Advances in Clinical and Experimental Medicine

MONTHLY ISSN 1899-5276 (PRINT) ISSN 2451-2680 (ONLINE) www.advances.umed.wroc.pl

2018, Vol. 27, No. 6 (June)

Impact Factor (IF) – 1.262
Ministry of Science and Higher Education – 15 pts.
Index Copernicus (ICV) – 155.19 pts.

Wroclaw Medical University

Advances
in Clinical and Experimental Medicine

ISSN 1899-5276 (PRINT) ISSN 2451-2680 (ONLINE) www.advances.umed.wroc.pl

MONTHLY 2018
Vol. 27, No. 6
(June)

Advances in Clinical and Experimental Medicine is a peer-reviewed open access journal published by Wroclaw Medical University. Its abbreviated title is Adv Clin Exp Med. Journal publishes original papers and reviews encompassing all aspects of medicine, including molecular biology, biochemistry, genetics, biotechnology, and other areas. It is published monthly, one volume per year.

Editorial Office
ul. Marcinkowskiego 2–6
50-368 Wrocław, Poland
Tel.: +48 71 784 12 05
E-mail: redakcja@umed.wroc.pl

Publisher
Wroclaw Medical University
Wybrzeże L. Pasteura 1
50-367 Wrocław, Poland

Online edition is the original version of the journal

Editorial Policy

Advances in Clinical and Experimental Medicine (Adv Clin Exp Med) is an independent multidisciplinary forum for exchange of scientific and clinical information, publishing original research and news encompassing all aspects of medicine, including molecular biology, biochemistry, genetics, biotechnology and other areas. During the review process, the Editorial Board conforms to the "Uniform Requirements for Manuscripts Submitted to Biomedical Journals: Writing and Editing for Biomedical Publication" approved by the International Committee of Medical Journal Editors (www.ICMJE.org/). The journal publishes (in English only) original papers and reviews. Short works considered original, novel and significant are given priority. Experimental studies must include a statement that the experimental protocol and informed consent procedure were in compliance with the Helsinki Convention and were approved by an ethics committee.

For all subscription related queries please contact our Editorial Office:

redakcja@umed.wroc.pl

For more information visit the journal's website:

www.advances.umed.wroc.pl

Pursuant to the ordinance no. 13/XV R/2017 of the Rector of Wroclaw Medical University (as of February 7, 2017) from February 8, 2017 authors are required to pay a fee amounting to 300 euros for each manuscript accepted for publication in the journal "Advances in Clinical and Experimental Medicine."

Pursuant to the ordinance no. 134/XV R/2017 of the Rector of Wroclaw Medical University (as of December 28, 2017) from January 1, 2018 authors are required to pay a fee amounting to 700 euros for each manuscript accepted for publication in the journal "Advances in Clinical and Experimental Medicine."

Indexed in: MEDLINE, Science Citation Index Expanded, Journal Citation Reports/Science Edition,

Scopus, EMBASE/Excerpta Medica, Ulrich's™ International Periodicals Directory, Index Copernicus

Typographic design: Monika Kolęda, Piotr Gil
DTP: Wydawnictwo UMW, TYPOGRAF
Cover: Monika Kolęda
Printing and binding: EXDRUK

Advances
in Clinical and Experimental Medicine

MONTHLY 2018, Vol. 27, No. 6 (June)

ISSN 1899-5276 (PRINT)
ISSN 2451-2680 (ONLINE)
www.advances.umed.wroc.pl

Contents

Original papers

Reviews

Protective effects of tumor necrosis factor alpha inhibitors on methotrexate-induced pancreatic toxicity

Tolga Mercantepe[1,A–E], Yıldıray Kalkan[1,A–E], Levent Tumkaya[1,A–E], İbrahim Sehitoglu[2,A–C], Filiz Mercantepe[3,D,E], Sermet Yıldırmıs[4,C]

[1] Departments of Histology and Embryology, Faculty of Medicine, Recep Tayyip Erdogan University, Rize, Turkey
[2] Department of Pathology, Faculty of Medicine, Recep Tayyip Erdogan University, Rize, Turkey
[3] Department of Internal Medicine, Faculty of Medicine, Recep Tayyip Erdogan University, Rize, Turkey
[4] Department of Pathology, Faculty of Medicine, Karadeniz Technical University, Trabzon, Turkey

A – research concept and design; B – collection and/or assembly of data; C – data analysis and interpretation;
D – writing the article; E – critical revision of the article; F – final approval of the article

Advances in Clinical and Experimental Medicine, ISSN 1899-5276 (print), ISSN 2451-2680 (online) *Adv Clin Exp Med*. 2018;27(6):715–720

Address for correspondence
Tolga Mercantepe
E-mail: tolgamercantepe@yahoo.com

Funding sources
This study was supported by the Scientific Research Department of Recep Tayyip Erdogan University, Turkey (Project No BAP: 2015.53001.106.01.03).

Conflict of interest
None declared

Received on January 12, 2016
Reviewed on January 27, 2017
Accepted on February 14, 2017

Abstract

Background. Methotrexate (MTX), a folate antagonist, is commonly used in the treatment of many different types of cancer and inflammatory diseases, including pancreatic cancer, although its side effects on the pancreas have not yet been researched. The mechanism of MTX-induced toxicity is not well known, and it has been reported in high-dose toxicity studies that the pancreas is sensitive to toxic effects.

Objectives. The aim of our study was to determine whether adalimumab (ADA) has a preventive effect on MTX-induced pancreas toxicity in rats.

Material and methods. The rats were equally and randomly divided into 3 groups (Group 1 comprised the healthy controls, Group 2 was the MTX group, and Group 3 was the MTX + ADA group). The rats in Groups 2 and 3 received an intraperitoneal (ip.) single-dose injection of MTX (20 mg/kg). A single dose of 5 mg/kg ADA (REMICADE®) was administered ip. to Group 3. All the rats were sacrificed under anesthesia 5 days after receiving the MTX injection.

Results. Significantly higher mean edema, necrotic cell, and inflammatory scores were recorded in Groups 2 and 3 compared to those recorded in Group 1. Significantly decreased edema, number of necrotic cells, and inflammatory scores were noted in Group 3 than in Group 2. A decrease in islets of Langerhans cell insulin and somatostatin-positive interneurons was demonstrated after the administration of MTX. An increase in insulin and somatostatin-positive cells in islets of Langerhans, as well as a remodeling of the structure of the pancreas, was shown following treatment with ADA.

Conclusions. Adalimumab was demonstrated to have a protective effect against MTX-induced pancreatic injury in this study.

Key words: adalimumab, methotrexate, pancreas, rat, toxicity

DOI
10.17219/acem/68967

Introduction

Methotrexate (MTX) was discovered in 1948 by Farber as an effective treatment for acute leukemia and is an antimetabolite, antifolate, and chemotherapeutic drug.[1,2] The effect of DNA synthesis in the "S" phase by inhibition and the affinity of dihydrofolic acid to inhibit the dihydrofolate reductase enzyme appear with the use of MTX. Thus, there is a drop in tetrahydrofolic acid levels and purine synthesis is inhibited.[3,4] Methotrexate is used to treat many different types of cancer (colorectal, breast, and pancreatic cancers) and inflammatory diseases (rheumatoid arthritis – RA, psoriatic arthritis, systemic lupus erythematosus, and dermatomyositis).[1–5] Nevertheless, its use is associated with side effects such as fibrosis affecting the liver, lung, and other organs.[1,2,5] Acute intense MTX side effects are dose-dependent. Bone marrow suppression, gastrointestinal upsets or ulcers, and liver fibrosis are well-known acute or common side effects of MTX therapy. It has been proposed in recent studies that MTX has a cytotoxic effect in reducing intracellular tetrahydrofolate, but the mechanism of MTX-induced toxicity is not well known.[1,2,4–11]

Methotrexate has been used in the treatment of pancreatic cancer, but there has been no research into its side effects on the pancreas, an organ which is relatively sensitive to various toxic substances and drugs. High-dose substances, causing oxidative stress, have been reported to have a toxic effect on the pancreas.[1,5–11] However, the development of tolerance to MTX has been reported in patients over time. The tolerance mechanism of the metabolites in MTX is not known.[1,2,4,5,11] Physicians increase the dosage of MTX to counter the development of tolerance. Accordingly, the risk of MTX toxicity increases. It was found in recent studies that an MTX overdose caused oxidative stress, leading to the release of proinflammatory cytokines and further tissue damage.[5,6,11]

Tumor necrosis factor alpha (TNF-α) plays a key role in the mechanism of immune-mediated inflammatory diseases, such as RA, ankylosing spondylitis, Crohn's disease, ulcerative colitis, psoriasis, and psoriatic arthritis. Inflammation induces the overproduction of inflammatory cytokines, such as TNF-α, interleukin: IL-1β, IL-6, IL-15, and IL-18, while TNF-α has been shown to increase the number of pancreatic cancer cells.[12] It has been reported in the literature that TNF-α cytokines modulate the autocrine growth regulatory pathways in pancreatic cancer cells.[13] Antagonists of TNF-α, such as adalimumab (ADA), infliximab, etanercept (ETN), golimumab, and certolizumab pegol, have been widely used in the treatment of RA. Inhibition of TNF results in the down-regulation of abnormal and progressive inflammatory processes, resulting in the prevention of target organ damage.[12,13]

It has been found that a combination of TNF-α antagonists and MTX improves the symptoms and signs of inflammation and physical function in RA patients who do not respond to MTX alone.[10–13] The combination of MTX and ADA has not been studied for its ability to counter toxicity in the pancreas. Irreversible tissue injury from edema and inflammatory and acinar necrosis has been reported in histopathological studies on pancreatic toxicity.[14–16]

The aim of this study was to determine whether TNF-α inhibitors have a preventive or toxicity-enhancing effect on MTX-induced pancreatic toxicity.

Material and methods

Animal testing

Thirty male albino Sprague Dawley® rats, aged 3 months and weighing 250–300 g, were procured from the Animal Care and Research Unit for this study (Recep Tayyip Erdogan University, Rize, Turkey). The animals were kept at a constant temperature (21 ±3°C) and according to a constant photoperiod and temperature regime (12-h light/dark cycle).

During the experimental period, all of the subjects were given fed ad libitum pellets containing 21% crude protein (purina) and given drinking water daily. The animals were selected according to the criteria outlined in the Guide for the Care and Use of Laboratory Animals, prepared by the National Academy of Sciences and published by the National Institutes of Health. Recep Tayyip Erdogan University Animal Care and Research Unit (Rize, Turkey).

This study was approved by the Institutional Animal Ethical Committee Recep Tayyip Erdogan University Animal Care and Research Unit (Rize, Turkey).

The subjects were randomly allocated to 3 groups of 8 rats each (n = 8), with similar biological and physiological characteristics: Group 1: control group (healthy), Group 2: MTX group and Group 3: MTX + ADA group.

Isotonic saline solution, mixed with an equal volume of MTX, was administered by ip. injection to Group 1.

A single-dose injection of MTX (Emthexate-s®, 50-mg ampule), at a dose of 20 mg/kg, was given by ip. injection to Groups 2 and 3, and a single dose of 5 mg/kg ADA (REMICADE®) was administered ip. to Group 3.

All the rats were sacrificed under anesthesia with ketamine hydrochloride 50 mg/kg, intramuscularly (Ketalar, Parke-Davis, Istanbul, Turkey) 5 days after receiving the MTX injection.

Histological preparation

Pancreatic tissue samples were fixed in 10% formalin. After fixation, the specimens were dehydrated in an ascending series of alcohol, cleared in xylene, and embedded in paraffin. The paraffin blocks were cut 4–5 µm thick, using a microtome (Leica® RM2125 RTS), and the sections were stained with hematoxylin and eosin (Applichem GmbH, Darmstadt, Germany), according to the guidelines that govern conventional light microscopes.

Immunohistochemical preparation

Paraffin blocks of the pancreatic samples were cut into 1–2 µm semi-thin sections. The sections obtained for immunohistochemical staining were left in xylene for 10 min, twice, and after being passed through an alcohol series (70–99%) for 5 min, were kept in a 3% H_2O_2 solution for 10 min. After washing with phosphate buffered saline solution (PBS), they were heated 4 times in a citrate buffer for 5–10 min at 800 W of power, and allowed to stand for 20 min in a secondary blocking agent. Each preparation was allowed to stand for 60–75 min in various dilutions (1/50–1/200) of anti-laminin antibody staining (Polyclonal Guinea Pig Anti-Insulin® [clinical application for IS002], and Polyclonal Rabbit Anti-Human Somtastatin® [clinical application for A0566], both Dako Denmark A/S, Denmark). The 3,3'-diaminobenzidine (DAB) solution was used as a chromogenic dye, and stained with Mayer's hematoxylin for contrast dye. Phosphate buffered saline solution was used for the negative controls instead of primary antibodies. The preparation was closed off with a suitable agent and photographed. According to the blind scoring evaluation performed by 2 histologists, the positivity was divided into the following 4 categories according to the percentage value: mild (+), moderate (++), severe (+++), and very severe (++++).

Pathological assessment of tissue

Parts of the tissue were fixed and embedded in paraffin for histological analysis. Blinded pathological scoring of the pancreas, by an experienced pathologist from Recep Tayyip Erdoğan University, Rize, Turkey, was performed with respect to edema, bleeding, inflammatory cell infiltration, and necrosis, according to Schmidt's report (Table 1).[14]

Statistical analysis

Statistical analysis was performed using SPSS® v. 18 (IBM; Chicago, USA). Schmidt's score was calculated.[14] The data was expressed as mean ±standard error of the mean (SEM). Statistical analysis was performed using one-way analysis of variance, followed by Tukey's test for each paired experiment value. A p-value of $p < 0.05$ was considered to be significant. The sections obtained by immunohistochemical staining were evaluated and graded by 2 blinded histologists and the positivity was expressed in terms of percentage and divided into 4 grade categories. Data was expressed as median ±standard deviation (SD). The obtained values were statistically compared with the Kruskal-Wallis test ($p < 0.05$) to each other.

Results

Histological results

The morphologic structure of the tissues in the control group was observed to have a normal histology (Fig. 1A, 1B).

The histopathologic features of the Group 2 samples were atypical islets of Langerhans, mild edema, necrosis, and inflammatory infiltration. Necrotic cells were observed in the islets of Langerhans and acinar cells. Necrotic acinar cells, with a pyknotic nucleus in the center, partial karyorrhexis, and a bright border due to cytoplasmatic shrinkage and cell degeneration, were observed. Connective tissue trabeculae were noted to increase considerably in volume with leukocytic infiltration (Fig. 1C–1E).

Complete destruction of islet of Langerhans cells, due to the toxicity of MTX, appeared in the Group II rats compared to Group 1 (Fig. 1A–1D).

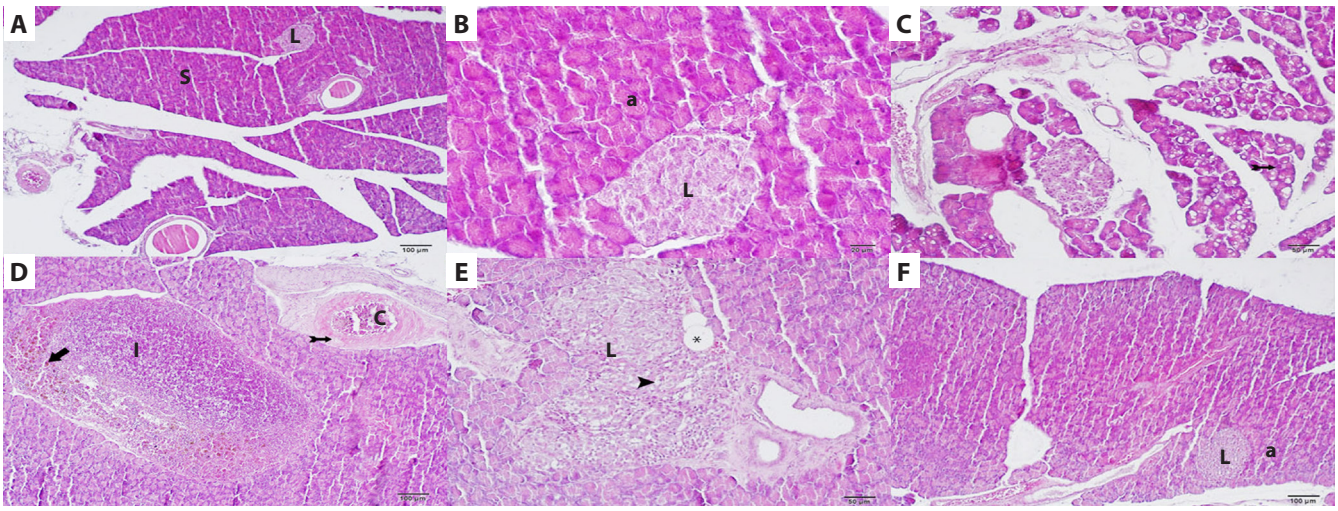

Fig. 1. A, B – histology of a normal pancreas (L – islets of Langerhans, a – acinar); C, D, E – MTX group C – MTX group demonstrating necrotic acinar cells with a pyknotic nucleus (tailed arrow), and edema (E); D – there are numerous entirely destroyed lobules with extreme leukocytic infiltration (i) and frequently widespread hemorrhage (thick arrow), capillary congestion (c), atypical blood vessel (thin arrow); E – edema (asterisk) and mononuclear leukocyte infiltration were observed in islets of Langerhans (spiral arrow); F – MTX + ADA group (L – islet of Langerhans, a – acinar); H&E stains.

Decreased edema, necrosis, and inflammatory infiltration was demonstrated in the Group 3 samples.

A decrease in necrotic cells was also observed in islets of Langerhans and acinar cells (Fig. 1F) after the administration of the ADA/MTX combination therapy.

Immunohistochemical results

The immunoreactivity rate for anti-insulin, together with islets of Langerhans, was found to be moderate (17%), severe (33%), and very severe (50%) in Group 1; mild (67%) and moderate (33%) in Group 2; and mild (17%), moderate (33%), severe (33%), and very severe (17%) in Group 3 (Fig. 2, 3).

Anti-somatostatin immunopositivity in islets of Langerhans was shown on immunohistochemical staining using the immunoperoxidase method, and was found to be mild (17%), moderate (17%), severe (33%), and very severe (33%) in Group 1; mild (83%) and moderate (17%) in Group 2; and mild (17%), moderate (33%), and very severe (50%) in Group 3 (Table 3).

Stereological results

All the study rats were scored by both investigators using Schmidt's histopathological scoring method. There was no more than a 0.5-point deviation in their discernment. Schmidt's histopathological scoring steps, shown in Table 2, were applied.

Statistical results

Significantly higher mean edema, necrotic cell, and inflammatory scores, compared to those obtained for Group 1, were recorded for Group 2 ($p < 0.05$). Significantly decreased edema, necrotic cell, and inflammatory scores were recorded for Group 3, when compared to Group 2 ($p < 0.05$) (Table 2).

Table 1. Schmidt's histopathologic scoring criteria

Edema	
0	Absent
0.5	Focal expansion of interlobular septae
1	Diffuse expansion of interlobular septae
1.5	Same as 1 + focal expansion of interlobular septae
2	Same as 1 + diffuse expansion of interlobular septae
2.5	Same as 2 + focal expansion of interacinar septae
3	Same as 2 + diffuse expansion of interacinar septae
3.5	Same as 3 + focal expansion of intercellular spaces
4	Same as 3 + diffuse expansion of intercellular spaces
Acinar necrosis	
0	Absent
0.5	Focal occurrence of 1–4 necrotic cells/HPF
1	Diffuse occurrence of 1–4 necrotic cells/HPF
1.5	Same as 1 + focal occurrence of 5–10 necrotic cells/HPF
2	Diffuse occurrence of 5–10 necrotic cells/HPF
2.5	Same as 2 + focal occurrence of 11–16 necrotic cells/HPF
3	Diffuse occurrence of 1 1–16 necrotic cells/HPF (foci of confluent necrosis)
3.5	Same as 3 + focal occurrence of >16 necrotic cells/HPF
4	>16 necrotic cells/HPF (extensive confluent necrosis)
Hemorrhage and fat necrosis	
0	absent
0.5	1 focus
1	2 foci
1.5	3 foci
2	4 foci
2.5	5 foci
3	6 foci
3.5	7 foci
4	8 foci
Inflammation and perivascular infiltrate	
0	0–1 intralobular or perivascular leukocytes/HPF
0.5	2–5 intralobular or perivascular leukocytes/HPF
1	6–10 intralobular or perivascular leukocytes/HPF
1.5	11–15 intralobular or perivascular leukocytes/HPF
2	16–20 intralobular or perivascular leukocytes/HPF
2.5	21–25 intralobular or perivascular leukocytes/HPF
3	26–30 intralobular or perivascular leukocytes/HPF
3.5	>30 leukocytes/HPF or focal microabscesses
4	>35 leukocytes/HPF or confluent microabscesses

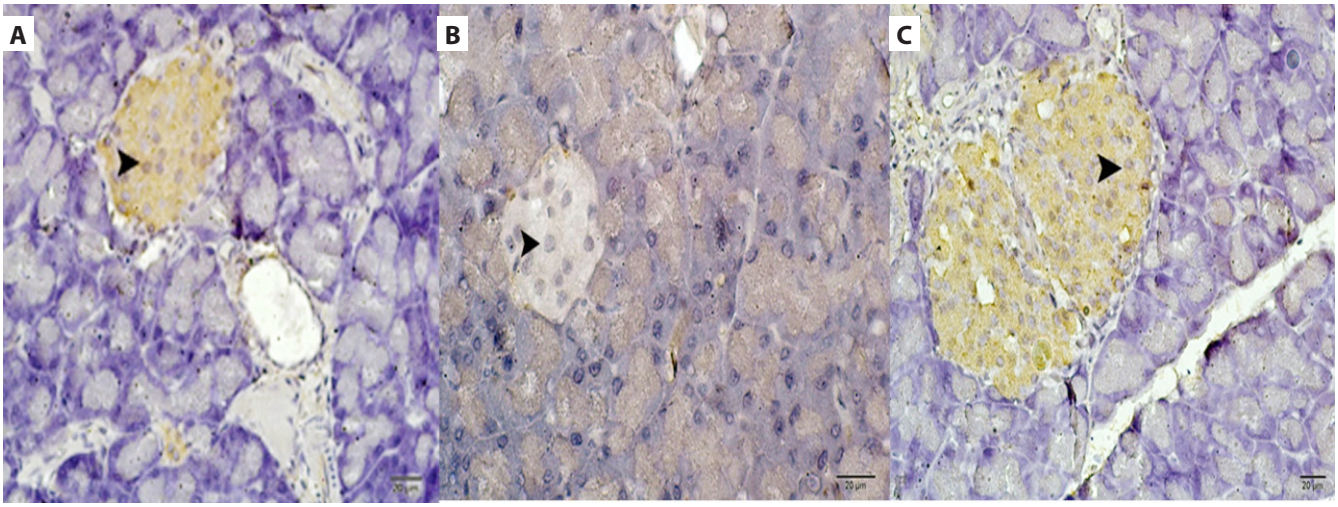

Fig. 2. Histopathologic examination of liver tissue stained by anti-insulin IHC staining method by light microscopy

A – control group, insulin positive area; B – MTX group, insulin negative area; C – MTX + ADA group, insulin positive area.

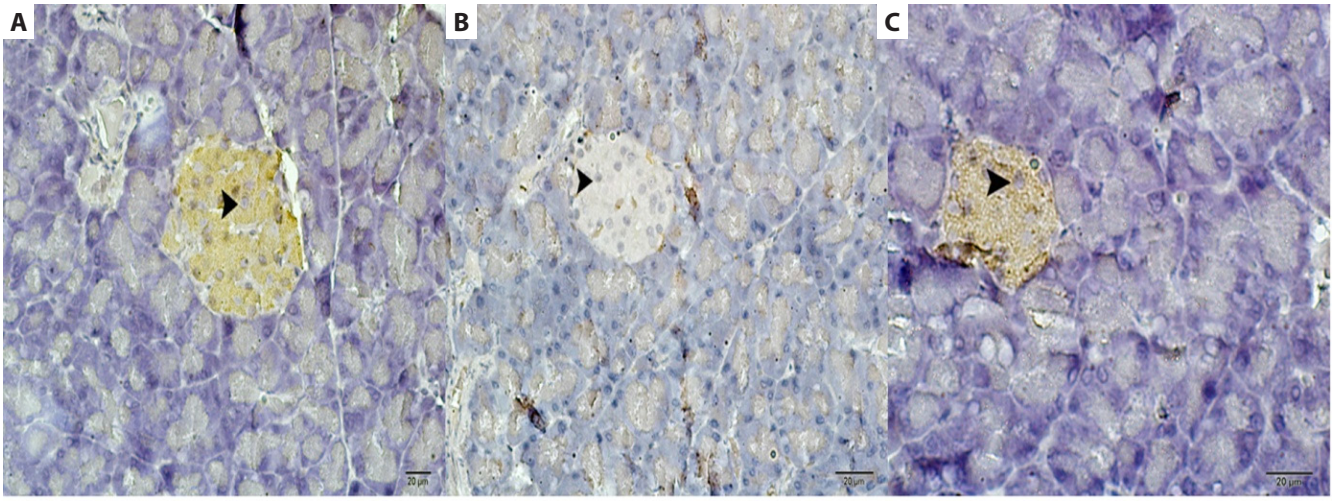

Fig. 3. Histopathologic examination of liver tissue stained by anti-somatostatin IHC staining method by light microscopy: A – control group, somatostatin positive area; B – MTX group, somatostatin negative area; C – MTX + ADA group, somatostatin positive area.

Table 2. Statistical results

Treatment	No. of rats	Edema	Acinar necrosis	Inflammatory infiltration	Perivascular infiltration
Control	8	0.19 ±0.09[b]	0.13 ±0.08[b]	0.06 ±0.06[b]	0.06 ±0.06[b]
MTX	8	1.75 ±0.66[a]	1.8 ±0.16[a]	1.88 ±0.08[a]	0.44 ±0.11[a]
MTX + ADA	8	0.5 ±0.09[b]	0.56 ±0.6[b]	0.05 ±0.09[b]	0.13 ±0.08[b]

Means in the same column by the same superscript letter are not statistically significantly different under the Tukey test (α = 0.05). Results are mean ±standard error of the mean.
[a] vs control Group $p < 0.05$; [b] vs MTX Group $p < 0.05$. MTX – methotrexate; ADA – adalimumab.

Table 3. Anti-insulin and anti-somatostatin shown in the pancreas tissues by the method of immunoperoxidase in immunohistochemical staining

Group	Anti-insulin median ±SD	Anti-somatostatin median ±SD
Control	3 ±0.75	3 ±1.17
MTX	1 ±0.52[a]	1 ±0.41[a]
MTX + ADA	2.5 ±1.05[b,c]	2.5 ±1.05

[a] In the statistical evaluations performed, significant differences were observed between the control and MTX groups in terms of anti-insulin and anti-somatostatin immunopositivity according to the Kruskal-Wallis test ($p < 0.05$). [b] In the statistical evaluations performed, significant differences were observed between the control and MTX + ADA groups in terms of anti-insulin and anti-somatostatin immunopositivity according to the Kruskal-Wallis test ($p < 0.05$). [c] In the statistical evaluations performed, significant differences were observed between the MTX and MTX + ADA groups in terms of anti-insulin and anti-somatostatin immunopositivity according to the Kruskal-Wallis test ($p < 0.05$).
MTX – methotrexate; ADA – adalimumab.

Discussion

The side effects of MTX on the pancreas have not been researched. However, high-dosage substances were reported to have a toxic effect on the pancreas. Irreversible tissue injury with edema, inflammation, and acinar necrosis was also found in histopathological studies on pancreatic toxicity.[16–23]

Increased edema, acinar edema, and necrotic cells were observed in islets of Langerhans and acinar cells in Group 2, compared to those found in Group 1 ($p < 0.05$) (Table 2) in our study on MTX-induced pancreatic toxicity. It was also found that atypical islets of Langerhans and connective tissue trabeculae were observed to increase considerably in volume. A reduction in the amount of insulin and somatostatin was also found. An accumulation of mast cells in the connective tissue was observed.

According to the literature, increased oxidative stress leads to the release of proinflammatory cytokines, leading to further tissue damage.[22–24] Methotrexate is used for the treatment of pancreatic cancer, but has been shown to destroy the beta cells of the pancreas, primarily through oxidative stress.[1,2,5,24] In support of the data in the literature, we determined that in our study the number of insulin and somatostatin-positive cells significantly decreased in Group 2, when compared to that in Group 1 (Fig. 2B, 3B).

It has been proposed in previous studies that MTX increases lipid peroxidation and oxidative stress, leading to an increase in reactive oxygen species (ROS).[5,24] It has also been reported that ROS play a key role in decreasing immune system defense.[5,24,25] In addition, intense proinflammatory cytokine release, due to excessive ROS formation, has been reported during MTX treatment for cancer and autoimmune diseases.[5,6,24,25] Accumulation of ROS leads to neutrophil infiltration and proinflammatory cytokine release, which triggers apoptosis.[5,6,24,25] Methotrexate is used for the treatment of pancreatic cancer, but has been shown to destroy the beta cells of the pancreas, primarily through oxidative stress.[5,6,24–26]

A decrease in islets of Langerhans insulin and somatostatin-immunopositive cells was shown in this study following the administration of MTX (Fig. 2B, 3B).

It has been suggested that TNF-α plays a key role in the mechanism of immune-mediated inflammation in recent studies. Inhibition of TNF results in the down-regulation of abnormal and progressive inflammatory processes, resulting in target organ damage.[4,5,10,11,19,27] It has been experimentally proven that TNF inhibitors prohibit organ tissue damage by suppressing the formation of TNF-α, proinflammatory cytokines, and nitric oxide.[5,26,27]

A decrease in edema, acinar cell edema, and necrotic cells was observed in Group 3 ($p < 0.05$) (Table 2) after the administration of ADA. An increase in islets of Langerhans insulin and somatostatin-positive cells was also demonstrated following the application of ADA treatment to Group 3 (Fig. 2C, 3C).

As a result, ADA was shown to have a protective effect against MTX-induced pancreatic injury. It was shown in this study that ADA reduced inflammatory levels and provided better protection to the insulin and somatostatin cells than that provided by MTX. This was a pilot study. Thus, further studies are needed in this regard to confirm our findings.

References

1. Sendur N, Karaman G, Savk E, Sahinkarakas E. Cutaneous ulceration as an early manifestation of methotrexate toxicity. *T Klin J Med Sci*. 2002;22:593–596.
2. Calvert AH, Walling JM. Clinical studies with MTA. *Br J Cancer*. 1998;78:35–40.
3. Selhub J, Dhar GJ, Rosenberg IH. Inhibition of folate enzymes by sulfasalazine. *J Clin Invest*. 1978;61:221–224.
4. Behrens F, Canete JD, Olivieri I, van Kuijk AW, McHugh N, Combe B. Tumour necrosis factor inhibitor monotherapy vs combination with Mtx in the treatment of PsA: A systematic review of the literature. *Rheumatology*. 2015;54:915–926.
5. Cure E, Kirbas A, Tumkaya L, et al. Protective effect of infliximab on methotrexate-induced liver injury in rats: Unexpected drug interaction. *J Cancer Res Ther*. 2015;11:164–169.
6. Moghadam AR, Tutunchi S, Namvaran-Abbas-Abad A, et al. Pre-administration of turmeric prevents methotrexate-induced liver toxicity and oxidative stress. *BMC Complement Altern Med*. 2015;15:246.
7. Kanter M, Yuncu M. Protective effects of vitamin E against methotrexate-induced mucosal damage of the small intestine in mice: An electron microscopic study. *TAD Journal*. 2006;4:1–6.
8. Güzel R. Rheumatoid arthritis and disease modifying antirheumatic drugs. *Turk J Phys Med Rehab*. 2008;54:25–30.
9. Salzer WL, Devidas M, Shuster JJ, et al. Intensified PEG-L-asparaginase and antimetabolite-based therapy for treatment of higher risk precursor-B acute lymphoblastic leukemia: A report from the Children's Oncology Group. *J Pediatr Hematol Oncol*. 2007;29:369-375.
10. Lipsky PE, van der Heijde DM, St. Clair EW, et al. Infliximab and methotrexate in the treatment of rheumatoid arthritis. *N Engl J Med*. 2000;30:1594–1602.
11. Harriman G, Harper LK, Schaible TF. Summary of clinical trials in rheumatoid arthritis using infliximab, an anti-TNFÆ treatment. *Ann Rheum Dis*. 1999;58:161–164. doi:10.1056/NEJM200011303432202
12. Goto Y, Yue L, Yokoi A, et al. A novel single-nucleotide polymorphism in the 3*-untranslated region of the human dihydrofolate reductase gene with enhanced expression. *Clin Cancer Res*. 2001;7:1952–1956.
13. Schmiegel W, Roeder C, Schmielau J, Rodeck U, Kalthoff H. Tumor necrosis factor alpha induces the expression of transforming growth factor alpha and the epidermal growth factor receptor in human pancreatic cancer cells. *Proc Natl Acad Sci*. 1993;90:863–867.
14. Schmidt J, Rattner DW, Lewandrowski K, et al. A better model of acute pancreatitis for evaluating therapy. *Ann Surg*. 1992;215:44–56.
15. Tinder TL, Subramani DB, Basu GD, et al. MUC1 enhances tumour progression and contributes toward immunosuppression in a mouse model of spontaneous pancreatic adenocarcinoma. *J Immunol*. 2008;181:3116–3125.
16. Gokalp O, Karakoyun I, Kaleli S, Ozer MK, Gultekin F. The effects of chlorpyrifos-ethyl on pancreas in rats. *Journal of Suleyman Demirel University Medicine*. 2005;12:19–22.
17. Gardi JE, Nyengaard JR, Gundersen HJ. Automatic sampling for unbiased and efficient stereological estimation using the proportionator in biological studies. *J Microsc*. 2005;230:108–120.
18. Maruyama H, Nakatsuji N, Sugihara S, et al. Anaplastic Ki-1-positive large cell lymphoma of the pancreas: A case report and review of the literature. *Jpn J Clin Oncol*. 1997;27:51–57.
19. Tasaka Y, Nakaya F, Matsumoto H, Omori Y. Effects of aminoguanidine on insulin release from pancreatic islets. *Endocr J*. 1994;41:309–313.
20. Hiramatsu S, Inoue K, Sako Y, Umeda F, Nawata H. Secretion of insulin and glucagon by the perfused pancreas of genetically obese (fa/fa) Zucker rats and its alteration with aging. *Endocr J*. 1995;42:563–567.
21. Kimura N, Schindler M, Kasai N, Kimura I. Immunohistochemical localization of somatostatin receptor type 2A in rat and human tissues. *Endocr J*. 2001;48:95–102.
22. Tasaka Y, Nakaya H, Omori Y. Effects of aminoguanidine on glucagon and insulin release from rat pancreatic islet. *Endocr J*. 1996;43:725–730.
23. Heitz PU, Kasper M, Polak JM, Kloppel G. Pathology of the endocrine pancreas. *J Histochem Cytochem*. 1979;27:1401–1402.
24. Sampaio AF, Silva M, Dornas WC, et al. Iron toxicity mediated by oxidative stress enhances tissue damage in an animal model of diabetes. *Biometals*. 2014;27:349–361.
25. Kalkan Y, Tumkaya L, Bostan H, et al. Effect of sugammadex on rocuronium induced changes in pancreatic mast cells. *Toxicol Ind Health*. 2015;31:738–746.
26. Tanaka T, Sekine A, Tsunoda Y, et al. Central nervous system manifestations of tuberculosis-associated immune reconstitution inflammatory syndrome during adalimumab therapy: A case report and review of the literature. *Intern Med*. 2005;54:847–851.
27. Rau R. Adalimumab (a fully human anti-tumour necrosis factor α monoclonal antibody) in the treatment of active rheumatoid arthritis: The initial results of five trials. *Ann Rheum Dis*. 2002;61:70–73.

The expression of selected molecular markers of immune tolerance in psoriatic patients

Joanna Bartosińska[1,A–E], Joanna Purkot[2,B,C], Małgorzata Kowal[1,B], Anna Michalak-Stoma[1,B], Dorota Krasowska[1,E,F], Grażyna Chodorowska[1,A,C,E,F], Krzysztof Giannopoulos[2,A,C,E,F]

[1] Department of Dermatology, Venereology and Pediatric Dermatology, Medical University of Lublin, Poland
[2] Department of Experimental Hematooncology, Medical University of Lublin, Poland

A – research concept and design; B – collection and/or assembly of data; C – data analysis and interpretation; D – writing the article; E – critical revision of the article; F – final approval of the article

Advances in Clinical and Experimental Medicine, ISSN 1899-5276 (print), ISSN 2451-2680 (online) *Adv Clin Exp Med*. 2018;27(6):721–725

Address for correspondence
Joanna Bartosińska
E-mail: jbartosinski@gmail.com

Funding sources
The study was supported by DS164 of the Medical University of Lublin.
The publication fee was covered by DS462/2016 of the Medical University of Lublin.

Conflict of interest
None declared

Received on July 14, 2017
Reviewed on July 31, 2017
Accepted on September 26, 2017

Abstract

Background. Psoriasis is a chronic autoinflammatory disease whose underlying molecular mechanisms remain unclear. The disease is mediated by the cells and molecules of both the innate and adaptive immune systems. Some T cell surface molecules, including neuropilin-1 (NRP1), programmed death 1 (PD-1) and the human leukocyte antigen G (HLA-G), are known to play a role in the maintenance of immune tolerance.

Objectives. The aim of this study was to investigate HLA-G, NRP1 and programmed cell death gene (PDCD1) mRNA expression in psoriatic patients.

Material and methods. The study included 72 psoriatic patients and 35 healthy individuals. Twenty-one patients (29.17%) suffered from concomitant psoriatic arthritis. The mRNA expression of HLA-G, NRP1, and PDCD1 were determined using quantitative real-time reverse transcription polymerase chain reaction (qRT-PCR). The severity of skin lesions was assessed by means of the Psoriasis Area and Severity Index (PASI), Body Surface Area (BSA), the Patient Global Assessment (PGA), and the Dermatology Life Quality Index (DLQI).

Results. The median value of the PASI was 11.5, and of BSA was 15.8%. The expressions of NRP1 and PDCD1, but not HLA-G, were significantly lower in psoriatic patients in comparison with the control group. The expression of HLA-G, NRP1 and PDCD1 were not significantly different in the psoriatic arthritis and psoriasis vulgaris patients.

Conclusions. The results of this study suggest that the molecular markers of immune tolerance, i.e., HLA-G, NRP1, and PD-1, may be involved in the immune response in psoriatic patients.

Key words: psoriasis, PD-1, HLA-G, NRP1

DOI
10.17219/acem/78020

Introduction

A disruption to the immune system is likely to compromise immune tolerance and may lead to the development of autoimmune and autoinflammatory conditions.

In psoriasis, whose pathogenesis involves keratinocyte hyperplasia and excessive angiogenesis, the role of genetic factors, environmental triggers and aberrant immune system regulation resulting in compromised immune tolerance is well understood. Here, the T cell immune response is activated by antigen-presenting cells (APCs) which will undoubtedly impair the balance between the effector and regulatory components of the immune system.[1]

Physiologically, in order to maintain undisturbed immune tolerance, various cellular and molecular mechanisms become activated. These include the central negative selection of autoreactive T cells in the thymus as well as peripheral anergy, clonal deletion, suppression, and exhaustion. This natural immune tolerance depends on the interaction between the T cells' stimulatory and inhibitory receptors and their ligands.[2] All of them form a complex network of molecules that interact in order to maintain peripheral tolerance or to enhance T cell immunity.

Since certain T cell surface molecules, including neuropilin-1 (NRP1), programmed death 1 (PD-1), and human leukocyte antigen G (HLA-G) play a vital role in the T cells' interactions with APCs (including dendritic cells [DCs], B cells, monocytes and macrophages), their compromised suppressive ability could insufficiently inhibit or even fail to inhibit the activity of the inflammatory cells in psoriasis.

Neuropilin-1, a transmembrane glycoprotein and a receptor involved in some physiological and pathological processes (including angiogenesis), acts as a co-receptor for the vascular endothelial growth factor (VEGF) and semaphorins 3A (Sema 3A).[3] Neuropilin-1 is preferentially expressed on regulatory T cells (Tregs) and myeloid cells (i.e., DCs), and it promotes long-term interactions between Tregs and immature DCs, thereby suppressing their activation and function.[4] A decreased number of NRP1-positive Treg cells, however, could possibly explain the inability of the immune system to suppress an immune response and restore immune tolerance.

Programmed death 1, a glycoprotein expressed on T cells – including Tregs – B cells, monocytes, and macrophages, is a known checkpoint inhibitor which blocks the effector T cells' function and promotes Treg activity. The co-expression of the PD-1 with its ligand 1 (PD-L1) on Tregs enhances their proliferation and favors the maintenance of self-tolerance.[5]

Human leukocyte antigen G, a nonclassical human leukocyte antigen (HLA), known as a tolerogenic molecule, is capable of downregulating the natural killer (NK) cells' cytotoxic activity, the inhibition of T cell migration, the induction of the apoptosis of activated CD8+ T cells, and the prevention of DC maturation. It induces the functional silencing of the immune response, which is indispensable in certain physiological settings, e.g., during pregnancy, but it also allows the tumor cells to escape the host's immune system.[6] This leukocyte affects the antigen presentation by the inhibition of HLA II upregulation and its interaction with co-stimulatory molecules.[7]

The 3 aforementioned molecules, i.e., HLA-G, NRP1 and PD-1, need to be better understood in terms of their function in psoriasis. Since all the molecular markers are capable of inhibiting the T cell function through the action on both innate and adaptive immunity, it is worth studying whether they are differently expressed in psoriatic patients compared to healthy individuals. If the coexistence of abnormal immunomodulatory properties of HLA-G, an absence of PD-1 co-inhibitory signal and a lack of NRP1 positive T cells with suppressive ability proved to be of significance in psoriasis, then chronic autoinflammatory disease, self-reactivity and the persistent T-cell activation in psoriasis could be better understood.

Material and methods

Study group

The study comprised 72 psoriatic patients, including 21 (29.17%) psoriatic arthritis patients, hospitalized in the Department of Dermatology, Venereology, and Pediatric Dermatology at the Medical University of Lublin, Poland, as well as 35 age- and gender-matched healthy volunteers.

The study inclusion criteria were a duration of psoriasis of at least 1 year, the presence of active psoriatic skin lesions, and an age of at least 18 years. The exclusion criteria were cardiovascular, cerebrovascular, hematologic, hepatic, or renal disease; neoplasm; chronic viral infections; erythrodermic, pustular, or guttate psoriasis; addiction to drugs; and systemic anti-psoriatic treatment.

The study was approved by the Local Ethics Committee at the Medical University of Lublin (KE-0254/81/2015). Informed consent was obtained from all participants.

Assessment of psoriasis severity

The severity of psoriatic skin lesions was assessed with the Psoriasis Area and Severity Index (PASI), Body Surface Area (BSA), Patient Global Assessment (PGA), the Dermatology Life Quality Index (the DLQI), and nail plate changes with the Nail Psoriasis Severity Index 80 (NAPSI 80). Psoriatic arthritis (PsA) was diagnosed using the Classification of Psoriasis Arthritis criteria (CASPAR). The severity of psoriatic arthritis was assessed with the Disease Activity Score 28 (DAS 28), the Patient Visual Analog Scale (VAS), the number of tender joints, the number of swollen joints, and a physician–patient Likert scale.

Assessment of gene expression

NRP1, *PDCD1* and *HLA-G* mRNA expression was measured by quantitative real-time reverse transcription-polymerase chain reaction (qRT-PCR).

First, peripheral blood mononuclear cells (PBMCs) from psoriatic patients and healthy volunteers were isolated by Ficoll density gradient centrifugation (Biochrom AG, Berlin, Germany) and cryopreserved at –80°C until the time of analysis. The viability of the PBMCs obtained was always >95%, as determined by Trypan blue staining. Viable cells were quantified in a Neubauer chamber (Zeiss, Oberkochen, Germany).

Next, total RNA was isolated from the PBMCs using a QIAamp RNA Blood Mini Kit (Qiagen, Venlo, Netherlands) and reverse-transcribed to cDNA using a QuantiTect Reverse Transcription Kit (Qiagen). cDNA was used in a qRT-PCR to measure the mRNA expression of *NRP1* (Hs00826128_m1), *PDCD1* (Hs0155088_m1) and *HLA-G* (Hs00365950_g1) using the TaqMan Gene Expression Assay methodology, according to the manufacturer's protocol (Applied Biosystems, Foster City, USA). Glyceraldehyde-3-phosphate dehydrogenase (*GAPDH*) was used as a constitutively expressed housekeeping gene and negative controls contained water instead of cDNA to ensure the purity of all reagents. The thermocycling program was set for 40 cycles of 15 s at 95°C and 1 min at 60°C on the ABI Prism 7300 Sequence Detector (Applied Biosystems).

The *NRP1*, *PDCD1*, and *HLA-G* mRNA expression was calculated as inverse ratios of the differences in the cycles of threshold ($1/\Delta C_t$), where ΔC_t is the C_t value of the target receptors minus the C_t value of *GAPDH*.

Statistical analysis

The results were statistically analyzed with STATISTICA v. 10.0 PL (StatSoft Inc., Tulsa, USA). The figures were created using the GraphPad Prism 5 software (GraphPad Software Inc., San Diego, USA). Median values with minimal and maximal values were estimated for continuous variables, or absolute (n) and relative numbers (%) of the occurrence of items for categorical variables. Mann-Whitney U test was used to compare the mRNA expressions of *NRP1*, *HLA-G*, and *PDCD1* between the psoriatic patients and the control group, as well as between the psoriatic patients with and without arthritis. Spearman's rank correlation coefficient was used to investigate the correlation between the mRNA expressions of *NRP1*, *HLA-G* and *PDCD1*, and the clinical features of psoriasis and psoriatic arthritis. A value of $p < 0.05$ was considered to be significant.

Results

Most of the patients were male, with an average age of 47 years and an average psoriasis duration of 15.5 years. The severity of psoriasis assessed by the PASI was 11.5, by BSA 15.8, and by the DLQI 12.0, on average. Psoriatic arthritis was present in the studied patients for 6 years on average. More than half of the PsA patients had the oligoarticular clinical subset of the disease (Table 1).

The psoriatic patients had a significantly lower mRNA expression of *NRP1* (median: 0.09) in comparison to the healthy controls (median: 0.14). Similarly, the psoriatic patients had a significantly lower mRNA expression of *PDCD1* (median: 0.08) in comparison to the healthy controls (median: 0.11). The mRNA expression of *HLA-G* did not significantly differ between the psoriatic patients (median: 0.05) and the healthy controls (median: 0.05) (Fig. 1).

None of the studied molecular markers of immune tolerance significantly differed between the psoriatic arthritis and psoriasis vulgaris patients (Fig. 2). The median mRNA expression of *NRP1* was 0.09, for *PDCD1* it was 0.08, and for *HLA-G* it was 0.05 for both psoriatic arthritis and psoriasis vulgaris patients.

The studied mRNA expression of *HLA-G* correlated negatively only with the age of the psoriatic patients. However, the studied mRNA expressions of *PDCD1* and *NRP1* did not correlate with any clinical features either in the psoriatic or the psoriatic arthritis patients (Table 2).

Table 1. Clinical data of psoriatic patients

Patients	Clinical data	Estimate
Psoriasis (n = 72)	age [years], median (min–max)	47 (21–76)
	female (n)	11
	male (n)	61
	duration of the disease [years], median (min–max)	15.5 (1–55)
	age at disease onset [years], median (min–max)	22 (1–71)
	positive family history (n, %)	27 (37.50)
	PASI, median (min–max)	11.5 (3–49)
	PGA, median (min–max)	3 (2–5)
	BSA (%), median (min–max)	15.8 (2–75)
	DLQI, median (min–max)	12 (1–30)
	NAPSI, median (min–max)	14 (0–64)
	diagnosis of psoriatic arthritis (n, %)	21 (29.17)
Psoriatic arthritis (PsA) (n = 21)	duration of psoriatic arthritis [years], median (min–max)	6 (1–20)
	number of tender joints, median (min–max)	5 (0–12)
	number of swollen joints, median (min–max)	0 (0–6)
	physician Likert, median (min–max)	2 (1–4)
	patient Likert, median (min–max)	3 (1–4)
	DAS28, median (min–max)	3.4 (1.0–5.5)
	VAS, median (min–max)	50 (0–70)
	clinical subsets of PsA (n) oligoarticular (≤5 joints) polyarticular distal interphalangeal predominant spondylitis predominant mutilans	 13 (61.90%) 6 (28.57%) 2 (9.53%) 0 0

PASI – Psoriasis Area and Severity Index; PGA - Patient Global Assessment; BSA – Body Surface Area; DLQI – Dermatology Life Quality Index; NAPSI – Nail Psoriasis Severity Index; DAS 28 – Disease Activity Score; VAS – Patient Visual Analog Scale.

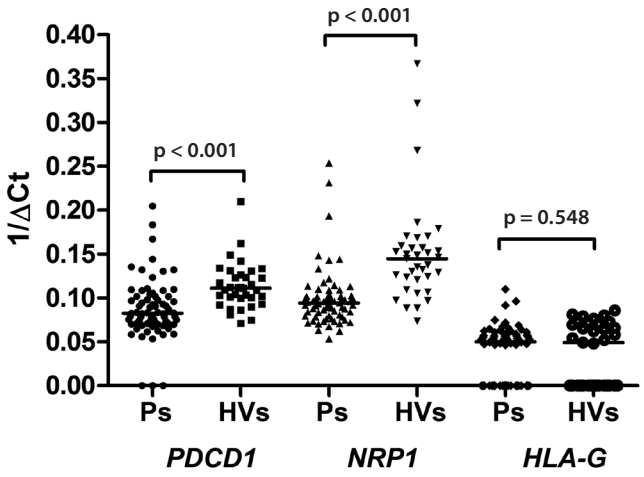

Fig. 1. Comparison of median *PDCD1*, *NRP1*, and *HLA-G* mRNA expression between psoriatic patients (Ps) and healthy volunteers (HVs)

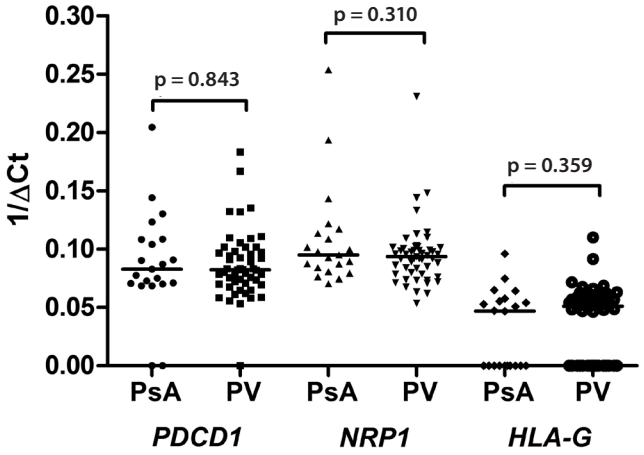

Fig. 2. Comparison of median *PDCD1*, *NRP1*, and *HLA-G* mRNA expression between psoriatic arthritis (PsA) and psoriasis vulgaris (PV) patients

Table 2. Correlation coefficients between the studied molecular markers and clinical data of psoriatic patients

Patients	Clinical data	*PDCD1*	*NRP1*	*HLA-G*
Psoriasis (n = 72)	age [years]	−0.08	−0.06	−0.36*
	duration of the disease [years]	−0.10	0.00	−0.19
	age at disease onset [years]	0.02	−0.08	−0.09
	PASI	−0.09	−0.10	0.10
	PGA	−0.04	−0.09	0.03
	BSA (%)	−0.07	−0.11	0.06
	DLQI	−0.08	−0.11	−0.04
	NAPSI	−0.13	−0.14	−0.07
Psoriatic arthritis (PsA) (n = 21)	duration of PsA [years]	−0.29	−0.18	−0.14
	age of PsA onset [years]	−0.05	−0.29	−0.40
	number of tender joints	−0.19	−0.18	−0.13
	number of swollen joints	−0.16	−0.14	0.01
	DAS28	−0.17	−0.09	0.16
	VAS	−0.05	−0.09	−0.09

* p < 0.05; PASI – Psoriasis Area and Severity Index; PGA – Patient Global Assessment; BSA – Body Surface Area; DLQI – Dermatology Life Quality Index; NAPSI – Nail Psoriasis Severity Index; DAS 28 – Disease Activity Score; VAS – Patient Visual Analog Scale.

Discussion

Any imbalance between the regulatory T cells (Tregs) and the effector T cells – including Th1, Th17, and Th22 – is pivotal in triggering psoriasis, while a subset of CD4+ T cells – Tregs with the CD25+Foxp-3+ (Forkhead box p3) phenotype – is known to prevent autoimmunity and to maintain immunological homeostasis and peripheral immune tolerance.[8] Nevertheless, under special circumstances, e.g., in inflammatory processes, the Tregs may undergo conversion into effector T cells (Th1 or Th17).[9] The number and function of Tregs are known to be downregulated in both the peripheral blood and skin lesions of psoriatic patients. The efficient inhibition of Th1 and Th17 activity requires the presence of interleukin 10 (IL-10) and transforming growth factor β (TGF-β), the major anti-inflammatory cytokines produced by various cells of the immune system, including Tregs.[10] Therefore, abnormally low levels of regulatory cytokines or their divergent action in inflammatory conditions – also observed in psoriasis – are not able to balance the enhanced Th1/Th17 response in this disease.[11]

Apart from the CD25+Foxp-3+ Tregs, HLA-G+ Tregs that emerge from the thymus also suppress T cell proliferation. Moreover, the HLA-G-negative APCs are able to induce the activation and proliferation of the T cells, while the HLA-G-positive APCs induce the differentiation of the Tregs.[12]

Interleukin 10 is the main upregulator of HLA-G expression, a molecule that may promote the development of the Tregs. However, not only anti-inflammatory cytokines, but also some growth factors and proinflammatory cytokines – such as IL-1β, IFN-α, IFN-β, IFN-γ, GM-CSF, and EGF – are capable of upregulating the *HLA-G* gene expression.[13]

In our study, no difference was found in the mRNA expression of *HLA-G* between the studied psoriatic patients and the healthy volunteers.

The research conducted so far has been focused on comparing the HLA-G protein levels in the psoriatic plaque and healthy skin.

In their immunohistochemical studies of psoriatic skin, Aractingi et al. found the presence of the HLA-G protein expression in all of the examined sections of the skin, which was not detected in the normal skin.[14] Since the HLA-G in Aractingi et al. study was mainly expressed by macrophages, the authors concluded that they could be representative of a control system which might be capable of counteracting the auto-reactive T cells.[14]

Similarly, Cardili et al. revealed an increased HLA-G expression in psoriatic skin in comparison with the skin of healthy individuals.[15] Sweeney C and Kirby B suggested that in psoriasis the HLA-G may promote the development of Tregs and prevent tissue destruction.[16]

Bearing in mind the results obtained by Aractingi and other researchers, as well as the results of our study, the presence of some inhibitory feedback mechanism powerful enough to downregulate the deleterious effect of the T cells and to prevent destruction in psoriatic skin is highly probable.

The analysis of NRP1 expression in psoriatic epidermis conducted by some authors has yielded contradictory results. Although some of them have reported an increased expression of NRP1 in psoriatic lesions, others have shown opposite results. Interestingly, in our study we observed a decreased mRNA expression of *NRP1* in the psoriatic patients in comparison to the healthy controls, which may confirm its role in disrupting immune tolerance in psoriatic patients.

Furthermore, Kou et al., in both immunostaining and mRNA expression studies, demonstrated lower *NRP1* and *Sema3A* in psoriatic skin samples compared with healthy skin samples.[17] Henno et al., however, showed an increased expression of not only NRP1 but also other pro-angiogenic factors, i.e., VEGF-A, VEGFR2, and PlGF, in psoriatic lesions compared to the uninvolved skin of the studied psoriatic patients.[18] The same authors also observed a significant overexpression of NRP1 in the nonlesional psoriatic skin in comparison to the skin of healthy volunteers.

The decreased NRP1 expression detected in our study may suggest the presence of some specific mechanisms of NRP1 regulation in peripheral blood, different from those in psoriatic plaques. The role of NRP1 as a co-receptor for VEGFR2 is important in the skin for blood vascular network expansion.

As in the case of PD-1, studies on its expression in psoriasis are scarce and performed on small series cases, they present contradictory results. Nevertheless, there are some reports pointing to the induction of psoriasis or a psoriasis-like disease during treatment with anti-PD-1 agents (i.e., nivolumab, pembrolizumab and pidilizumab).[19] This is not unusual since PD-1 is a molecule capable of suppressing T cell activity and favoring Treg proliferation. Therefore, its blockage will provoke a shift of cellular reactivity towards the pro-inflammatory Th1/Th17 lymphocytes.

Kim et al., in their quantitative real-time RT-PCR, western blotting, and immunohistochemistry studies have found a decreased expression of PD-1 ligands (PD-L1 and PD-L2) in the psoriatic epidermis in comparison to the healthy controls.[20] They suggested that it could result from an impairment of the Tregs' function in psoriasis and that it could allow continuous T cell activation.

Kim et al., in their animal study on imiquimod-treated mice, demonstrated overexpressed PD-1 on IL-17A-producing T cells.[21] The same authors observed similar results in the skin of psoriatic patients in whom immunofluorescent staining also revealed an overexpression of PD-1 on IL-17A-producing T cells.

Contrary to the studies conducted so far, which focused on the PD-1 expression in the skin, our present investigation provides some insight into the mRNA *PDCD1* expression. In our study, mRNA *PDCD1* expression has proven to be lower in the psoriatic patients, which is in agreement with its mechanisms of immune response. One possible limitation of our study may be the number of patients in the psoriatic arthritis group.

The study results for the molecular markers of immune tolerance, i.e., *HLA-G*, *NRP1*, and *PDCD1*, conducted so far give reasonable grounds for making further efforts to broaden scientific knowledge about the possible mechanisms involved in the induction and maintenance of the immune response in psoriatic patients.

References

1. Deng Y, Chang C, Lu Q. The inflammatory response in psoriasis: A comprehensive review. *Clin Rev Allergy Immunol*. 2016;50(3):377–389.
2. Bardhan K, Anagnostou T, Boussiotis VA. The PD1:PD-L1/2 pathway from discovery to clinical implementation. *Front Immunol*. 2016;12(7): 550. doi: 10.3389/fimmu.2016.00550
3. Oussa NA, Dahmani A, Gomis M, et al. VEGF requires the receptor NRP-1 to inhibit lipopolysaccharide-dependent dendritic cell maturation. *J Immunol*. 2016;197(10):3927–3935.
4. Sarris M, Andersen KG, Randow F, Mayr L, Betz AG. Neuropilin-1 expression on regulatory T cells enhances their interactions with dendritic cells during antigen recognition. *Immunity*. 2008;28(3):402–413.
5. Chen Z, Pang N, Du R, et al. Elevated expression of programmed death-1 and programmed death ligand-1 negatively regulates immune response against cervical cancer cells. *Mediators Inflamm*. 2016;2016:6891482.
6. Urosevic M. HLA-G in the skin – friend or foe? *Semin Cancer Biol*. 2007;17(6):480–484.
7. Amodio G, Sales de Albuquerque R, Gregori S. New insights into HLA-G mediated tolerance. *Tissue Antigens*. 2014;84(3):255–263.
8. Wang Y, Wang L, Yang H, Yuan W, Ren J, Bai Y. Activated circulating T follicular helper cells are associated with disease severity in patients with psoriasis. *J Immunol Res*. 2016;2016:7346030.
9. Smilek DE, Ehlers MR, Nepom GT. Restoring the balance: Immunotherapeutic combinations for autoimmune disease. *Dis Model Mech*. 2014;7(5):503–513.
10. Borghi A, Fogli E, Stignani M, et al. Soluble human leukocyte antigen-G and interleukin-10 levels in plasma of psoriatic patients: Preliminary study on a possible correlation between generalized immune status, treatments and disease. *Arch Dermatol Res*. 2008;300(10):551–559.
11. Han G, Li F, Singh TP, Wolf P, Wang X-J. The pro-inflammatory role of TGFβ1: A paradox? *Int J Biol Sci*. 2012;8(2):228–235.
12. Brenol CV, Veit TD, Chies JA, Xavier RM. The role of the HLA-G gene and molecule on the clinical expression of rheumatologic diseases. *Rev Bras Reumatol*. 2012;52(1):82–91.
13. Moreau P, Flajollet S, Carosella ED. Non-classical transcriptional regulation of HLA-G: An update. *J Cell Mol Med*. 2009;13(9B):2973–2989.
14. Aractingi S, Briand N, Le Danff C, et al. HLA-G and NK receptor are expressed in psoriatic skin: A possible pathway for regulating infiltrating T cells? *Am J Pathol*. 2001;159(1):71–77.
15. Cardili RN, Alves TG, Freitas JC, et al. Expression of human leucocyte antigen-G primarily targets affected skin of patients with psoriasis. *Br J Dermatol*. 2010;163(4):769–775.
16. Sweeney C, Kirby B. Does HLA-G prevent tissue destruction in psoriasis? *Br J Dermatol*. 2011;164(5):1118–1119.
17. Kou K, Nakamura F, Aihara M, et al. Decreased expression of semaphorin-3A, a neurite-collapsing factor, is associated with itch in psoriatic skin. *Acta Derm Venereol*. 2012;92(5):521–528.
18. Henno A, Blacher S, Lambert CA, et al. Histological and transcriptional study of angiogenesis and lymphangiogenesis in uninvolved skin, acute pinpoint lesions and established psoriasis plaques: An approach of vascular development chronology in psoriasis. *J Dermatol Sci*. 2010;57(3):162–169.
19. Ruiz-Bañobre J, García-González J. Anti-PD-1/PD-L1-induced psoriasis from an oncological perspective. *J Eur Acad Dermatol Venereol*. Epub 2017 Apr 3. doi: 10.1111/jdv.14217
20. Kim DS, Je JH, Kim SH, et al. Programmed death-ligand 1, 2 expressions are decreased in the psoriatic epidermis. *Arch Dermatol Res*. 2015;307(6):531–538.
21. Kim JH, Choi YJ, Lee BH, et al. Programmed cell death ligand 1 alleviates psoriatic inflammation by suppressing IL-17A production from programmed cell death 1-high T cells. *J Allergy Clin Immunol*. 2016; 137(5):1466–1476.

Design of a hybrid model for cardiac arrhythmia classification based on Daubechies wavelet transform

Rekha Rajagopal[B–F], Vidhyapriya Ranganathan[A]

Department of Information Technology, PSG College of Technology, Coimbatore, India

A – research concept and design; B – collection and/or assembly of data; C – data analysis and interpretation;
D – writing the article; E – critical revision of the article; F – final approval of the article

Advances in Clinical and Experimental Medicine, ISSN 1899–5276 (print), ISSN 2451–2680 (online) *Adv Clin Exp Med*. 2018;27(6):727–734

Address for correspondence
Rekha Rajagopal
E-mail: rekha.psgtech@gmail.com

Funding sources
None declared

Conflict of interest
None declared

Acknowledgements
The authors express their sincere and heartfelt thanks to the management and to the principal of PSG College of Technology, Coimbatore for extending the essential support and infrastructure to carry out this work.

Received on March 16, 2016
Reviewed on August 17, 2016
Accepted on February 14, 2017

Abstract

Background. Automation in cardiac arrhythmia classification helps medical professionals make accurate decisions about the patient's health.

Objectives. The aim of this work was to design a hybrid classification model to classify cardiac arrhythmias.

Material and methods. The design phase of the classification model comprises the following stages: preprocessing of the cardiac signal by eliminating detail coefficients that contain noise, feature extraction through Daubechies wavelet transform, and arrhythmia classification using a collaborative decision from the K nearest neighbor classifier (KNN) and a support vector machine (SVM). The proposed model is able to classify 5 arrhythmia classes as per the ANSI/AAMI EC57: 1998 classification standard. Level 1 of the proposed model involves classification using the KNN and the classifier is trained with examples from all classes. Level 2 involves classification using an SVM and is trained specifically to classify overlapped classes. The final classification of a test heartbeat pertaining to a particular class is done using the proposed KNN/SVM hybrid model.

Results. The experimental results demonstrated that the average sensitivity of the proposed model was 92.56%, the average specificity 99.35%, the average positive predictive value 98.13%, the average F-score 94.5%, and the average accuracy 99.78%.

Conclusions. The results obtained using the proposed model were compared with the results of discriminant, tree, and KNN classifiers. The proposed model is able to achieve a high classification accuracy.

Key words: support vector machine, biomedical data classification, decision support systems

DOI
10.17219/acem/68982

Introduction

Cardiovascular disease is a leading cause of global mortality. Hence, there is a need to develop automation strategies for the management of sudden cardiac death.[1] The objective of this work is to automate cardiac arrhythmia classification. An abnormality in the normal rhythm of a heartbeat causes arrhythmia. The ANSI/AAMI EC57: 1998 classification standard categorizes arrhythmias into 5 classes, namely: non-ectopic beat (N), supra-ventricular ectopic beat (S), ventricular ectopic beat (V), fusion beat (F), and unknown beat (Q). The diagnosis of a specific class of arrhythmia is done by careful monitoring of a long-term electrocardiograph (ECG) signal. Automation in ECG arrhythmia classification is very essential in order to make a fast and accurate decision about the arrhythmia class. The key requirements of an automated system are reduced complexity, fast decision making, and less memory. Several research projects have been carried out for automation in arrhythmia classification. In general, the algorithm used for automated classification includes (i) preprocessing, (ii) feature extraction, and (iii) feature classification. The preprocessing of recorded ECG signals is done in order to eliminate the important noises that degrade the classifier performance, such as baseline wandering, motion artifact, power line interference, and high frequency noise. Currently, researchers use many filtering techniques like morphological filtering, integral coefficient band stop filtering, finite impulse response filtering, 5–20 Hz band pass filtering, median filtering, and wavelet-based denoising for preprocessing.[2–7,9,25]

Commonly extracted ECG features include (i) temporal features of heartbeat, such as the P–Q interval, the QRS interval, the S–T interval, the Q–R interval, the R–S interval, and the R–R interval between adjacent heartbeats, (ii) amplitude-based features, such as P peak amplitude, Q peak amplitude, R peak amplitude, S peak amplitude, and T peak amplitude, (iii) wavelet transform-based features that include Haar wavelets, Daubechies wavelets, and discrete Meyer wavelets at various decomposition levels of 4, 6, and 8, and (iv) Stockwell transform-based features, including statistical features taken from a complex matrix of Stockwell transform, time-frequency contour and time-max amplitude contour.

A support vector machine (SVM),a probabilistic neural network (PNN), a multilayer perceptron neural network (MLPNN), a linear discriminant classifier, a mixture of experts, and unsupervised clustering are commonly used by researchers for the classification of ECG arrhythmia.[5,6,9–16,21,24–26] Parameters such as accuracy, sensitivity, and specificity are used in the literature for evaluating the performance of a classifier. Most of the research works reported more than 90% average accuracy, average sensitivity, and average specificity taken over all 5 classes. However, the classifier outputs very poor sensitivity when the sensitivity of individual classes is considered. The reason is that, in a medical scenario, the number of training examples for each class of ECG arrhythmia may not be uniform. Usually, the normal class of heart beats dominates the entire population, which leads to biased classification towards classes with larger examples.

Some of the common limitations in the literature are listed as follows:

1. Time interval features are used in many automated systems.[2,5,7,8] Hidden information in the ECG signal cannot be completely recovered from those time domain features.
2. Few researchers have used the entire data set of MIT_BIH arrhythmia database for experimentation. A random selection of only a few records from the entire database may not provide the actual result of their proposed system.[2,5,7–9,23,24,28]
3. A few research works did not follow a standard classification scheme, such as the ANSI/AAMI EC57: 1998 standard.[2,12,13,16,23,24]
4. Classes with major and minor training examples are treated equally in almost all projects, and this may lead to biased results towards major classes. The distinction between ventricular ectopic beats and supra-ventricular ectopic beats should be considered very important because some drugs for supra-ventricular ectopic beats can worsen the clinical state if the rhythm is a ventricular ectopic beat.
5. Class N and class S show a highly overlapped pattern. No special care is taken to overcome this issue.

This work eliminates the above limitations by extracting features from the time-frequency representation of an ECG signal through wavelet transform. The entire dataset of a benchmark database (i.e., the MIT_BIH arrhythmia database) is used and the proposed model adheres to the classification standard. The proposed model trains the classifier in such a way that the classifier better predicts the minority class using a hybrid approach.

Material and methods

The MIT_BIH arrhythmia database was used in this work. It contains 48 half-h excerpts of 2-channel ambulatory ECG recordings which were obtained from 47 subjects studied by the BIH arrhythmia laboratory. The recordings were digitized at 360 samples per second per channel with 11-bit resolution over a 10-mV range. The reference annotations for each beat were included in the database. Four records containing paced beats (102, 104, 107, and 217) were removed from the analysis as specified by the AAMI. The total number of heart beats in each class is given in Table 1. Figure 1 shows the architecture of the proposed work. The entire experiments were carried out using Matlab R2012a (MathWorks, Natick, USA). The details of the methodology followed are summarized below.

Table 1. Number of heartbeats in each class

Heartbeat type	N	S	V	F	Q
Full database	87643	2646	6792	794	15

N – non-ectopic beat; S – supra-ventricular ectopic beat; V – ventricular ectopic beat; F – fusion beat; Q – unknown beat.

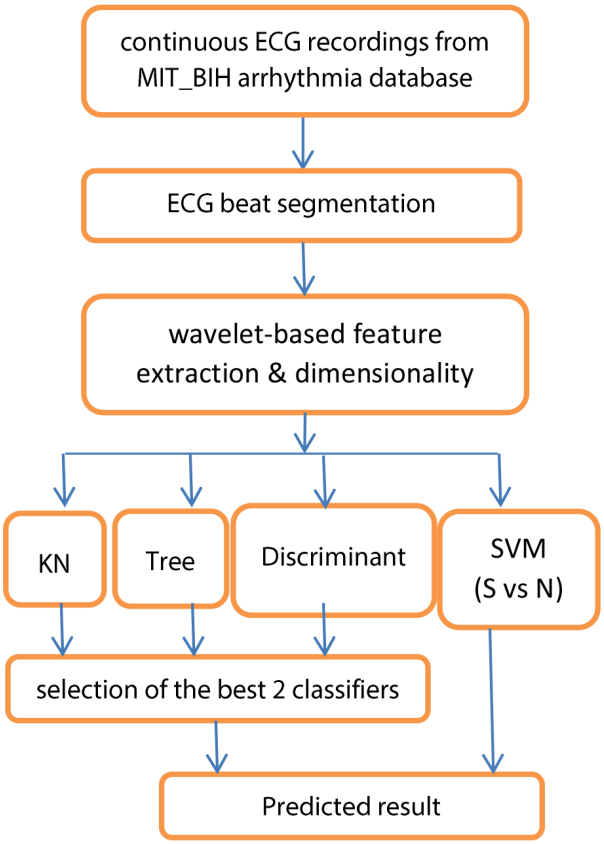

Fig. 1. Architecture of the proposed work

Data preprocessing

The records contain continuous ECG recordings of a duration of 30 min. The raw ECG signals include baseline wander, motion artifact, and power line interference noise. The discrete wavelet transform (DWT) is used for denoising the ECG signal and for extracting the important features from the original ECG signal.[22,27] The DWT captures both temporal and frequency information. The DWT of the original ECG signal is computed by successive high pass and low pass filtering of that signal. This can be mathematically represented as follows in equations (1) and (2),

$$(1)\ y_{high}[k] = \sum_{n}^{\infty} = {}_{-\infty} x[n]\ g[2k-n]$$

$$(2)\ y_{low}[k] = \sum_{n}^{\infty} = {}_{-\infty} x[n]\ h[2k-n]$$

where x[n] is the original ECG signal samples, g and h are the impulse responses of the high pass and low pass filters, respectively, and are the outputs of the high pass and low pass filters after sub-sampling by 2. This procedure is repeated until the required decomposition level is reached. The low frequency component is called approximation and the high frequency component is called detail.

In this work, the raw ECG signals sampled at 360 Hz were decomposed into approximation and detail sub bands up to level 9 using Daubechies ('db8') wavelet basis function.[18] The first and second level detail coefficients were made zero and were not used for reconstruction of the denoised signal, since most of the ECG information is contained within the 40-Hz frequency range and sub bands at the first and second levels contain the frequency ranges 90–180 Hz and 45–90 Hz, respectively. Moreover, power line interference noise occurs at 50 Hz or 60 Hz. Baseline wander noise occurs in the frequency range of <0.5 Hz, and therefore, the level 9 approximation sub band in the frequency range of 0–0.351 Hz was not used for reconstruction. The denoised signal was obtained by applying inverse DWT to the required detail coefficients of levels 3, 4, 5, 6, 7, 8, and 9. The coefficients of detail sub bands 1 and 2 and the approximation sub band 9 were made 0.

After denoising, the continuous ECG waveform was segmented into individual heartbeats. This segmentation is done by identifying the R peaks using the Pan-Tompkins algorithm and by considering the 99 samples before the R peak and the 100 samples after the R peak.[19] This choice of 200 samples, including the R peak for segmentation, was made because it constitutes one cardiac activity with P, QRS, and T waves. Figure 2 shows a segment of a recorded ECG waveform of patient No. 123 before and after preprocessing.

Feature extraction

The entire database (97,890 heartbeats) is divided into 10 sets, each containing 9,789 heartbeats. Nine sets are used for training (88,101 heartbeats) and 1 set for testing (9,789 heartbeats). From each heartbeat, wavelet-based features are extracted by using Daubechies wavelet ('db4'). A Daubechies wavelet with level 4 decomposition was selected in this project after making performance comparisons with a discrete Meyer wavelet and other levels of Daubechies wavelets, including 'db2' and 'db6'. A total of 107 features were produced by the 4^{th} level approximation sub-band and another 107 features by the 4^{th} level detail sub-band. Principal component analysis (PCA) was applied to reduce redundant information on the extracted features and to reduce the dimensionality. After dimensionality reduction was applied separately to the approximation and detail sub-bands, a total of 12 features were obtained. The choice of 6 features from each sub-band was made since there is no significant improvement in classification when more than 6 features are used.

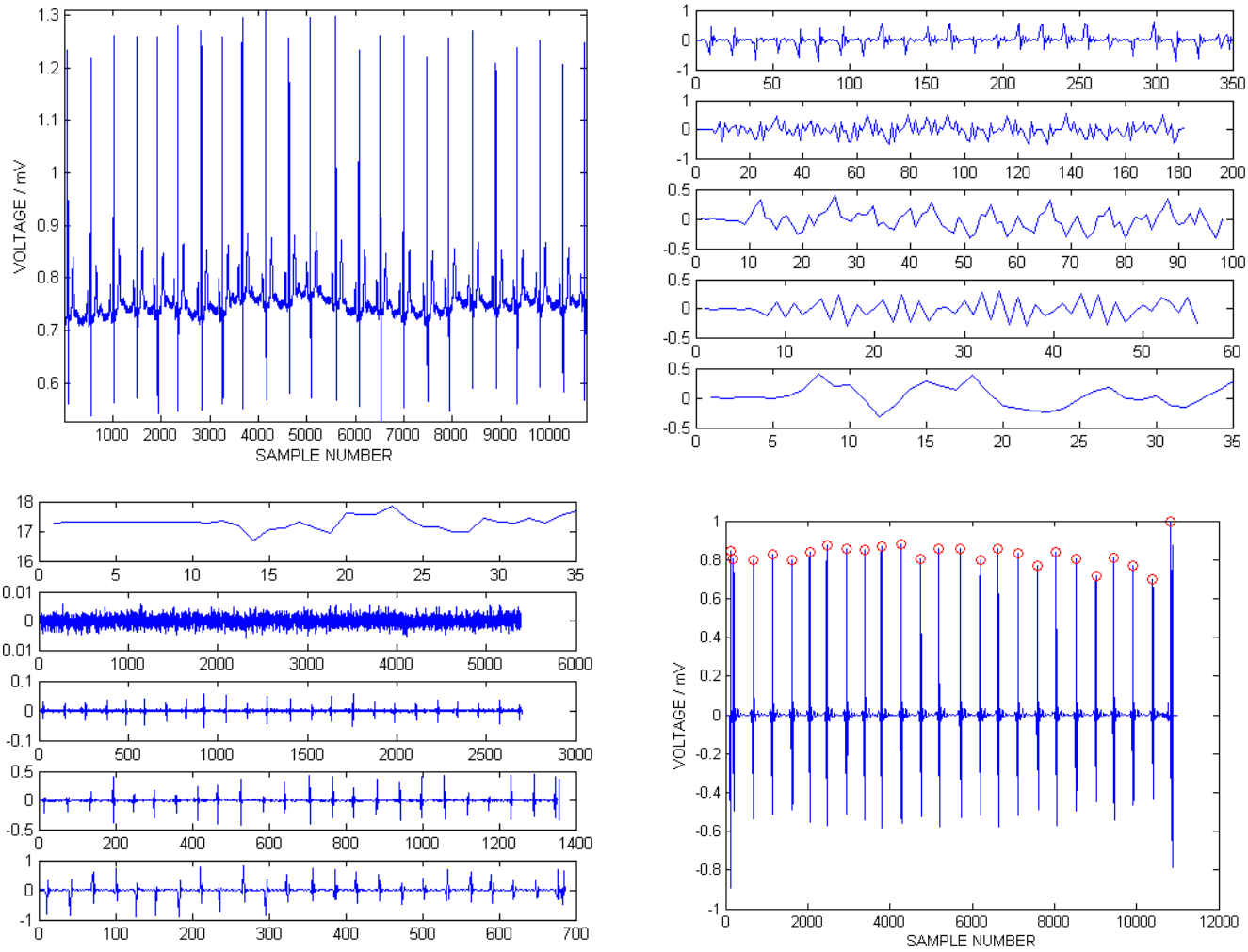

Fig. 2. A segment of an ECG waveform before and after preprocessing

A – raw ECG signal; B – approximation subband level 9 and detail subband levels 1–4 (bottom left corner); C – detail subband levels 5–9 (top right corner); D – preprocessed ECG waveforms with R peaks detected.

Training of classifiers

The training and testing matrix was computed, in which each row represents an ECG heartbeat and the features occupy the columns. The KNN (with distance metrics such as Euclidean, correlation, Mahalanobis, standardized Euclidean, and Spearman), tree, and discriminant (linear and quadratic) classifiers are trained with a training matrix 88,101 × 12 in size, which includes training examples from all 5 classes. The sensitivity, specificity, accuracy, positive predictivity, and F-score of those classifiers in classifying ECG arrhythmias were compared. The classifier that produced the best sensitivity and F-score was selected at level 1 of the proposed model. The radial basis function SVM was used at level 2 of the proposed model and was trained with examples from the entire class S and down-sampled examples from class N. Random down-sampling of class N is done in order to match the sample size of class S (2,646 × 12). The reason for this design is that samples from classes S and N are highly overlapped and many class S samples are wrongly predicted as class N at level 1 because of the large number of class N training examples (87,643 × 12). More weight is given to a decision from the SVM classifier while determining a test heartbeat to be other than class S. The advantage of the SVM classifier is that it performs well on datasets that have many attributes, even when there are few training examples available. But the drawback of SVM is its limitation in speed and size during both training and testing. Because of this limitation, SVM is not used for the training and classification of all classes. SVM is used only to make a final decision of a highly overlapped minority class. A description of the classifiers used is discussed in the following sections.

K nearest neighbor classifier

KNN is an instance-based simple classification algorithm. For a training data set of N points and its corresponding labels, given by $\{(x_1, y_1), (x_2, y_2) \ldots (x_N, y_N)\}$,

where (x_i, y_i) represents a data pair 'i' with 'x_i' as the input feature vector and 'y_i' as its corresponding target class label, the most likely class of test beat 'x' is determined by finding the K closest training points to it. The prediction of a class is determined by majority vote. The distance is taken as the weighting factor for voting. The main advantage in selecting the KNN classifier is that complex tasks can be learned using simple procedures by local approximation. The training process for KNN only consists of storing feature vectors and their corresponding labels. It also works well on classes with different characteristics for different subsets.[20]

Tree-based classifier

The decision tree algorithm works by selecting the best attribute to split the data and expand the leaf nodes of the tree until the stopping criterion is met. After building the tree, tree pruning is performed to reduce the size of the decision tree. This is done in order to avoid overfitting and to improve the generalization capability of decision trees. The class of a test heartbeat is determined by following the branches of the tree until a leaf node is reached. The class of that leaf node is then assigned to the test heartbeat. The advantage of this algorithm is its simplicity and good performance for larger data sets. Gini's diversity index is used as the split criterion in this work.

Discriminant classifier

The algorithm creates a new variable from one or more linear combinations of input variables. Linear discriminant analysis is done by calculating the sample mean of each class. Sample covariance is calculated by subtracting the sample mean of each class from the observations of that class, and taking the empirical covariance matrix of the result. In the linear discriminant model, only the means vary for each class, but the covariance matrix remains the same. For quadratic discriminant analysis, both the mean and covariance of each class varies.

Support vector machine

The support vector machine (SVM) constructs a hyper plane in such a way that the margin of separation between positive examples (minority class S) and negative examples (majority class N) is maximized. Since classes S and N overlap very much, the hyper plane cannot be linearly separable and cannot be constructed without a classification error. For such overlapped patterns, SVM performs nonlinear mapping of the input vector into a high dimensional feature space. An optimal hyper plane is constructed for separation of these newly mapped features. The hyper plane is constructed in such a way that it minimizes the probability of a classification error. For a training set X with N number of training examples, if {(x_i, d_i)} is the i^{th} training example, where x_i is the input vector for the i^{th} example and d_i is its corresponding target output, α_i is the i^{th} Lagrange multiplier, K(x, x_i) is the inner product kernel, and b is the bias, then the optimal separating hyper plane is defined as in Equation (3):

$$(3)\quad f(x) = \sum_{i=1}^{N} a_1\, d_1\, K(x, x_i) + b$$

A radial basis function SVM was used in this work instead of polynomial and two-layer perceptron because of its higher discrimination ability. The inner product kernel K(x, x_i) of a radial basis function with width σ is given by equation (4):

$$(4)\quad K(x, x_i) = \exp\left(\frac{-1}{2^{\wedge 2}} \| x - x_i \|^2\right)$$

The performance of the proposed model was evaluated using performance metrics such as sensitivity, specificity, positive predictivity, F-score, and accuracy. These metrics are computed by calculating true positive (TP), true negative (TN), false positive (FP), and false negative (FN) counts and are defined as follows: sensitivity = TP / (TP + FN), specificity = TN / (TN + FP), positive predictivity = TP / (TP + FP), F-score = 2TP / (2TP + FP +FN), and accuracy = (TP + TN) / (TP + FP + FN +TN). The process is repeated 10 times so that each set is used once for testing. The overall performance of the classifier is computed by taking the average of all 10 folds.

Results and discussion

The reliability of a classifier in accurately predicting the test heartbeat's class is measured mainly by the sensitivity and F-score. The reason for not considering accuracy is that even a poor classifier can show good accuracy in favoring a class with more training examples. It can be observed from Fig. 3 that a discriminant classifier with linear and quadratic function produces consistently less sensitivity than KNN and tree classifiers. The KNN with Euclidean distance metric produces the highest sensitivity.

Figure 4 shows the specificity of all classifiers in each of the 10 folds. The discriminant classifier produces the least specificity. The KNN classifier produces the highest specificity. Figure 5 shows the F-score of all classifiers in all 10 folds. The discriminant classifier with a linear function produces the lowest F-score. The tree classifier and the quadratic discriminant classifier produce a nearly uniform F-score, while the KNN classifier achieves the highest F-score.

The KNN with Euclidean distance metric achieves the highest accuracy compared to other classifiers and is shown in Fig. 6.

Table 2 shows the average classification results of all classifiers at level 1. One can see from Table 2 that the KNN with Euclidean distance metric and 4 neighbors produces

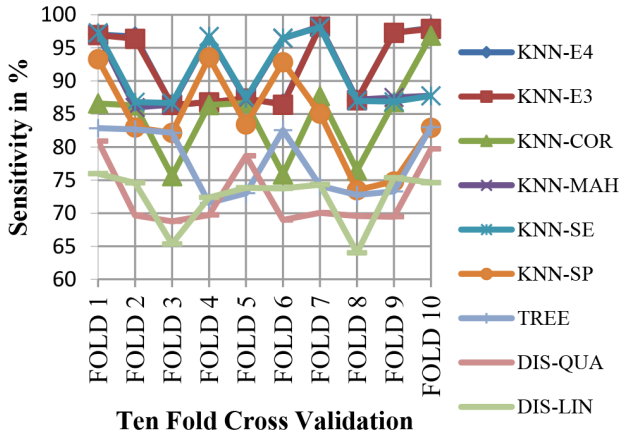

Fig. 3. Results of sensitivity for 10 different folds of KNN, tree, and discriminant classifiers

KNN-E4 – K-nearest neighbour classifier with Euclidean distance 4; KNN-E3 – K-nearest neighbour classifier with Euclidean distance 3; KNN-COR – K-nearest neighbour classifier with correlation distance metric; KNN-MAH – K-nearest neighbour classifier with Mahalanobis distance metric; KNN-SE – K-nearest neighbour classifier with standardized Euclidean distance metric; KNN-SP – K-nearest neighbour classifier with Spearman distance metric; TREE – tree classifier; DIS-QUA – discriminant classifier with quadratic function; DIS-LIN – discriminant classifier with linear function.

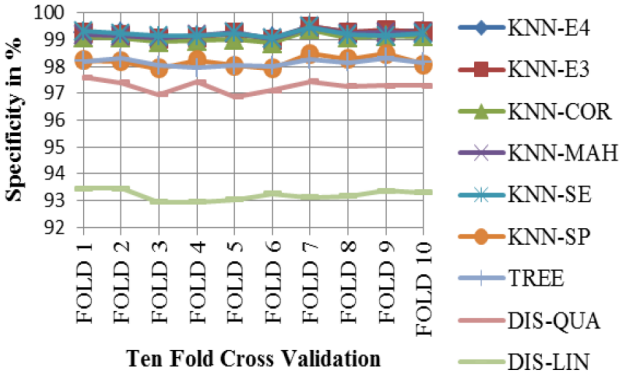

Fig. 4. Results of specificity for 10 different folds of KNN, tree, and discriminant classifiers

KNN-E4 – K-nearest neighbour classifier with Euclidean distance 4; KNN-E3 – K-nearest neighbour classifier with Euclidean distance 3; KNN-COR – K-nearest neighbour classifier with correlation distance metric; KNN-MAH – K-nearest neighbour classifier with Mahalanobis distance metric; KNN-SE – K-nearest neighbour classifier with standardized Euclidean distance metric; KNN-SP – K-nearest neighbour classifier with Spearman distance metric; TREE – tree classifier; DIS-QUA – discriminant classifier with quadratic function; DIS-LIN – discriminant classifier with linear function.

a better sensitivity, specificity, positive predictivity, F-score, and accuracy than the other 2 classifiers which were considered. Hence, KNN is used at level 1 of the proposed model. KNN with 3 neighbors also produces comparable results to KNN with 4 neighbors. Compared to KNN with 4 neighbors, the KNN classifier with 3 neighbors has a greater discrimination capability for class S.

From the confusion matrix obtained from tenfold cross validation using different classifiers, it was found that a high number of class S heartbeats are misclassified

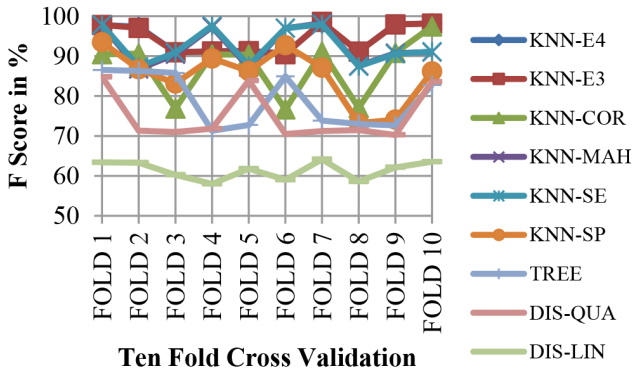

Fig. 5. Results of F-score for 10 different folds of KNN, tree, and discriminant classifiers

KNN-E4 – K-nearest neighbour classifier with Euclidean distance 4; KNN-E3 – K-nearest neighbour classifier with Euclidean distance 3; KNN-COR – K-nearest neighbour classifier with correlation distance metric; KNN-MAH – K-nearest neighbour classifier with Mahalanobis distance metric; KNN-SE – K-nearest neighbour classifier with standardized Euclidean distance metric; KNN-SP – K-nearest neighbour classifier with Spearman distance metric; TREE – tree classifier; DIS-QUA – discriminant classifier with quadratic function; DIS-LIN – discriminant classifier with linear function.

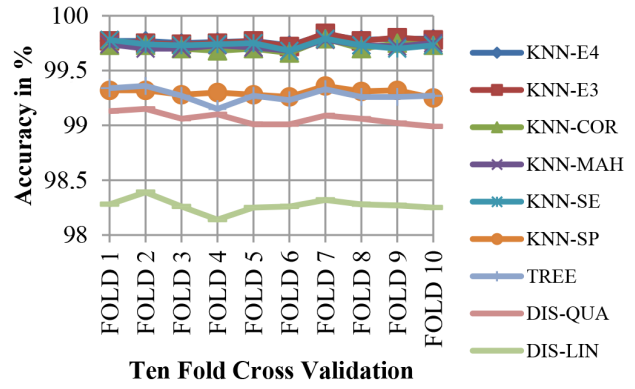

Fig. 6. Results of accuracy for 10 different folds of KNN, tree, and discriminant classifiers

KNN-E4 – K-nearest neighbour classifier with Euclidean distance 4; KNN-E3 – K-nearest neighbour classifier with Euclidean distance 3; KNN-COR – K-nearest neighbour classifier with correlation distance metric; KNN-MAH – K-nearest neighbour classifier with Mahalanobis distance metric; KNN-SE – K-nearest neighbour classifier with standardized Euclidean distance metric; KNN-SP – K-nearest neighbour classifier with Spearman distance metric; TREE – tree classifier; DIS-QUA – discriminant classifier with quadratic function; DIS-LIN – discriminant classifier with linear function.

as normal class N. This is because of the close resemblance of class S to the normal class and because the number of training examples for class N is higher than class S. A sample confusion matrix of the KNN classifier with 4 neighbors at level 1 is shown in Table 3.

Moreover, the number of training examples for class N (78,879 heartbeats) is much greater than class S (2,381 heartbeats) training examples. This may be the reason why the KNN with 3 neighbors can classify class S better than the KNN with 4 neighbors. For other classes, KNN with 4 neighbors performed well. To achieve better results, the SVM classifier is used along with KNN. SVM is trained

Table 2. Average classification results of tenfold cross validation for classifiers at level 1

Classifier	Average sensitivity	Average specificity	Average positive predictivity	Average F-score	Average accuracy
KNN-Euclidean 4	92.14	99.24	98.56	94.48	99.77
KNN-Euclidean 3	92.07	99.23	98.53	94.43	99.76
KNN-correlation	84.53	99.07	97.92	87.16	99.71
KNN-Mahalanobis	91.05	99.21	94.74	92.39	99.72
KNN-standardized Euclidean	91.11	99.22	94.97	92.53	99.73
KNN-Spearman	84.45	98.19	89.09	85.23	99.30
Tree classifier	77.80	98.15	83.72	78.98	99.28
Discriminant-linear	72.42	93.20	60.87	61.41	98.28
Discriminant-quadratic	72.56	97.27	92.68	74.97	99.06

Table 3. Confusion matrix (KNN 4 fold 2)

n = 9789 (where 'n' is the total number of test samples in fold 2)	Predicted					
Actual	arrhythmia class	S	V	F	N	Q
	S	234	1	0	30	0
	V	0	674	2	3	0
	F	0	0	76	3	0
	N	13	2	1	8748	0
	Q	0	0	0	0	2

N – non-ectopic beat; S – supra-ventricular ectopic beat; V – ventricular ectopic beat; F – fusion beat; Q – unknown beat.

Table 4. Confusion matrix (proposed model fold 2)

n = 9789 (where 'n' is the total number of test samples in fold 2)	Predicted					
Actual	arrhythmia class	S	V	F	N	Q
	S	242	1	0	22	0
	V	0	674	2	3	0
	F	0	0	76	3	0
	N	13	2	1	8748	0
	Q	0	0	0	0	2

N – non-ectopic beat; S – supra-ventricular ectopic beat; V – ventricular ectopic beat; F – fusion beat; Q – unknown beat.

to classify class S from class N. The classification result of KNN with Euclidean distance metric (4 and 3 neighbors) was compared with the predicted result of Support vector machine (SVM). A test heartbeat is concluded to be class S if at least 2 classifiers predict it as class S. A sample confusion matrix of the proposed hybrid model is shown in Table 4.

Table 5. Sensitivity and F-score of class S before and after using the proposed model

Fold number	Sensitivity of class S		F-Score of class S	
	KNN – EUC 4	Proposed	KNN – EUC 4	Proposed
Fold 1	88.68	90.56	92.16	92.30
Fold 2	88.30	91.32	91.40	93.07
Fold 3	85.28	87.54	90.58	90.62
Fold 4	88.67	91.69	92.33	92.74
Fold 5	88.67	90.56	91.79	92.13
Fold 6	85.66	88.30	89.90	90.00
Fold 7	92.07	93.58	94.02	93.23
Fold 8	89.43	90.56	92.75	92.13
Fold 9	90.18	91.69	93.35	92.57
Fold 10	92.07	94.33	93.84	93.80

KNN-EUC 4 – K-nearest neighbour classifier with Euclidean distance 4.

Sensitivity and F-score results before and after the usage of the proposed model are shown in Table 5. It is clear that the sensitivity of class S improves considerably through this hybrid model. The performance of other classes remains unaltered and the classification performance of class N gets slightly reduced by an average sensitivity percentage of 0.09 and an average F-score percentage of 0.01. Class N is the normal class and the problem of normal class misclassified as class S is less compared to a class S beat misclassified as normal class N. Hence, the proposed model improves sensitivity in the prediction of all heartbeat classes.

Conclusions

In this paper, a hybrid classification model is proposed which inherits the abilities of both SVM and KNN. Instead of using a simple classifier as KNN for predicting highly overlapped classes, this mixed model improves the sensitivity of minority classes, which is dominated by the majority class. SVM is specifically trained to classify overlapped classes. At the same time, the low complex KNN classifier is trained to classify all 5 classes. Hence, the final decision of a test heartbeat is done using classifiers at both levels of the hierarchy. The performance of this model is supported by experimental results on the entire MIT/BIH arrhythmia database. Future work will experiment with other combinations of classifiers.

References

1. Mehra R. Global public health problem of sudden cardiac death. *J Electrocardiol*. 2007; 40(6 Suppl):118–122.
2. Kim J, Shin HS, K, Shin, Lee M. Robust algorithm for arrhythmia classification in ECG using extreme learning machine. *Bio Medical Engineering Online*. 2009. https://doi.org/10.1186/1475-925X-8-31
3. Liang W, Zhang Y, Tan J, Li Y. A novel approach to ECG classification based upon two-layered HMMs in body sensor networks. *Sensors*. 2014;14(4):5994–6011.
4. Kim H, Yazicioglu RF, Merken P, Van Hoof C, Yoo HJ. ECG signal compression and classification algorithm with quad level vector for ECG holter system. *IEEE Trans Inf Technol Biomed*. 2010;14(1):93–100.
5. Asl BM, Setarehdan SK, Mohebbi M. Support vector machine – based arrhythmia classification using reduced features of heart rate variability signal. *Artif Intell Med*. 2008;1(44):51–64.
6. Huang K, Zhang L. Cardiology knowledge free ECG feature extraction using generalized tensor rank one discriminant analysis. *EURASIP J Appl Signal Processing*. 2014. https://doi.org/10.1186/1687-6180-2014-2
7. Zhu B, Ding Y, Hao K. A novel automatic detection for ECG arrhythmias using maximum margin clustering with immune evolutionary algorithm. *Comput Math Methods Med*. 2013. http://dx.doi.org/10.1155/2013/453402
8. Chazal P, Dwyer MO, Reilly RB. Automatic classification of heartbeats using ECG morphology and heartbeat interval features. *IEEE Trans Biomed Eng*. 2004;7(51):1196-1206.
9. Roshan Joy Martis, Rajendra Acharya U, Lim Choo Min. ECG beat classification using PCA, LDA, ICA and discrete wavelet transform. *Biomed Signal Process Control*. 2013;5(8):437–448.
10. Manab Kumar Das, Samit Ari. ECG beats classification using mixture of features. *Int Sch Res Notices*. 2014;2014:178436. doi: 10.1155/2014/178436
11. Das MK, Ari S. Electrocardiogram beat classification using S-Transform based feature set. *J Mech Med Biol*. 2014;5(14):1450066.
12. Rai HM, Trivedi A, Shukla S. ECG signal processing for abnormalities detection using multi-resolution wavelet transform and artificial neural network classifier. *Measurement*. 2013;9(46):3238–3246.
13. Song MH, Lee J, Lee KJ, Yoo SK. Support vector machine based arrhythmia classification using reduced features. *Int J Control Autom*. 2005;4(3):571–579.
14. Zidelmal Z, Amirou A, Ould Abdeslam D, Merckle J. ECG beat classification using a cost sensitive classifier. *Comput Meth Prog Bio*. 2013;3(111):570–577.
15. Daamouche A, Hamami L, Alajlan N, Melgani F. A wavelet optimization approach for ECG signal classification. *Biomed Signal Process Control*. 2012;(7):342 –349.
16. Ubeyli ED. Usage of Eigen vector methods in implementation of automated diagnostic systems for ECG beats. *Digit Signal Process*. 2008;33(18):33–48.
17. Moody GB, Mark RG. The impact of the MIT_BIH arrhythmia database. *IEEE Eng Med Biol*. 2001;3(20):45–50.
18. Singh BN, Tiwari AK. Optimal selection of wavelet basis function applied to ECG signal denoising. *Digit Signal Process*. 2006;3(16): 275–287.
19. Pan J, Tompkins JW. A real time QRS detection algorithm. *IEEE Trans Biomed Eng*. 1985;3(32). https://doi.org/10.1109/TBME.1985.325532
20. Kim J, Kim BS, Savarese S. Comparing image classification methods: K Nearest Neighbor and Support Vector Machines. *Applied Mathematics in Electrical and Computer Engineering*. 2012; 133–138.
21. Ghoraani B, Krishnan S. Discriminant non-stationary signal features clustering using hard and fuzzy cluster labeling. *EURASIP J Adv Signal Process*. 2012. https://doi.org/10.1186/1687-6180-2012-250
22. Mazomenos EB, Biswas D, Acharyya A, et al. A low-complexity ECG feature extraction algorithm for mobile healthcare applications. *IEEE J Biomed Health Inform*. 2013;2(17):459–569.
23. Sufi F, Khalil I,Mahmood AN. A clustering based system for instant detection of cardiac abnormalities from compressed ECG. *Expert Syst Appl*. 2011;5(38):4705–4713.
24. Melgani F, Bazi Y. Classification of electrocardiogram signals with support vector machines and particle swarm optimization. *IEEE Trans Inf Technol Biomed*. 2008;5(12):667–677.
25. Oresko JJ, Jin Z, Huang S, Sun Y, Duschl, Cheng AC . A wearable smart phone based platform for real time cardiovascular disease detection via electrocardiogram processing. *IEEE Trans Inf Technol Biomed*. 2010;3(14):734–740.
26. Wiens J, Guttag JV. Patient adaptive ectopic beat classification using active learning. *Comput Cardiol*. 2010;37:109–112.
27. Li D, Pedrycz W, Pizzi JN. Fuzzy wavelet packet based feature extraction method and its application to biomedical signal classification. *IEEE Trans Biomed Eng*. 2005;6(52):1132–1139.
28. Luz E, Menotti D. How the choice of samples for building arrhythmia classifiers impact their performances. *Proc Conf IEEE Eng Med Biol Soc*. 2011;4988–4991.

The inhibition of c-MYC transcription factor modulates the expression of glycolytic and glutaminolytic enzymes in FaDu hypopharyngeal carcinoma cells

Robert Kleszcz[A–D], Jarosław Paluszczak[A–C,E,F], Violetta Krajka-Kuźniak[B], Wanda Baer-Dubowska[C,E,F]

Department of Pharmaceutical Biochemistry, Poznan University of Medical Sciences, Poland

A – research concept and design; B – collection and/or assembly of data; C – data analysis and interpretation;
D – writing the article; E – critical revision of the article; F – final approval of the article

Advances in Clinical and Experimental Medicine, ISSN 1899-5276 (print), ISSN 2451-2680 (online) *Adv Clin Exp Med*. 2018;27(6):735–742

Address for correspondence
Wanda Baer-Dubowska
E-mail: baerw@ump.edu.pl

Funding sources
This study was supported by a grant from Poznan University of Medical Sciences, No. 502-14-03302403-41154.

Conflict of interest
None declared

Acknowledgements
The authors would like to thank prof. dr hab. Marek Murias for obtaining the DMU-212 compound used in this research.

Received on July 6, 2016
Reviewed on October 23, 2016
Accepted on February 14, 2017

Abstract

Background. Cancer cells are dependent on aerobic glycolysis for energy production and increased glutamine consumption. HIF-1α and c-MYC transcription factors regulate the expression of glycolytic and glutaminolytic genes. Their activity may be repressed by SIRT6. Head and neck carcinomas show frequent activation of c-MYC function and SIRT6 down-regulation, which contributes to a strong dependence on glucose and glutamine availability.

Objectives. The aim of this study was to compare the influence of HIF-1α and c-MYC inhibitors (KG-548 and 10058-F4, respectively) and potential SIRT6 inducers – resveratrol and its synthetic derivative DMU-212 with the effect of glycolysis and glutaminolysis inhibitors (2-deoxyglucose and aminooxyacetic acid, respectively) on the metabolism and expression of metabolic enzymes in FaDu hypopharyngeal carcinoma cells.

Material and methods. Cell viability was assessed by means of an MTT assay. Quantitative PCR was performed to evaluate the expression of *SIRT6*, *HIF-1a*, *c-MYC*, *GLUT1*, *SLC1A5*, *HK2*, *PFKM*, *PKM2*, *LDHA*, *GLS*, and *GDH*. The release of glycolysis and glutaminolysis end-products into the culture medium – lactate and ammonia, respectively – was assessed using standard colorimetric assays.

Results. Lactate production was significantly inhibited by 10058-F4, KG-548, and 2-deoxyglucose. Moreover, 10058-F4 strongly reduced the amount of ammonia release. The effects of 10058-F4 activity can be attributed to a reduction in the expression of *PKM2* and *LDHA*. On the other hand, the induction of *SIRT6* expression by resveratrol and DMU-212 was not associated with significant modulation of the expression of metabolic enzymes.

Conclusions. Overall, the results of this study indicate that the inhibition of c-MYC may be considered to be a promising strategy of the modulation of cancer-related metabolic changes in head and neck carcinomas.

Key words: c-MYC, energy metabolism, the Warburg effect, 10058-F4, FaDu cells

DOI
10.17219/acem/68979

Introduction

Cancer cells, in contrast to normal cells, generate energy by increasing aerobic glycolysis, a phenomenon termed "the Warburg effect".[1] Altered energy metabolism supporting continuous cell growth and proliferation was pointed out as a new hallmark of cancer cells.[2] Several hypotheses have been proposed to explain the maintenance of this seemingly wasteful catabolic state. Recent investigations into the mechanisms that underlie the Warburg effect indicate that beside the direct involvement of overexpressed uncoupling proteins (UCP) in the Warburg effect, the alterations in the glycolytic pathway itself may be equally or even more important. In this regard, it has been suggested that pyruvate kinase M2 (PKM2) or hexokinase 2 (HK2) might be the key mediators of aerobic glycolysis and promote tumor growth, at least in certain types of tumors.[3–5] Moreover, PKM2 was shown to function as a co-activator of hypoxia inducible factor 1 (HIF-1).[6]

The HIF-1 factor may be considered a driver molecule of glycolytic control. It is composed of an HIF-1α subunit, which is susceptible to changes in oxygen concentration (stabilized in hypoxic conditions), and HIF-1β being constitutively expressed.[7] Typically, HIF-1α is expressed in hypoxia, whereas under oxygen stimuli, prolyl hydroxylase 2 (PHD2) promotes HIF-1α association with von Hippel-Lindau tumor suppressor (VHL), which finally leads to the ubiquitination and proteasomal degradation of HIF-1α.[8,9] However, oncogenic H-Ras and phosphatidylinositol 3-kinase signaling can maintain an elevated HIF-1α level even in aerobic conditions.[9] Moreover, inactivating mutations of genes encoding succinate dehydrogenase and fumarase lead to an accumulation of succinate and fumarate, which results in the stabilization of HIF-1α in normoxia via the inhibition of prolyl hydroxylase.[7,9]

There are also suggestions that aerobic glycolysis may represent a shift to the oxidative metabolism of non-glucose carbon sources, particularly glutamine – an amino acid that is ultimately converted to α-ketoglutarate in the mitochondria to enter the citric acid cycle (CAC).[4] Indeed, glutamine seems to be a nutrient as important as glucose for some types of malignant cells. For instance, the proliferation and survival of head and neck squamous cell carcinoma cells (HNSCC) strongly depend on both glucose and glutamine availability, where cell proliferation can be maximized only in the presence of glutamine.[10] The c-MYC transcription factor is suggested to be important in the regulation of both glutamine and glucose metabolism.[11] Cells overexpressing *c-MYC* are glutamine-addicted, which is related to an increased glutaminase 1 (GLS1) level.[12] c-MYC is responsible for the direct promotion of the expression of glutamine transporters enhancing glutamine's cellular entry[11,12] and is capable of supporting HIF-1α functions by up-regulating, e.g., *HK2*, phosphofructokinase (*PFK1*), *PKM2*, and lactate dehydrogenase (*LDH*), contributing to the enhancement of glycolysis intensity as well.[8]

The transcriptional activity of HIF-1α and c-MYC may be regulated by an interaction with other proteins including epigenetic modulatory proteins. Sirtuins have recently emerged as important regulators of energy metabolism in mammalian cells.[13] Sirtuins (SIRTs) belong to Class III of the histone deacetylase (HDACs) family and are the only HDACs that require NAD^+ for their proper enzymatic activity.[14] Histone acetylation is known to promote the local transcriptional activity of chromatin, whereas histone deacetylases, by removing acetyl groups, lead to the formation of tightly packed and transcriptionally inactive heterochromatin. SIRT6 is thought to be especially important in metabolic orchestration, and its depletion may be connected with the development of a metabolic environment conducive to cancer. Both HIF-1α and SIRT6 influence the expression of several crucial glycolytic genes, e.g., *PFK1*, aldolase (*ALD*), pyruvate dehydrogenase kinase 1 (*PDK1*), *LDH* and, additionally, glucose transporter *GLUT-1*.[15] Lack of SIRT6 leads to the up-regulation of glycolytic genes via HIF-1α derepression. Similarly, a decreased expression of SIRT6 relieves the repression of c-MYC transcriptional activity. Altogether, SIRT6 depletion may result in the enhancement of HIF-1α and c-MYC target gene expression, which contributes to a characteristic glucose (HIF-1α and c-MYC)[16] and glutamine (c-MYC) addiction.[17] Importantly, the level of the expression of SIRT6 is decreased in head and neck squamous cell carcinomas.[18] The activity of SIRT1 may be induced by resveratrol and possibly other stilbene derivatives, and SIRT1 may indirectly induce the expression of SIRT6.[19]

Head and neck squamous cell carcinomas (HNSCCs) are the fifth most common type of cancer[20] characterized by a poor survival rate, particularly for patients with aggressive tumors, and regional and distant metastases.[21] A better understanding of tumor metabolism in HNSCCs may provide new therapeutic strategies for the treatment of this type of cancer. The data on the regulation of energetic metabolism in HNSCCs, although limited,[22] suggests that head and neck cancer cell proliferation depends on glucose and glutamine metabolism. The aim of this study was to evaluate the influence of small molecules – inhibitors of specific regulators of both c-MYC inhibitor (10058-F4) and HIF-1 inhibitor (KG-548) pathways – on the proliferation and metabolism of the hypopharyngeal carcinoma FaDu cells. Direct inhibitors of glycolysis (2-deoxyglucose) and transamination (aminooxyacetic acid) were used for comparison. Additionally, we tested whether resveratrol and its synthetic derivative DMU-212 are capable of inducing *SIRT6* and, therefore, affecting energy metabolism in FaDu cells.

Material and methods

Cell culture and viability assay

The hypopharyngeal carcinoma FaDu cell line was purchased from ATCC (Manassas, Virginia, USA). The cells were grown in Dulbecco's Modified Eagle's Medium

(DMEM), containing 10% fetal bovine serum (FBS) (Biowest SAS, Nuaillé, France) and antibiotics – penicillin and streptomycin 1% (Sigma-Aldrich, St. Louis, USA) – at 37°C in a 95% humidified and 5% CO_2 atmosphere.

The effects of KG-548, 10058-F4, 2-deoxyglucose, resveratrol (Sigma-Aldrich, St. Louis, USA), and DMU-212 (obtained from the Department of Toxicology, Poznań University of Medical Sciences) and aminooxyacetic acid (MP Biomedicals, Illkirch, France) on FaDu cell viability were assessed by the MTT assay according to standard protocols. Briefly, 10^4 cells were seeded per well in a 96-well plate. After 24 h of pre-incubation in DMEM supplemented with 5% FBS and antibiotics, the tested compounds were added to the culture medium in various concentrations and the cells were incubated for 24 h. Afterwards, the cells were washed twice with PBS buffer, and a fresh medium containing MTT salt (0.5 mg/mL) was added. After 4 h of incubation, formazan crystals were dissolved in acidic isopropanol and absorbance was measured at 570 and 690 nm. All the experiments were repeated 3 times with 3 measurements per assay. In all the subsequent experiments, non-toxic concentrations (viability level >70%) of the compounds were used. The chemical structure of the studied compounds is presented in Fig. 1.

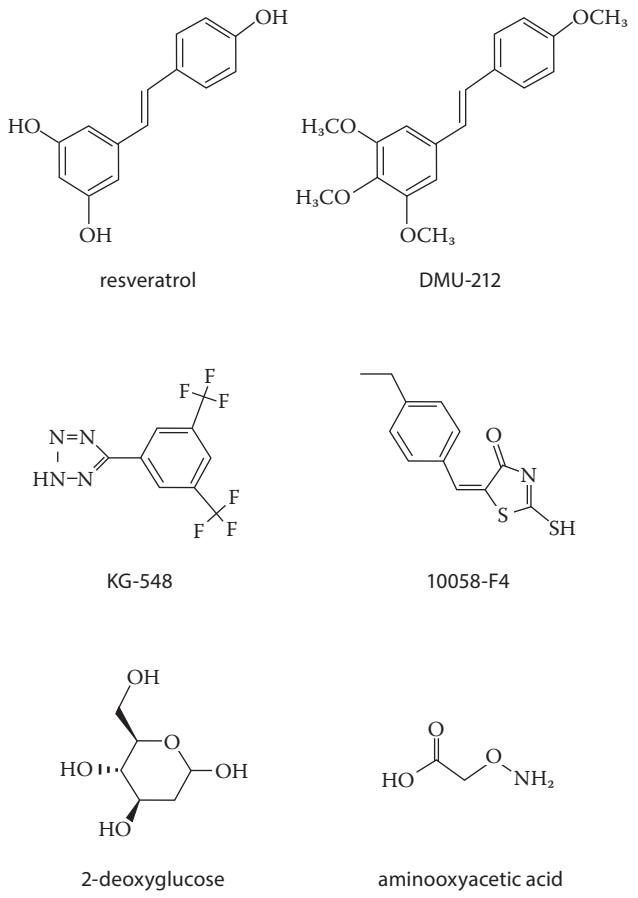

Fig. 1. The chemical structure of the tested compounds

Isolation of total RNA and cDNA synthesis

1 × 10^6 cells were seeded in 100-mm culture dishes, and after 24 h of pre-incubation in DMEM containing 5% FBS, the cells were treated with 10 μM of resveratrol, 2 μM of DMU-212, 50 μM of KG-548 and 10058-F4, 1 or 2 mM of 2-deoxyglucose (2-DG), and 0.1 or 0.2 mM of aminooxyacetic acid (AOAA) or vehicle control. After a 24-h incubation, total RNA was isolated using a Universal RNA Purification Kit (EURx, Gdańsk, Poland) and subsequently subjected to reverse transcription using a RevertAid First Strand cDNA Synthesis Kit (Thermo Fisher Scientific Inc., Waltham, USA), according to the manufacturer's recommendations.

Quantitative real-time polymerase chain reaction

Quantitative real-time polymerase chain reaction (PCR) was performed using the Maxima SYBR Green qPCR Master Mix (2X) (Thermo Fisher Scientific, Waltham, USA)

Table 1. The sequence of starters used in real-time PCR reactions

Primer		Sequence	Product size
PBGD	*forward*	5'CCGCATCTGGAGTTCAGGAGTATTC	101 bp
	reverse	5'CCAGCTGTTGCCAGGATGATG	
TBP	*forward*	5'GGCACCACTCCACTGTATC	183 bp
	reverse	5'GGGATTATATTCGGCGTTTCG	
SIRT6	*forward*	5'ACTGGCGAGGCTGGTCTG	157 bp
	reverse	5'GCTCTCAAAGGTGGTGTCG	
HIF-1a	*forward*	5'CAGTAACCAACCTCAGTGTG	199 bp
	reverse	5'AAGTTCTTCTGGCTCATATCC	
c-MYC	*forward*	5'TTACAACACCCGAGCAAG	133 bp
	reverse	5'AATCCAGCGTCTAAGCAG	
GLUT1	*forward*	5'GCCAAGAGTGTGCTAAAG	107 bp
	reverse	5'ATGGTGACCTTCTTCTCC	
SLC1A5	*forward*	5'CTGCCTTTGGGACCTCTTC	93 bp
	reverse	5'AACGGCTGATGTGCTTGG	
HK2	*forward*	5'GTCCGTAACATTCTCATCG	125 bp
	reverse	5'AGGCAGTCACTCTCAATC	
PFKM	*forward*	5'GCCCGTGTCTTCTTTGTC	161 bp
	reverse	5'AGTCGTCCTTCTCGTTCC	
PKM2	*forward*	5'AGAGAAGGGAAAGAACATCAAG	175 bp
	reverse	5'GCACCGTCCAATCATCATC	
LDHA	*forward*	5'TCAGCCCGATTCCGTTACC	119 bp
	reverse	5'ACATTCATTCCACTCCATACAGG	
GLS	*forward*	5'ATGATGTGCTGGTCTCCTC	177 bp
	reverse	5'ATTTATCACTGACTTTACCCTTTG	
GDH	*forward*	5'GGATTCTAACTACCACTTGCTC	171 bp
	reverse	5'GAACGCTCCATTGTGTATGC	

on a Chromo4 thermal cycler (BioRad Laboratories, Hercules, USA). The primer sequences which are listed in Table 1 were generated using Beacon Designer software and synthesized at the Institute of Biochemistry and Biophysics, Warszawa, Poland. All the reactions were run in triplicate. The protocol started with a 10 min enzyme activation at 95°C, followed by 40 cycles of 95°C for 15 s, 56°C for 20 s, 72°C for 40 s, and the final elongation at 72°C for 5 min. The melting curve analysis was used to confirm the generation of a single amplification product. Experiments were normalized for the mean expression of the TATA-box binding protein (*TBP*) and porphobilinogen deaminase (*PBGD*). The Pfaffl relative method was used for fold-change quantification.

Lactate and ammonia concentration analysis

Lactate concentration in the culture medium was measured using an L-Lactate Assay Kit, and the ammonia concentration was tested using an Ammonia Assay Kit (ScienCell Research Laboratories, Carlsbad, USA) according to the manufacturer's instructions. Immediately after acquisition, the media samples were divided into 2 portions and 1 was passed through Amicon Ultra 10K filters (Millipore, Cork, Ireland) in order to remove any LDH activity which could interfere with lactate assessment.

Statistical analysis

Statistical analysis was performed by one-way ANOVA using STATISTICA software (v. 10). The statistical significance between the experimental groups and their respective controls was assessed by Tukey's post hoc test, with $p < 0.05$ considered significant.

Results

Cell viability analysis

Cell viability was assessed by the MTT assay (Fig. 2). 2-deoxyglucose reduced cell viability in a dose-dependent manner (Fig. 2C), in contrast to AOAA, which exerted weaker effects (Fig. 2D). KG-548 did not significantly affect

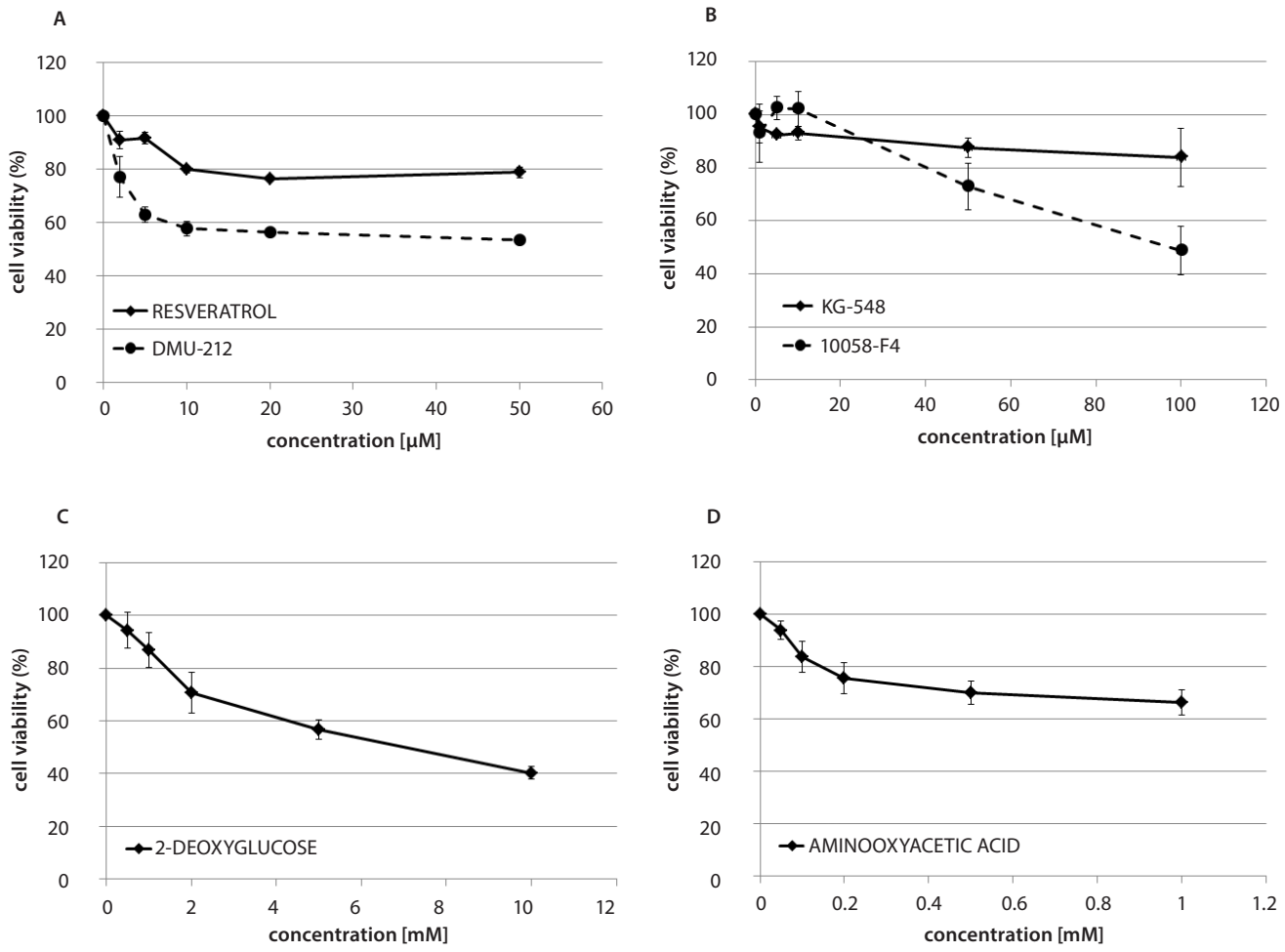

Fig. 2. The effect of the tested compounds on the viability of FaDu cells

Mean values +/- SEM from 3 independent experiments are shown. The viability of vehicle-treated cells was considered to be 100%.

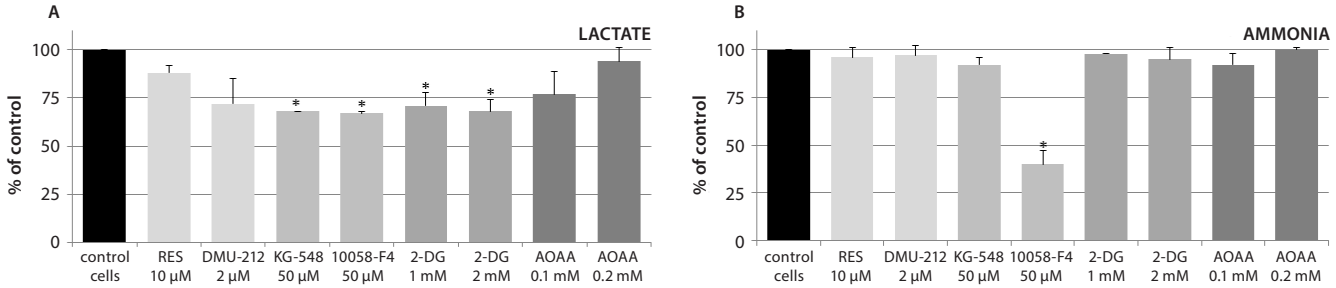

Fig. 3. The effect of resveratrol, DMU-212, and small molecule inhibitors KG-548, 10058-F4, 2-deoxyglucose (2-DG), and aminooxyacetic acid (AOAA) on lactate (A) and ammonia (B) release into the culture medium

Mean values +/- SEM from 2 independent experiments are shown. The level of vehicle-treated cells was considered to be 100%. An asterisk above a bar denotes statistically significant differences from the control group, $p < 0.05$.

cell viability up to 100 µM, while 10058-F4 decreased cell viability only at high concentrations (Fig. 2B). DMU-212 showed stronger anti-proliferative effects than its parent compound, resveratrol (Fig. 2A). In all the subsequent experiments, non-toxic concentrations of the tested compounds (viability above 70%) were used.

Lactate and ammonia concentration analysis

The release of glycolysis and glutaminolysis end-products – lactate and ammonia, respectively – into the culture medium was assessed in order to evaluate the effect of the tested modulators on these pathways. Lactate concentration was significantly reduced after treatment with KG-548 (HIF-1 inhibitor), 10058-F4 (c-MYC inhibitor), and 2-deoxyglucose (glycolysis inhibitor). Resveratrol, DMU-212, and AOAA showed a tendency to reduce lactate production; however, the changes were not statistically significant (Fig. 3A). Ammonia production remained unaltered after the FaDu cells were treated with the compounds, with the exception of 10058-F4, which diminished the ammonia level in media samples by almost 60% (Fig. 3B).

Gene expression analysis

Figure 4 presents the results of the quantitative PCR which was performed to evaluate the expression of genes associated with the metabolism of glucose (glucose transporter [*GLUT1*], hexokinase 2 [*HK2*], phosphofructokinase M [*PFKM*], pyruvate kinase M2 [*PKM2*], and lactate dehydrogenase A [*LDHA*]) and glutamine (glutamine transporter [*SLC1A5*], glutaminase [*GLS*], and glutamate dehydrogenase [*GDH*]) and genes which encode regulatory proteins: sirtuin 6 (*SIRT6*), hypoxia inducible factor 1α (*HIF-1α*), and transcription factor *c-MYC*. Although resveratrol and DMU-212 induced the expression of *SIRT6* (Fig. 4A), they did not significantly change the expression of genes related to the metabolism of glucose and glutamine, with the exception of *HK2* up-regulation after exposure to DMU-212 (Fig. 4F). KG-548 also did not affect the expression of glucose and glutamine metabolism genes except for *GLUT1* (Fig. 4D); however, it did lead to a significant induction of *c-MYC* expression (Fig. 4C). The strongest modulation of the expression of the studied genes was exerted by the MYC inhibitor, 10058-F4. This compound decreased the expression of genes engaged in the last stage of glycolysis – *PKM2* (Fig. 4H) and *LDHA* (Fig. 4I) – by approx. 60%. Interestingly, this compound induced the expression of glutamine transporter (Fig. 4E), but had a slight inhibitory effect on the expression of glutaminase (Fig. 4J). Although 2-deoxyglucose reduces lactate generation mainly through the direct inhibition of glycolysis, the treatment of FaDu cells with this compound also led to a decrease in the expression of *GLUT1* (Fig. 4D) and *HK2* (Fig. 4F).

Discussion

Head and neck squamous cell carcinomas (HNSCCs) are characterized in most cases by unfavorable outcome rates. Thus, a better understanding of the molecular pathways involved in the malignant transformation of HNSCCs is essential for the development of novel therapies. A shift in glucose degradation from glucose oxidation to aerobic glycolysis and the induction of glutaminolysis are considered to be hallmarks of cancer cell metabolism. However, the data on the regulation of these pathways in HNSCCs are limited and somehow controversial. The aim of this study was to attempt to assess the role of these processes along with SIRT6 activation in FaDu cells derived from hypopharyngeal SCC using small molecule inhibitors of specific target elements of these pathways.

The results pointed to the c-MYC inhibitor, 10058-F4, as the most effective modulator of both pathways. This was the only compound among the tested modulators which decreased both lactate and ammonia production, the end-products of glycolysis and glutaminolysis, respectively. Moreover, the c-MYC inhibitor decreased the expression of the *LDHA* gene encoding a major molecular mediator of the Warburg effect as well as the *PKM2* gene and slightly decreased glutaminase expression. Interestingly,

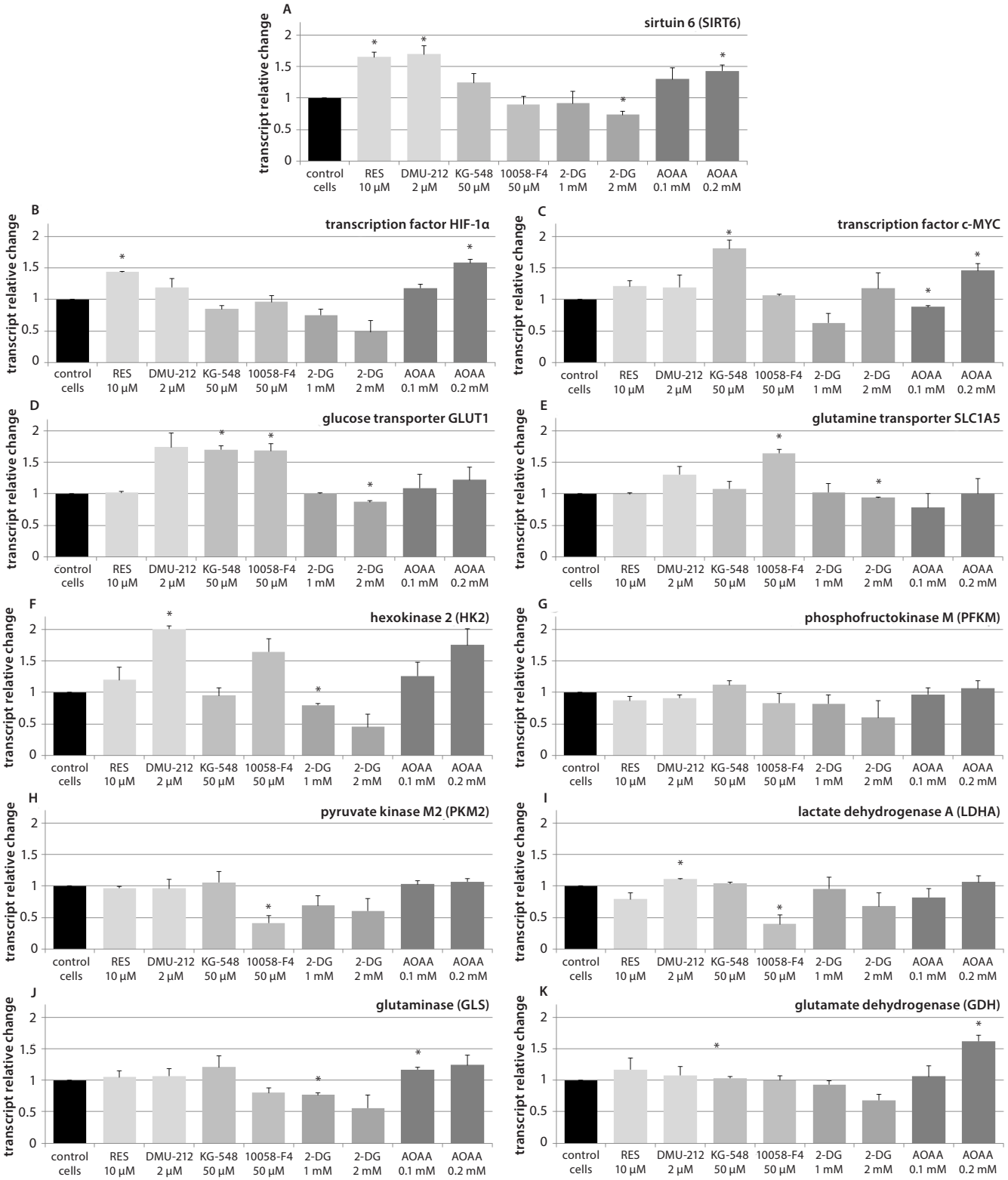

Fig. 4. The effect of resveratrol (RES), DMU-212, and small molecule inhibitors KG-548, 10058-F4, 2-deoxyglucose (2-DG), and aminooxyacetic acid (AOAA) on the expression of *SIRT6* (A), *HIF-1α* (B), *c-MYC* (C), glucose (D), and glutamine (E) transporters, on key glycolysis enzymes *HK2* (F), *PFKM* (G), *PKM2* (H), and *LDHA* (I), as well as on key glutaminolysis enzymes *GLS* (J) and *GDH* (K) in FaDu cells

Mean values +/- SEM from 2 independent experiments are shown. The level of vehicle-treated cells was considered to be 1. An asterisk above a bar denotes statistically significant differences from the control group, $p < 0.05$.

the inhibition of HIF-1 by KG-548, although resulting in a reduced production of lactate, did not affect the expression of glycolytic enzymes. Thus, these results suggest that the upregulation of proto-oncogene c-MYC plays a major role in the regulation of glycolysis in FaDu cells. To a certain extent, our results also confirm the observation that glucose, not glutamine, is the dominant energy source required for the proliferation and survival of HNSCC cells.[22] On the other hand, the induction of *SLC1A5* by 10058-F4 is consistent with the results of other authors who showed an elevated expression of this transporter as a response to c-MYC inhibition in human P-493 B lymphoma and PC3 prostate cancer cells.[12,23] However, the mechanism which leads to the decrease in ammonia production is elusive since it cannot be explained by changes in the gene expression level alone. It may be hypothesized that ammonia secretion is reduced passively through the blocking of lactate production, which may favor mitochondrial consumption of pyruvate and thus reduce the use of glutamine for anaplerosis.

SIRT6 has recently emerged as a novel tumor suppressor which regulates aerobic glycolysis in cancer cells. Moreover, it has been proposed that SIRT6 functions as a co-repressor of HIF-1a and c-MYC by deacetylating H3K9 and H3K56 at HIF-1a and c-MYC target gene promoters, respectively.[13,24]

Since SIRT6 is downregulated in many tumors, including HNSCCs, SIRT6 upregulation may be expected to reverse the tumorigenic metabolic profile. To test this hypothesis, we used 2 stilbene derivatives, resveratrol and its methoxy-analogue, DMU-212, as possible activators since resveratrol was previously described as an activator of SIRT1.[25]

Both resveratrol and DMU-212 induced the expression of *SIRT6*, but only slightly affected the expression of genes whose products are involved in glucose and glutamine metabolism. These results suggest that SIRT6 does not play a critical role in the regulation of the transcriptional activity of HIF-1 and c-MYC in FaDu cells. However, more detailed studies are required to confirm this observation.

Among the other modulators used in this study, 2-deoxyglucose effectively inhibited glycolysis as expected, leading to a decreased viability of FaDu cells. This observation indicates that targeting glycolysis may be a valid anti-proliferative strategy in HNSCCs, as has been recently suggested.[26] The anti-proliferative effects of 2-deoxyglucose are related to blocking the consumption of glucose in glycolysis and the depletion of the cellular ATP level due to the accumulation of 2-deoxyglucose-6-phosphate (2-DG-6-P), which can neither be transformed into fructose derivative nor utilized in the pentose phosphate pathway.[27,28] Accumulated 2-DG-6-P may reach levels 20-fold higher than G-6-P concentrations. 2-deoxyglucose also affects the protein N-glycosylation, induces the accumulation of misfolded proteins, and disrupts proper protein translocation to the cell membrane.[29,30]

AOAA, a glutaminolysis inhibitor, also reduced FaDu cell viability; however, this effect cannot be attributed to the modulation of either glutaminolysis or glycolysis. AOAA's lack of effect on ammonia production may be related to the induction of glutamate metabolism by glutamate dehydrogenase, which may be associated with the induction of c-MYC expression.[31] Thus, our results support the hypothesis that AOAA mediates cytotoxic effects through a stress response pathway.[32]

Overall, the results of the study indicate that the c-MYC transcription factor, rather than HIF-1α, plays a major role in the regulation of glycolytic and glutaminolytic enzyme expression in head and neck carcinoma cells. This suggests that c-MYC inhibitors, as with 2-deoxyglucose, may show anti-proliferative activity in HNSCCs by modulating dysregulated metabolic pathways.

References

1. Warburg O. On the origin of cancer cells. *Science*. 1956;123:309–314.
2. Hanahan D, Weinberg RA. Hallmarks of cancer: The next generation. *Cell*. 2011;144:646–674.
3. Samudio I, Fiegl M, Andreeff M. Mitochondrial uncoupling and the Warburg effect: Molecular basis for the reprogramming of cancer cell metabolism. *Cancer Res*. 2009;69:2163–2166.
4. Ward PS, Thompson CB. Signaling in control of cell growth and metabolism. *Cold Spring Harb Perspect Biol*. 2012;4(7):a006783. doi: 10.1101/cshperspect.a006783
5. Dando I, Fiorini C, Pozza ED, et al. UCP2 inhibition triggers ROS-dependent nuclear translocation of GAPDH and autophagic cell death in pancreatic adenocarcinoma cells. *Biochim Biophys Acta*. 2013;1833:672–679.
6. Wang HJ, Hsieh YJ, Cheng WC, et al. MJD5 regulates PKM2 nuclear translocation and reprograms HIF-1α-mediated glucose metabolism. *Proc Natl Acad Sci USA*. 2014;111:279–284.
7. Bell EL, Emerling BM, Ricoult SJ, Guarente L. SirT3 suppresses hypoxia inducible factor 1α and tumor growth by inhibiting mitochondrial ROS production. *Oncogene*. 2011;30:2986–2996.
8. Hammoudi N, Ahmed KB, Garcia-Prieto C, Huang P. Metabolic alterations in cancer cells and therapeutic implications. *Chin J Cancer*. 2011;30:508–525.
9. Kim JW, Dang CV. Cancer's molecular sweet tooth and the Warburg effect. *Cancer Res*. 2006;66:8927–8930.
10. Sandulache VC, Myers JN. Altered metabolism in head and neck squamous cell carcinoma: An opportunity for identification of novel biomarkers and drug targets. *Head Neck*. 2012;34:282–290.
11. Wise DR, DeBerardinis RJ, Mancuso A, et al. Myc regulates a transcriptional program that stimulates mitochondrial glutaminolysis and leads to glutamine addiction. *Proc Natl Acad Sci USA*. 2008;105:18782–18787.
12. Gao P, Tchernyshyov I, Chang TC, et al. c-Myc suppression of miR-23a/b enhances mitochondrial glutaminase expression and glutamine metabolism. *Nature*. 2009;458:762–765.
13. Kleszcz R, Paluszczak J, Baer-Dubowska W. Targeting aberrant cancer metabolism – The role of sirtuins. *Pharmacol Rep*. 2015;67:1068–1080.
14. Nakagawa T, Guarente L. Sirtuins at a glance. *J Cell Sci*. 2011;124:833–838.
15. Zhong L, Mostoslavsky R. SIRT6: A master epigenetic gatekeeper of glucose metabolism. *Transcription*. 2010;1:17–21.
16. Sebastián C, Zwaans BM, Silberman DM, et al. The histone deacetylase SIRT6 is a tumor suppressor that controls cancer metabolism. *Cell*. 2012;151:1185–1199.
17. Lyssiotis CA, Cantley LC. SIRT6 puts cancer metabolism in the driver's seat. *Cell*. 2012;151:1155–1156.
18. Lai CC, Lin PM, Lin SF, et al. Altered expression of SIRT gene family in head and neck squamous cell carcinoma. *Tumor Biol*. 2013;34:1847–1854.
19. Kim HS, Xiao C, Wang RH, et al. Hepatic-specific disruption of SIRT6 in mice results in fatty liver formation due to enhanced glycolysis and triglyceride synthesis. *Cell Metab*. 2010;12:224–236.

20. Rezende TM, de Souza Freire M, Franco OL. Head and neck cancer: Proteomic advances and biomarker achievements. *Cancer*. 2010;116:4914–4925.
21. Pignon JP, le Maître A, Maillard E, Bourhis J. MACH-NC Collaborative Group: Meta-analysis of chemotherapy in head and neck cancer (MACH-NC): An update on 93 randomised trials and 17,346 patients. *Radiother Oncol*. 2009;92:4–14.
22. Sandulache VC, Ow TJ, Pickering CR, et al. Glucose, not glutamine, is the dominant energy source required for proliferation and survival of head and neck squamous carcinoma cells. *Cancer*. 2011;117:2926–2938.
23. Dang CV. Rethinking the Warburg effect with Myc micromanaging glutamine metabolism. *Cancer Res*. 2010;70:859–862.
24. Cai J, Zuo Y, Wang T, Cao Y, Cai R, Chen FL. A crucial role of SUMOylation in modulating Sirt6 deacetylation of H3 at lysine 56 and its tumor suppressive activity. *Oncogene*. 2016;35:4949-4956.
25. Price NL, Gomes AP, Ling AJ, et al. SIRT1 is required for AMPK activation and the beneficial effects of resveratrol on mitochondrial function. *Cell Metab*. 2012;15:675–690.
26. Sobhakumari A, Orcutt KP, Love-Homan L, et al. 2-Deoxy-d-glucose suppresses the in vivo antitumor efficacy of erlotinib in head and neck squamous cell carcinoma cells. *Oncol Res*. 2016;24:55–64.
27. Pietzke M, Zasada C, Mudrich S, Kempa S. Decoding the dynamics of cellular metabolism and the action of 3-bromopyruvate and 2-deoxyglucose using pulsed stable isotope-resolved metabolomics. *Cancer Metab*. 2014;2:9.
28. Warmoes MO, Locasale JW. Heterogeneity of glycolysis in cancers and therapeutic opportunities. *Biochem Pharmacol*. 2014;92:12–21.
29. Pelicano H, Martin DS, Xu RH, Huang P. Glycolysis inhibition for anticancer treatment. *Oncogene*. 2006;25:4633–4646.
30. Kurtoglu M, Gao N, Shang J, et al. Under normoxia, 2-deoxy-D-glucose elicits cell death in select tumor types not by inhibition of glycolysis but by interfering with N-linked glycosylation. *Mol Cancer Ther*. 2007;6:3049–3058.
31. Coller HA. Is cancer a metabolic disease? *Am J Pathol*. 2014;184:4–17.
32. Korangath P, Teo WW, Sadik H, et al. Targeting glutamine metabolism in breast cancer with aminooxyacetate. *Clin Cancer Res*. 2015;21:3263–3273.

Lost life years due to premature mortality caused by diseases of the respiratory system

Irena Maniecka-Bryła[1,A,F], Paulina Paciej-Gołębiowska[1,C,D], Elżbieta Dziankowska-Zaborszczyk[1,B], Marek Bryła[2,E]

[1] Department of Epidemiology and Biostatistics, Medical University of Lodz, Poland
[2] Department of Social Medicine, Medical University of Lodz, Poland

A – research concept and design; B – collection and/or assembly of data; C – data analysis and interpretation;
D – writing the article; E – critical revision of the article; F – final approval of the article

Advances in Clinical and Experimental Medicine, ISSN 1899-5276 (print), ISSN 2451-2680 (online) *Adv Clin Exp Med*. 2018;27(6):743–748

Address for correspondence
Paulina Paciej-Gołębiowska
E-mail: paulina.paciej@stud.umed.lodz.pl

Funding sources
The study was financed by the National Science Center based on decision No. DEC-2013/11/B/HS4/00465.

Conflict of interest
None declared

Received on December 1, 2016
Reviewed on February 1, 2017
Accepted on February 28, 2017

Abstract

Background. In Poland, as in most other European countries, diseases of the respiratory system are the 4th leading cause of mortality; they are responsible for about 8% of all deaths in the European Union (EU) annually. To assess the socio-economic aspects of mortality, it has become increasingly common to apply potential measures rather than conventionally used ratios.

Objectives. The aim of this study was to analyze years of life lost due to premature deaths caused by diseases of the respiratory system in Poland from 1999 to 2013.

Material and methods. The study was based on a dataset of 5,606,516 records, obtained from the death certificates of Polish residents who died between 1999 and 2013. The information on deaths caused by diseases of the respiratory system, i.e., coded as J00–J99 according to the International Statistical Classification of Diseases and Related Health Problems, 10th revision (ICD-10), was analyzed. The Standard Expected Years of Life Lost (SEYLL) indicator was used in the study.

Results. In the years 1999–2013, the Polish population suffered 280,519 deaths caused by diseases of the respiratory system (4.69% of all deaths). In the period analyzed, a gradual decrease in the standardized death rate was observed – from 46.31 per 100,000 inhabitants in 1999 to 41.02 in 2013. The dominant causes of death were influenza and pneumonia (J09–J18) and chronic lower respiratory diseases (J40–J47). Diseases of the respiratory system were the cause of 4,474,548.92 lost life years. The Standard Expected Years of Life Lost per person ($SEYLL_p$) was 104.72 per 10,000 males and 52.85 per 10,000 females. The Standard Expected Years of Life Lost per death ($SEYLL_d$) for people who died due to diseases of the respiratory system was 17.54 years of life on average for men and 13.65 years on average for women.

Conclusions. The use of the SEYLL indicator provided significant information on premature mortality due to diseases of the respiratory system, indicating the fact that they play a large role in the health status of the Polish population.

Key words: years of life lost, premature mortality, respiratory system, Poland

DOI
10.17219/acem/69227

Introduction

Diseases of the respiratory system are an important health problem faced by the population of Europe. It is estimated that they cause about 8% of all deaths in the European Union (EU) each year. Additionally, in many highly-developed member nations, this percentage is often higher than the EU average, accounting for more than 10% of deaths (e.g., in 2012: Great Britain – 14.1%; Denmark – 11.2%; Belgium – 10.5%; and the Netherlands – 10.4%).[1]

In Poland, as in most other European countries, diseases of the respiratory system are the 4th leading cause of mortality, after diseases of the circulatory system, malignant neoplasms, and external causes.[2,3] However, the proportional mortality rate due to these diseases is lower than the EU average (5.2% in 2012). On the other hand, the increasing number of deaths caused by diseases of the respiratory system is alarming.[1,4]

To assess the socioeconomic aspects of deaths, it has become increasingly common to apply potential measures which take into account the lifetime potential of the individuals in the population, rather than the conventionally used ratios.[5,6] These measures consider not only the number of deaths, but also the age of the individuals at the moment of death, so they can be used to analyze the problem of premature mortality. Knowledge about the scope of the problem and its changes over time plays a pivotal role in planning the public health policy in every population.[7,8]

The aim of this study was to assess the years of life lost due to premature deaths caused by diseases of the respiratory system in Poland between 1999 and 2013, using the Standard Expected Years of Life Lost (SEYLL), Standard Expected Years of Life Lost per person ($SEYLL_p$), and Standard Expected Years of Life Lost per death ($SEYLL_d$).

Material and methods

This study was based on a dataset of 5,606,516 records provided by the Statistical Office in Poland, which contained information from the death certificates of Poles who died between 1999 and 2013. The analysis was performed on the records reporting deaths caused by diseases of the respiratory system, i.e., coded as J00–J99 according to the International Statistical Classification of Diseases and Related Health Problems, 10th revision (ICD-10).

In the study, proportional and specific death ratios were used. The measures were standardized using the direct method for age, with the use of the European population as a reference.

The SEYLL indicator was used as a potential measure. It was calculated according to the method developed by Murray and Lopez:[5]

$$SEYLL = \sum_{\chi=0}^{I} d_\chi e^*_\chi$$

where:

e^*_χ – the average life expectancy for a particular age based on a standard population;

d_χ – the number of deaths at age χ;

χ – the age of death;

I – the oldest age in the population.

The life expectancies for particular ages were determined from the life tables published by the World Health Organization (WHO) in 2012.[9] According to this source, the expected lifespan for both genders is 86.02 years. The values given in the table were not adjusted for age or discounted.

In this study, 2 additional calculations were performed: $SEYLL_p$, the ratio of the SEYLL to the number of inhabitants of a country in the year analyzed (calculated per 10,000 inhabitants in this study); and $SEYLL_d$, the quotient of the SEYLL and the number of deaths caused by a particular disease, i.e., calculated per 1 death.

Results

From 1999 to 2013, the Polish population suffered 280,519 deaths caused by diseases of the respiratory system, which accounted for 4.69% of all deaths. The ratio between men and women was 1.45 (Table 1).

In the period studied, the values of the standardized death rate due to diseases of the respiratory system gradually decreased for both men and women. In 2013, compared to 1999, the value of this rate had decreased by 8.21 for men (per 100,000 males) and by 3.52 for women (per 100,000 females) (Fig. 1).

The majority of deaths attributed to diseases of the respiratory system occurred in the age group of 65 years and above. In 1999, 78.29% of all deaths of men due to diseases of the respiratory system were noted in this age group, and in 2013 this figure was 77.54%. For women, 87.26% and 86.71% of all deaths due to these diseases were found in this age group in 1999 and 2013, respectively.

The prevailing causes of deaths due to diseases of the respiratory system were influenza and pneumonia (J09–J18), as well as chronic lower respiratory diseases (J40–J47). Over the period analyzed, the percentage of deaths due to influenza and pneumonia increased from 48.01% to 58.73%, but dropped for all other respiratory diseases; for example, deaths due to chronic lower respiratory diseases fell from 42.59% to 33.65%.

In 1999, the dominant cause of death due to diseases of the respiratory system among men were chronic lower respiratory diseases, while in 2013 it was influenza and pneumonia. The percentage of male deaths decreased for all other groups of diseases over the period of 1999–2013. Only the group of other respiratory diseases principally affecting the interstitium (J80–J84) demonstrated such high incidence.

For women, on the other hand, while respiratory deaths were predominantly caused by influenza and pneumonia over the study period, the percentage of deaths due to these

Table 1. Deaths caused by diseases of the respiratory system in Poland from 1999 to 2013

Year	Men		Women		General	
	number of deaths	proportional mortality ratio	number of deaths	proportional mortality ratio	number of deaths	proportional mortality ratio
1999	10,427	5.11	7,496	4.23	17,923	4.70
2000	10,491	5.37	7,819	4.53	18,310	4.98
2001	9,284	4.81	6,474	3.80	15,758	4.34
2002	9,342	4.87	6,195	3.69	15,537	4.32
2003	10,185	5.25	7,145	4.17	17,330	4.74
2004	10,175	5.23	6,697	3.97	16,872	4.64
2005	11,066	5.62	7,481	4.36	18,547	5.04
2006	11,126	5.61	7,341	4.28	18,467	5.00
2007	11,778	5.82	7,644	4.37	19,422	5.15
2008	11,569	5.72	7,728	4.36	19,297	5.09
2009	12,206	5.99	8,446	4.66	20,652	5.36
2010	11,487	5.75	7,846	4.39	19,333	5.11
2011	11,868	5.99	8,108	4.57	19,976	5.32
2012	11,715	5.80	8,433	4.62	20,148	5.24
2013	13,106	6.50	9,841	5.30	22,947	5.92
Total	165,825	5.23	114,694	4.08	280,519	4.69

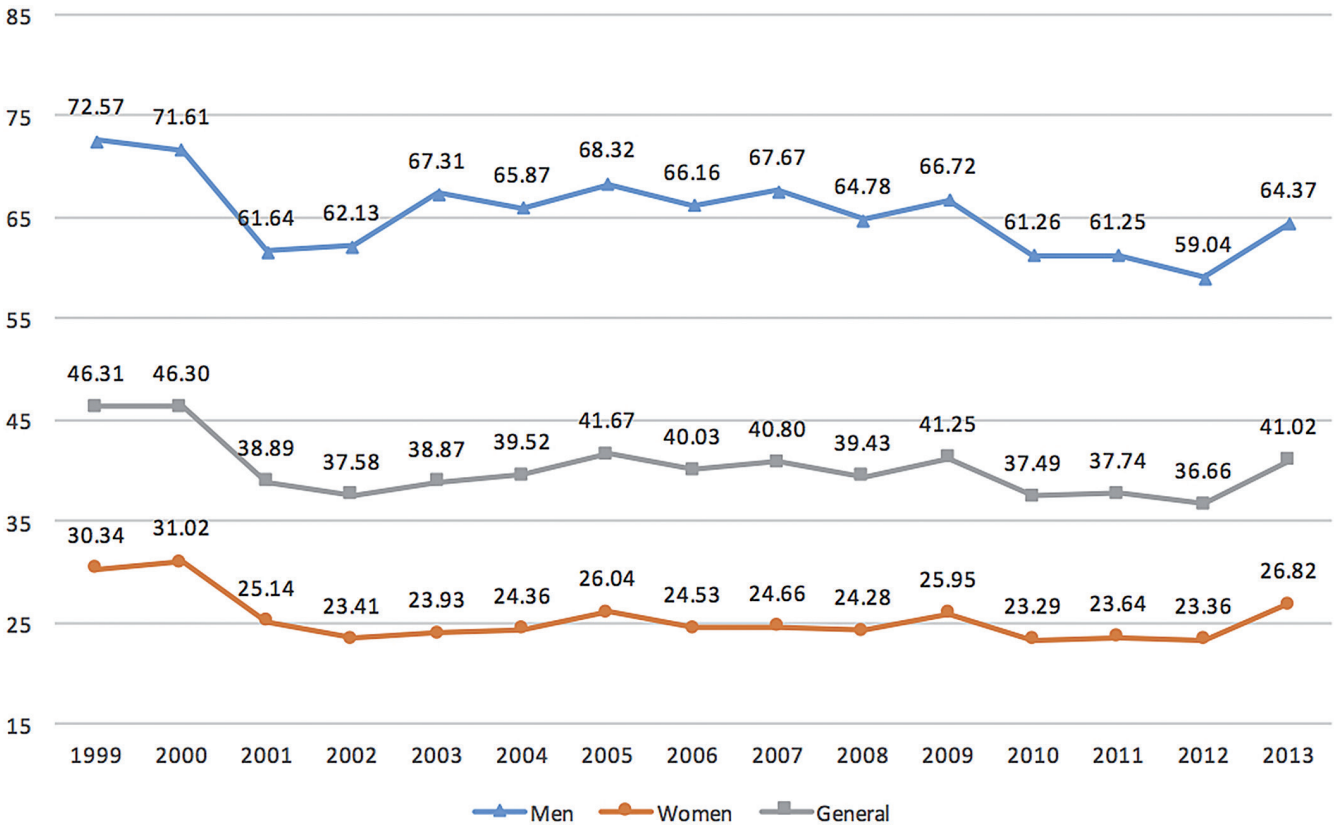

Fig. 1. Standardized death rate due to diseases of the respiratory system in Poland from 1999 to 2013, calculated per 100,000 inhabitants according to sex

diseases grew from 60.22% to 65.03% by the end of 2013. It was also observed that the percentage of deaths caused by lung diseases due to external causes (J60–J70) increased from 1.77% to 2.02%. The deaths caused by other groups of respiratory diseases fell (Table 2).

In Poland, between 1999 and 2013, deaths due to diseases of the respiratory system accounted for 4,474,548.92 years of lost life (SEYLL): 2,908,777.99 years for men and 1,565,770.93 years for women. These figures translate to 104.72 prematurely lost life years ($SEYLL_p$) per

Table 2. Deaths due to diseases of the respiratory system in Poland in 1999 and 2013 according to cause and sex

Cause of death	1999			2013		
	men	women	general	men	women	general
Acute upper respiratory infections (J00–J06)	12 (0.12%)	10 (0.13%)	22 (0.12%)	5 (0.04%)	3 (0.03%)	8 (0.03%)
Influenza and pneumonia (J09–J18)	4,090 (39.23%)	4,514 (60.22%)	8,604 (48.01%)	7,078 (54.01%)	6,399 (65.03%)	13,477 (58.73%)
Influenza (J09–J11)	5 (0.12%)	4 (0.09%)	9 (0.10%)	47 (0.66%)	50 (0.78%)	97 (0.72%)
Pneumonia (J12–J18)	4,085 (99.88%)	4,510 (99.91%)	8,595 (99.90%)	7,031 (99.34%)	6,349 (99.22%)	13,380 (99.28%)
Other acute lower respiratory infections (J20–J22)	55 (0.53%)	35 (0.47%)	90 (0.50%)	11 (0.08%)	35 (0.36%)	46 (0.20%)
Other diseases of upper respiratory tract (J30–J39)	11 (0.11%)	3 (0.04%)	14 (0.08%)	2 (0.02%)	2 (0.02%)	4 (0.02%)
Chronic lower respiratory diseases (J40–J47)	5,316 (50.98%)	2,317 (30.91%)	7,633 (42.59%)	5,037 (38.43%)	2,685 (27.28%)	7,722 (33.65%)
Chronic obstructive pulmonary disease (J40–J44, J47)	4,444 (83.60%)	1,706 (73.63%)	6,150 (80.57%)	4,819 (95.67%)	2,372 (88.34%)	7,191 (93.12%)
Asthma (J45–J46)	872 (16.40%)	611 (26.37%)	1,483 (19.43%)	218 (4.33%)	313 (11.66%)	531 (6.88%)
Lung diseases due to external agents (J60–J70)	245 (2.35%)	133 (1.77%)	378 (2.11%)	254 (1.94%)	199 (2.02%)	453 (1.97%)
Other respiratory diseases principally affecting the interstitium (J80–J84)	290 (2.78%)	254 (3.39%)	544 (3.04%)	366 (2.79%)	301 (3.06%)	667 (2.91%)
Suppurative and necrotic conditions of the lower respiratory tract (J85–J86)	165 (1.58%)	54 (0.72%)	219 (1.22%)	159 (1.21%)	55 (0.56%)	214 (0.93%)
Other diseases of the pleura (J90–J94)	53 (0.51%)	31 (0.41%)	84 (0.47%)	32 (0.24%)	21 (0.21%)	53 (0.23%)
Other diseases of the respiratory system (J95–J99)	190 (1.82%)	145 (1.93%)	335 (1.87%)	162 (1.24%)	141 (1.43%)	303 (1.32%)
Total	10,427 (100%)	7,496 (100%)	17,923 (100%)	13,106 (100%)	9,841 (100%)	22,947 (100%)

10,000 men, and 52.85 years per 10,000 females. The number of lost life years was found to increase over the period for both men and women, with $SEYLL_p$ being the highest in the final year of observation: for men it was 118.43 and for women 64.68. $SEYLL_p$ for men was lower than 100 only in the years 2001–2004. During this time, the lowest values for women were also recorded (<50).

The analysis of $SEYLL_d$ indicated that a man who died due to a disease of the respiratory system in Poland from 1999 to 2013 lost 17.54 years on average, and a woman 13.65 years on average. Over the period studied, $SEYLL_d$ fell from 18.55 in 1999 to 16.83 in 2013 for men, and from 14.23 to 13.06 for women (Table 3).

Discussion

Poland belongs to the group of European countries with a low mortality rate for diseases of the respiratory system, which contribute to about 5% of all Polish deaths. However, the results of the authors' research indicate that this percentage may increase in the coming years. It was at its highest point in the last year of observation, at 5.92%, which was 0.62% higher compared to the previous year and 1.60% higher than the lowest value recorded during the study period (4.32% in 2002). In 2012, the highest proportional mortality rate from all the EU countries was noted in Great Britain. It was 14.1% during that time. The available data indicates that the values of this ratio may also increase in this population.[10]

This study examines the changes in the standardized death rate due to diseases of the respiratory system in Poland. Its value gradually decreased over the study period, but a significant increase was noted in the final year. A similar trend in the standardized death rate was observed for Great Britain and the EU as a whole.[4] In Poland, the standardized death rate due to diseases of the respiratory system for the general population now has a value almost equal to the EU average (41.02 vs 41.64 per 100,000 inhabitants in 2013). For men, the EU average value was exceeded in 2006, and this upward trend has continued to the present (64.37 vs 47.47 per 100,000 males in 2013). For women, the values were lower than the EU average throughout the entire period analyzed (26.82 vs 31.05 per 100,000 females in 2013).

An analysis of deaths due to diseases of the respiratory system according to age helps in interpreting the changes seen in the values of the standardized death rate and the

Table 3. Lost life years due to diseases of the respiratory system in Poland from 1999 to 2013 according to sex

Year	Men			Women		
	SEYLL	$SEYLL_p$ (per 10,000)	$SEYLL_d$	SEYLL	$SEYLL_p$ (per 10,000)	$SEYLL_d$
1999	193,469.35	104.29	18.55	106,636.32	54.18	14.23
2000	190,250.70	102.63	18.13	110,094.03	55.94	14.08
2001	168,229.24	90.80	18.12	92,308.27	46.89	14.26
2002	165,801.98	89.65	17.75	85,753.37	43.55	13.84
2003	178,431.09	96.60	17.52	97,005.11	49.07	13.58
2004	179,390.11	97.21	17.63	91,381.37	46.44	13.65
2005	191,275.33	103.65	17.28	100,332.88	50.92	13.41
2006	195,384.50	106.03	17.56	99,130.22	50.32	13.50
2007	208,624.72	113.31	17.71	103,710.97	52.63	13.57
2008	202,709.79	110.08	17.52	104,962.05	53.22	13.58
2009	214,432.55	116.36	17.57	116,547.91	59.05	13.80
2010	200,072.87	107.26	17.42	106,641.92	53.65	13.59
2011	205,439.20	110.13	17.31	112,886.45	56.77	13.92
2012	194,633.75	104.36	16.61	109,876.38	55.26	13.03
2013	220,632.81	118.43	16.83	128,503.68	64.68	13.06
Total	2,908,777.99	104.72	17.54	1,565,770.93	52.85	13.65

proportional mortality rate over time. The results of the presented study indicate that the highest number of deaths caused by these diseases occurred in people at the age of 65 years or older.

The main respiratory diseases that caused the most deaths in Poland were influenza and pneumonia (J09–J18). An analysis of the number of vaccinations against influenza received by the Polish population suggests that many deaths could be prevented by the vaccine against this virus.[11] While the European Council recommends that at least 75% of the population are vaccinated, this number has not exceeded even 5% in Poland for many years.[12,13] Moreover, despite the regular advancements in the influenza vaccination, its use has been gradually decreasing in recent years, from 6.8% in 2009 to 3.4% in 2015.[14,15] It is also worth noting that one of the current indications for vaccination against influenza is an age of 65 years or older, regardless of additional risk factors.[15,16]

Beside influenza and pneumonia, the greatest mortality due to diseases of the respiratory system observed in Poland, as in most other European countries, is in chronic lower respiratory diseases (J40–J47), such as bronchial asthma and chronic obstructive pulmonary disease (COPD).[1] Despite considerable research on the causality of these diseases, certain data on the factors determining their development is lacking. One of the most probable causes of asthma is hypersensitivity to inhaled allergens, and the best documented factor facilitating the progress of asthma is tobacco smoke.[17] Smoking cigarettes is also a main factor in the progress of COPD.[18,19] WHO data indicates that in 2013, 29.4% of Poles aged ≥15 years regularly smoked cigarettes. At the same time, the mean value in the EU was 27.5%, and 20.3% in Great Britain.[4]

From a socioeconomic point of view, SEYLL is more important than a simple interpretation of death rates. Of particular concern is the significant increase in $SEYLL_p$ observed in the last year studied. This means that the number of years of life lost due to diseases of the respiratory system calculated per 10,000 inhabitants has increased, and it indicates that there is a need to continue observing premature mortality in the Polish population. Additionally, the decrease in $SEYLL_d$ confirms that deaths due to diseases of the respiratory system have shifted to older age groups over time. This may indicate that the prophylactic and therapeutic methods used to treat these diseases have improved.

Diseases of the respiratory system are the 4th highest cause of mortality in Poland, after diseases of the circulatory system, malignant neoplasms, and external causes. Influenza and pneumonia, as well as chronic lower respiratory diseases, including bronchial asthma and chronic obstructive pulmonary disease, are the dominant respiratory diseases contributing to the observed mortality.

The analysis of the health status of a population by a potential measure, like SEYLL, gives significant information on premature mortality.[19–22] Diseases of the respiratory system over a 15-year period caused the loss of 4,474,548.92 years of life in the Polish population. This disproportionately affected men, with an average of 104.72 lost life years per 10,000 males, compared to 52.85 lost life years per 10,000 females. This means that, on average, a man who died due to a disease of the respiratory system lost 17.54 years and a woman lost 13.65 years. The values of SEYLL indicate that diseases of the respiratory system play an important socioeconomic role in the health status of the Polish population.

References

1. Statistical Office of the European Communities. Respiratory diseases statistics. Eurostat: statistics explained. http://ec.europa.eu/eurostat/statistics-explained/index.php/Respira-tory_diseases_statistics. Published October, 2016. Updated December 16, 2016. Accessed December 20, 2016.
2. Dmochowska H, ed. *Statistical Yearbook of the Republic of Poland 2015*. Warszawa: Central Statistical Office; 2015.
3. World Health Organization. World Health Statistics Report 2008. http://www.who.int/whosis/whostat/EN_WHS08_Full.pdf. Accessed December 20, 2016.
4. World Health Organization Regional Office for Europe. European health for all database. http://data.euro.who.int/hfadb/. Published 2002. Updated June, 2016. Accessed December 20, 2016.
5. Murray CJL, Lopez AD. *The Global Burden of Disease. A comprehensive Assessment of Mortality and Disability from Diseases, Injuries and Risk Factors in 1990 and Projected to 2010*. Boston, MA: Harvard University Press; 1996.
6. Marshall RJ. Standard Expected Years of Life Lost as a measure of disease burden: An investigation of its presentation, meaning and interpretation. In: Preedy VR, Watson RR, eds. *Handbook of Disease Burdens and Quality of Life Measures*. Berlin: Springer; 2009:3421–3434.
7. Selb Semerl J, Sesok J. Years of potential life lost and valued years of potential life lost in assessing premature mortality in Slovenia. *CMJ.* 2002;43:439–445.
8. Santric Milicevic M, Bjegovic V, Terzic Z, et al. Serbia within the European context: An analysis of premature mortality. *Popul Health Metr.* 2009;7:12.
9. Supplement to: Murray CJL, Ezzati M, Flaxman AD, et al. GBD 2010: Design, definitions, and metrics. *Lancet*. 2012;380:2063–2066.
10. Office for National Statistics. Deaths registered in England and Wales: 2015. http://ons.gov.uk. Published July, 2016. Accessed December 20, 2016.
11. Preaud EDL, Macabeo B, Farkas N, et al. Annual public health and economic benefits of seasonal influenza vaccination: A European estimate. *BMC Public Health*. 2014;14:813.
12. Council of the European Communities. *Proposal for a Council Recommendation on Seasonal Influenza Vaccination*. Brussels; 2009.
13. Raise Awareness of Influenza Strategies in Europe. *Szczepienia przeciw grypie: podstawowe fakty dla lekarzy pierwszego kontaktu w Europie*. Warszawa; 2016.
14. Kolegium Lekarzy Rodzinnych w Polsce. *Profilaktyka i leczenie grypy*. Łódź; 2006.
15. Ogólnopolski Program Zwalczania Grypy. Raport. Ernst & Young. http://instytutoz.org/wp-content/uploads/2013/12/Raport_II_Ogolnopolski_Program_Zwalczania_Grypy.pdf. Published June, 2013. Accessed December 20, 2016.
16. Polish Ministry of Health. *Komunikat Głównego Inspektora Sanitarnego w sprawie Programu Szczepień Ochronnych na rok 2016*. Warszawa: Dziennik Urzędowy Ministra Zdrowia; 2016.
17. Subbarao P, Mandhane PJ, Sears MR. Asthma: Epidemiology, etiology and risk factors. *CMAJ.* 2009;181(9):E181–E190.
18. Rabe KF, Hurd S, Anzueto A, et al. Global strategy for the diagnosis, management and prevention of chronic obstructive pulmonary disease. *Am J Respir Crit Care Med.* 2007;6(176):532–555.
19. Shavelle RM, Paculdo DR, Kush SJ, Mannino DM, Strauss DJ. Life expectancy and years of life lost in chronic obstructive pulmonary disease: Findings from the NHANES III Follow-up Study. *Int J Chron Obstruct Pulmon Dis*. 2009;4:137–148.
20. Maniecka-Bryła I, Bryła M, Bryła P, et al. The burden of premature mortality in Poland analysed with the use of standard expected years of life lost. *BMC Public Health*. 2015;15:101.
21. Gènova-Maleras R, Catalá-López F, de Larrea-Baz NF, et al. The burden of premature mortality in Spain using standard expected years of life lost: A population-based study. *BMC Public Health*. 2011;11:787.
22. Burnet NG, Jefferies SJ, Benson RJ, et al. Years of life lost (YLL) from cancer is an important measure of population burden – and should be considered when allocating research funds. *Brit J Cancer.* 2005;92(2):241–245.

The influence of a 3-week body mass reduction program on the metabolic parameters and free amino acid profiles in adult Polish people with obesity

Małgorzata Moszak[1,A–D], Agnieszka Klupczyńska[2,A–D], Alina Kanikowska[1,A,B,D,E], Zenon Kokot[2,A,C,E,F], Agnieszka Zawada[1,B,C], Małgorzata Grzymisławska[3,B,C], Marian Grzymisławski[1,A,C,E,F]

[1] Department of Gastroenterology, Human Nutrition and Internal Diseases, Poznan University of Medical Sciences, Poland
[2] Department of Inorganic and Analytical Chemistry, Poznan University of Medical Sciences, Poland
[3] Department and Chair of Anatomy, Poznan University of Medical Sciences, Poland

A – research concept and design; B – collection and/or assembly of data; C – data analysis and interpretation; D – writing the article; E – critical revision of the article; F – final approval of the article

Advances in Clinical and Experimental Medicine, ISSN 1899-5276 (print), ISSN 2451-2680 (online) *Adv Clin Exp Med*. 2018;27(6):749–757

Address for correspondence
Małgorzata Moszak
E-mail: mmoszak@ump.edu.pl

Funding sources
None declared

Conflict of interest
None declared

Received on January 9, 2017
Reviewed on January 31, 2017
Accepted on April 27, 2017

Abstract

Background. Previous studies have shown differences in the amino acid (AA) composition in the plasma of people with obesity when compared to lean individuals, but the perturbations of AA concentrations in obesity and the dynamics of AA changes after weight loss are not fully understood.

Objectives. The objective of the study was to evaluate the effect of a short-term weight reduction program on the metabolic status and plasma AA levels in individuals with obesity.

Material and methods. A total of 24 adult Polish patients with a BMI between 34 and 49 kg/m^2 were enrolled in a 3-week controlled body mass reduction program based on everyday physical activity and a hypocaloric diet (25–30% less than total daily energy requirements). At baseline and after the program, anthropometric measurements, biochemical parameters and free AA profiles were determined.

Results. After the weight loss program, significant changes in body mass and metabolic parameters (e.g., low-density lipoprotein, triglyceride, fasting glucose, and insulin levels) were observed. Positive changes in a homeostatic model assessment of insulin resistance (HOMA-IR) and quantitative insulin sensitivity check index (QUICKI) following the program were also found. The levels of 10 AAs (α-amino-n-butyric acid, alanine, citrulline, glutamine, glycine, hydroxyproline, isoleucine, proline, sarcosine, and threonine) had significantly increased following weight loss. Only aspartic acid was present at a significantly lower concentration after the program.

Conclusions. Using a 3-week controlled body mass reduction program based on physical activity and a hypocaloric diet, we were able to demonstrate significant changes in biochemical parameters and free AA profiles. To better understand these changes, future studies should involve a long-term program with more patients.

Key words: obesity, amino acids, metabolic profile, body mass reduction

DOI
10.17219/acem/70796

Introduction

Obesity is a significant public health problem reaching the level of pandemic in the developed world. It not only predisposes individuals to serious chronic conditions, such as type 2 diabetes, cardiovascular diseases and certain cancers, but it is also a leading cause of premature death worldwide. The etiology of obesity is multifactorial and includes interactions between genetic and environmental factors. Obesity results from energy homeostasis disorders, caused by an excessive intake of calories in relation to energy expenditure, and other lifestyle-related factors, such as a sedentary job and inactivity.[1,2]

In recent years, there has been a growing interest in the study of the human metabolome in obesity. The term "metabolome" is defined as the complete set of all metabolites in the body, tissues or cells (e.g., amino acids, lipids, carbohydrates, or nucleotides).[3] Free amino acids (AAs) constitute a particularly interesting group of metabolites.[4,5]

Previous studies showed significant differences in plasma AA composition in people with obesity compared to individuals with normal body mass.[6–9] Newgard et al. observed that among a total of 16 AAs measured in the serum of adult African-American subjects, 8 amino acids (alanine, valine, leucine/isoleucine, phenylalanine, tyrosine, glutamate/glutamine, aspartate/asparagine, and arginine) were found in dramatically higher levels in obese participants (median body mass index – BMI: 36.6 kg/m^2) vs lean participants (median BMI: 23.2 kg/m^2).[10] Only the glycine level was lower in patients with obesity.

Strong discrepancies between the branched-chain amino acid (BCAA) and AA levels in children with obesity (8–18 years old) compared to lean individuals were also described by McCormack et al.[11] A report on Japanese subjects with obesity showed that plasma levels of alanine, glycine, glutamate, tryptophan, tyrosine, and BCAAs were associated with high visceral fat accumulation and could be dependent on genetic and environmental factors.[12] Moreover, Yamakado et al. hypothesized that the amount of visceral fat changes AA profile, and that the multivariate logistic regression model of free AAs in plasma can discern non-apparent visceral obesity in adult Asian individuals.[12] The associations between the BCAA levels and tyrosine with visceral adiposity – irrespective of ethnicity, lifestyle or environmental conditions – were also studied by Marti et al.[13]

Despite the great interest in and development of the state of knowledge about metabolic profiles in people with obesity, the perturbations in AA concentrations in the serum of adult patients suffering from obesity after weight loss are not fully understood. The previous studies in this area focused on describing the changes in metabolic profile after weight loss achieved by bariatric surgery or long-term body mass reduction programs based on lifestyle intervention. In addition, previous studies evaluated the AA changes in groups of people of different races or with different baseline BMI levels, and used other metabolomic assay techniques. Only a few studies investigated the effect of weight reduction on the level of amino acids in time points shorter than 1 year on a Caucasian population. An intriguing issue is the dynamics of changes in the metabolome under weight loss intervention.

This is the first study which demonstrates alterations in AA profiles and a number of biochemical parameters: fasting serum glucose, fasting serum insulin and a homeostatic model assessment of insulin resistance (HOMA-IR), quantitative insulin sensitivity check index (QUICKI), C-reactive protein (CRP), total cholesterol (TC), high-density lipoprotein (HDL), low-density lipoprotein (LDL), triglyceride (TG), alanine aminotransferase (AlAT), and aspartate aminotranferase (AspAT) after a 3-week program based on a controlled, energy-restricted diet (25–30% less than daily energy requirements) of a strictly specified macronutrient composition and physical activity. The panel of free AAs analyzed was the most comprehensive among all previously conducted studies and it covered concentrations of 42 metabolites.

Material and methods

Participants and study design

The study was conducted in the Department of Internal Diseases, Metabolism and Nutrition of the Heliodor Swiecicki University Hospital in Poznań, Poland, between September 2014 and June 2015. Twenty-four Polish patients (10 men and 14 women) with a BMI between 34 and 49 kg/m^2 (mean BMI: 40 ±4 kg/m^2) were enrolled. Mean age was 46 ±12 years and ranged from 24 to 66 years. Diabetes mellitus type 1 or uncontrolled type 2 diabetes, a vegetarian or any other alternative diet, cancer, a history of eating disorders, or chronic diseases related to metabolism (e.g., chronic liver, kidney or pancreatic diseases, inborn metabolic diseases, autoimmune diseases, or inflammatory bowel diseases) were considered to be exclusion criteria. The occurrence of diseases listed in the exclusion criteria was checked through the use of specific diagnostic tests and medical histories. None of the patients smoked.

The study protocol was approved by the Bioethics Committee at Poznan University of Medical Sciences (No. 333/14), and was performed in accordance with the Declaration of Helsinki. All the patients signed statements of informed consent before they participated in the study.

The subjects were hospitalized for 3 weeks and received controlled daily aerobic physical training, under the supervision of a physical therapist, and a hypocaloric diet based on a 25–30% reduction of caloric dietary intake compared to their total estimated energy requirement. The total daily energy requirement was calculated on actual body weight using the Harris-Benedict formula and the physical activity level index (PAL). To more accurately determine total

energy expenditure and to assess the caloric value of the diet before the program, subjects completed a 3-day intake assessment prior to the study (the 24-hour dietary assessment covers 3 days). The subjects received the same type of diet prepared by dietetic food caterers based on the planned menu. The average value of total daily energy intake before the program was 2,935.6 ±490.2 kcal (2,764.0 ±406.1 kcal for women; 3,340.5 ±284.5 for men), and the average value during the body mass reduction program was 2,016.0 ±281.7 kcal (1,880.0 ±234.0 kcal for women; 2,220.0 ±219.1 for men).

Each patient received a diet with an identical composition of macronutrients (especially proteins) derived from the same products. The diet consisted of 20% of calories from protein, 25–30% from fat, and 50–55% from carbohydrates. The daily fiber intake from the diet was over 25 g. Physical training included active and passive breathing exercises for 30 min a day, cardiovascular aerobic exercise (Nordic walking or cycling) twice a day for 60 min and resistance training for 30 min daily. Each patient who participated in the study was educated on proper nutrition and nutritional recommendations for obesity by a qualified nutritionist.

Serum assays

Serum glucose (3.3–5.8 mmol/L), TC (3.4–5.2 mmol/L), HDL (>1.6 mmol/L), TG (0.5–1.9 mmol/L), AspAT (5–40 U/L), and AlAT (5–40 U/L) were determined by a fully automated Modular P-800 Roche (Diamond Diagnostic, Holliston, USA). LDL was measured indirectly using the Friedewald equation. Insulin (2.0–25.0 mU/L) was determined by a micro-particle enzyme immunoassay (Abbot, Abbot Park, USA). Serum CRP was analyzed by a commercial assay (Dade Behring, Marburg, Germany). The QUICKI was calculated using the inverse of the sum of the logarithms of fasting insulin and fasting glucose levels: 1/[log(fasting insulin μU/mL) + log(fasting glucose mg/dL)]. The HOMA-IR was calculated according to this formula: fasting insulin μU/L × fasting glucose nmol/L/22.5.

An important element of the study was the analysis of the serum profiles of 42 AAs in obese patients and their possible changes after weight loss. Fasting plasma was collected for AA analysis in the morning after 10 h of fasting and was stored in −80°C before analysis. The determination of free AA serum profiles was performed using the fully validated, highly selective liquid chromatography-tandem mass spectrometry method (LC-MS/MS). Samples were prepared using aTRAQ-based methodology (Sciex, Framingham, USA), and then analyzed by a high-performance liquid chromatograph 1260 Infinity (Agilent Technologies, Santa Clara, USA) interfaced to a triple-quadrupole mass spectrometer 4000 QTRAP (Sciex, Framingham, USA). The detailed sample preparation protocol, LC-MS/MS parameters and validation results using serum samples were presented in the previous reports.[14,15]

Anthropometric measures

For each patient, anthropometric measurements were carried out at baseline and after the 3-week weight reduction program. Height was measured to the nearest centimeter using a stadiometer. Weight and analysis of body composition was performed by Tanita MC 980 MA – bodyfat analyzer (TANITA, Tokio, Japan) based on the measurement of bioelectrical impedance, with a tetrapolarfoodpad-style electrode arrangement. The subjects stood on the metal contacts in bare feet, as recommended in the manual. Body mass index was defined as the individual's body mass divided by the square of their height, with the value given in kg/m^2. Waist–hip ratio (WHR) was the ratio of waist circumference to hip circumference, measured in cm with the use of medical measuring tape (SECA, Hamburg, Germany).

Statistical analysis

In order to examine changes in the anthropometric and biochemical parameters, as well as free AA serum profiles induced by the weight loss program, the Shapiro-Wilk test of normality was used in the first step. Variables with normal distribution were then subjected to the paired t-test. For the analysis of variables that were not normally distributed, the Wilcoxon signed-rank test was used. In all tests, a p-value of ≤0.05 was considered to be statistically significant. Additionally, in order to evaluate the influence of a reduction in body weight on the free AA levels in the serum, a principal component analysis (PCA) was conducted. PCA is used to bring out any patterns in the study dataset and to visualize the differences among groups of analyzed samples. Since PCA is conducted without any prior information on sample classification, it is defined as an unsupervised statistical method. Prior to PCA, normalization by sum and by autoscaling of the amino acid concentrations were performed. The statistical analyses were carried out using STATISTICA v. 10.0 (StatSoft, Kraków, Poland) and the MetaboAnalyst 3.0 web portal.[16]

Results

Anthropometric and biochemical characteristics of the study population

The differences in the anthropometric and biochemical parameters measured before and after the 3-week weight loss program are presented in Table 1.

After the applied weight loss program, significant decreases in body mass, BMI, waist circumference, and hip circumference were observed. The average reduction in body mass was 6.0 kg (5.1%), which significantly decreased the BMI level (39.7 ±4.1 kg/m^2 vs 37.7 ±3.9 kg/m^2; $p < 0.0000$). The average waist and hip circumferences

changed from 121.8 ±11.7 cm to 118.0 ±11.1 cm (p = 0.0000) and from 129.0 ±9.1 cm to 126.0 ±8.3 cm (p = 0.0000), respectively. After the 3-week program, we observed an 8.7% reduction in fat mass. A reduction in muscle mass and total body water was also noticed in the study group (Table 1).

Table 1. Anthropometric characteristics, biochemical parameters and free AA concentrations of the study population before and after the weight loss program

Parameter	Before the program	After the program	After – before the program		p-value*
	mean ±SD	mean ±SD	mean ±SD	% difference	
Anthropometric parameters					
Body weight [kg]	116.1 ±14.8	110.1 ±13.6	–6.0 ±3.0	–5.1	<0.0000**
BMI [kg/m^2]	39.7 ±4.1	37.7 ±3.8	–2.0 ±1.0	–5.2	<0.0000**
Waist circumference [cm]	121.8 ±11.7	118.0 ±11.1	–3.8 ±2.8	–3.2	0.0000**
Hip circumference [cm]	129.0 ±9.1	126.0 ±8.3	–3.0 ±1.6	–2.3	0.0000**
Fat mass [kg]	46.3 ±8.7	42.2 ±8.3	–4.1 ±2.0	–8.7	0.0000**
FFM [kg]	69.8 ±11.5	67.9 ±11.6	–1.9 ±2.1	–2.8	0.0002**
Muscle mass [kg]	66.3 ±10.9	64.4 ±11.2	–1.9 ±2.0	–2.9	0.0001**
TBW [kg]	50.0 ±8.7	48.7 ±8.8	–1.3 ±2.2	–2.7	0.0064**
Biochemical parameters					
Triglycerides [mg/dL]	152.7 ±87.3	133.6 ±58.1	–19.1 ±48.9	–12.5	0.1004
LDL [mg/dL]	119.2 ±35.6	105.9 ±32.9	–13.3 ±32.9	–11.3	0.0560
CRP [mg/L]	4.1 ±2.7	4.0 ±3.2	–0.1 ±3.0	–3.4	0.3606
Glucose [mg/dL]	108.9 ±19.6	101.9 ±12.2	–7.0 ±14.3	–6.4	0.0082**
Insulin [µU/mL]	21.3 ±16.4	18.0 ±15.8	–3.3 ±4.7	–15.7	0.0006**
HOMA-IR	6.1 ±5.4	4.8 ±4.8	–1.3 ±1.8	–20.4	0.0029**
QUICKI	0.2 ±0.0	0.2 ±0.0	0.0 ±0.0	5.6	0.0244**
ALAT [U/L]	35.3 ±17.9	31.6 ±18.0	–3.7 ±9.4	–10.4	0.0355**
AspAT [U/L]	25.3 ±13.2	24.7 ±16.3	–0.6 ±6.2	–2.5	0.2373
Amino acids [µM]					
1-methylhistidine	6.09 ±4.77	8.03 ±6.30	1.96 ±7.60	32.0	0.1451
3-methylhistidine	3.20 ±1.12	3.61 ±1.59	0.42 ±1.49	13.0	0.1322
α-aminoadipic acid	0.79 ±0.40	0.79 ±0.41	–0.0001 ±0.43	0.0	0.7701
α-amino-n-butyric acid	25.05 ±6.06	30.00 ±6.20	4.95 ±6.21	19.8	0.0007**
Alanine	382.44 ±112.01	452.68 ±128.73	70.24 ±150.26	18.4	0.0315
Arginine	65.72 ±17.40	71.04 ±12.21	5.32 ±15.47	8.1	0.1055
Asparagines	38.37 ±8.15	40.07 ±5.78	1.70 ±8.38	4.4	0.3306
Aspartic acid	11.63 ±3.73	9.83 ±2.38	–1.80 ±3.42	–15.5	0.0169**
β-aminoisobutyric acid	2.64 ±0.88	2.88 ±1.01	0.24 ±0.77	8.9	0.1462
β-alanine	22.42 ±4.29	22.01 ±2.94	–0.41 ±3.39	–1.8	0.5573
Citrulline	18.56 ±7.53	22.26 ±8.30	3.70 ±7.56	19.9	0.0251**
Cystine	47.11 ±14.87	49.23 ±13.17	2.13 ±13.18	4.5	0.4373
Ethanolamine	7.11 ±1.87	6.96 ±1.37	–0.15 ±1.38	–2.1	0.5994
Glutamine	444.59 ±85.25	503.76 ±75.65	59.17 ±79.85	13.3	0.0014**
Glutamic acid	48.13 ±14.44	45.03 ±13.90	–3.10 ±13.86	–6.5	0.2842
Glycine	221.77 ±53.58	261.28 ±54.53	39.51 ±43.12	17.8	0.0002**
Histidine	63.32 ±13.77	63.06 ±7.93	–0.26 ±11.04	–0.4	0.9078
Hydroxylysine	8.18 ±3.51	9.89 ±3.63	1.71 ±5.12	20.9	0.0199**
Isoleucine	65.08 ±13.85	72.20 ±18.54	7.13 ±16.62	11.0	0.0469**
Leucine	117.50 ±25.05	120.41 ±27.43	2.91 ±29.53	2.5	0.8639
Lysine	181.17 ±40.80	183.58 ±34.84	2.41 ±42.42	1.3	0.7833
Methionine	20.10 ±5.31	20.45 ±4.54	0.35 ±5.55	1.8	0.7584

Table 1 (cont.).

Parameter	Before the program	After the program	After – before the program		p-value*
	mean ±SD	mean ±SD	mean ±SD	% difference	
Ornithine	65.91 ±16.94	71.03 ±17.76	5.12 ±19.05	7.8	0.2010
Phosphoethanolamine	1.79 ±0.62	1.74 ±0.46	−0.04 ±0.64	−2.5	0.7394
Phenylalanine	50.60 ±9.04	48.66 ±7.59	−1.94 ±10.24	−3.8	0.3642
Proline	146.42 ±44.28	190.51 ±53.79	44.09 ±66.76	30.1	0.0014**
Sarcosine	1.31 ±0.66	1.62 ±0.86	0.31 ±0.48	23.9	0.0040**
Serine	106.88 ±24.21	112.35 ±25.04	5.47 ±24.60	5.1	0.2873
Taurine	93.74 ±25.84	88.95 ±21.94	−4.79 ±22.37	−5.1	0.3053
Threonine	91.94 ±21.87	109.08 ±31.94	7.14 ±31.85	18.6	0.0148**
Tryptophan	42.41 ±10.99	42.16 ±7.24	−0.25 ±8.35	−0.6	0.8854
Tyrosine	42.51 ±11.20	46.81 ±14.16	4.30 ±11.54	10.1	0.0810
Valine	211.71 ±42.25	227.04 ±37.33	15.33 ±42.31	7.2	0.0892

* obtained based on paired t-test or Wilcoxon test ; ** statistically significant; BMI – body mass index; FFM – free fat mass, TBW – total body water; LDL – low-density lipoprotein; CRP – C-reactive protein; HOMA-IR – homeostatic model assessment of insulin resistance; QUICKI – quantitative insulin sensitivity check index; AlAT – alanine aminotransferase; AspAT – aspartate aminotransferase.

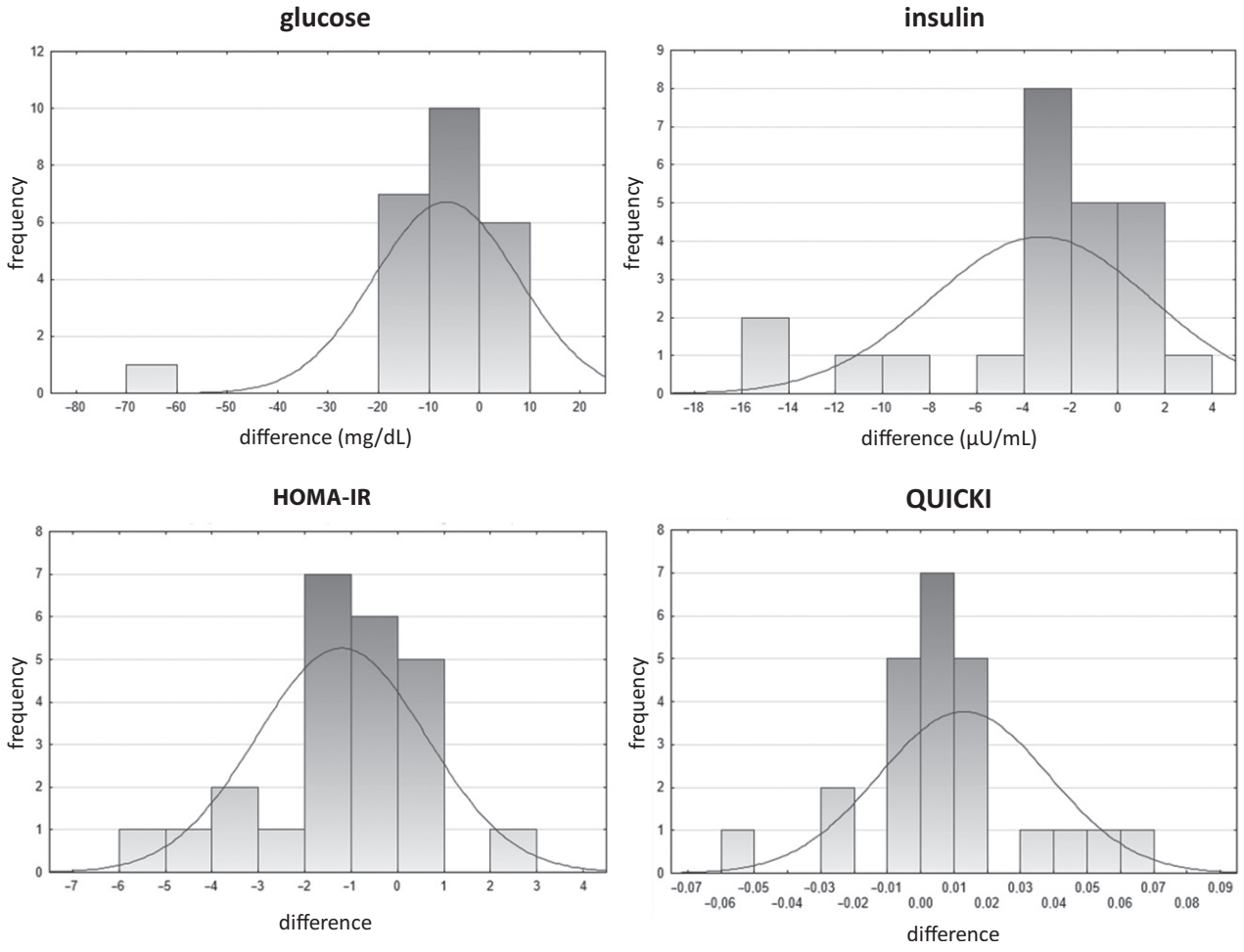

Fig. 1. Histograms of the differences in parameters associated with carbohydrate metabolism measured before and after the 3-week weight loss program

HOMA-IR – homeostatic model assessment of insulin resistance; QUICKI – quantitative insulin sensitivity check index.

Baseline median fasting blood glucose levels in patients with obesity were elevated compared to the values after body mass reduction (Table 1). Similarly, the fasting insulin levels in patients at baseline were significantly higher than at the end of the study. We observed positive changes in HOMA-IR after weight loss (Fig. 1). Other important changes observed after weight loss were the reductions in TG concentration (12.5%), the LDL-cholesterol level (11.4%) and CRP (3.4%); however, those differences were not statistically significant.

AA profiles of serum

The analysis of free AA profiles in the serum samples collected before and after the 3-week weight loss program revealed a number of significant changes in the metabolic profile of the patients. Although the applied methodology allows for measurements of 42 free AAs, both proteinogenic and non-proteinogenic, not all of the metabolites occurred in measurable concentrations in the samples. For this reason, the following 9 AAs were excluded from further statistical analysis: phosphoserine, argininosuccinic acid, homocitrulline, anserine, carnosine, homocysteine, γ-amino-n-butyric acid, cystathionine, and δ-hydroxylysine. The remaining 33 metabolites, along with their concentrations as measured in the analyzed serum samples, are listed in Table 1. The levels of 10 AAs (α-amino-n-butyric acid, alanine, citrulline, glutamine, glycine, hydroxyproline, isoleucine, proline, sarcosine, and threonine) were significantly higher after weight loss compared with their values before the program. Only aspartic acid was lower in patients after the program. According to the univariate statistical analyses performed, the highest differences in serum levels were observed for the following metabolites: glycine ($p = 0.0002$), α-amino-n-butyric acid ($p = 0.0007$), proline ($p = 0.0014$), and glutamine ($p = 0.0014$).

The influence of weight loss on AA profiles was also investigated using multivariate statistical analysis – PCA – which involves a group of variables simultaneously. Free AA profiles were analyzed by PCA to determine any clusters with respect to the 2 groups of samples: before and after intervention. In Fig. 2, points corresponding to the analyzed serum samples are contained in the space spanned by the first 2 principal components (PC 1 vs PC 2). Although the 2 groups of samples did not form separate clusters, a partial separation between samples was observed (Fig. 2). The results of PCA indicate that the changes in free AA profiles were strong enough to cause grouping of the samples according to their inclusion in one of the groups studied.

Discussion

This paper presents a comprehensive picture of the metabolic changes in Polish patients with obesity after a 3-week weight loss program. Although the duration of the body mass reduction program was relatively short, it is noteworthy that the weight reduction was carried out under strictly controlled conditions. All patients were treated with the same type of diet prepared by dietetic food caterers and the level of compliance remained under supervision during the entire 3 weeks. The implemented program of physical exercise was also the same in all study participants.

The weight loss achieved in all patients during the 3-week program (based on a hypocaloric diet of a strictly defined macronutrient composition and physical activity) was very satisfactory and it affected the measured

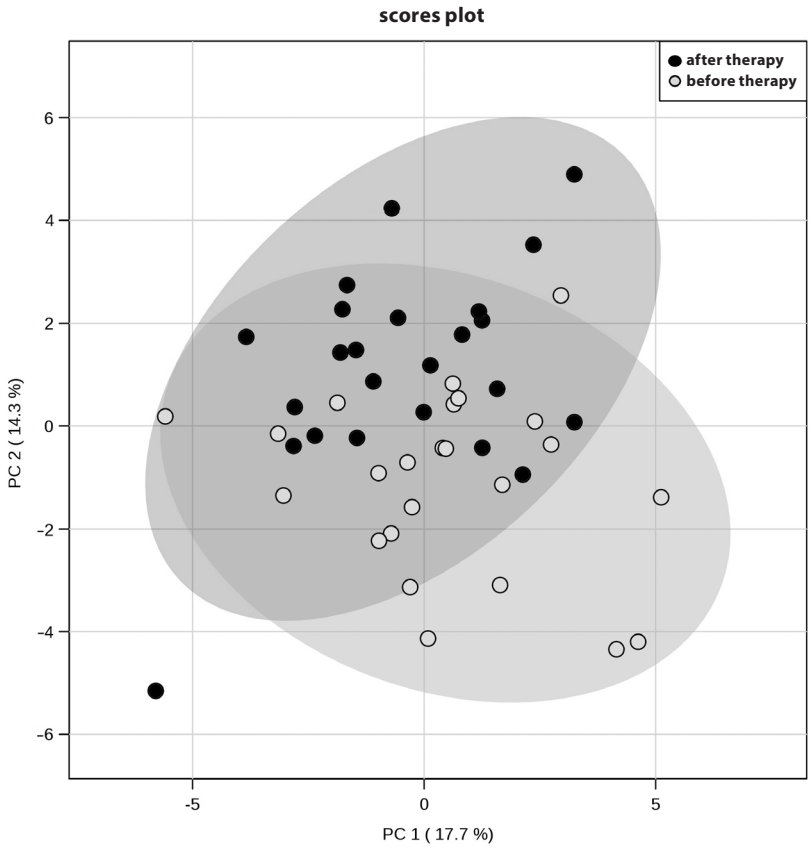

Fig. 2. Score plot from PCA model classifying the serum samples according to their inclusion in one of the studied groups (before or after weight loss)

PCA – principal component analysis.

metabolic parameters and body mass composition. It has been already demonstrated that a 5% weight loss reduces or eliminates disorders associated with obesity; it improves both TC and TG, and causes a reduction in plasma glucose level.[17] Similar trends were observed in this study, even though the body mass reduction was achieved after a short-term program. The TG and LDL-cholesterol levels were reduced in response to weight loss, though those differences were not statistically significant. As a result of weight reduction, positive changes in carbohydrate profiles were observed (Fig. 1). We noticed positive changes in HOMA-IR and QUICKI after weight loss. The HOMA-IR and QUICKI are widely validated and applied in the estimation of insulin sensitivity.[18] High HOMA-IR and low QUICKI were independently and significantly associated with an increased risk of impaired glucose tolerance (IGT) and type 2 diabetes. The HOMA-IR cut off value which correlates with an increased risk of metabolic and cardiovascular diseases was estimated in several studies, in which its dependence on age, gender and ethnicity was noted.[19] In the study population, HOMA-IR was elevated, but we observed a reduction after the intervention ended ($p = 0.0029$) (Table 1).

Our study involved the application of a targeted metabolomic approach focused on the profiles of free AAs and their derivatives in the serum of adult Polish patients with obesity at baseline and after 3 weeks of a weight loss program. The previous studies described the changes in biochemical parameters after weight loss, but only a few studies assessed the impact of the reduction in body mass and body composition changes on free AA profiles. The available conclusions on this relationship mainly come from studies of patients after bariatric surgery or long-term weight reduction programs. However, it has been shown that bariatric surgery caused differential metabolic changes in AA profiles of patients with obesity compared with dietary intervention, despite identical weight loss of the subjects.[20,21] Additionally, only a few studies investigated the effect of weight reduction on the AA levels in time points shorter than 1 year. An intriguing issue is the dynamics of changes in the metabolome of people with obesity during weight loss. Moreover, the previous studies on changes in AA profiles during weight loss were conducted on a group of patients of varying races (especially among Asians and Americans), which may have influenced the observations. The results obtained in the previous studies may have also depended on the technique of metabolomic assays. The advantages of the analytical methodology used in the current study were confirmed in the available literature and include high sensitivity and specificity, short time of analysis and a very wide range of analytes, since it enables the quantification of 42 AAs, both proteinogenic and non-proteionogenic.[15,16] As 9 AAs of the identified 42 AAs occurred in concentrations below measurable values, the final analysis included 33 metabolites.

In this study, we observed that the levels of 10 AAs (α-amino-n-butyric acid, alanine, citrulline, glutamine, glycine, hydroxyproline, isoleucine, proline, sarcosine, and threonine) had increased significantly after weight loss compared to their values before the program, while the aspartic acid level had decreased. According to the univariate statistical analyses performed, the highest differences in serum levels were observed for the following metabolites: glycine, α-amino-n-butyric acid, proline, and glutamine (Table 1). An elevation in the glycine and threonine levels was also observed in a population of overweight, older German adults, following an 8-week calorie-restricted (15% less than daily energy requirements) weight loss and physical activity program.[22]

An elevation of the BCAA levels has been reported in humans with obesity and in animal models of obesity, and many studies have described a decrease in the levels of BCAAs after weight loss.[12,22–24] Some studies demonstrated a decrease in concentrations of BCAA and metabolites derived from BCAA oxidation after bariatric surgery.[25,26] The increased plasma BCAA concentration may be the result of the impaired BCAA-catabolizing capacity of the adipose tissue, an improper high-fat and high-protein diet (dietary protein comprised of >20% BCAA) and increased catabolic pathways of BCAAs.[13,20,27,28] So far, only a few studies rated the changes in the BCAA levels after weight loss through diet and physical activity, but those studies were conducted on different populations (especially Caucasian and Japanese subjects) and used another model of body mass reduction program (based on nutritional recommendation and lifestyle intervention, but not a strictly composed diet). A 7-year prospective KORA study on a group of Caucasian patients with obesity showed a significant correlation between the average percentage increase in body weight and the increase in the BCAA, phenylalanine, tyrosine, and glutamate levels.[29] In our study, we observed that the valine, isoleucine and leucine levels increased (Table 1) despite the body mass reduction. Tochikubo et al. noted that a 3-month diet and exercise intervention based on individual dietary guidance caused a normalization in circulating BCAA.[30] In their study on Japanese subjects, Tochikubo et al. first observed that the initial plasma concentrations of AAs predict the success or lack thereof of a 3-month standardized diet and exercise weight loss program.[30]

The 1-year body mass reduction program based on lifestyle intervention (changes in diet and exercise habits) conducted by Reinehr et al., showed an increased level of serine, glutamine and methionine, but not proline, after the body mass reduction in a group of German children with obesity.[31] Wahl et al. described that the proline levels were reduced in children suffering from obesity compared to children with normal weight.[26] Moreover, Wahl et al. demonstrated that methionine and glutamine were diminished at baseline in children with obesity who reduced weight during lifestyle intervention, as compared with

children without the body mass reduction in the same kind of intervention.[26] The same relationship was described by Pathmasiri et al. in a study on an adult population with obesity, which leads to the hypothesis that dysregulation in the AA levels might be a consequence of poor lifestyle habits (diet and exercise).[32]

Some inconsistencies between our findings and the data obtained from previous studies were found. These differences may have been caused by different duration and methods of the weight reduction program, or by additional factors, such as the ethnicity or age of the study population, baseline BMI values and the level of weight loss achieved, or the protein content of the patients' normal diet. The current study was conducted on Polish patients (Caucasian race), while the previous study involved mainly Asian populations. In our study, the subjects were hospitalized for 3 weeks in a controlled environment. Additionally, each patient received the same type of a hypocaloric diet based on a 25–30% reduction in caloric dietary intake compared to total energy requirement. To eliminate the possible effect of diet composition on the levels of circulating AAs, a diet with an identical composition and sources of macronutrients (especially proteins) was administered to all patients. Moreover, the mean BMI in our study population after the weight loss program was lower, but still above 35 kg/m^2, which could account for the differences in the AA changes in our study compared to previous data.

Conclusions

This study is the first to describe the changes in 42 free AA profiles during a 3-week body mass reduction program in adult Polish patients with obesity. Our study shows that the metabolic profile of patients undergoing a strictly controlled weight reduction program were characterized by high dynamics of change and were visible after 3 weeks of body mass reduction.

The 3-week diet and physical activity program caused significant changes in body mass and biochemical parameters (e.g., the fasting glucose and insulin levels, HOMA-IR, CRP, and TG) and changes in free AA profiles. We observed that the levels of 10 out of the 42 AAs measured were significantly higher after weight loss. The highest differences in serum levels were observed for the following metabolites: glycine, α-amino-n-butyric acid, proline, and glutamine. Some variations between our findings and the data obtained from previous studies were found. These differences may have been caused by different duration and methods of the weight reduction program, or by additional factors, such as the ethnicity or age of the study population, baseline BMI values and the level of weight loss achieved, the protein content of the patients' normal diet, or the impact of physical activity on the metabolism of AA. To better understand these changes, future studies should involve a long-term program with more patients.

References

1. Baboota R, Bishnoi M, Ambalam P, et al. Functional food ingredients for the management of obesity and associated co-morbidities: A review. *J Funct Foods*. 2013;5:997–1012.
2. Conroy KP, Davidson IM, Warnock M. Pathogenic obesity and nutraceuticals. *Proc Nutr Soc*. 2011;70:426–438.
3. Patti GJ, Yanes O, Siuzdak G. Innovation: Metabolomics: The apogee of the omicstrilogy. *Nat Rev Mol Cell Biol*. 2012;13:263–269.
4. Wu G. Amino acids: Metabolism, functions and nutrition. *Amino Acids* 2009;37:1–17.
5. Wang TJ, Larson MG, Vasan RS. Metabolite profiles and the risk of developing diabetes. *Nat Med*. 2011;17:448–453.
6. Morris C, O'Grada C, Ryan M, et al. The relationship between BMI and metabolomic profiles: A focus on amino acids. *Proc Nutr Soc*. 2012;71:634–638.
7. Wery JP. Application of proteomics technologies to biomarker discovery and development: Challenges and solutions. *Curr Sep*. 2007;22:15–17.
8. Mayeux R. Biomarkers: Potential uses and limitations. *NeuroRx*. 2004; 1:182–188.
9. Chevalier S, Marliss EB, Morais JA, et al. Whole-body protein anabolic response is resistant to the action of insulin in obese women. *Am J Clin Nutr*. 2005;82:355–365.
10. Newgard CB, An J, Bain JR, et al. A branched-chain amino acid-related metabolic signature that differentiates obese and lean humans and contributes to insulin resistance. *Cell Metab*. 2009;9:311–326.
11. McCormack SE, Shaham O, McCarthy MA, et al. Circulating branched-chain amino acid concentrations are associated with obesity and future insulin resistance in children and adolescents. *Pediatr Obes*. 2013;8:52–61.
12. Yamakado M, Tanaka T, Nagao K, et al. Plasma amino acid profile is associated with visceral fat accumulation in obese Japanese subjects. *Clin Obes*. 2012;2:29–40.
13. Marti FPJ, Montoliu I, Collino S, et al. Topographical body fat distribution links to amino acid and lipid metabolism in healthy non obese women. *PLoS One*. 2013;8:e73445.
14. Held PK, White L, Pasquali M. Quantitative urine amino acid analysis using liquid chromatography tandem mass spectrometry and aTRAQ reagents. *J Chromatogr B*. 2011;879:2695–2703.
15. Matysiak J, Dereziński P, Klupczyńska A, et al. Effects of a honeybee sting on the serum free amino acid profile in humans. *PLoS One*. 2014;9:e103533.
16. Xia J, Sinelnikov IV, Han B, et al. MetaboAnalyst 3.0: Making metabolomics more meaningful. *Nucleic Acids Res*. 2015;43:W251–257.
17. Blackburn G. Effect of degree of weight loss on health benefits. *Obes Res*. 1995;3:211–216.
18. Foss-Freitas MC, Foss MC. Comparison of HOMA, QUICKI and forearm metabolic data in humans. *Braz J Med Biol Res*. 2004;37:663–668.
19. Song Y, Manson J, Tinker L. Insulin sensitivity and insulin secretion determined by homeostasis model assessment and risk of diabetes in a multiethnic cohort of women. *Diabetes Care*. 2007;30:1747–1752.
20. Oberbach A, von Bergen M, Bluher S. Combined serum proteomic and metabolomic profiling after laparoscopic sleeve gastrectomy in children and adolescents. *J Laparoendosc Adv Surg Tech A*. 2012;22: 184–188.
21. Laferrere B, Reilly D, Arias S, et al. Differential metabolic impact of gastric bypass surgery versus dietary intervention in obese diabetic subjects despite identical weight loss. *Sci Transl Med*. 2011;3:80–82.
22. Perez-Cornago A, Brennan L, Ibero-Baraibar I, et al. Metabolomics identifies changes in fatty acid and amino acid profiles in serum of overweight older adults following a weight loss intervention. *J Physiol Biochem*. 2014;70:593–602.
23. Shah SH, Crosslin DR, Haynes CS. Branched-chain amino acid levels are associated with improvement in insulin resistance with weight loss. *Diabetologia*. 2012;55:321–330.
24. Herman MA, She P, Peron OD. Adipose tissue branched chain amino acid (BCAA) metabolism modulates circulating BCAA levels. *J Biol Chem*. 2010;285:11348–11356.
25. Lips MA, van Klinken JB, van Harmelen V. Roux-en-Y gastric bypass surgery, but not calorie restriction, reduces plasma branched-chain amino acids in obese women independent of weight loss or the presence of type 2 diabetes. *Diabetes Care*. 2014;37:3150–3156.

26. Wahl S, Yu Z, Kleber M, et al. Childhood obesity is associated with changes in the serum metabolite profile. *Obes Facts*. 2012;5:660–670.
27. O'Connell TM. The complex role of branched chain amino acids in diabetes and cancer. *Metabolites*. 2013;3:931–945.
28. She P, Van Horn C, Reid,T et al. Obesity-related elevations in plasma leucine are associated with alterations in enzymes involved in branched-chain amino acid metabolism. *Am J Physiol Endocrinol Metab*. 2007;293:E1552–1563.
29. Wahl S, Vogt S, Stückler F, et al. Multi-omic signature of body weight change: Results from a population-based cohort study. *BMC Medicine*. 2015;13:48.
30. Tochikubo O, Nakamura H, Jinzu H, et al. Weight loss is associated with plasma free amino acid alterations in subjects with metabolic syndrome. *Nutrition & Diabetes*. 2016;6:e197;1–6.
31. Reinehr T, Wolters B, Knop C, et al. Changes in the serum metabolite profile in obese children with weight loss. *Eur J Nutr*. 2015,54:173–181.
32. Pathmasiri W, Pratt KCD, Lutes L, et al. Integrating metabolomic signatures and psychosocial parameters in responsivity to an immersion treatment model for adolescent obesity. *Metabolomics*. 2012;8: 1037–1051.

The assessment of skeletal status in young patients with Turner syndrome by 2 densitometric techniques: Phalangeal quantitative ultrasound and dual energy X-ray absorptiometry

Beata Wikiera[1,A–D,F], Agata Mierzwicka[2,B,C], Aleksander Basiak[1,A–C], Jowita Halupczok-Żyła[2,B,C], Diana Jędrzejuk[2,A–C], Magdalena Cabała[3,B], Anna Noczyńska[1,A,E], Marek Bolanowski[2,A,E,F], Kornel Mikołajczyk[4,B,E], Zenon P. Halaba[5,A–F]

[1] Department and Clinic of Endocrinology and Diabetology for Children and Adolescents, Wroclaw Medical University, Poland
[2] Department and Clinic of Endocrinology, Diabetes and Isotope Therapy, Wroclaw Medical University, Poland
[3] Department of Pediatrics, Division of Propedeutics of Pediatrics and Rare Disorders, Wroclaw Medical University, Poland
[4] Faculty of Rehabilitation, The Józef Piłsudski University of Physical Education in Warsaw, Poland
[5] Department of Medical Simulation, University of Opole, Poland

A – research concept and design; B – collection and/or assembly of data; C – data analysis and interpretation; D – writing the article; E – critical revision of the article; F – final approval of the article

Advances in Clinical and Experimental Medicine, ISSN 1899-5276 (print), ISSN 2451-2680 (online) *Adv Clin Exp Med*. 2018;27(6):759–764

Address for correspondence
Zenon P. Halaba
E-mail: zhalaba@uni.opole.pl

Funding sources
None declared

Conflict of interest
None declared

Acknowledgements
We thank Prof. Laura K. Bachrach from Stanford University for her assistance in calculating the height-adjusted Z-score based on the Z-score calculator of the Bone Mineral Density in Childhood Study (BMDCS) for Hologic systems.

Received on December 18, 2016
Reviewed on February 26, 2017
Accepted on June 8, 2017

DOI
10.17219/acem/74598

Abstract

Background. Studies using dual energy X-ray absorptiometry (DXA) demonstrate a reduction in bone mineral density (BMD) in children and adolescents with Turner syndrome (TS). However, these studies do not take into account changes in bone size, which influence BMD in the case of short-statured patients. Phalangeal quantitative ultrasound (phQUS) measurements have shown an ability to reveal changes due to skeletal growth, aging, and bone and mineral disorders. There is limited data on bone mineral status in girls with TS assessed by 2 different techniques, i.e., DXA and phQUS.

Objectives. The aim of this study was to investigate the potential negative impact of TS on bone status and to assess whether densitometric values were related to former fractures.

Material and methods. In 43 TS girls aged 5–18 years, we evaluated bone status by 2 different densitometric techniques, DXA and phQUS.

Results. The mean lumbar spine areal bone mineral density (LS aBMD) Z-score was significantly lower than 0 (the hypothetical mean) compared to the reference population ($p < 0.001$). The mean LS aBMD height-adjusted Z-score did not differ significantly from 0. The amplitude-dependent speed of sound (Ad-SoS) Z-score was significantly lower than 0 compared with a Polish reference population. There were no significant differences between fractured and fracture-free patients as regards Ad-SoS Z-score and LS aBMD height-adjusted Z-score.

Conclusions. Girls with TS have normal bone density adjusted for height, but significantly decreased phQUS values. Neither DXA nor phalangeal Ad-SoS can identify young TS patients with former fractures.

Key words: fractures, quantitative ultrasound, Turner syndrome, dual energy X-ray absorptiometry

Introduction

An increased risk of fracture is a feature of Turner syndrome (TS). However, the reason for this is unclear, and forearm fractures have been estimated to be more prevalent in the TS population.[1] Some studies also reported an increase in fracture prevalence during childhood in these patients.[2] Exogenous recombinant human growth hormone (rhGH) is often used in childhood to increase height. The role of growth hormone (GH) treatment in promoting bone accrual has not yet been completely defined, although the administration of GH is known to increase bone mineral density (BMD) in children without TS.[3,4] Studies using dual energy X-ray absorptiometry (DXA) demonstrate a reduction in BMD in children and adolescents with TS.[5–7] However, these studies do not take into account changes in bone size, which influence BMD in the case of short-statured patients. DXA studies, when adjusted for bone size, find no differences in volumetric BMD (vBMD) between TS girls and controls.[8] Peripheral quantitative computed tomography (pQCT) is able to provide precise measurements of 3-dimensional bone density without being influenced by bone size. In TS girls, pQCT data suggests that cortical density is reduced with sparing of trabecular bone.[9] In recent years, another promising method of assessing skeletal status was introduced. This method is based on ultrasound waves, which are transmitted through the bone tissue. Phalangeal quantitative ultrasound (phQUS) measurements have demonstrated an ability to reveal changes due to skeletal growth, aging, and bone and mineral disorders.[10–14] Quantitative ultrasound (QUS) is also devoid of ionizing radiation, and is cost-effective, easy to use and portable – all highly desirable features in pediatrics. There is data on girls with TS whose bone mineral status was assessed by 2 different techniques, i.e., DXA and phQUS. Despite its pitfalls, DXA is recommended as a monitoring tool in children with chronic disease who are at risk of developing osteoporosis; phQUS, however, is able to provide measurements of bone quality without being influenced by bone size. The objective of our study was to assess bone status in young girls with TS by 2 different densitometric techniques, DXA and phQUS, and to evaluate the relationship between low bone density and the prevalence of fracture.

This is the first study to concurrently examine the lumbar spine (LS) BMD height-adjusted Z-score and amplitude-dependent speed of sound (Ad-SoS) Z-score in Polish TS girls.

Material and methods

Patients

In the study, 43 Caucasian Polish girls with TS aged 13.7 ±3.4 years (range 5.3–18.3) were enrolled as outpatients to the Department and Clinic of Endocrinology and Diabetology for Children and Adolescents or the Department and Clinic of Endocrinology, Diabetes and Isotope Therapy of Wroclaw Medical University, Poland. They were sent an invitation with an informational letter. After consent was given, a questionnaire detailing fracture history was completed by the participants and/or their parents or guardians. The diagnosis of TS was made by karyotyping (45,X = 22, deletion = 4 and mosaic = 17). The clinical characteristics of the study group are presented in Table 1.

Table 1. Clinical findings in TS girls

Variable	Mean ±SD (range)	p-value
Age [years]	13.7 ±3.4 (5.3–18.3)	NA
Height SDS	–1.9 ±1.1 (–5.4–0.3)	0.001*
Weight SDS	–0.26 ±1.3 (–2.0–3.6)	NS*
BMI SDS	1.1 ±1.7 (–1.5–4.8)	0.01*
Age at diagnosis [years]	6.1 ±4.9 (0.1–15.1)	NA
Age at start of rhGH therapy [years]	8.1 ±3.9 (3.6–14.3)	NA
Cumulative dose of rhGH [mg]	2375 ±1802	NA
Ad-SoS Z-score	–1.1 ±1.26 (–3.9–1.8)	0.001*
LS aBMD Z-score	–0.84 ±1.04 (–3.9–0.9)	0.001*
LS aBMD height-adjusted Z-score	–0.21 ±1.1 (–3.7–1.6)	NS*

* comparison of SDS axiological and Z-score densitometric variables with the hypothetical mean of 0.0; SDS – standard deviation score; BMI – body mass index; rhGH – recombinant human growth hormone; Ad-SoS – amplitude-dependent speed of sound; LS aBMD – lumbar spine areal bone mineral density; NS – not significant; NA – not applicable.

None of our patients suffered from other conditions known to be associated with disrupted mineral metabolism. Recombinant human growth hormone was administered at a dose of 0.33 mg/kg/week. In all patients diagnosed before puberty, pubertal development was induced at the age of 12 with the most physiological form of estrogen available for replacement. Starting from a daily dose of 0.25 mg, 17β-estradiol was administered orally in increasing doses. Progesterone was added after at least 1 year of estrogenization. In case of a late diagnosis of TS, rhGH was administered first, and pubertal induction began 1 year later. Twenty-three girls had been treated with estrogens and only 6 with hormone replacement therapy (HRT).

Study design

In order to assess skeletal status in all patients, we evaluated LS BMD by DXA, and Ad-SoS using QUS. Phalangeal QUS results were compared with reference data for

Polish girls and the Ad-SOS Z-score was calculated.[13,14] From the DXA results – in order to avoid misdiagnosis in the case of the assessment of short individuals – we calculated LS aBMD height-adjusted Z-score based on the Z-score calculator of the Bone Mineral Density in Childhood Study (BMDCS) for Hologic Systems, which was sponsored by the Eunice Kennedy Shriver National Institute of Childhood and Human Development (NICHD). The normative data from this project is currently considered to be the gold standard for pediatric norms.[15] The LS aBMD height-adjusted Z-score deals better with the stature issue than bone mineral apparent density (BMAD) Z-score.[16] Standing height was measured with a floor-mounted stadiometer, body weight was measured to the nearest 0.1 kg with a standard medical scale, and body mass index (BMI) was calculated [kg/m^2]. Height, weight, and BMI were expressed as a standard deviation score (SDS) and were calculated using references from the Polish general population.

Informed verbal consent was obtained from all girls and written consent was given by parents/guardians and the girls who were older than 18 years. The study was approved by the Ethics Committee at Wroclaw Medical University.

Assessment of bone mineral status and the prevalence of fracture

Phalangeal QUS was measured using a DBM Sonic Bone Profiler (Igea, Carpi, Modena, Italy), which measures the amplitude-dependent speed of sound [m/s] at the proximal phalanges of dominant-hand fingers. Ad-SoS [m/s] was measured in the distal metaphyses of the proximal phalanges of the 2nd–5th fingers of the dominant hand, taking into account the first signal with an amplitude of at least 2 mV at the receiving probe. Thus, the measured speed of sound is specified as "amplitude-dependent." All phQUS measurements were performed by the same operator (ZPH). The precision error for QUS results was previously established by 5 serial measurements and expressed as the root-mean-square coefficient of variation (RMS-%CV). RMS-%CV for Ad-SoS was 0.64%.

Lumbar spine areal bone mineral density (LS aBMD) was measured by a Discovery W densitometer (Hologic Inc., Bedford, USA) using APEX software (release 4.5.2.1, Hologic Inc.), and the LS aBMD Z-score was calculated. The coefficient of precision was about 1% for LS aBMD.

For all patients, the frequency and severity of injury and the sites of fractures were recorded and classified according to the Landin severity scale.[17]

Statistical analysis

From the phQUS and DXA results obtained, Z-scores were calculated as the difference between the patient's value and the age-specific mean, divided by the reference group's standard deviation (SD) [Z-score = (test result for patient – age-specific mean in reference population)/age-specific SD in reference population].

All calculations were done using R v. 3.2.4 (R Foundation for Statistical Computing, Vienna, Austria). Descriptive statistics were presented as mean values, standard deviations, and value ranges for continuous variables. Distribution normality was tested by the Shapiro-Wilk test of normality. In the case of nonparametric data, the Yeo-Johnson transformation was used to reduce skewness and to approximate normality. For a comparative analysis of normally distributed variables, the ANOVA algorithm, Student's t-test, and multiple comparisons of means by Tukey contrasts were used. For comparative analysis of non-normal distributed variables, the Fisher-Pitman permutation test was used. Depending on the distribution of the variables analyzed, Pearson's or Spearman's correlation coefficients were used to estimate the associations between 2 variables. Significance was assumed at $p < 0.05$.

Results

A total of 43 girls with genetically confirmed TS aged 5–18 years participated in the study. The mean height SDS was significantly below that of age-matched Polish girls, whereas the mean weight SDS did not differ significantly from that of age-matched Polish girls, and the mean BMI SDS was significantly greater (Table 1). Of the 43 girls, 7 (16%) were prepubertal, 22 (51%) had reached Tanner stage 2 or higher pubarche or breast development without menarche, and 14 (33%) were postmenarche. Although the mean LS aBMD Z-score was significantly lower than 0 (the hypothetical mean) when compared with a reference population ($p = 0.001$), the mean LS aBMD height-adjusted Z-score did not differ significantly from 0 (Fig. 1). The Ad-SoS Z-score was significantly lower than 0 compared to a Polish reference population ($p = 0.001$) (Fig. 2). The LS aBMD height-adjusted Z-score was ≤–2 in 1 out of 43 girls (2%), and the Ad-SoS Z-score was ≤–2 in 11 out of 43 girls (26%). None of the patients reported pathological fractures. Nine girls had fractures caused by medium-force-trauma (21%), including 1 patient who reported 2 fractures. All fractures involved the appendicular skeleton, but not vertebral or femoral sites. We did not find significant differences between patients with and without fractures as regards the Ad-SoS and LS aBMD height-adjusted Z-scores. Only 1 girl, who had sustained 2 fractures, had an LS aBMD height-adjusted Z-score of <–2; the others showed normal values. The Ad-SoS Z-score was ≤–2 in 3 girls with a positive history of fracture (including the girl with 2 fractures). We did not find any differences in Ad-SoS and BMD values in relation to karyotype or age of diagnosis. The DXA and QUS parameters did not correlate with age at the start of GH therapy and cumulative doses of GH. The LS BMD values differed significantly between girls with breast Tanner stage 4 or lower (mean ±SD: –0.39 ±1.06), and those with stage 5 (mean ±SD: 0.87 ±0.64) ($p < 0.03$). Ad-SoS

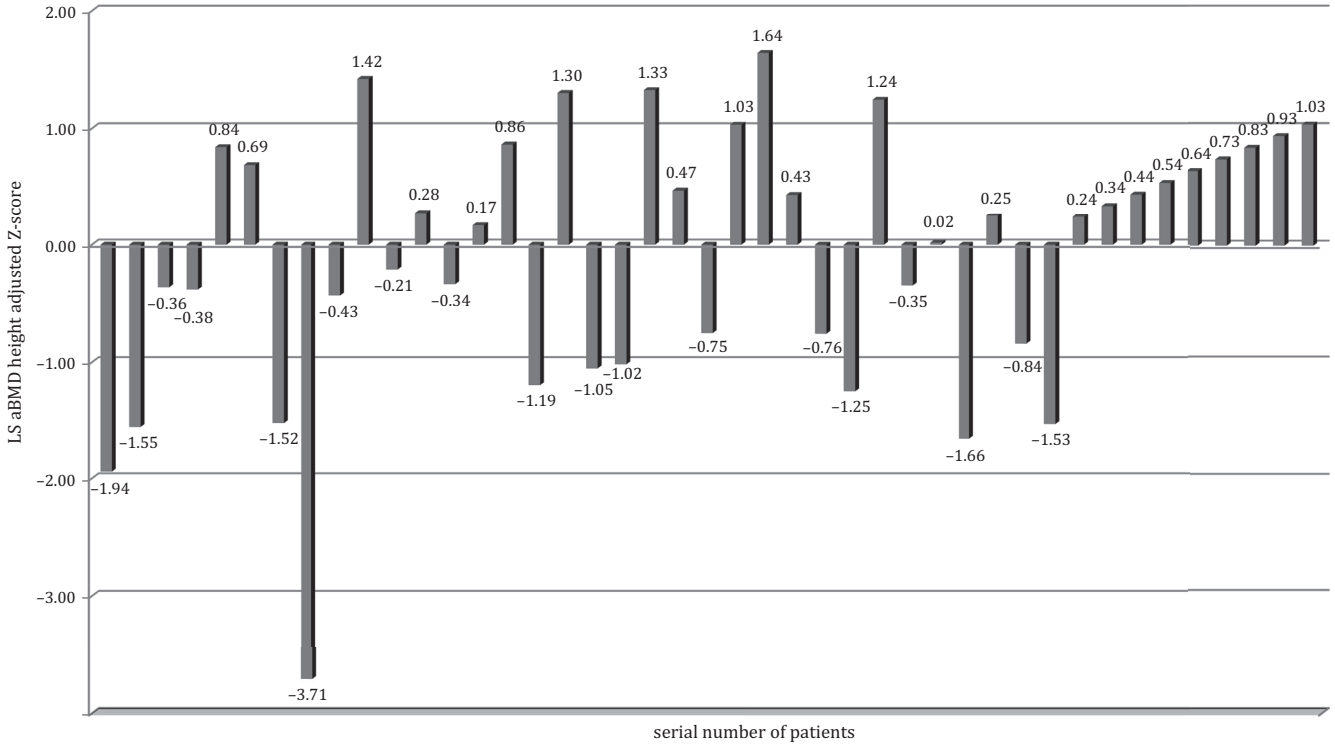

Fig. 1. Individual values of LS aBMD height-adjusted Z-score

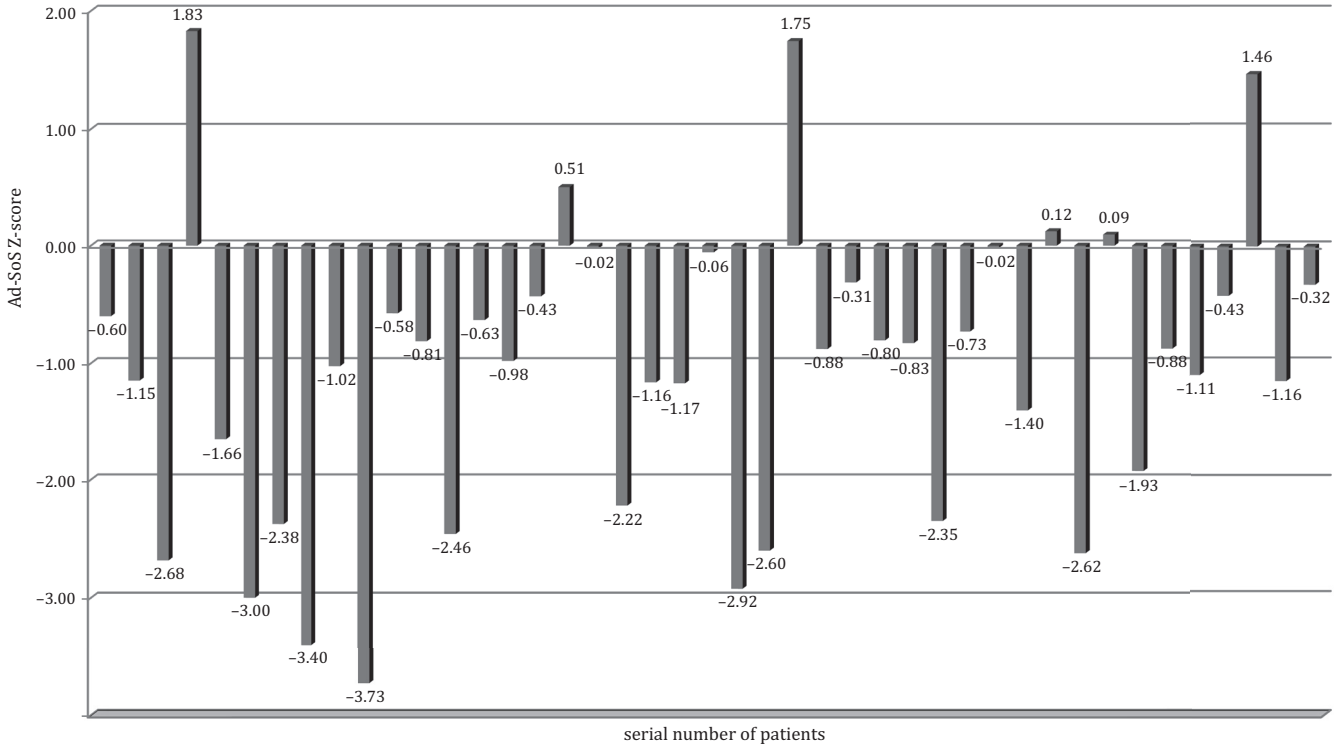

Fig. 2. Individual values of Ad-SoS Z-score

values – but not DXA values – showed only a significantly negative correlation with the presence of menstrual disturbances ($p < 0.03$).

Discussion

Although short stature is the most common clinical feature of TS, skeletal abnormalities encompass more than poor linear growth. One of the biggest concerns is that

of increased fracture risk and decreased bone density. Studies using DXA show decreased BMD, but small size leads to underestimation, and when the results are adjusted for body size, patients with TS usually have normal BMD in the spine, i.e., in trabecular bone.[2,18,19] This phenomenon also occurred in our study, showing that apparent BMD may be misleading when evaluating patients with short stature. Although the majority of studies indicate that the abnormalities seem to be only in cortical bone, some studies show compromised trabecular microarchitecture in patients with TS.[20,21] However, reduced cortical BMD in young TS patients is not proven to lead to increased fractures.[22–24]

We assessed the skeletal status of a group of young females with TS at 2 different skeletal sites using 2 different densitometric techniques. Phalangeal QUS measurements have shown an ability to reveal changes due to skeletal disorders and seem to be less influenced by bone size.[10–12] Furthermore, as proximal phalanges of the hands consist primarily of cortical bone (>60%), a phalangeal QUS evaluation may provide more information on bone health in TS girls than DXA. Our patients had statistically significantly lower Ad-SoS values compared to healthy Polish girls, but not LS BMD values after adjusting for height. These findings are in agreement with other studies demonstrating that in young TS girls, at a site with predominantly trabecular bone (i.e., the lumbar spine), BMD does not differ from controls after adjusting for body size.[2,9,18,19,25] However, reduced BMD may be present at sites of predominantly cortical bone, such as the 1/3 distal radius.[23] Also, the studies that used pQCT, a method which is able to independently provide measurements of 3-dimensional bone density and an assessment of trabecular and cortical bone density, have revealed significantly reduced cortical volumetric BMD (vBMD) and cortical thickness at some sites, and lower bone strength.[20–22] Holroyd et al. showed by this method not only a significant reduction in cortical vBMD at the proximal radius, but in cortical thickness as well (Z-score of –2.58 and –2.89, respectively).[9] Moreover, they found no differences in the total vBMD Z-score or the trabecular vBMD Z-score at the distal radius. Using ultrasound methods, comparable results were obtained by Zuckerman-Levin et al. and Vierucci et al.[24,26] As in our study, they found reduced phalangeal Ad-SoS, and radial and tibial SoS in girls and women with TS. As with pQCT data, abnormal QUS results may imply structural abnormalities in cortical bone in TS. In contrast, Soucek et al. questioned the findings that the cortical BMD is decreased in TS. They concluded that the partial volume effect is probably responsible for this outcome.[27] The fracture prevalence in our patients was 21%, and was similar to other observations.[28,29] This percentage is not higher than in a healthy population, because fractures are also common in youth, with 1/3 of all children sustaining at least 1 fracture before the age of 17 years.[30,31] Our finding varies from a paper by Vierucci et al.[26] They found a slightly increased risk of fracture in TS girls. In the study, 62.5% of their TS patients had an Ad-SoS Z-score of <–2 and only 1 TS patient with positive history of fracture had normal QUS values, whereas 67% of our TS girls with a previous history of fracture had an Ad-SoS Z-score of >–2. We also did not find any differences in Ad-SoS values between TS girls with and without a positive history of fracture. Unfortunately, we did not assess bone transmission time (BTT), which was shown by Vierucci et al. to have a strong correlation with previous fractures. These differences are difficult to explain. Perhaps this conflicting data resulted from the earlier age of our patients at the start of rhGH therapy, but we found no correlation between QUS values and the onset of GH treatment. Also, the relatively small number of subjects included in these studies may be behind the dissimilarities encountered. Unlike Vierucci et al., we examined the dominant hand, because the Polish reference values were calculated on the basis of dominant hand measurements,[14] but studies by Shönau et al. and Baroncelli et al. have showen that there is no significant difference between measurements of the two hands.[32,33] Although GH administration, the standard treatment for TS patients, is considered to promote bone accrual and strength, we found no correlation between the cumulative dose of GH and densitometric results.[21] Similar results have been obtained by other authors.[5,34,35] Furthermore, karyotype did not influence densitometric Z-score values, which was also in an agreement with previous studies.[34,36]

Our study may have been limited by its cross-sectional design and the small number of subjects studied. However, the rarity of TS limits the potential for enrollment. Indeed, other studies assessing skeletal status in young TS patients encompass a similar number of subjects. A longitudinal study in patients with TS is in progress, and the results of this study may furnish further important data.

Conclusions

We concluded that TS girls have normal bone density adjusted for height, but significantly decreased phQUS values. Neither DXA nor phalangeal Ad-SoS can identify young TS patients with former fractures.

References

1. Gravholt CH, Vestergaard P, Hermann AP, Mosekilde L, Brixen K, Christiansen JS. Increased fracture rates in Turner's syndrome: A nationwide questionnaire survey. *Clin Endocrinol*. 2003;59:89–96.
2. Ross JL, Long LM, Feuillan P, Cassorla F, Cutler GB Jr. Normal bone density of the wrist and spine and increased wrist fractures in girls with Turner's syndrome. *J Clin Endocrinol Metab*. 1991;73:355–359.
3. Saggese G, Baroncelli GI, Bertoelloni S, Barsanti S. The effect of long-term growth hormone (GH) treatment on bone mineral density in children with GH deficiency. Role of GH in the attainment of peak bone mass. *J Clin Endocrinol Metab*. 1996;81:3077–3083.
4. Conway GS, Szarras-Czapnik M, Racz K, et al. Treatment for 24 months with recombinant human GH has a beneficial effect on bone mineral density in young adults with childhood-onset GH deficiency. *Eur J Endocrinol*. 2009;160(6):899–907.

5. Aycan Z, Cetinkaya E, Darendeliler F, et al. The effect of growth hormone treatment on bone mineral density in prepubertal girls with Turner syndrome: A multicentre prospective clinical trial. *Clin Endocrinol* (*Oxf*). 2008;68(5):769–772.
6. Davies MC, Gulekli B, Jacobs HS. Osteoporosis in Turner's syndrome and other forms of primary amenorrhoea. *Clin Endocrinol*. 1995;43: 741–746.
7. Landin-Wilhelmsen K, Bryman I, Windh M, Wilhelmsen L. Osteoporosis and fractures in Turner syndrome: Importance of growth promoting and oestrogen therapy. *Clin Endocrinol*. 1999;51:497–502.
8. Nadeem M, Roche EF. Bone health in children and adolescent with Turner syndrome. *J Pediatr Endocrinol Metab*. 2012;25:823–833.
9. Holroyd CR, Davies JH, Taylor P, et al. Reduced cortical bone density with normal trabecular bone density in girls with Turner syndrome. *Osteoporos Int*. 2010;21:2093–2099.
10. Pluskiewicz W, Łuszczyńska A, Halaba Z, Drozdzowska B, Sońta-Jakimczyk D. Skeletal status in survivors of childhood acute lymphoblastic leukemia assessed by quantitative ultrasound: A pilot cross-sectional study. *Ultrasound Med Biol*. 2002;28:1279–1284.
11. Pluskiewicz W, Adamczyk P, Drozdzowska B, Pyrkosz A, Halaba Z. Quantitative ultrasound and peripheral bone densitometry in patients with genetic disorders. *Ultrasound Med Biol*. 2006;32:523–528.
12. Halaba ZP. The usefulness of phalangeal quantitative ultrasound in the assessment of skeletal status in children and adolescents. *Curr Med Imaging Rev*. 2008;4:194–201.
13. Drozdzowska B, Pluskiewicz W, Halaba Z, Misiołek H, Beck B. Quantitative ultrasound at the hand phalanges in 2850 females aged 7 to 77 yr: A cross-sectional study. *J Clin Densitom*. 2005;8(2):216–221.
14. Halaba ZP, Pluskiewicz W. Quantitative ultrasound in the assessment of skeletal status in children and adolescents. *Ultrasound Med Biol*. 2004;30(2):239–243.
15. Eunice Kennedy Shriver National Institute of Child Health and Human Development: Bone mineral density in childhood study. https://bmdcs.nichd.nih.gov/zscore.htm Accessed December 14, 2015 – April 10, 2016.
16. Zemel BS, Leonard MB, Kelly A, et al. Height adjustment in assessing dual energy X-ray absorptiometry measurements of bone mass and density in children. *J Clin Endocrinol Metab*. 2010;95:1265–1273.
17. Landin LA. Fracture patterns in children. Analysis of 8,682 fractures with special reference to incidence, etiology and secular changes in a Swedish urban population 1950–1979. *Acta Orthop Scand Suppl*. 1983;202:1–109.
18. Gravholt CH, Lauridsen AL, Brixen K, Mosekilde L, Heickendorff, Christiansen JS. Marked disproportionality in bone size and mineral, and distinct abnormalities in bone markers and calcitropic hormones in adult Turner syndrome: A cross-sectional study. *J Clin Endocrinol Metab*. 2002;87:2798–2808.
19. Bakalov V, Chen M, Baron J, et al. Bone mineral density and fractures in Turner syndrome. *Am J Med*. 2003;115(4):259–264.
20. Hansen S, Brixen K, Gravholt CH. Compromised trabecular microarchitecture and lower finite element estimates of radius and tibia bone strength in adults with turner syndrome: A cross-sectional study using high-resolution-pQCT. *Bone Miner Res*. 2012;27(8):1794–1803.
21. Nour MA, Burt LA, Perry RJ, Stephure DK, Hanley DA, Boyd SK. Impact of growth hormone on adult bone quality in Turner syndrome: A HR-pQCT study. *Calcif Tissue Int*. 2016;98(1):49–59.
22. Bechtold S, Rauch F, Noelle V, et al. Musculoskeletal analyses of the forearm in young women with Turner syndrome: A study using peripheral quantitative computed tomography. *J Clin Endocrinol Metab*. 2001;86:5819–5823.
23. Bakalov VK, Axelrod L, Baron J, et al. Selective reduction in cortical bone mineral density in Turner syndrome independent of ovarian hormone deficiency. *J Clin Endocrinol Metab*. 2003;88:5717–5722.
24. Zuckerman-Levin N, Yaniv I, Schwartz T, Guttmann H, Hochberg Z. Normal DXA bone mineral density but frail cortical bone in Turner's syndrome. *Clin Endocrinol*. 2007;67:60–64.
25. Neely EK, Marcus R, Rosenfeld RG, Bachrach L. Turner syndrome adolescents receiving growth hormone are not osteopenic. *J Clin Endocrinol Metab*. 1993;76(4):861–866.
26. Vierucci F, Del Pistoia M, Erba P, Federico G, Saggese G. Usefulness of phalangeal quantitative ultrasound in identifying reduced bone mineral status and increased fracture risk in adolescents with Turner syndrome. *Hormones*. 2014;13(3):353–360.
27. Soucek O, Schonau E, Lebl J, Sumnik Z. Artificially low cortical bone mineral density in Turner syndrome is due to the partial volume effect. *Osteoporos Int*. 2015;26(3):1213–1218.
28. Bakalov V, Bondy CA. Fracture risk and bone mineral density in Turner syndrome. *Rev Endocr Metab Disord*. 2008;9(2):145–151.
29. Soucek O, Lebl J, Snajderova M, et al. Bone geometry and volumetric bone mineral density in girls with Turner syndrome of different pubertal stages. *Clin Endocrinol* (*Oxf*). 2011;74:445–452.
30. Cooper C, Dennison EM, Leufkens HG, Bishop N, van Staa TP. Epidemiology of Childhood Fractures in Britain: A study using the general practice research database. *J Bone Miner Res*. 2004;19:1976–1981.
31. Konstantynowicz J, Bialokoz-Kalinowska I, Motkowski R, et al. The characteristics of fractures in Polish adolescents aged 16–20 years. *Osteoporos Int*. 2006;16(11):1397–1403.
32. Schönau E, Radermacher A, Wentzlik U, Klein K, Michalk D. The determination of ultrasound velocity in the os calcis, thumb and patella during childhood. *Eur J Pediatr*. 1994;153:252–256.
33. Baroncelli GI, Federico G, Bertelloni S, et al. Bone quality assessement by quantitative ultrasound of proximal phalanxes of the hand in healthy subjects aged 3–21 years. *Pediatr Res*. 2001;49(5):713–718.
34. Nadeem M, Roche EF. Bone mineral density in Turner's syndrome and the influence of pubertal development. *Acta Paediatr*. 2014;103(1): e38–42.
35. Ari M, Bakalov VK, Hill S, Bondy CA. The effects of growth hormone treatment on bone mineral density and body composition in girls with turner syndrome. *J Clin Endocrinol Metab*. 2006;91:4302–4305.
36. Högler W, Briody J, Moore B, Garnett S, Lu PW, Cowell CT. Importance of estrogen on bone health in Turner syndrome: A cross-sectional and longitudinal study using dual-energy X-ray absorptiometry. *J Clin Endocrinol Metab*. 2004;89:193–199.

Quality control of riboflavin-treated platelet concentrates using Mirasol® PRT system: Polish experience

Elżbieta Lachert[1,A–D], Jolanta Kubis[1,A–D], Jolanta Antoniewicz-Papis[1,A–D], Aleksandra Rosiek[1,C], Jolanta Woźniak[1,B,C], Dariusz Piotrowski[2,B], Zofia Przybylska[2,B], Agata Mikołowska[1,A–D], Susanne Marschner[3,E,F], Magdalena Łętowska[1 E,F]

[1] Institute of Hematology and Transfusion Medicine, Warszawa, Poland
[2] Regional Blood Transfusion Center, Warszawa, Poland
[3] Terumo BCT Biotechnologies, Lakewood, USA

A – research concept and design; B – collection and/or assembly of data; C – data analysis and interpretation; D – writing the article; E – critical revision of the article; F – final approval of the article

Advances in Clinical and Experimental Medicine, ISSN 1899-5276 (print), ISSN 2451-2680 (online) *Adv Clin Exp Med*. 2018;27(6):765–772

Address for correspondence
Elżbieta Lachert
E-mail: elachert@ihit.waw.pl

Funding sources
None declared

Conflict of interest
None declared

Acknowledgements
The authors would like to thank Ms Krystyna Dudziak for her contribution and assistance.

Received on October 18, 2016
Reviewed on November 15, 2017
Accepted on February 9, 2017

Abstract

Background. The quality of platelet concentrates (PCs) is affected by preparation, storage, the type of container, and pathogen reduction technology (PRT). The Mirasol® Pathogen Reduction Technology (PRT) system (Terumo BCT Inc., Lakewood, USA), which uses riboflavin and ultraviolet (UV) light, has recently been proven effective against bacteria, viruses, parasites, and leukocytes.

Objectives. The aim of the study was to evaluate the effect of the Mirasol® PRT system, based on riboflavin and UV light exposure, on the most common in vitro platelet quality parameters of PCs prepared from whole blood-derived buffy coats.

Material and methods. The study included 15 trials (n = 15). For each trial, 2 PCs were used: 1 for treatment with the Mirasol® PRT system (M) and 1 for a control (C). In the M group, PCs were illuminated. In the C group, saline solution was added. PCs from groups M and C were stored at 20–24°C, with agitation. Samples were collected on days 1, 3 and 5 to determine platelet concentration, total platelet count/unit, mean platelet volume (MPV), power of hydrogen (pH), glucose and beta-thromboglobulin concentration (BTG), hypotonic shock response (HSR), aggregation, CD42b and CD62P expression, pCO_2, and pO_2.

Results. No significant differences in HSR or CD42b expression were observed between groups M and C. All pH values were stable during the whole storage period (7.1–7.5). On storage day 1, CD62P expression in group C was significantly higher than in group M. In the Mirasol® group, significantly higher glucose consumption was noted on storage days 3 and 5. On day 5, a 2–3-fold increase in BTG was observed in both groups as compared to day 1; on day 5, BTG concentration was 32% higher in group M than in group C. On all storage days, pCO_2 was comparable in groups M and C; lower pO_2 values were reported for group M.

Conclusions. In vitro results demonstrated that pH, HSR, aggregation, CD42b antigen expression, and MPV and platelet count parameters were comparable in groups M and C.

Key words: pathogen, platelets, inactivation

DOI
10.17219/acem/68901

Introduction

Blood and blood components have never been as safe as they are nowadays. Significant improvements have been made to safety through restricted donor selection, closed system preparation, implementation of higher sensitivity serological and molecular biology tests, and the exclusive use of quarantine plasma. Additionally, the implementation of the Quality Assurance (QA) system has greatly contributed to the higher quality of blood components.[1]

Regardless of those preventive measures, blood components are still not safe enough. We must constantly be prepared for new and emerging pathogens, pathogens for which no tests are yet available or for which tests are not routinely used. Such was the case in the 1970s, when thousands of hemophilia patients were infected with hepatitis C virus (HCV) when they were administered coagulation factor concentrates which were not subjected to inactivation.[2]

There is also another factor that needs to be considered as an additional risk of disease transmission, namely, migration. As a result of migration, diseases like malaria, Chagas disease, or West Nile virus, which are characteristic of one geographical region, may also appear in other geographical locations. The original sources of these pathogens are Africa, Mediterranean countries and occasionally Europe, but in the period of 1999–2003, these viruses spread to the territory of the United States and Canada, where the transfusion transmissible infection (TTI) risk for West Nile virus, for example, was calculated at 1.46–12.33 per 10,000 donations and resulted in the immediate implementation of screening tests (polymerase chain reaction – PCR) for single donations in all American blood banks.[3,4]

Not only viruses are a potential threat to blood safety. Statistical data regarding post-transfusion adverse reactions demonstrates a high risk of bacterial contamination for platelet concentrates (PCs) that are mostly stored at room temperature, which favors bacterial proliferation. Bacteria-related adverse reactions following PC transfusions have been estimated at 1/2000 transfusions.[5]

This explains why pathogen inactivation methods which were previously in use only for plasma fractionation are now becoming increasingly popular for inactivation in cellular blood components. Inactivation methods promise additional protection both from already known infectious agents and those yet unrecognized but which may pose a threat to safe blood supply. One such method is the Mirasol® Pathogen Reduction Technology (PRT) system (Terumo BCT Inc., Lakewood, USA) for pathogen inactivation in plasma and platelet concentrates. The system offers a nucleic acid-targeted pathogen reduction technique based on ultraviolet (UV) light and riboflavin. Riboflavin molecules form complexes with the nucleic acid of the pathogen. Exposure to UV light activates riboflavin causing a chemical alteration in the functional groups of the nucleic acid (primary guanine bases), rendering the pathogen unable to replicate. Although riboflavin is most effective for lipid-enveloped viruses, reports in the literature also describe reductions for the non-enveloped parvovirus B19, as well as for some bacteria and protozoa. Multicenter trials by Cardo et al. have shown the riboflavin method to be effective for killing *Leishmania* and other emerging plasma and platelet pathogens (5–7 log reduction).[6,7] Numerous studies have also confirmed this method to be effective for white blood cell inactivation. Clinical trials have proved the safety of Mirasol® PRT system-treated blood components and lack of neoantigen formation.[8–11]

Nowadays, the Mirasol® PRT system is in routine use in many European countries. In Poland, the system has been used since 2009 for pathogen inactivation in plasma, but in some regional blood transfusion centers also for PCs. In our country, more than 90% of pooled PCs for clinical use are buffy coat-derived, which explains why this type of PCs were dedicated for pathogen reduction technology.

Objectives

The objective of our study was to evaluate the quality parameters of buffy coat-derived PCs inactivated with the Mirasol® PRT system and stored for 5 days. The inactivation effect of the Mirasol® PRT system on in vitro cell quality in PCs was evaluated and the results were compared to quality parameters of untreated control platelets.

Material and methods

The experiments (n = 15) were performed with pairs of identical buffy coat-derived PCs. PC preparation was done according to current Polish blood transfusion service regulations.[1] The study included 15 pooled PCs obtained from buffy coats (150 buffy coats, 30 plasma units) by the use of whole blood centrifugation and separation of red blood cells and plasma. The procedure was performed in the Regional Blood Transfusion Center in Warszawa using the ATREUS system (Terumo BCT Inc., Lakewood, USA). Before pooling, the bags with buffy coats (65 mL each) were left without agitation for 18 h.

For each experiment, 2 PCs were used: 1 for treatment with the Mirasol® PRT system (M) and 1 for a control (C).

Platelet concentrate preparation

In sterile conditions (TSCD; Terumo BCT, Lakewood, USA), 10 units of ABO-compatible buffy coats and 2 units of plasma were pooled in 1000 mL bags (JMS, Hiroshima, Japan), mixed and transferred into 600 mL bags, then centrifuged at 2240 g/min for 4.5 min at 22°C (J-6 M/E; Beckman, Porton, UK) in order to obtain PCs. The PC parameters (volume, platelet concentration and total platelet count/unit) met the Mirasol® PRT system incoming product specifications. After centrifugation, all PCs were

pooled into 1 collective 1000 mL bag, mixed and left for 1 h without agitation. Each PC unit was then divided into 2 aliquots – one was transferred into the Mirasol® PRT system illumination bag (M) and the other was transferred into a control bag (C).

All PC units were stored at 20–24°C, with agitation.

Equipment handling and inactivation process

Prior to each illumination process, the PCs were identified by donation number and batch scanning. Riboflavin solution (500 µM) was added to the PC for PRT treatment (M) at a volume of 35 mL, while the same volume (35 mL) of saline solution (0.9% NaCl; Ravimed, Łajski, Poland) was added to the PC control group (C). After removing air, the Mirasol® illumination bags were inactivated for approx. 6 min (illuminator; 6.2 J/mL). All PCs were placed on a horizontal flatbed shaker at 20–24°C at 30 cycles/min (Helmer; Fresenius Kabi, Lake Zurich, USA).

Storage and sampling

Twenty-four h after buffy coat preparation and illumination, the first 20 mL study samples were collected in sterile conditions (TSCD; Terumo BCT) from both PC groups (M and C). Consecutive samples were collected on storage days 3 and 5. All riboflavin-treated PC bags were stored at no risk of exposure to light. PCs were not subjected to filtration as this is not a routine procedure in the Polish blood transfusion service.

Evaluation of in vitro platelet concentrates quality on 1st, 3rd and 5th day of storage

- Platelet concentration and mean platelet volume (MPV) were immediately tested on a hematological analyzer (Beckman Coulter ACD diff, High Wycombe, USA).
- Power of hydrogen (pH), pO_2 and pCO_2 concentration measurements were performed within 15 min of sample collection in aseptic conditions on a self-calibrated blood gas analyzer (Rapidlab®1260; Bayer HealthCare, Leverkusen, Germany).
- Hypotonic shock response (HSR) was determined using a 2-channel Lambda 12 spectrophotometer (Perkin Elmer, Waltham, USA) at a wavelength of 620 nm.
- The aggregation ability of cells in adenosine diphosphate (ADP) (Chrono-Lume®Reagents, Havertown, USA) was studied with a Chrono-Log aggregometer (Chrono-Log Corporation, Havertown, USA) using the turbidimetric method of light transmission which differentiates between PPP (platelet poor plasma) and PRP (platelet rich plasma) samples.
- Cytofluometric analysis was used to study antigen expression on the platelet surfaces. After plasma washing and paraformalehyde fixing, the platelets were incubated with monoclonal antibodies directed against CD42b and CD62P antigens (Beckman Coulter Co, Villepinte, France). We used monoclonal IgG1 class antibodies labeled with fluorescein isothiocyanate (FITC). Class IgG1 anti-murine antibodies were used as a negative control. Readings were performed on a Cytoron Absolute flow cytofluorometer (Ortho Diagnostics, New Jersey, USA); the labeled cell distribution and fluorescence intensity were observed as well.
- Glucose concentration was determined in Cobas Integra 400 Plus Roche biochemical analyzer (Roche Diagnostics Ltd., Rotkreuz, Switzerland).
- Beta-thromboglobulin (BTG) was determined with ELISA (Asserachrom β-TG kit, Asnières, France).

Statistical analysis

All reported values were calculated with a statistical software program STATISTICA (Tibco, Palo Alto, USA). The results are presented as mean and standard deviation (SD). The p-value for paired results was calculated with ANOVA, and $p < 0.05$ was considered significant.

Results

Study results are presented in Table 1 and in Fig. 1–6. Statistical significance was determined by comparing the results for PRT-treated PCs (M) and untreated PCs (C) on storage days 1, 3 and 5. The average PC volume after treatment and after collection of study samples was 227 mL in both the M and C groups (min volume: 183 mL; max volume: 327 mL). On storage days 3 and 5, 20 mL of PCs was collected in both PC groups (C, M). The volume decreased to 206 mL on day 3, and to 184 mL on day 5 of storage. For both study groups (C, M), the differences in volume prepared on each storage day were not statistically significant.

In both the C and M groups, the platelet (PLT) concentration in PCs decreased slightly with storage time, from $1316 \pm 208 \times 10^3/\mu L$ to $1275 \pm 212 \times 10^3/\mu L$ in group M PCs, and from $1338 \pm 209 \times 10^3/\mu L$ to $1288 \pm 182 \times 10^3/\mu L$ in control PCs (C). Statistical significance was observed for Mirasol®-treated PCs (M) and control PCs on storage days 1 ($p < 0.005$) and 3 ($p < 0.05$).

On storage day 1, the average platelet count/unit was $3.0 \pm 0.5 \times 10^{11}$ in both study groups, and on storage day 5 it was $2.3 \pm 0.5 \times 10^{11}$ in M and $2.4 \pm 0.4 \times 10^{11}$ in C. Platelet loss was mostly due to study sample collection. No statistical significance was found between the studied groups on individual storage days.

Statistically significant differences in MPV were observed for PCs in both study groups for storage days 1, 3 and 5 ($p < 0.005$, $p < 0.05$ and $p < 0.0005$, respectively). Over 5 days of storage, MPV decreased from 7.6 fL to 7.0 fL in group C and from 7.5 fL to 7.2 fL in group M.

The pH values in both groups increased slightly by storage day 3, and decreased by day 5 to 7.4 for C and to 7.2 for M. It is worth noting that the pH value in all studied PCs was very stable and ranged from 7.1 to 7.5 during the whole storage period. Statistical significance was observed when inactivated PCs were compared with control PCs on storage days 3 and 5 ($p < 0.0005$ and $p < 0.0005$, respectively).

We observed a 16% decrease of glucose concentration in PRT-treated PCs from day 1 to day 3 of storage and an 11% decrease in the control group. Glucose consumption increased on storage day 5 (25% for M and 12% for C group as compared to storage day 3). Statistical significance was found for storage days 3 and 5 ($p < 0.0005$ and $p < 0.0005$, respectively).

The same average values for HSR were observed in both groups for the whole storage period (about 80–90%). No statistical significance was observed when inactivated PCs were compared with control PCs on individual storage days (Fig. 1).

Table 1. Effect of Mirasol® PRT system on the quality of PCs

Parameters	Day 1			Day 3			Day 5		
	control (C)	Mirasol® PRT system (M)	p-value	control (C)	Mirasol® PRT system (M)	p-value	control (C)	Mirasol® PRT system (M)	p-value
Volume [mL]	227 ±32	227 ±31	>0.05	206 ±31	206 ±31	>0.05	184 ±31	184 ±31	>0.05
PLT concentration [$\times 10^3/\mu L$]	1338 ±209	1316 ±208	<0.005*	1293 ±173	1280 ±188	<0.05*	1288 ±182	1275 ±212	>0.05
Total PLTs [$\times 10^{11}$/unit]	3.0 ±0.5	3.0 ±0.5	>0.05	2.7 ±0.4	2.6 ±0.4	>0.05	2.4 ±0.4	2.3 ±0.5	>0.05
MPV [fL]	7.6 ±0.9	7.5 ±0.8	<0.005*	7.5 ±0.1	7.0 ±0.4	<0.05*	7.0 ±0.5	7.2 ±0.5	<0.0005*
pH	7.1 ±0.1	7.1 ±0.1	>0.05	7.5 ±0.1	7.4 ±0.1	<0.0005*	7.4 ±0.1	7.2 ±0.1	<0.0005*
Glucose [mg/dL]	231.6 ±12.2	228.5 ±12.7	>0.05	206.1 ±14.8	190.9 ±16.6	<0.0005*	181.0 ±18.5	143.5 ±27.7	<0.0005*

PLT – platelet; MPV – mean platelet volume; pH – power of hydrogen; * statistical significance.

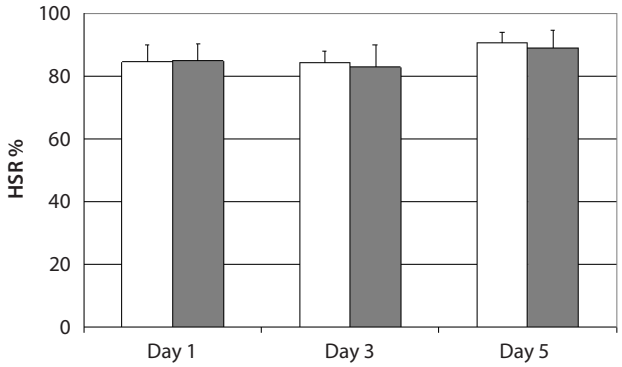

Fig. 1. Effect of Mirasol® PRT system on the quality of PCs – HSR [%]

☐ – Mirasol®; ■ – control.

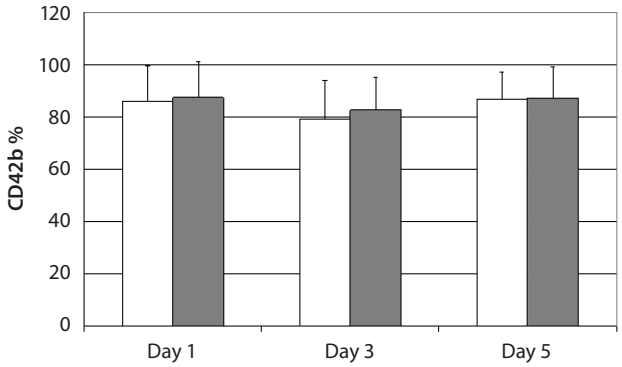

Fig. 2. Effect of Mirasol® PRT system on the quality of PCs – CD42b [%]

☐ – Mirasol®; ■ – control.

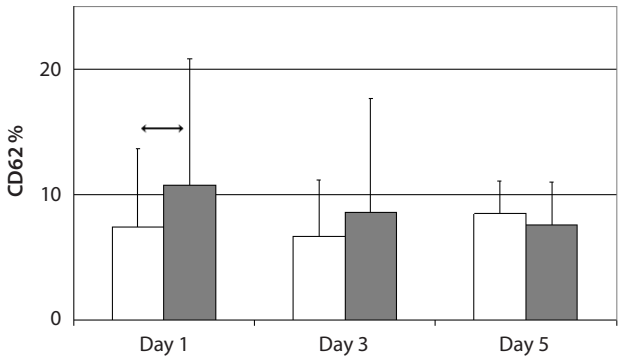

Fig. 3. Effect of Mirasol® PRT system on the quality of PCs – CD62 [%]

☐ – Mirasol®; ■ – control; ↔ – statistical significance.

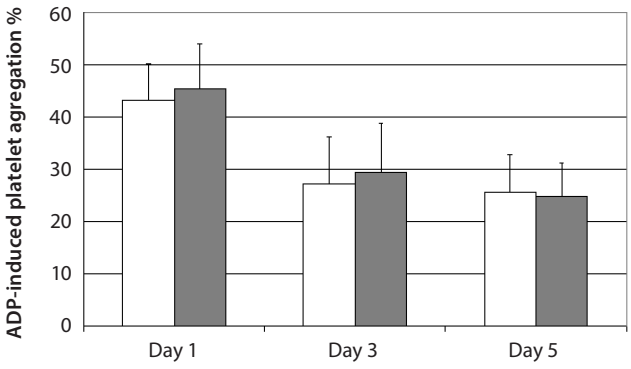

Fig. 4. Effect of Mirasol® PRT system on the quality of PCs – ADP-induced platelet aggregation [%]

☐ – Mirasol®; ■ – control.

Antigen expression on the surface of the platelets is one of the most sensitive platelet activation tests. The average CD42b expression in both study groups was observed at 80–90% and did not change significantly throughout storage. A slight decrease in the CD42b expression was observed on storage day 3 and it returned to the value of day 1 by storage day 5 (Fig. 2).

The CD62P antigen expression was slightly lower for group M as compared to group C on storage days 1 and 3. On storage day 5, the CD62P antigen expression in group M was slightly higher compared to group C. Statistical significance was found only for storage day 1 ($p < 0.05$) (Fig. 3).

The average ADP aggregation was observed at 43.3% for group M and at 45.4% for group C on storage day 1. By storage day 3, the aggregation value in group M dropped by 37% and in group C by 35%. On storage day 5, aggregation capability further decreased in both groups, to 25.6% in M and to 24.9% in C group. No statistical significance was observed (Fig. 4).

The concentration of beta-thromboglobulin, a protein found in the alpha granularity, increased with PC storage time and platelet activation. A 3-fold increase of BTG was observed in group M and more than a 2-fold increase in group C over 5 days of storage. Statistical significance was observed on storage day 5 ($p < 0.05$) (Fig. 5).

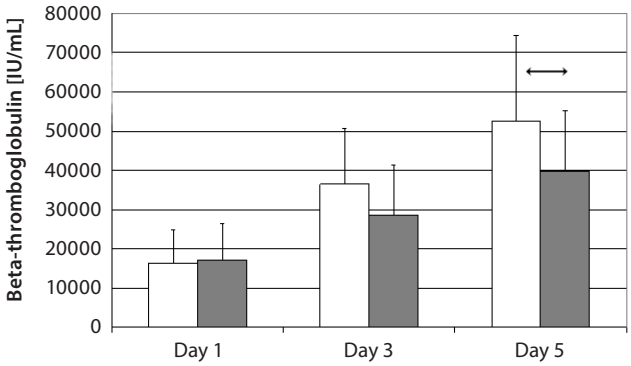

Fig. 5. Effect of Mirasol® PRT system on the quality of PCs – beta-thromboglobulin [IU/mL]

☐ – Mirasol®; ■ – control; ↔ – statistical significance.

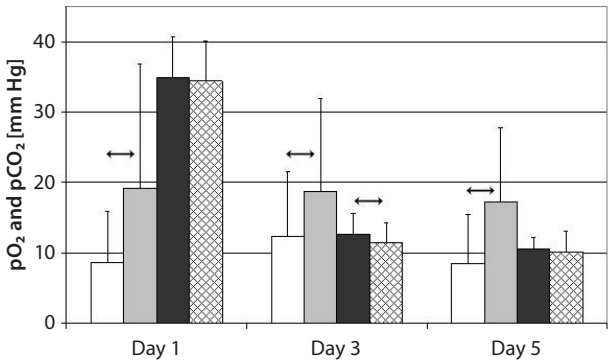

Fig. 6. Effect of Mirasol® PRT system on the quality of PCs – pO_2 and pCO_2 [mm Hg]

☐ – pO_2 Mirasol®; ■ – pO_2 control; ■ – pCO_2 Mirasol®; ☒ – pCO_2 control; ↔ – statistical significance.

The pCO_2 value decreased with storage in both PC groups. Statistical significance was observed on storage day 3 ($p < 0.0005$). The pO_2 values were significantly lower in inactivated PCs than in control PCs ($p < 0.05$, $p < 0.0005$ and $p < 0.005$ on respective days 1, 3 and 5) (Fig. 6).

Discussion

Transfusions of platelet concentrates are becoming more and more common for the prevention of bleeding. The ultimate aim of every blood transfusion service is therefore to prepare safe PCs of high therapeutic quality to induce hemostasis in the recipient's circulatory system. The methods of PC preparation in routine use are apheresis (from a single donor) or the conventional method from whole blood (from buffy coats or platelet rich plasma). Pooled buffy coats carry a higher risk of pathogen transmission as compared to PCs obtained from a single donor.[12] This is one of the reasons why we used PCs from buffy coats to evaluate the efficacy of PCs inactivated in the Mirasol® PRT system; the other reason is that this method of PC preparation is more common in Poland than the method of obtaining PCs from PRP.

The aim of the study was to evaluate the effect of PRT based on riboflavin and UV light exposure on PC functional characteristics. During collection, preparation and storage, PCs are subjected to procedures such as centrifugation, resuspension and agitation, which are responsible for platelet activation.[13] The platelet functional characteristics are then impaired and platelet survival time in the recipient's circulatory system may also be reduced. The Mirasol® PRT system may impose additional stress on the platelets.

The study aim was to evaluate the most common in vitro parameters of PRT-treated PCs.[13] One of the parameters that determines PC quality is the pH value. It is worth noting that PC storage bags, which facilitate free gas exchange, may cause PC alkalization (especially when platelet count is low) through excessive CO_2 diffusion from the plasma. Alkalization or low pH (<6.2) may correlate with low post-transfusion platelet viability.[14,15]

No additional effect of PRT treatment on the PC platelet count was determined. The platelet count decreased over time, as already demonstrated by Moroff et al., who evaluated this parameter in various kinds of PCs (illuminated, filtered, etc.) during a 5-day storage period.[16,17]

Many studies have shown that a drop in the pH during storage to 6.4 or 6.2 causes swelling of the platelets and a decrease in the number of transfused platelets. A pH value <6.1 has been reported to result in irreversible shape changes in transfused platelets and a pH value <6.2 results in a 50% decrease in the number of platelets remaining in circulation after transfusion and a 50% decrease in the half-life of the platelets in circulation.[17] These changes are believed to decrease the efficacy of transfused platelets and are the basis for the lower

pH limit for transfused platelets in the regulations. Murphy et al. observed the ideal pH value to be 6.8–7.4 and found that the mean platelet volume and platelet count are equally significant for PC quality control.[18] According to Rinder and Smith, most authors claim that the pH of platelets stored in gas-permeable bags should be closer to 7.0. In fact, considering the low platelet yields found in PCs, there is more concern about an alkaline pH (close to or >8.0), since storage at this pH is also known to be deleterious to platelet function and post-transfusion recovery.[19] The degranulation of stored platelets at low pH was one factor that led us to examine if lesser but significant degrees of platelet release and activation occurred under more physiological storage conditions.[18]

Platelets stored in an acidic environment (pH < 6.0) lose their oxygen-absorbing capability, undergo degranulation and are rapidly removed from the recipient's circulatory system.

A statistical significance in pH value in group M was observed on storage days 3 and 5, although the values were within normal range. On storage day 3, slight PC alkalization was noted in both PCs groups (C and M), but it was attributed to the procedure of sample collection, which resulted in a lower volume and a lower platelet count, while the O_2/CO_2 exchange surface remained the same.

Li et al. evaluated the PRT-treated PCs obtained through apheresis. They observed similar pH values (7.45 for controls and 7.51 for Mirasol® PRT system) on storage day 1 and the same value – 6.90 – for Mirasol® PRT system and for control on storage day 5. Clinical studies have demonstrated that pH value is a simple parameter which indirectly indicates the condition of platelets and correlates with in vivo platelet recovery.[19,20] It has been determined that the mean platelet volume decreases in all components stored at room temperature, which confirms the satisfactory condition of cells.

Goodrich et al. showed the highest correlation between pH and lactate production in PCs and in vivo recovery of Mirasol®-treated platelets.[21] In the 1970s, Valeri demonstrated a correlation between HSR and platelet viability in the recipient's circulatory system.[22] A similar correlation was reported by Handin, who recognized HSR as the most significant in vitro parameter to reflect in vivo platelet functions.[23] In our study, we observed HSR changes to be very slight compared to the results obtained by other study centers. After 5 days of storage, the PCs in group M showed no statistically significant HSR differences compared to control PCs, which only shows that platelets are capable of "removing water out of the cell."[21,24]

The turbidimetric method was used to evaluate platelet aggregation capacity by inducing with ADP, an agonist which defines the adhesion and aggregation capacity. ADP-related aggregation depends on the presence of ADP receptors, IIb/IIIa receptors for fibrinogen and proper alpha granule release. The aggregation capacity of platelets decreases with storage time, which was observed in both PC groups (C and M). Similar results were obtained by Rijkers et al., who studied platelet aggregation in PCs. No additional effect of PRT treatment on platelet aggregation was reported.[25]

Flow cytometry is a routine method for studying platelet activation mechanisms. Monoclonal antibodies used for the evaluation of platelet activation help to determine cell fractions that express on the platelet membrane. The appearance of new antigens (absent in a resting-stage), as well as quantity changes of antigens expressed on platelet membranes, result from platelet activation and intracellular granule release. In consequence, the intraplatelet vesicle membrane fuses with the cytoplasmatic membrane, and the glycoproteins from granular membranes disseminate into the cytoplasmatic membrane and are expressed on the platelet membrane. The level of platelet activation on the cytoplasmatic membrane is usually expressed by 3 antigens. With an increase of platelet activation, the expression of P-selectine increases as well (PADGEM antigen, GMP-140 glycoprotein, CD62P antigen) as a result of intensive alpha granule release. Simultaneously, the expression of the α fragment (the von Willebrand receptor) for glycoprotein Ib (antigen CD42b) is reduced, and the expression of the active form of fibrinogen receptor GP IIb-IIIa (CD41) increases.[26,27]

To evaluate the effect of PRT treatment on PCs, we decided to concentrate on the 2 most characteristic parameters of platelet activation, namely the CD42b and CD62P antigens.

In contrast to the results concerning the CD42b antigen expression reported by other authors, in our study, a slight decrease of glycoprotein Ib (antigen CD42b) expression on cells in both study groups was observed on storage day 3. On storage day 5, however, a return to the initial values was noted. Glycoprotein Ib is the basic receptor during the initial adhesion of platelets to the vessel wall, and a lack or decrease of this expression results in aggregation impairment.[13] No correlation between the CD42b antigen expression and platelet aggregation capacity was found.

P-selectin is also a significant activation marker. Most authors involved in PC quality control use this parameter as an indirect measure of platelet function. George et al. studied the CD62P antigen expression in PCs stored for 7 days under different agitation conditions. The percentage of the CD62P antigen expression on cells was 3-fold higher as compared to the initial values.[28] Fijnheer et al. observed that P-selectin expression correlates with the PC platelet count.[29] According to his observations, after 5 days of storage, a 15% increase in the number of activated platelets occurred if the platelet count was below 1×10^9/mL, and a 30% increase occurred if the platelet concentration was above 1.4×10^9/mL. In our study, we observed minimal platelet activation (higher P-selectin expression) on storage day 5 for PRT-treated PCs, though the values were not statistically significant compared to control PCs. Rinder and Smith suggest that P-selectin-positive platelets

are the first to be removed from the recipient's circulatory system and are phagocytosed by granulocytes and monocytes.[19]

Glucose is a compound that participates in ATP synthesis via metabolism of lactic acid along the glycolytic pathway. There occurs a direct correlation between depletion of glucose resources and prolongation of storage time. Additionally, in our study we report a statistically significant decrease in glucose concentration for inactivated platelets (M) on days 3 and 5 which was also confirmed by other authors.[18,19]

Rinder and Smith report that beta-thromboglobulin concentration may be an alternative to the costly and complicated isotope-stained studies which predict in vivo platelet recovery and survival. The higher beta-thromboglobulin release from alpha granules in PRT-treated PCs also indicates slight activation on all storage days as confirmed by the statistically significant difference observed for PCs after 5 days of storage.[19]

The pO_2 and pCO_2 values confirm proper gas exchange in the stored PCs, both control and PRT-treated. The lower pO_2 values in group M compared to group C indicate higher aerobic respiration, a requirement for adequate ATP production in cell mitochondria.

The aim of the study was to evaluate the in vitro biological parameters of PCs. Many authors claim that parameters such as aggregation capacity or HSR represent the in vivo hemostatic functions of platelets, but the most reliable, conclusive method of demonstrating PC transfusion effectiveness would be to evaluate the patient's clinical state following the transfusion of PRT-treated PCs.[20,30]

Independently of the above-described in vitro studies, each regional blood transfusion center involved in PC inactivation also performs routine quality control of inactivated PCs and monitors the components. If the percentage of components within a normal range falls below 75%, corrective measures are launched which consist of monitoring all stages of inactivated PC preparation.

Conclusions

The in vitro results demonstrate that pH, HSR, aggregation, CD42b antigen expression, MPV, and platelet count are comparable in groups M and C. It is commonly acknowledged that pH, HSR, CD42b antigen expression, MPV, and platelet count in the in vitro studies correlate with platelet survival time in the recipient's circulatory system. We can therefore assume that the therapeutic value of PRT-treated PCs is comparable to that of untreated conventional PCs, even though the values for glucose consumption and the CD62P antigen expression in group M are slightly higher on storage day 5, and for BTG the increase is statistically significant.

However, the most desired clinical outcome is the achievement of hemostasis; therefore, further in vivo studies are required to confirm the correlation between the in vitro and in vivo results.

References

1. Lachert E, Kubis J, Dąbrowska A. Quality system in blood transfusion service. In: Łętowska M, ed. *Medical Standards for Collection, Preparation and Distribution of Blood and Blood Components*. 3rd ed. Warszawa: Institute of Hematology and Transfusion Medicine; 2014:41–105.
2. Klein HG, Bryant BJ. Pathogen-reduction methods: Advantages and limits. *Vox Sang*. 2009;4:154–160.
3. Hayes EB, Komar N, Nasci RS, Montgomery SP, O'Leary DR, Campbell GL. Epidemiology and transmission dynamics of West Nile virus disease. *Emerg Infect Dis*. 2005;11:1167–1173.
4. Biggerstaff BJ, Petersen LR. Estimated risk of transmission of the West Nile virus through blood transfusion in the US, 2002. *Transfusion*. 2003;43:1007–1017.
5. Canellini G, Waldvogel S, Anderegg K, Tissot JD. Bacterial contamination of platelet concentrates: Perspectives for the future. *Labmedicine*. 2010;41(5):301–305.
6. Cardo LJ, Rentas FJ, Ketchum L, et al. Pathogen inactivation of Leishmania donovani infantum in plasma and platelet concentrates using riboflavin and ultraviolet light. *Vox Sang*. 2006;90:85–91.
7. Ruane PH, Edrich R, Gampp D, Keil SD, Leonard RL, Goodrich RP. Photochemical inactivation of selected viruses and bacteria in platelet concentrates using riboflavin and light. *Transfusion*. 2004;44:877–885.
8. Fast LD, DiLeone G, Li J, Goodrich R. Functional inactivation of white blood cells by Mirasol treatment. *Transfusion*. 2006;46:642–648.
9. Fiebig E, Hirschkorn DF, Maino VC, Grass JA, Lin L, Busch MP. Assessment of donor T-cell function in cellular blood components by the CD69 induction assay: Effects of storage, γ radiation, and photochemical treatment. *Transfusion*. 2000;40:761–770.
10. Ambruso DR, Thurman G, Marschner S, Goodrich RP. Lack of antibody formation to platelet neoantigens after transfusion of riboflavin and ultraviolet light-treated platelet concentrates. *Transfusion*. 2009;49:2631–2636.
11. Cazenave JP, Follea G, Bardiaux L, et al. A randomized controlled clinical trial evaluating the performance and safety of platelets treated with MIRASOL pathogen reduction technology. *Transfusion*. 2010;50:2362–2375.
12. Ness P, Braine H, King K, et al. Single-donor platelets reduce the risk of septic platelet transfusion reactions. *Transfusion*. 2001;41:857–861.
13. Ali SF. Platelet activation in stored platelet concentrates: Comparison of two methods preparation. *J Hematol*. 2012;1:15–19.
14. Slichter SJ, Corson J, Jones MK, Christoffel T, Pellham E, Bolgiano D. Platelet concentrates prepared after a 20- to 24-hour hold of the whole blood at 22°C. *Transfusion*. 2012;52:2043–2048.
15. Tudisco C, Jett BW, Byrne K, Oblitas J, Leitman SF, Stroncek DF. The value of pH as a quality control indicator for apheresis platelets. *Transfusion*. 2005;45:773–778.
16. Picker SM. In vitro assessment of platelet function. *Transfus Apher Sci*. 2011;44:305–319.
17. Moroff G, George VM, Siegl AM, Luban NLC. The influence of irradiation on stored platelets. *Transfusion*. 1986;26:453–456.
18. Murphy S, Rebulla P, Bertolini F, et al. In vitro assessment of the quality of stored platelet concentrates. *Transfus Med Rev*. 1994;8:29–36.
19. Rinder HM, Smith BR. In vitro evaluation of stored platelets: Is there hope for predicting post-transfusion platelet survival and function? *Transfusion*. 2003:43:2–6.
20. Li J, Lockerbie O, de Korte D, Rice J, McLean R, Goodrich RP. Evaluation of platelet mitochondria integrity after treatment with Mirasol pathogen reduction technology. *Transfusion*. 2005;45:920–926.
21. Goodrich RP, Li J, Pieters H, Crookes R, Roodt J, Heyns A. Correlation of in vitro platelet quality measurements with in vivo platelet viability in human subjects. *Vox Sang*. 2006;90:279–285.
22. Valeri CR, Feingold H, Marchionni LD. The relation between response to hypotonic stress and the 51Cr recovery in vivo of preserved platelets. *Transfusion*. 1974;14:331–337.
23. Handin RI, Fortier NL, Valeri CR. Platelet response to hypotonic stress after storage at 4°C or 22°C. *Transfusion*. 1970;10:305–309.
24. Kraemer L, Raczat T, Weiss DR, Strobel J, Eckstein R, Ringwald J. Correlation of the hypotonic shock response and extent of shape change with the new ThromboLUX™. *Vox Sang*. 2015;9:194–196.
25. Rijkers M, van der Meer PF, Bontekoe IJ, et al. Evaluation of the role of the GPIb-IX-V receptor complex in development of the platelet storage lesion. *Vox Sang*. 2016. doi:10.1111/vox.12416

26. Shrivastava M. The platelet storage lesion. *Transfus Apher Sci*. 2009;41:105–113.
27. Macher S, Sipurzynski-Budrass S, Rosskopf K, et al. Function and activation state of platelets in vitro depend on apheresis modality. *Vox Sang*. 2010;99:332–340.
28. George JN. Changes in platelet membrane glycoproteins during blood bank storage. *Blood Cells*. 1992;18:501–511.
29. Fijnheer R, Modderman PW, Veldman H, et al. Detection of platelet activation with monoclonal antibodies and flow cytometry: Changes during platelet storage. *Transfusion*. 1990;30:20–25.
30. Fijnheer R, Pietersz RN, de Korte D, et al. Platelet activation during preparation of platelet concentrates: A comparison of the plateletrich plasma and the buffy coat methods. *Transfusion*. 1990;30:634–638.

Surgical and oncological outcomes of free dermal fat graft for breast reconstruction after breast-conserving surgery

Fabrizio de Biasio[1,A–F], Serena Bertozzi[2,A–F], Ambrogio P. Londero[3,A–F], Daria Almesberger[1,A–F], Chiara Zanin[1,A–F], Andrea Marchesi[4,D–F], Carla Cedolini[2,A–F], Andrea Risaliti[2,D–F], Pier C. Parodi[1,A–F]

[1] Clinic of Plastic and Reconstructive Surgery, Department of Medical Area, University of Udine, Italy
[2] Clinic of Surgery, Department of Medical Area, University of Udine, Italy
[3] Clinic of Obstetrics and Gynecology, University of Udine, Italy
[4] Department of Plastic and Reconstructive Surgery, IRCCS Policlinico San Donato, University of Milan, Italy

A – research concept and design; B – collection and/or assembly of data; C – data analysis and interpretation; D – writing the article; E – critical revision of the article; F – final approval of the article

Advances in Clinical and Experimental Medicine, ISSN 1899-5276 (print), ISSN 2451-2680 (online) *Adv Clin Exp Med*. 2018;27(6):773–780

Address for correspondence
Serena Bertozzi
E-mail: dr.bertozzi@gmail.com

Funding sources
None declared

Conflict of interest
None declared

Acknowledgements
We are grateful to Dunya Bernardon for her suggestions on style and composition of our text in English.

Received on June 16, 2016
Reviewed on September 26, 2016
Accepted on February 14, 2017

Abstract

Background. Oncoplastic breast surgery originated in order to improve the esthetic result of breast-conserving surgery (BCS). Autologous free dermal fat graft (FDFG) is an emerging oncoplastic technique to improve the cosmetic outcome of breast-conserving surgery.

Objectives. The aim of this study was to analyze our experience with FDFGs in breast reconstruction after breast-conserving surgery. Oncological outcomes, surgical complications and cosmetic results were considered.

Material and methods. This retrospective chart review study considered all consecutive oncoplastic breast treatment by means of FDFG reconstruction during the period between September 2011 and September 2012 in our Clinic of Surgery (University of Udine, Italy). The data collected included patient and tumor characteristics and outcomes (cosmetic and oncological).

Results. During the study period, 37 women were treated by breast cancer surgery and immediate breast reconstruction by FDFG. At a 3-year follow-up, we found no cases of recurrence among breast cancer patients treated by FDFG; at a 18-month follow-up, we found a prevalence of 75.0% of women extremely satisfied with their oncoplastic surgery and a high prevalence of excellent or good cosmetic outcomes (70.3%) according to objective and subjective cosmetic assessment.

Conclusions. Immediate breast reconstruction by FDFG after BCS in a population selected for a low risk of breast cancer recurrence seems to be an oncologically safe option, with a good cosmetic outcome and a high prevalence of women satisfied with the treatment.

Key words: breast cancer, disease-free survival, free dermal fat graft, oncoplastic surgery, breast-conserving surgery

DOI
10.17219/acem/68977

Introduction

During the past 2 decades, breast cancer surgery underwent an important evolution through the introduction of a new concept of oncoplastic breast surgery, which integrates the principles of oncological demolition and plastic reconstruction.[1,2] Oncoplastic breast surgery initially originated in order to improve the esthetic result of breast-conserving surgery (BCS), the indications of which have grown significantly in recent years, ranging from small, wide excisions limited to 10–15% of the breast to partial mastectomies.[1] In particular, the dissatisfaction rate after BCS has been reported to be actually 30–40%.[3]

Oncoplastic breast surgery techniques have been classified into 2 main categories: one consists of the residual breast tissue mobilization, and the other requires distant tissue transplantation within the residual breast.[4] The first category includes all glandular and dermo-glandular flaps described in recent years as well as techniques based on resection patterns typical of reducing mastoplasty.[4] On the other hand, the latter category consists of the myocutaneous flaps of the latissimus dorsi in its all possible variants, the perforant adipo-fascial flaps of the chest wall and the free flaps of the abdominal region.[4,5]

The optimal choice regarding the best oncoplastic solution depends on the proportion between the resected tissue volume and the whole breast volume as well as on the breast lesion site. Tissue mobilization techniques are generally preferred, because they are easier and quicker to carry out, and, furthermore, do not increase morbidity in different donation sites. However, there are some peremptory indications for tissue transplantation techniques, i.e., when the remaining tissue after breast demolition is insufficient for reconstructing a breast of adequate shape and volume. Unfortunately, choices related to the reconstruction may also be affected by the surgeon's experience, as the learning curve for the flap surgery – and especially microsurgery – often proves to be particularly long; thus, sometimes BCS is turned into mastectomy in order to simplify the surgical procedure.

Among various tissue transplantation techniques, a very important role is played by the free dermal fat graft (FDFG), which is a simple, traditional technique for breast reconstruction. In 2007, Kijima et al. described their experience with this procedure especially for the reconstruction of upper-inner quadrantectomies and in the case of patients who did not qualify for postoperative radiotherapy.[5,6]

Our study aims to analyze our experience with FDFG in breast reconstruction after BCS. In particular, we assessed the surgical outcomes in terms of morbidity and esthetic results, along with the oncological outcomes in terms of overall survival and disease-free survival.

Material and methods

We collected retrospective data on all patients who underwent reconstructive procedures after BCS for invasive breast cancer between September 2011 and September 2012 in our Clinic of Surgery (University of Udine, Italy). This study follows the dictates of the general authorization law on processing personal data for scientific research purposes on behalf of the Italian Data Protection Authority.

All patients underwent preoperative mammography, breast ultrasound and breast magnetic resonance imaging (MRI) when not contraindicated (e.g., obese women, patients with important comorbidities or those with metallic implants) in order to better define the cancer size and to exclude its eventual multifocality or multicentricity.[7]

About 10 days before surgery, all women were visited by both the breast surgeon and the plastic surgeon in order to plan the incision site and extension as well as the breast site and excision volume, and to discuss the best reconstructive option. All patients gave their informed consent to both demolitive and reconstructive operations.

Indications of FDFG include all breast tissue defects following breast oncological surgery that are located in an area where the graft can rest on the pectoral muscle, and in which the simple dermal and parenchymal remodeling (local tissue mobilization techniques) alone does not yield a satisfactory esthetic result.

The day before surgery, patients with non-palpable lesions underwent the imaging-guided placement of a wire hook together with a radiotracer injection for the sentinel lymph node biopsy as previously described, and were instructed to guide the breast surgeon's excision.[8] The site of graft sampling was chosen together with the patient based on the potential presence of scars (e.g., cesarean section scar) and the clothing preferences.

All patients underwent general anesthesia and the sentinel lymph node biopsy was performed before breast surgery in order to have the lymph node intraoperatively analyzed.[8] The incision site for the sentinel lymph node biopsy coincided with the site for breast resection only in the case of upper-outer quadrant lesions. Breast-conserving surgery consisted of the excision of the lesion with adequate margins, including both the skin over the breast lesion and the muscle fascia under it. The specimen was measured and weighed in order to be intraoperatively analyzed later (in order to control the margin negativity). Additionally, in each case, a cavity shave margin excision of about 1 cm was carried out.

Based on the specimen size and weight, the FDFG site was drawn on the inferior abdominal wall (Fig. 1). Unlike the traditional Kijiama technique – in which the surgeon excises abundant sovrapubic tissue to then design it on the breast defect site, consequently wasting some tissue – we excised a tissue lozenge with a major and a minor diameter and cut it into 2 parts to duplicate its minor diameter.

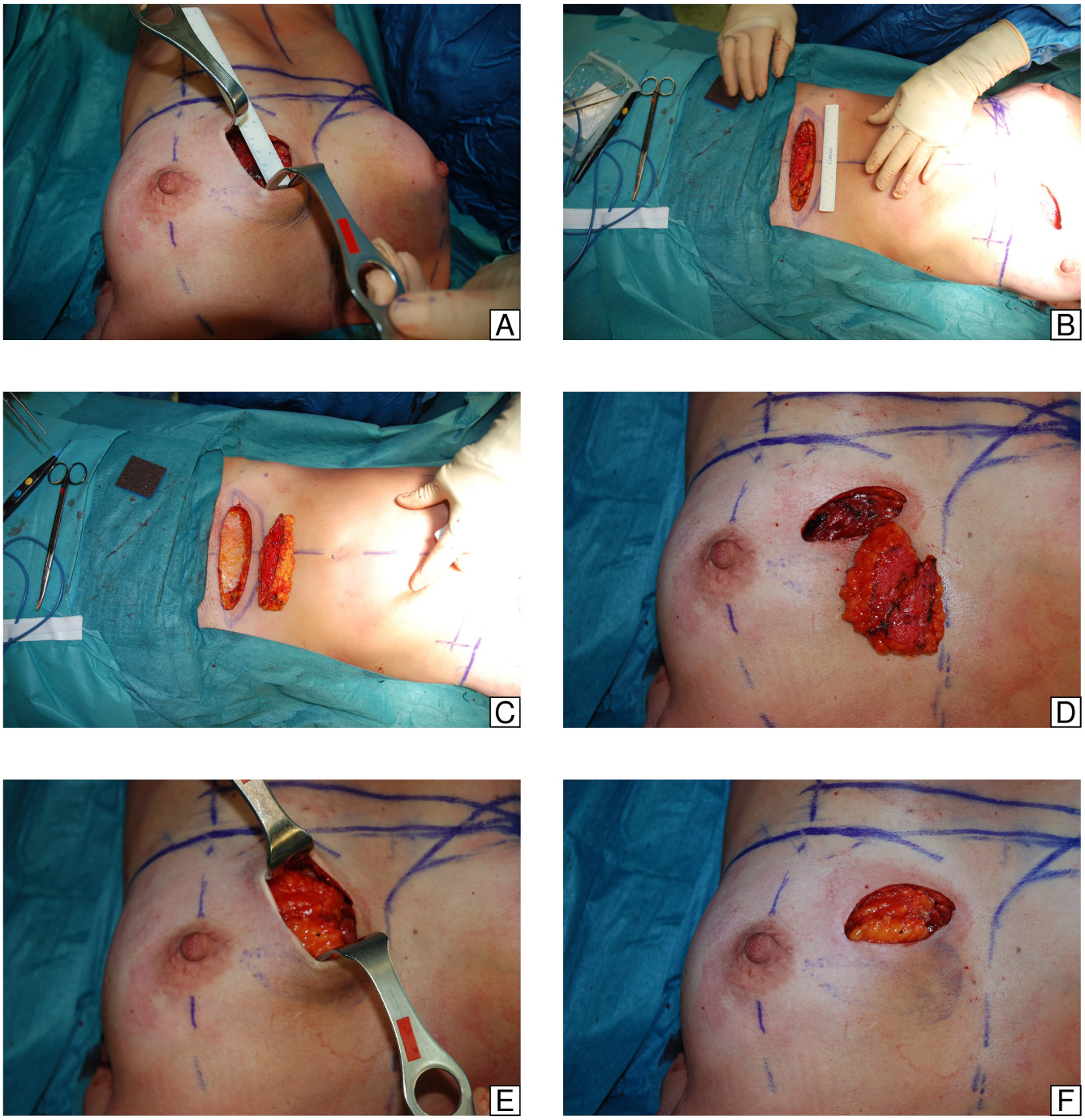

Fig. 1. Surgical procedure

After measuring the size of breast tissue to be replaced after breast cancer excision (A), the plastic surgeon draws the abdominal area of the FDFG site (B), from where he takes the dermo-hypodermic graft (C). Thereafter, the abdominal wall graft is placed and sutured into the breast tissue target area (D–F).

In accordance with Kijiama, we observed that the graft size is well maintained even after the passage of time; thus, it is not required to over-size it.

Sovrapubic tissue was then transferred to any breast defects on an adequate receiving bed, that is to say, on the pectoralis muscle. In particular, the sovrapubic area was initially shaved and then accurately conserved by means of derma vascularization, which is very important for its consequent engraftment. After that, the graft was excised by means of a cold scalpel with a maximum thickness of 2.5 cm, cut and sutured as previously described, then weighed, and finally transferred to the receiving breast area. The graft dermal side was sutured to the pectoralis muscle surface using separate stitches of Vycril 3/0 (Ethicon, Somerville, USA) (Fig. 1).

Before the closure of the wound, drainage was placed in the site of the FDFG, which was maintained in aspiration modality for about 24–48 h. Medication of the donor and the receiving areas was performed with a mild compression and plate dressing, respectively.

All patients underwent postoperative external breast radiotherapy, and even adjuvant chemotherapy or hormonal therapy were administered when required. Patient follow-up included a yearly oncological examination in order to exclude possible local or distant recurrences, together with a semi-annual check-up until 18 months after surgery for the evaluation of the esthetic results, as some authors described this time interval as the best time to assess definite esthetic outcomes, also including any possible late effects of radiotherapy.[9]

In particular, cosmetic assessment was performed using a score introduced by Sawai et al. and accepted by the Japanese Breast Cancer Society, calculated by summing up the following parameters: breast size (2 – no visual difference, 1 – a slight difference, 0 – a significant difference); breast shape (2 – no visual difference, 1 – a slight difference, 0 – a significant difference); scars (2 – unapparent, 1 – apparent, 0 – significantly apparent); breast softness (2 – equivalent and soft, 1 – slightly firm or partially firm, 0 – quite firm); size and shape of the nipple-areola complex (1 – no difference, 0 – some difference); color of the nipple-areola complex (1 – no difference, 0 – some difference); level of the nipple – the difference in the distance from the suprasternal notch between the bilateral nipples (1 – <2 cm, 0 – >2 cm); and the lowest point of the breast – the difference between the bilateral breasts (1 – a difference of <2 cm, 0 – a difference of >2 cm).[5,10] Total scores of 12 were considered to be excellent, 9–11 were considered good, 5–8 fair, and 0–4 poor. Furthermore, the patients were also asked to give their satisfaction rate according to a 4-point scale (excellent, good, fair, or poor).

The data collected included the following patients characteristics: age and body mass index (BMI) at the time of diagnosis, family history of breast cancer, menopause, and the use of hormonal oral contraceptives.[8,11,12] Among tumor characteristics, we considered the following: histological type, tumor-nodes-metastasis (TNM) classification and stage, possible extra-axillary lymph node involvement (internal mammary chain and subclavear), nuclear grading, Mib-1/Ki-67 proliferation index, estrogen and progesterone receptor expression, Her2/neu status, and molecular subtypes.[8,11,12] We also took into consideration other microscopic and histological characteristics which are present in more recent classifications put forward by Arnone et al., and which include the following: multifocality/multicentricity, extensive intraductal component, perivascular invasion, peritumoral inflammation, lymph node extracapsular invasion, and the bunching of the lymph nodes together.[8,11–13] Regarding surgery, we took into account operative and hospitalization time as well as potential surgical morbidity (defined as surgical site complications happening within 30 days after surgery).

The data was analyzed by R (v. 3.1.2), with $p < 0.05$ considered significant. The data is presented as proportions (and absolute values), mean (±SD; standard deviation), median (and interquartile range), or percentage of disease-free survival with the relative 95% confidence interval (CI), where appropriate. Furthermore, survival analysis was performed in order to compare the patients treated with FDFG to our general breast cancer population treated during the same period.

Results

During the study period, 230 women were treated by means of breast cancer surgery and 125 by BCS. In 37 women, an immediate oncoplastic breast reconstruction by FDFG was carried out.

The mean age of women treated by FDFG was 39.84 years (±10.25) and the mean BMI was 25.85 kg/m^2 (±5.80) (Table 1). The mean follow-up was 33.76 months (±4.43). In 11 women (29.7%), co-morbidities (3 with hyperthyroidism, 6 with hypertension and 3 with hypercholesterolemia) were present. In total, 13.5% of these women presented a family history of cancer.

The majority of the treated cancers were ductal invasive cancers, luminal A subtype with a low TNM stage that was mainly 0 or I (Tables 2, 3). The mean weight of the excised breast tissue was 49.49 g (±30.13) and the mean surgical time was 38.92 min (±5.02) (Table 4). Complications developed in 6 cases (16.2%): 1 case of FDFG necrosis after intraoperative radiotherapy requiring reintervention, 1 hematoma requiring reintervention, 3 seromas, and 1 wound separation managed by outpatient facilities.

Table 1. Description of the population

Age [years]	39.84 (±10.25)
BMI [kg/m^2]	25.85 (±5.8)
Follow-up [months]	17.76 (±4.43)
Comorbidities	29.7% (11/37)
Tobacco smoke	24.3% (9/37)
Family history of cancer	13.5% (5/37)
Previous use of estrogens	2.7% (1/37)
Post-menopausal status	56.8% (21/37)
1st breast surgical intervention	
BCS	94.6% (35/37)
NSM	5.4% (2/37)
2nd breast surgical intervention	
nothing	82.9% (29/35)
margin widening	14.3% (5/35)
SSM	2.9% (1/35)
Definitive axilla surgery	
SLNB	89.2% (33/37)
CALND	10.8% (4/37)
Non-surgical treatments	
neoadjuvant chemotherapy	0% (0/37)
adjuvant radiotherapy	86.5% (32/37)
adjuvant chemotherapy	35.1% (13/37)
adjuvant hormonal therapy	75.7% (28/37)

BMI – body mass index; BCS – breast-conserving surgery; NSM – nipple sparing mastectomy; SSM – skin sparing mastectomy; SLNB – sentinel lymph node biopsy; CALDN – complete axilla lymph node dissection.

Table 2. Tumor characteristics

Histological type	
ductal invasive carcinoma	67.6% (25/37)
lobular invasive carcinoma	5.4% (2/37)
ductal and lobular invasive carcinoma	8.1% (3/37)
other invasive carcinoma	8.1% (3/37)
ductal in situ carcinoma	10.8% (4/37)
Tumor characteristics	
Mib-1 > 20%	29% (9/31)
comedo-like necrosis	13.5% (5/37)
multifocality/multicentricity	8.1% (3/37)
EIC	16.2% (6/37)
PVI	18.9% (7/37)
Molecular subtype	
luminal A	59.4% (22/37)
luminal B	27% (10/37)
basal-like	8.1% (3/37)
luminal Her	2.7% (1/37)
Her enriched	2.7% (1/37)
Lymph node characteristics	
non axilla locoregional lymph node metastasis	0% (0/37)
ITC	2.7% (1/37)
micrometastasis	0% (0/37)
extracapsular lymph node invasion	2.7% (1/37)
axilla lymph node bunching	0% (0/37)

EIC – extended intraductal component; PVI – peritumoral vascular invasion; ITC – isolated tumor cells.

Table 3. TNM staging

Tumor size	
Tis	10.8% (4/37)
T1	83.8% (31/37)
T2	5.4% (2/37)
Nodal status	
N0	89.2% (33/37)
N1	8.1% (3/37)
N2	2.7% (1/37)
TNM stage	
stage 0	10.8% (4/37)
stage I	75.7% (28/37)
stage II	13.5% (5/37)
Tumor grading	
G 1	22.9% (8/35)
G 2	42.9% (15/35)
G 3	34.3% (12/35)

Table 4. Characteristics of reconstructive surgery

Weight of excised breast tissue [g]	49.49 (±30.33)
Surgical time [min]	38.92 (±5.02)
Hospitalization time [days]	3.27 (±0.61)
Complications	16.2% (6/37)
Margin involvement	2.7% (1/37)

Table 5. Objective and subjective assessment (Sawai's cosmetic assessment, Japanese Breast Cancer Society)

Size of the breast	
no visual difference (2)	67.6% (25/37)
a slight difference (1)	24.3% (9/37)
a significant difference (0)	8.1% (3/37)
Shape of the breast	
no visual difference (2)	70.3% (26/37)
a slight difference (1)	16.2% (6/37)
a significant difference (0)	13.5% (5/37)
Scar	
unapparent (2)	70.3% (26/37)
apparent (1)	21.6% (8/37)
significantly apparent (0)	8.1% (3/37)
Softness of the breast	
equivalent and soft (2)	32.4% (12/37)
slightly firm or partially firm (1)	56.8% (21/37)
quite firm (0)	10.8% (4/37)
Size and shape of nipple-areola	
no difference (1)	81.1% (30/37)
some difference (0)	18.9% (7/37)
Color of the nipple-areola	
no difference (1)	86.5% (32/37)
some difference (0)	13.5% (5/37)
Level of the nipple	
a difference of <2 cm (1)	89.2% (33/37)
a difference of >2 cm (0)	10.8% (4/37)
Level of the lowest point of the breast	
a difference of <2 cm (1)	91.9% (34/37)
a difference of >2 cm (0)	8.1% (3/37)
Total score (assessment)	9.49 (±1.92)
excellent (12)	5.4% (2/37)
good (9–11)	64.9% (24/37)
fair (5–8)	29.7% (11/37)
poor (0–4)	0% (0/37)

Margin involvement was found in 1 case (2.7%) after definitive histological examination – it required another surgery for margin widening. In 1 case, a skin sparing mastectomy was required because of multicentricity/multifocality found after definitive histological examination.

In the study group, 75% (27/36) of women declared an excellent esthetic result at a 18-month follow-up, the other 25.0% (9/36) declared a good or fair esthetic result, and none declared a poor result. Furthermore, in Table 5 we show the cosmetic assessment according to the Sawai score at a 18-month follow-up; the majority of cases presented an excellent or good total score (Table 5, Fig. 2).

During the follow-up, among the 37 cases treated by means of FDFG, we found no cases of local or distant recurrence. During the same period, in the cases treated by BCS, we registered a disease-free survival at a 3-year follow-up of 95.1% (95% CI 90.9–99.6%) (p – nonsignificant). No case of a cancer-related death in either group was observed.

Discussion

At a 3-year follow-up, we found high disease-free survival among breast cancer patients treated with FDFG, and at a 18-month follow-up, we found a high prevalence of women extremely satisfied by oncoplastic surgery and an excellent level of a cosmetic outcome.

Although oncological safety regarding breast surgery surely constitutes the most important aim while treating breast cancer, great attention is always given to the esthetic result, and oncoplastic breast surgery represents the most important progress achieved in the last 2 decades.

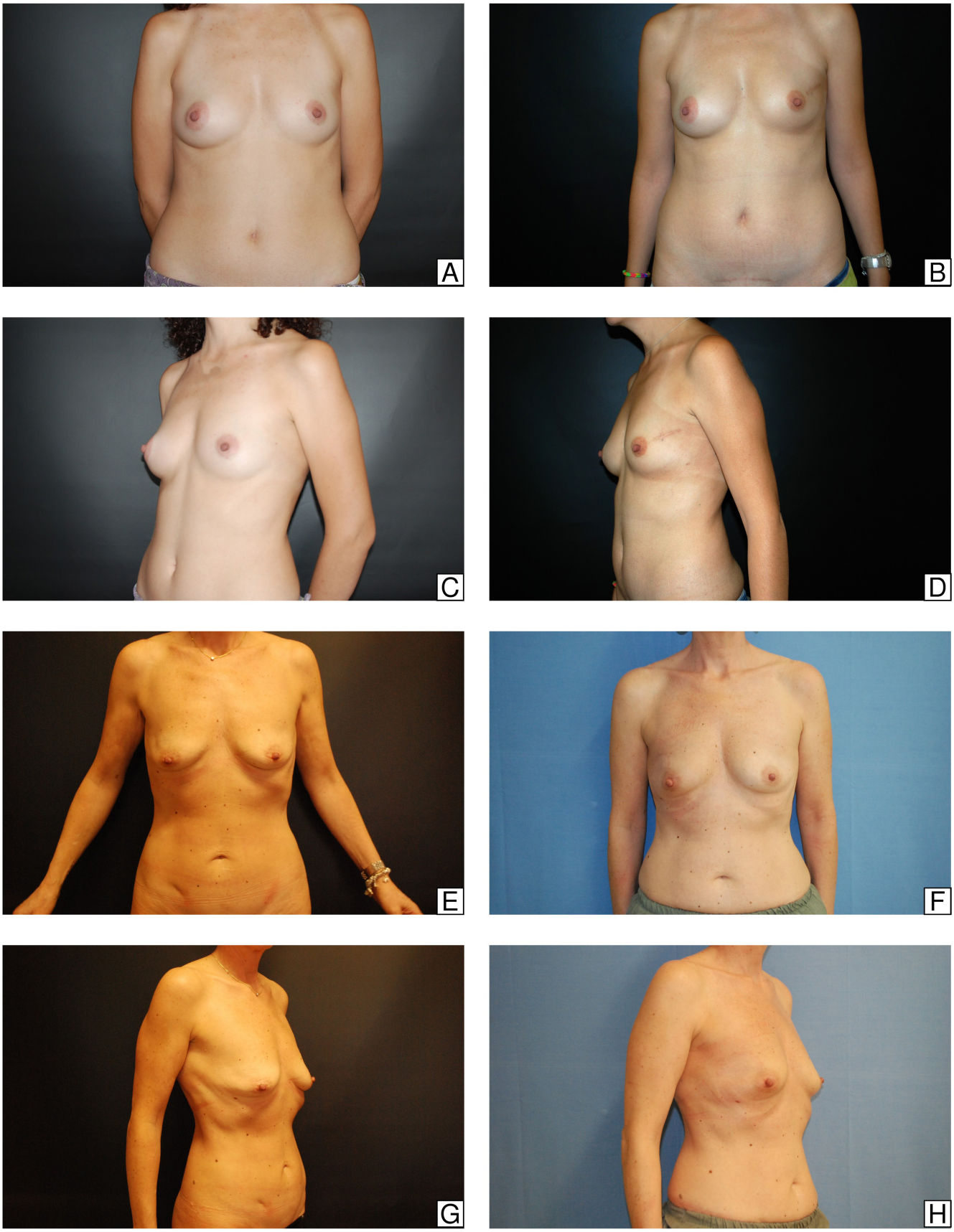

Fig. 2. Cosmetic assessment at a 18-month follow-up

Two cases are shown in the panels. A and C are pre-surgery case 1; B and D are post-surgery case 1 (surgery site in the left breast upper external quadrant). E and G are pre-surgery case 2; F and H are post-surgery case 2 (surgery site in the right breast upper external quadrant).

In fact, Clough et al. demonstrated that the introduction of oncoplastic surgical techniques allowed the excision of a 4 times greater tissue volume than in the case of traditional quadrantectomy.[14] A meta-analysis of Haloua et al. revealed that oncoplastic surgical techniques significantly reduced margin positivity rates of BCS from about 20–40% in the case of traditional quadratectomy to 3–16% in oncoplastic surgery, and significantly increased esthetic satisfaction rates up to 84–89%.[4]

Despite the great results of oncoplastic surgery described in the recent literature, in our experience some difficulties occurred which must be considered, such as an unfavorable proportion of breast volume to excised tissue volume. In particular, demolition involving less than 20% of the breast generally allows for adequate reconstruction independently of breast size; in fact, medium- and large-sized breasts may be submitted so as to reduce mastoplasty with good esthetic results, especially for women who desire a reduction in their breast size. On the other hand, demolition involving more than 20% of the breast in the cases of small-sized breasts may compromise the esthetic result of BCS and lead the surgeon to choose a mastectomy, also due to the long surgical time and the significant morbidity of traditional flap surgery; these women represent the group of patients who would have greater benefits thanks to the introduction of FDFG.

Thanks to the preoperative breast MRI study and the intraoperative resection margin evaluation, the 5-year recurrence rate after BCS in our population was 0% at a 3-year follow-up, and 75% of the women declared an excellent esthetic result. Of the remaining 25%, the majority were women with an unfavorable proportion between breast volume and excised tissue volume.

An intraoperative margin evaluation, as well as a subsequent systematic cavity shave margin excision, aim to further reduce the margin positivity rate, especially since some authors observed evident difficulty in margin widening after oncoplastic surgery with a consequent increased rate of secondary mastectomies.[4] Free dermal fat graft allows breast surgeons to excise as much tissue as it is required in a more tranquil manner so as to reach oncological radicality. Furthermore, a graft size which may influence its engraftment is not so much a question of length but of thickness, so in the case of large breast defects, a larger sovrapubic tissue excision is required. In any case, if margin widening is required, it is always possible to perform the 2nd intervention followed by traditional tissue mobilization techniques.

Free dermal fat graft proves to allow very simple and quick execution, and does not require particular skills, so the majority of breast surgeons can perform it.

In the current literature, FDFG has an early and late morbidity of 20% and 10%, respectively. In our specific cases, we registered a complication prevalence of 16.2% – mainly minor ones, treated in outpatient facilities. Furthermore, only a single case of graft loss was reported in a woman who underwent intraoperative radiotherapy, which was consequently considered to be an absolute contraindication.

The main limitation of the present study is the short oncological follow-up; however, the use of this kind of procedure is limited and only minor studies with short follow-up periods have been published.[5,15] In fact, most of the recurrences in breast cancer occur between the 3rd and the 6th year of follow-up.[16] However, recent studies analyzing the oncological outcome of autologous fat grafting have declared this procedure to be safe even with a shorter mean follow-up than ours (<21 months of follow-up vs 34 months).[15,17] It must be stressed that in all aspects considered in the current literature, so far nothing has demonstrated the worsening of oncological outcomes as a result of using these techniques.[5,15,17–19] Finally, there is a cosmetic improvement achieved by using these techniques in oncoplastic surgery, as they allow the reconstruction of defects in areas difficult to repair, such as upper inner quadrants, or in small and medium-sized breasts.

To summarize, FDFG oncoplastic surgery, in a population of breast cancer patients selected for low oncological risk, seems to be oncologically safe, with a good cosmetic outcome and a high level of satisfaction of the women treated.

References

1. Driul L, Bernardi S, Bertozzi S, Schiavon M, Londero AP, Petri R. New surgical trends in breast cancer treatment: Conservative interventions and oncoplastic breast surgery. *Minerva Ginecol*. 2013;65:289–296.
2. Urban C, Lima R, Schunemann E, Spautz C, Rabinovich I, Anselmi K. Oncoplastic principles in breast conserving surgery. *Breast*. 2011; 20(Suppl 3):92–95.
3. Blondeel PN, Hijjawi J, Depypere H, Roche N, Van Landuyt K. Shaping the breast in aesthetic and reconstructive breast surgery: An easy three-step principle. Part III – Reconstruction following breast conservative treatment. *Plast Reconstr Surg*. 2009;124:28–38.
4. Haloua MH, Krekel NMA, Winters HAH, et al. A systematic review of oncoplastic breast-conserving surgery: Current weaknesses and future prospects. *Ann Surg*. 2013;257:609–620.
5. Kijima Y, Yoshinaka H, Funasako Y, et al. Immediate breast reconstruction using autologous free dermal fat grafts provides better cosmetic results for patients with upper inner cancerous lesions. *Surg Today*. 2011;41:477–489.
6. Kijima Y, Yoshinaka H, Owaki T, Aikou T. Early experience of immediate reconstruction using autologous free dermal fat graft after breast conservational surgery. *J Plast Reconstr Aesthet Surg*. 2007;60:495–502.
7. Del Frate C, Borghese L, Cedolini C, et al. Role of pre-surgical breast MRI in the management of invasive breast carcinoma. *Breast*. 2007;16: 469–481.
8. Cedolini C, Bertozzi S, Seriau L, et al. Eight-year experience with the intraoperative frozen section examination of sentinel lymph node biopsy for breast cancer in a North-Italian university center. *Int J Clin Exp Pathol*. 2014;7:364–371.
9. Vrieling C, Collette L, Fourquet A, et al.; EORTC Radiotherapy and Breast Cancer Cooperative Groups. The influence of patient, tumor and treatment factors on the cosmetic results after breast-conserving therapy in the EORTC 'boost vs no boost' trial. *Radiother Oncol*. 2000;55:219–232.
10. Ozaki S, Ohara M, Shigematsu H, et al. Technical feasibility and cosmetic advantage of hybrid endoscopy-assisted breast-conserving surgery for breast cancer patients. *J Laparoendosc Adv Surg Tech A*. 2013;23:91–99.
11. Cedolini C, Bertozzi S, Londero AP, et al. Type of breast cancer diagnosis, screening, and survival. *Clin Breast Cancer*. 2014;14:235–240.

12. Cedolini C, Bertozzi S, Seriau L, et al. Feasibility of conservative breast surgery and intraoperative radiation therapy for early breast cancer: A single-center, open, non-randomized, prospective pilot study. *Oncol Rep*. 2014;31:1539–1546.
13. Arnone P, Zurrida S, Viale G, et al. The TNM classification of breast cancer: Need for change. *Updates Surg*. 2010;62:75–81.
14. Clough KB, Lewis JS, Couturaud B, Fitoussi A, Nos C, Falcou MC. Oncoplastic techniques allow extensive resections for breast-conserving therapy of breast carcinomas. *Ann Surg*. 2003;237:26–34.
15. Biazus JV, Falcão CC, Parizotto AC, et al. Immediate reconstruction with autologous fat transfer following breast-conserving surgery. *Breast J*. 2015; 21(3):268–275.
16. Bernardi S, Bertozzi S, Londero AP, et al. Nine years of experience with the sentinel lymph node biopsy in a single Italian center: A retrospective analysis of 1,050 cases. *World J Surg*. 2012;36:714–722.
17. Petit JY, Lohsiriwat V, Clough KB, et al. The oncologic outcome and immediate surgical complications of lipofilling in breast cancer patients: A multicenter study – Milan-Paris-Lyon experience of 646 lipofilling procedures. *Plast Reconstr Surg*. 2011;128:341–346.
18. Semprini G, Cattin F, Lazzaro L, Cedolini C, Parodi PC. About locoregional recurrence risk after lipofilling in breast cancer patients. *Ann Oncol*. 2012;23:802–804.
19. Semprini G, Cattin F, Zanin C, et al. About locoregional recurrence risk after lipofilling in breast cancer patients: Our experience. *Minerva Chir*. 2014;69:91–96.

Validation of the Portuguese version of Addenbrooke's Cognitive Examination III in mild cognitive impairment and dementia

Bruno Peixoto[1,2,A–F], Milene Machado[3,B,C,E,F], Patricia Rocha[3,B,C,E,F], Carla Macedo[3,B,C,E,F], António Machado[3,B,C,E,F], Élia Baeta[4,A,C–F], Gerly Gonçalves[5,B,C,E,F], Paulo Pimentel[6,A–C,E,F], Emanuela Lopes[5,A,C,E,F], Luis Monteiro[1,A,C,E,F]

[1] University Institute of Health Sciences, Advanced Polytechnic and University Cooperative (CESPU), Gandra, Portugal
[2] NeuroGen – Center for Health Technology and Services Research (CINTESIS), Porto, Portugal
[3] Institute of Research and Advanced Training in Health Sciences and Technologies, Advanced Polytechnic and University Cooperative (CESPU), Gandra, Portugal
[4] The Alto Minho Hospital Center, Viana do Castelo, Portugal
[5] The Alto Ave Hospital Center, Guimarães, Portugal
[6] The Trás-os-Montes and Alto Duoro Hospital Center, Vila Real, Portugal

A – research concept and design; B – collection and/or assembly of data; C – data analysis and interpretation;
D – writing the article; E – critical revision of the article; F – final approval of the article

Advances in Clinical and Experimental Medicine, ISSN 1899-5276 (print), ISSN 2451-2680 (online) *Adv Clin Exp Med*. 2018;27(6):781–786

Address for correspondence
Bruno Peixoto
E-mail: bruno.peixoto@iscsn.cespu.pt

Funding sources
None declared

Conflict of interest
None declared

Received on September 12, 2016
Reviewed on November 12, 2016
Accepted on February 14, 2017

Abstract

Background. Cognitive assessment is central to the diagnosis of cognitive impairment and dementia, and it should be performed in all patients in the early stages of the disease. Recently, the 3rd version of Addenbrooke's Cognitive Examination (ACE-III) has been developed in order to improve the previous versions.

Objectives. The aim of this study was to determine the psychometric properties of the Portuguese version of ACE-III, namely: reliability and discriminative validity (sensitivity and specificity) in the identification of mild cognitive impairment (MCI) and dementia, in comparison to other neuropsychological screening tests, as well as to establish its concurrent and divergent validity.

Material and methods. The study encompassed a sample of 90 participants distributed into 3 groups: Control (n = 30), MCI (n = 30) and Dementia (n = 30). In addition to ACE-III, Clinical Dementia Rating (CDR) and Montreal Cognitive Assessment (MoCA) were also used.

Results. The reliability of ACE-III was very good ($\alpha = 0.914$). ACE-III significantly differentiated the 3 groups. The receiver operating characteristic (ROC) curves significantly favored ACE-III in comparison to another screening test – MoCA. ACE-III presented higher levels of sensitivity and specificity. Its total score correlated positively with the results on MoCA ($\rho = 0.912$; $p < 0.001$) and negatively with a depression scale ($\rho = -0.505$; $p < 0.001$).

Conclusions. The Portuguese version of ACE-III has very good reliability and high diagnostic capacity in the context of MCI and dementia. ACE-III also holds concurrent and divergent validity.

Key words: Alzheimer's disease, screening test, neuropsychological assessment

DOI
10.17219/acem/68975

Introduction

Dementia and cognitive impairment constitute a serious worldwide problem. Dementia is in the top 10 of the leading causes of the burden of disease in high-income countries.[1]

The prevalence of dementia in Western Europe in people over 60 years of age is estimated at 7.3% and increases exponentially with age, doubling every 6.3 years.[2]

Cognitive assessment is central to the diagnoses of cognitive impairment and dementia, and should be performed in all patients in the early stages of the disease.[3] Furthermore, patients with mild cognitive impairment (MCI) should be recognized due to an increased risk of subsequent dementia.[4]

Therefore, the use of screening tests with high diagnostic utility, simplicity and celerity, and with normative data for the target population, is important in a time-constrained environment.[5,6]

Recently, the 3rd version of Addenbrooke's Cognitive Examination (ACE-III) has been developed in order to improve certain weaknesses in some domains, such as repetition, comprehension and visuospatial items.[7] With a mean administration time of 15 min, ACE-III meets the requirements of a screening test, evaluating different cognitive dimensions and enabling an overall picture of a subject's neurocognitive functioning.

The 3rd version of Addenbrooke's Cognitive Examination is scored out of 100 and assesses 5 cognitive domains: attention (max score = 18 points), assessed through orientation, immediate verbal evocation of words and serial subtraction tasks; nemory (max score = 26 points), evaluated by verbal delayed recall (free recall and recognition), verbal learning and semantic memory tasks; verbal fluency (max score = 14 points), including phonetic and semantic fluency tasks; language (max score = 26 points), assessed through comprehension, repetition, naming, reading, and writing tasks; visuospatial (max score = 16 points), including visuoconstructive tasks (e.g., copying a cube and drawing a clock) and spatial perceptive tasks (counting dots and identifying incomplete letters).[7]

To date, several ACE-III validation and normative studies have been published and translated into several languages, including Portuguese.[7–10] However, there is a need to further determine the validity of the test in different clinical populations and to compare it with other tests.[7,10,11]

This study aims to determine the psychometric properties of the Portuguese version of ACE-III, namely: reliability and discriminant validity (sensitivity and specificity) in the identification of MCI and dementia, in comparison to other neuropsychological screening tests, as well as to establish its concurrent and divergent validity.

Material and methods

Participants

The study included a sample of 90 participants distributed into 3 groups: the Control group, made up of 30 subjects ranging between 61 and 81 years of age from the ACE-III Portuguese normative study, without any subjective complaint of memory loss and completely independent in everyday activities; the MCI group, composed of 30 subjects ranging between 47 and 79 years of age and fulfilling Petersen's criteria for MCI; and the Dementia group, made up of 30 subjects ranging between 59 and 87 years of age, with dementia according to National Institute of Neurological and Communicative Disorders and Stroke (NINCDS) and the Alzheimer's Disease and Related Disorders Association (ADRDA) criteria (Table 1).[10,12,13] Individuals with a prior history of neuropsychiatric or systemic pathologies, liable to directly interfere with neurocognitive functioning, and those who are illiterate, were excluded.

Groups did not differ according to age (p = 0.673), schooling (p = 0.593) or gender (p = 0.679). The participants included in the MCI and Dementia groups were recruited from the neurology outpatient clinics of 3 different Portuguese hospitals. Clinical diagnoses were established by those services and complemented with the results of the Clinical Dementia Rating (CDR) to determine the severity of MCI and dementia.

Table 1. Sociodemographic and clinical characteristics of the sample

Variables	Control (n = 30)	MCI (n = 30)	Dementia (n = 30)
Age in years (M ±SD)	68.6 ±6.2	67.2 ±9.3	69.2 ±10.3
Years of education (M ±SD)	5.6 ±3	5.5 ±2.3	5.42 ±3.3
Gender (n)			
male	11	13	12
female	19	17	18
CDR (M ±SD)	0 ±0	0.5 ±0.25	1.25 ±0.75
Diagnosis (n)			
multiple domain		16	
amnestic		9	
non-amnestic		5	
Alzheimer's disease			16
vascular dementia			9
frontotemporal dementia (behavioral variant)			3
mixed etiology			2

MCI – mild cognitive impairment; CDR – clinical dementia rating; M – mean; SD – standard deviation.

Neuropsychological assessment

In addition to ACE-III, the following instruments were used: CDR, Montreal Cognitive Assessment (MoCA) and Geriatric Depression Scale (GDS).[14–16] The MoCA test was selected to determine convergent validity of ACE-III due to its high specificity and sensitivity in detecting MCI

and dementia.[14] Geriatric Depression Scale was applied in order to establish divergent validity of ACE-III.

The scoring criteria of ACE-III followed the norms of the English version of the test.[17]

Procedures

This study was approved by the ethical committees of the Alto Minho Hospital Center (Viana do Castelo, Portugal), the Alto Ave Hospital Center (Guimarães, Portugal) and the Trás-os-Montes and Alto Duoro Hospital Center (Vila Real, Portugal). All participants gave their informed consent.

The assessment occurred in a single session in a private room. The CDR and GDS tests were administered first, followed by ACE-III and MoCA. The order of the 2 neurocognitive tests alternated for all the participants in order to control for fatigue.

Statistical analysis

Statistical analysis was carried out using the program IMB Statistics v. 22 for Windows (IBM, Armonk, USA).

Reliability was determined by Cronbach's alpha. The comparison of the groups' performance from the tests was made through univariate analysis of variance (ANOVA) with subsequent comparisons by the Scheffe's test. The sensitivity and specificity of ACE-III in the distinction of the 3 groups were determined by the receiver operating characteristic (ROC) curves. Pearson's correlations were used to establish concurrent and divergent validity of ACE-III.

Results with $p \leq 0.05$ were considered significant.

Results

The value of Cronbach's alpha for the ACE-III total score is considered very good ($\alpha = 0.914$).

Table 2 shows the results obtained and the comparisons between the groups from the neuropsychological tests. The ANOVA was significant for each test and for the subscales of ACE-III. The Control and MCI groups' results were significantly different on most of the tests, except the Attention and Visuospatial subtests. The MCI and Dementia groups did not differ regarding the level of depression.

Table 3 presents the characteristics of the ROC curves generated by the ACE-III and MoCA scores (Fig. 1–3). All the generated curves are significant for both tests, but the area under the curve for the 3 clinical settings favors ACE-III. Cut-off scores and corresponding values of sensitivity and specificity were extracted (Table 4). A cut-off score of 82 on ACE-III differentiates the Control and MCI groups with a sensitivity of 87.5% and a specificity of 57.14%. A cut-off score of 66 on ACE-III differentiates the MCI and Dementia participants with a sensitivity of 89.9% and a specificity of 71.43%. A cut-off score of 74 on ACE-III discriminates the Control

Table 2. Differences between the groups on the GDS, the MoCA and ACE-III

Neuropsychological tests	Control (n = 30)	MCI (n = 30)	Dementia (n = 30)	F	p-value	Control vs MCI p-value	MCI vs Dementia p-value
GDS (M ±SD)	7.66 ±4.18	13.9 ±5.32	17.5 ±6.67	21.2	<0.001	<0.001	0.076
MoCA (M ±SD)	26.25 ±2.5	21.55 ±4.93	13.07 ±5.77	46.6	<0.001	<0.001	<0.001
ACE-III (total) (M ±SD)	89.41 ±5.9	78.79 ±11.23	58.36 ±18.52	37.3	<0.001	0.002	<0.001
Attention (M ±SD)	16.9 ±1.67	15.34 ±2.62	11.36 ±4.12	21.6	<0.001	0.076	<0.001
Memory (M ±SD)	24 ±2.59	20.07 ±4.36	12.86 ±6.97	31.9	<0.001	0.001	<0.001
Fluency (M ±SD)	9.53 ±1.61	7.41 ±2.48	5.43 ±2.43	20.2	<0.001	0.001	0.018
Language (M ±SD)	25.06 ±1.37	22.82 ±3.16	18.5 ±5.26	21.7	<0.001	0.025	<0.001
Visuospatial (M ±SD)	13.91 ±1.94	12.41 ±3	10.21 ±3.64	8.88	<0.001	0.115	0.05

MDI – mild cognitive impairment; GDS – Geriatric Depression Scale; MoCA – Montreal Cognitive Assessment; ACE-III – Addenbrooke's Cognitive Examination III.

Table 3. Characteristics of the ROC curves generated by ACE-III and MoCA

Groups	Neuropsychological tests	Area under the curve	Standard error	p-value	Confidence interval	
					upper bound	lower bound
Control vs MCI	ACE-III	0.816	0.054	<0.001	0.711	1
	MoCA	0.776	0.052	<0.001	0.673	0.878
MCI vs Dementia	ACE-III	0.901	0.052	<0.001	0.798	1
	MoCA	0.815	0.064	<0.001	0.688	0.941
Control vs Dementia	ACE-III	0.973	0.0234	<0.001	0.927	1
	MoCA	0.953	0.024	<0.001	0.905	1

ROC – receiver operating characteristic; ACE-III – Addenbrooke's Cognitive Examination III; MoCA – Montreal Cognitive Assessment; MCI – mild cognitive impairment.

Table 4. Sensitivity and specificity of ACE-III and MoCA between the groups and for different cut-off scores

Groups	ACE-III			MoCA		
	cut-off	sensitivity [%]	specificity [%]	cut-off	sensitivity [%]	specificity [%]
Control vs MCI	78	96.88	36	19	97	17.90
	80	96.88	42.86	20	91	32.10
	81	90.63	50.00	21	86	39.30
	82	87.50	57.14	22	84	53.60
	83	84.38	60.71	23	82	53.60
	84	81.25	67.86	24	75	53.60
MCI vs Dementia	62	96.43	64	12	97	42.9
	63	92.86	64.29	13	96.4	42.9
	65	89.29	64.29	14	90.4	52.4
	66	89.29	71.43	15	82.9	61.9
	68	85.71	71.43	16	80.3	66.7
	69	85.71	78.57	17	78.3	76.2
Control vs Dementia	57	100	50	16	100	33
	63	100	64.29	17	100	43
	66	100	71.43	18	100	52
	74	100	78.57	19	100	62
	81	93.75	78.57	20	98	67
	83	93.75	85.71	21	96	81

ACE-III – Addenbrooke's Cognitive Examination III; MoCA – Montreal Cognitive Assessment; MCI – mild cognitive impairment.

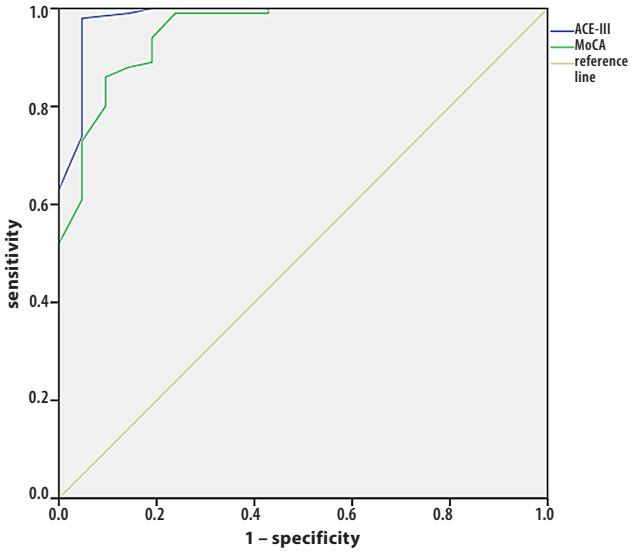

Fig. 1. ROC for the discrimination between the Control and MCI groups on ACE-III and MoCA

ROC – receiver operating characteristic; MCI – mild cognitive impairment; ACE-III – Addenbrooke's Cognitive Examination III; MoCA – Montreal Cognitive Assessment.

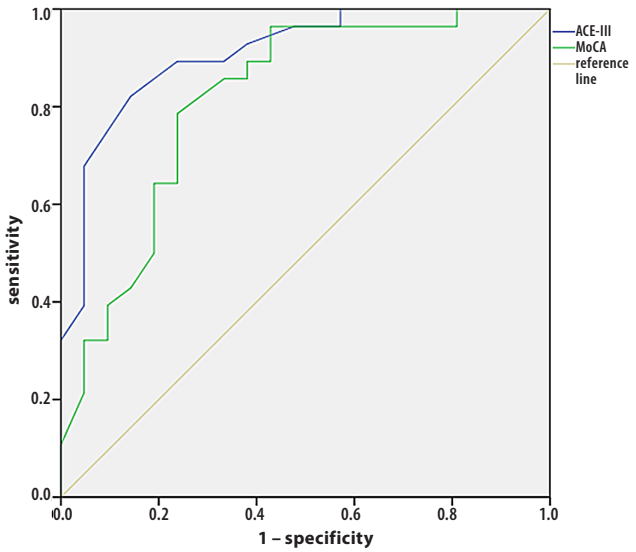

Fig. 2. ROC for the discrimination between the MCI and Dementia groups on ACE-III and MoCA

ROC – receiver operating characteristic; MCI – mild cognitive impairment; ACE-III – Addenbrooke's Cognitive Examination III; MoCA – Montreal Cognitive Assessment.

and Dementia group patients with a sensitivity of 100% and a specificity of 78.57%. Therefore, ACE-III holds sensitivity and specificity values higher than MoCA in all the domains.

The ACE-III total score correlated positively with the results on MoCA ($\rho = 0.912$; $p < 0.001$) and negatively with the GDS scores ($\rho = -0.505$; $p < 0.001$).

Discussion

The present study shows that the Portuguese version of ACE-III has very good reliability and high diagnostic capacity in the context of MCI and dementia, even when compared with another widely used screening

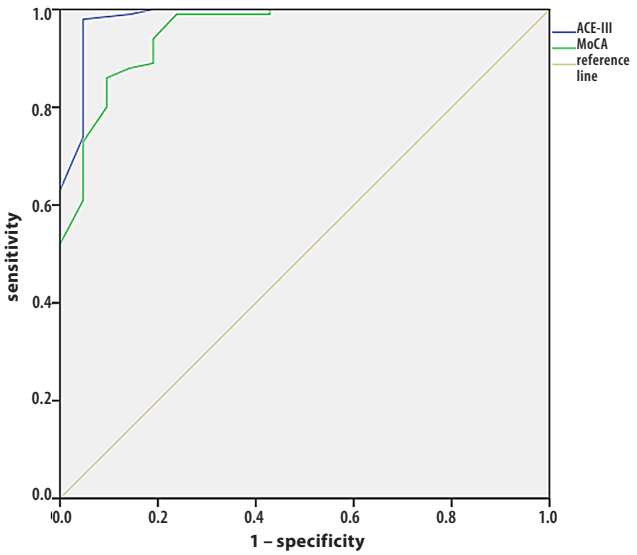

Fig. 3. ROC for the discrimination between the Control and Dementia groups on ACE-III and MoCA

ROC – receiver operating characteristic; ACE-III – Addenbrooke's Cognitive Examination III; MoCA – Montreal Cognitive Assessment.

test. Moreover, ACE-III also holds concurrent and divergent validity.

Reliability determined by Cronbach's alpha was high and very similar to that obtained in a Spanish study of the test (α = 0.927), and also slightly higher than in a study with the original version (α = 0.88) and in a Portuguese normative study (α = 0.732).[7,8,10]

The ACE-III results were significantly different between the 3 groups. The MCI group obtained lower results in comparison to the Control group in the majority of the domains, except for the Attention and Visuospatial domains. The differentiation of the Memory, Fluency and Language domains could be related to the fact that the majority of the participants in the MCI group had a multi-domain form of MCI. In addition to the registered differences between the Control and MCI groups, the generated ROC curve was significant and with an area under the curve greater than the one generated by the MoCA test. Unfortunately, there was no possibility to compare this remark regarding the Portuguese version of ACE-III to other versions, since, to our knowledge, this is the first study to analyze the discrimination capacity of ACE-III in MCI. However, in comparison to other widely used screening tests – like the Mini-Mental State Examination (MMSE) with a sensitivity level for MCI of 64.6%, and the MoCA test with a sensitivity level of 84.1% – the sensitivity values obtained for different ACE-III cut-off points are encouraging.[14,18] Future studies must determine whether the specificity values found in our study are due to the characteristics of our MCI sample or to the specifications of the instrument.

In our study, ACE-III also demonstrated good discrimination capacity between the MCI and Dementia groups. In direct comparison with MoCA, the cut-off scores were associated with more balanced levels of sensitivity and specificity.

The discrimination between the Control and Dementia groups was very satisfactory, with a significant area under the curve and values of sensitivity and specificity close to those of other versions of the test. In the original version, a cut-off score of 82 revealed a sensitivity of 93% and a specificity of 100%.[7] The high level of specificity found in this study could be due to the inclusion of a subgroup of participants with a diagnosis of primary progressive aphasia; since the test is highly weighted toward language tasks, it could have positively affected discrimination capacity. A study of the Spanish version of ACE-III determined levels of sensitivity (83.1%) and specificity (80.4%) closer to ours.[8] In fact, the Dementia group in that study was mainly composed of participants diagnosed with Alzheimer's disease and vascular dementia in the mild stage, as in our study. However, the cut-off score in the Spanish study was lower (65.5). This may be related to the fact that the participants in that study were older, as it is known that age is a determinant for performance in ACE-III.[8,10] Once more, discrimination capacity of ACE-III in direct comparison to MoCA was slightly higher. One of the desirable properties of a cognitive assessment tool is its sensitivity to the deficits of aging and dementia.[19] The inclusion of "true positives" and the exclusion of "true negatives" can accelerate the diagnostic process through the identification of cases for further testing. However, since further assessment requires more time and effort, specificity must be also observed. Thus, the suggested ACE-III cut-off scores were based on the equilibrium of this ratio (sensitivity/specificity).

Concurrent validity was also established, which is in line with other language versions of ACE-III. The original version found high correlations between the domains of ACE-III and standard cognitive tests (e.g., the Rey Osterrieth Complex Figure Test), and the Spanish version established convergence through the Kappa index with MMSE.[7,8] The negative correlation between ACE-III and the measure of depression (GDS) was expected, since the inverse relation between depressive mood and cognitive functioning is well-established.[20]

Conclusions

The current study has some limitations. The reduced number of participants makes it hard to determine the diagnostic utility of ACE-III in the differentiation between various types of MCI and dementia. Concurrent validity could have been determined by using a more comprehensive neuropsychological assessment battery; however, it would have been very time-consuming, and since the standard neuropsychological assessment was so diverse in the 3 hospitals, we were unable to present additional neuropsychological data common to all the participants.

Therefore, in conclusion, the Portuguese version of ACE-III has proven to be a valid instrument in the context of MCI and dementia. In comparison to MoCA, ACE-III shows better discrimination capacity. This is especially relevant for the prompt identification of patients that need a more extensive neuropsychological and neurological assessment.

References

1. Lopez AD, Mathers CD, Ezzati M, Jamison DT, Murray CJ. Global and regional burden of disease and risk factors, 2001: Systematic analysis of population health data. *Lancet*. 2006;367(9524):1747–1757.
2. Prince M, Bryce R, Albanese E, Wimo A, Ribeiro W, Ferri CP. The global prevalence of dementia: A systematic review and metaanalysis. *Alzheimers Dement*. 2013;9(1):63–75.e2.
3. Sorbi S, Hort J, Erkinjuntti T, et al. EFNS-ENS guidelines on the diagnosis and management of disorders associated with dementia. *Eur J Neurol*. 2012;19(9):1159–1179.
4. Petersen R, Stevens J, Ganguli M, et al. Practice parameter: Early detection of dementia: Mild cognitive impairment (an evidence-based review). Report of the Quality Standards Subcommittee of the American Academy of Neurology. *Neurology*. 2001;56(9):1133–1142.
5. Boustani M, Peterson B, Hanson L, Harris R, Lohr KN. Screening for dementia in primary care: A summary of the evidence for the US Preventive Services Task Force. *Ann Intern Med*. 2003;138(11):927–937.
6. Sánchez LB, Muñoz MA, López MDB, et al. Estudio de validez del Test de las Fotos en el cribado de deterioro cognitivo en atención primaria. *Revista Clínica de Medicina de Familia*. 2007;2:57–62.
7. Hsieh S, Schubert S, Hoon C, Mioshi E, Hodges JR. Validation of the Addenbrooke's Cognitive Examination III in frontotemporal dementia and Alzheimer's disease. *Dement Geriatr Cogn Disord*. 2013;36(3–4):242–250.
8. Matias-Guiu JA, de Bobadilla RF, Escudero G, et al. Validación de la versión española del test Addenbrooke's Cognitive Examination III para el diagnóstico de demencia. *Neurología*. 2015;30(9):545–551.
9. Qassem T, Khater MS, Emara T, et al. Normative data for healthy adult performance on the Egyptian-Arabic Addenbrooke's Cognitive Examination III. *Middle East Current Psychiatry*. 2015;22(1):27–36.
10. Machado A, Baeta E, Pimentel P, Peixoto B. Psychometric and normative indicators of the Portuguese version of the Addenbrooke's Cognitive Examination III: Preliminary study on a sample of healthy subjects. *Acta Neuropsychol*. 2015;13(2):127–136.
11. Velayudhan L, Seung-Ho R, Raczek M, et al. Review of brief cognitive tests for patients with suspected dementia. *Int Psychogeriatr*. 2014;26(8):1247–1262.
12. Petersen RC. Mild cognitive impairment as a diagnostic entity. *J Intern Med*. 2004;256(3):183–194.
13. McKhann GM, Knopman DS, Chertkow H, et al. The diagnosis of dementia due to Alzheimer's disease: Recommendations from the National Institute on Aging-Alzheimer's Association workgroups on diagnostic guidelines for Alzheimer's disease. *Alzheimers Dement*. 2011;7(3):263–269.
14. Freitas S, Simões MR, Martins C, Vilar M, Santana I. Estudos de adaptação do Montreal Cognitive Assessment (MoCA) para a população portuguesa. *Avaliação Psicológica*. 2010;9(3):345–357.
15. Nasreddine ZS, Phillips NA, Bédirian V, et al. The Montreal Cognitive Assessment, MoCA: A brief screening tool for mild cognitive impairment. *J Am Geriatr Soc*. 2005;53(4):695–699.
16. Yesavage JA, Brink TL, Rose TL, et al. Development and validation of a geriatric depression screening scale: A preliminary report. *J Psychiatr Res*. 1983;17(1):37–49.
17. Frontier – NeuRA. https://www.neura.edu.au/frontier/research/test-downloads/. Accessed September 8, 2016.
18. Santana I, Duro D, Lemos R, et al. Mini-Mental State Examination: Avaliação dos novos dados normativos no rastreio e diagnóstico do défice cognitivo. *Acta Medica Portuguesa*. 2016;29(4):240–248.
19. Ritchie CW, Terrera GM, Quinn TJ. Dementia trials and dementia tribulations: Methodological and analytical challenges in dementia research. *Alzheimers Res Ther*. 2015;7(1):31.
20. Austin MP, Mitchell P, Goodwin GM. Cognitive deficits in depression: Possible implications for functional neuropathology. *Br J Psychiatry*. 2001;178:200–206.

The relationship between event-related potentials, stress perception and personality type in patients with multiple sclerosis without cognitive impairment: A pilot study

Marta Waliszewska-Prosół[1,A–D], Marta Nowakowska-Kotas[1,A–D], Roman Kotas[2,B,D], Tomasz Bańkowski[3,C], Anna Pokryszko-Dragan[1,A,C,E,F], Ryszard Podemski[1,E,F]

[1] Department of Neurology, Wroclaw Medical University, Poland
[2] Department of Psychiatry, Regional Specialist Hospital, Legnica, Poland
[3] Department of Cardiology, Wroclaw Medical University, Poland

A – research concept and design; B – collection and/or assembly of data; C – data analysis and interpretation; D – writing the article; E – critical revision of the article; F – final approval of the article

Advances in Clinical and Experimental Medicine, ISSN 1899-5276 (print), ISSN 2451-2680 (online) *Adv Clin Exp Med*. 2018;27(6):787–794

Address for correspondence
Marta Waliszewska-Prosół
E-mail: marta.waliszewska@gmail.com

Funding sources
None declared

Conflict of interest
None declared

Received on September 4, 2016
Reviewed on January 2, 2017
Accepted on February 13, 2017

Abstract

Background. The clinical course of multiple sclerosis (MS) can vary significantly among patients and is affected by exogenous and endogenous factors. Among these, stress and personality type have been gaining more attention.

Objectives. The aim of this study was to investigate the parameters of event-related potentials (ERPs) with regards to stress perception and personality type, as well as cognitive performance in MS patients.

Material and methods. The study group consisted of 30 MS patients and 26 healthy controls. Auditory ERPs were performed in both groups, including an analysis of P300 and N200 response parameters. The Perceived Stress Scale (PSS) was used in the MS group to measure the perception of stress. The D-type Scale (DS14) scale was used to determine the features of Type D personality, characterized by social inhibition and negative affectivity.

Results. The score on the PSS corresponded with a moderate or high level of stress perception in 63% of MS patients, while 23% of patients presented with a Type D personality. P300 latencies were significantly longer ($p = 0.001$), N200 amplitudes were significantly higher ($p = 0.004$), and N200 latencies were longer in MS patients than in the controls. Strong positive correlations were found between N200 and P300 amplitudes, as well as between the DS14 and PSS results.

Conclusions. Most MS patients experience moderate to severe stress. ERP abnormalities were found in MS patients who did not have overt cognitive impairment and showed correlations with stress levels and negative affectivity. Event-related potentials may be useful in assessing the influence of stress and emotions on the course of MS.

Key words: multiple sclerosis, event-related potentials, stress perception, personality type

DOI
10.17219/acem/68944

Introduction

Multiple sclerosis (MS) is a central nervous system inflammatory/autoimmune disorder. Multifocal demyelinating lesions are accompanied by axonal loss due to neurodegenerative processes.[1] The clinical course of MS can vary significantly among patients. This renders it less predictable, especially at the onset of the disease. Among other factors, stress and personality type have recently been increasingly associated with the individual course of MS. A relationship between the course of MS and stress has been found. Stress can aggravate MS symptoms, while disability and the chronicity of the disease result in stress, creating a vicious circle. However, studies in this field are inconclusive and the value of the tests used to measure the intensity of stress is constantly disputed.[2–4]

Event-related potentials (ERPs) are an electrophysiological method considered to reflect a subject's cognitive and emotional reaction to a mental task. Parameters of ERPs, particularly the most commonly analyzed P300 component, are mainly used in combination with neuropsychological tools as a measure of cognitive impairment in the course of various central nervous system (CNS) diseases, including MS. Those parameters may be affected by stress and anxiety.[5] Therefore, it seems interesting to analyze ERPs in combination with the patient's susceptibility to stress and the intensity of stress itself. Such analysis could prove the usefulness of the method as a biomarker in this field.

The aim of our pilot study was to analyze event-related potential parameters in MS patients, with regard to the perceived stress level and personality features.

Material and methods

The study was carried out on 30 patients with relapsing–remitting MS (26 women and 4 men; mean age: 34.9 years) and 26 healthy controls, matched to the patients with regard to age, gender and education level (22 women and 4 men; mean age: 34.6 years). The patients enrolled in the study were diagnosed with clinically definite MS by an experienced neurologist according to the McDonald criteria.[6] All patients underwent at least 1 magnetic resonance imaging (MRI) examination, which revealed dissemination of lesions in both space and time. The duration of the disease varied from 1 to 18 years (mean: 6.2 years; standard deviation (SD): 4.3) and the mean Expanded Disability Status Scale (EDSS) score was 1.8 (range: 1–3.5; median score: 1.5).[7] All the patients were in the course of treatment with disease-modifying agents, including interferon beta and glatiramer acetate. Exclusion criteria included severe cognitive impairment (patients unable to follow the test instructions), mood disorders (such as depression), progressive forms of MS, concomitance of other neurological or systemic disorders that may have influenced the cognitive performance and/or ERP results, severely decreased visual acuity, and hearing loss.

The study was approved by the Commission of Bioethics at the Wroclaw Medical University. All the subjects provided informed consent prior to their inclusion in the study.

A battery of tests was performed in the MS group to measure the perception of stress, the presence of Type D personality, and the basic level of cognitive performance (Symbol Digit Modalities Test – SDMT).[8,9]

The Perceived Stress Scale (PSS) was developed to measure the degree to which a recent situation in one's life is perceived as stressful – the higher the score (range 0–40), the higher the perception of stress.[10] In this study, Polish 10-point version of the scale was used.[11] In addition, sten scores were calculated; they indicated an individual's approximate score with respect to the whole population (sten scores of 1–4 corresponded with a low perception of stress, sten scores of 5–6 corresponded with moderate stress perception and sten scores of 7–10 corresponded with a high level of perceived stress).[11]

The D-type Scale (DS14) is a questionnaire used to determine the features of the so-called Type D personality, believed to be associated with a higher risk of morbidity and a higher susceptibility to stress. In order to be classified as Type D, one has to score more than 10 out of 14 points in the 2 dimensions of the scale: negative affectivity and social inhibition.[12]

The Symbol Digit Modalities Test (SDMT) is regarded as a reliable screening test for cognitive performance (including attention and executive functions) of MS patients.[13] In our study, it was performed in order to exclude patients with overt cognitive dysfunction, as well as to comparatively analyze the relationships between ERP parameters and stress, personality type and cognitive performance.

Event-related potentials were obtained from the MS patients and the controls. The multimodal ERPs were recorded in the Evoked Potential laboratory of the Department of Neurology of the Wroclaw Medical University. ERPs were induced after auditory stimulation with tones that differed in frequency (1 kHZ and 2 kHz) but had the same duration (200 ms) and intensity (70 dB). These tones were delivered binaurally through headphones. The oddball paradigm was used, where the eliciting stimuli were randomly presented in between neutral stimuli. The target stimuli occurred less frequently and constituted 20% of all stimuli, while the neutral stimuli made up 80% of each series. The recording Ag/AgCl electrodes were placed in the sagittal plane on the head in the frontal (Fz), central (Cz), and parietal (Pz) regions according to the 10–20 system of electrode placement. Two earlobe electrodes were used as reference electrodes, and the ground electrode was placed on the forearm. Electrode impedance was controlled and kept below 5000 Ω. The patient was recumbent with his/hers eyes closed. The series consisting of 30 to 40 target stimuli was presented to the patient at 2 time-points, and the patient was asked to count the stimuli. The response within the filter bandpass target (between 0.3 and 70 Hz, for 1000 ms) was averaged separately for target stimuli and neutral stimuli.

The N200 and P300 components were distinguished and their latencies and peak-to-peak amplitudes were determined.

The procedure used to record the ERPs was compliant with the International Federation of Clinical Neurophysiology (IFCN) and the standards recommended by the American Society of Electroencephalography.[14] The same ERP protocol was used in the earlier studies on MS patients conducted at our site.[5]

The ERP parameters obtained from MS patients and controls were compared, and the relationship between ERP and PSS, personality type and the SDMT was analyzed.

Statistical analysis

The statistical analysis was performed using of STATISTICA v. 10 software (StatSoft Inc., Tulsa, USA). The normality of distribution was verified with the Shapiro-Wilk test. If a normal distribution was stated, the groups were compared using the parametric Student's t-test. If the parameter value distributions differed significantly from a normal distribution, the non-parametric Mann-Whitney U test was used to compare the groups. The ANOVA test was used to compare more than 2 variables in the non-combined groups. Correlation coefficients were calculated and assessed using a standard Pearson coefficient. To assess relationships between 2 variables, $p \leq 0.05$ was considered statistically significant and p-value of 0.02–0.05 indicated a p-trend.

Results

Symbol Digit Modalities Test results

A SDMT was performed in all the patients, and a mean result of 55.6 ±7.94 points was obtained. None of the patients obtained scores lower than those corresponding to normal for the age range. The result of the SDMT did not correlate significantly with P300 or N200 latencies and amplitudes. A negative correlation ($R = -0.41$; $p < 0.05$) was found between the SDMT and the negative affectivity subscale of the DS14. No other correlations were found between the SDMT and the remaining test results.

Perceived Stress Scale and D-type Scale personality test results

The perceived level of stress was measured using the PSS. The mean score was 16.6 points (range: 5–26 points). The level of stress was determined as low in 11 individuals (37%), moderate in 6 individuals (20%) and high in 13 individuals (43%) when expressed in sten scores. A high level of stress was observed in 50% of men and 42% of women. A moderate level of stress was found in 0% of men and 23% of women, and low stress levels were seen in 50% of men and 34% of women. A Type D personality was found in 7 individuals (23% of the total study group), all of whom were women.

P300/N200 between groups

The 2 components of the ERP – N200 and P300 – were performed in all the subjects. The mean N200 amplitude values and P300 latency values registered in all 3 recording sites (Fz, Cz and Pz) were significantly higher in the group of MS patients than in the controls. A trend was also noted in the group of patients with MS toward longer latencies of the N200 recorded in the Fz and Pz sites ($p = 0.17$ and $p = 0.18$, respectively) than in the control group (Table 1).

Table 1. The mean value of the latency [ms] and amplitude [uV] of N200 and P300 potentials in patients with MS and in the control group

ERP	Patients with MS (n = 30)		Control group (n = 26)		p-value
	mean	SD	mean	SD	
Latency [ms]					
N200 Fz	211.7	21.6	207.0	21.1	0.17
Cz	208.8	20.5	205.3	20.7	0.53
Pz	214.2	26.1	205.8	19.0	0.18
P300 Fz	338.4	23.5	314.5	20.3	0.0002
Cz	336.4	23.9	315.6	22.3	0.001
Pz	338.6	21.4	318.3	23.4	0.001
Amplitude [uV]					
N200 Fz	7.0	3.5	4.5	3.9	0.006
Cz	6.7	4.0	3.9	3.6	0.001
Pz	5.9	5.4	2.9	2.3	0.004
P300 Fz	8.9	6.4	8.6	8.0	0.7
Cz	8.7	5.7	8.4	8.0	0.8
Pz	8.4	7.1	8.4	6.9	0.59

ERP – event-related potential; MS – multiple sclerosis; SD – standard deviation; Fz – frontal region; Cz – central region; Pz – parietal region.

N200 and DS14

The presence of a Type D personality, determined by the DS14 test, did not correlate significantly with any latency or amplitude values of the N200 component. However, a trend toward an inverse correlation between a Type D personality and the latency of N200 in the Pz recording site was observed (Table 2). Similarly, no statistically significant correlations were found between the latencies of the N200 at any of the recording sites and the components of the DS14 test, i.e., negative affectivity and social inhibition. An inversely proportional correlation was found between the N200 latencies recorded at the Cz and Pz sites and the 2 constituents of DS14. In the case of the N200 latency recorded at the Cz and Pz sites, there was an inversely proportional correlation between individual components of the DS14 (Table 3). The amplitude of N200 in the Fz, Cz and Pz sites strongly correlated with negative affectivity. No such tendency was found in the case of social inhibition (Table 4). When comparing patients with and without Type D personality, a trend towards longer N200 latencies was found at the Cz and Pz sites recorded in the group of patients without Type D features (212.5 ±16.5 vs 196.7 ±28.3, p = 0.07 and 219.3 ±23.7 vs 197.6 ±28.4, p = 0.05, respectively).

Table 2. The correlation of Type D personality and parameters of the N200 wave

Correlation	R*	p-value
D – type & N200 Cz lat	0.33	0.07
D – type & N200 Pz lat	–0.36	0.05
D – type & N200 Fz lat	–0.20	0.3
D – type & N200 Cz amp	–0.0033	0.99
D – type & N200 Pz amp	0.1137	0.55
D – type & N200 Fz amp	0.0570	0.77

Fz – frontal region; Cz – central region; Pz – parietal region; amp – amplitude.

Table 3. Correlation of negative affectivity and social inhibition estimated using the DS14 scale and CERP latencies assessed using the standard Pearson coefficient

Correlation	R*	p-value
NA & N200 Cz lat	–0.28	0.13
NA &N200 Pz lat	–0.28	0.14
NA &N200 Fz lat	–0.15	0.43
NA & P300 Cz lat	0.02	0.91
NA & P300 Pz lat	–0.04	0.83
NA & P300 Fz lat	–0.04	0.85
SI & N200 Cz lat	–0.25	0.19
SI &N200 Pz lat	–0.32	0.09
SI &N200 Fz lat	–0.1	0.59
SI & P300 Cz lat	0.18	0.35
SI & P300 Pz lat	0.11	0.58
SI & P300 Fz lat	0.19	0.30

NA – negative affectivity; SI – social inhibition; Fz – frontal region; Cz – central region; Pz – parietal region; lat – latency.

Table 4. Correlation of negative affectivity and social inhibition estimated using the DS14 scale and CERP amplitudes assessed using the standard Pearson coefficient

Correlation	R*	p-value
NA & N200 Fz amp	0.40	0.03
NA & N200 Cz amp	0.46	0.01
NA & N200 Pz amp	0.53	0.001
SI & N200 Fz amp	–0.13	0.51
SI & N200 Cz amp	–0.08	0.69
SI & N200 Pz amp	0.07	0.72
NA & P300 Fz amp	–0.21	0.27
NA & P300 Cz amp	–0.28	0.13
NA & P300 Pz amp	–0.03	0.87
SI & P300 Fz amp	0.01	0.94
SI & P300 Cz amp	–0.23	0.23
SI & P300 Pz amp	–0.22	0.25

Fz – frontal region; Cz – central region; Pz – parietal region; NA – negative affectivity; SI – social inhibition; amp – amplitude.

P300 and DS14

Type D personality did not correlate with any parameter of the P300 wave (Table 5). No correlation was found between the latency and amplitude values of P300 and the components of the DS14 scale at any of the recording sites (Table 3). An inverse correlation was observed between the amplitude of P300 at the Cz site and negative affectivity (R = –0.28; p = 0.13) (Table 4).

Table 5. Correlation of Type D personality and parameters of the P300 wave

Correlation	R*	p-value
D – type & P300 Cz lat	0.1237	0.52
D – type & P300 Pz lat	0.0920	0.63
D – type & P300 Fz lat	0.0716	0.71
D – type & P300 Cz amp	–0.2074	0.27
D – type & P300 Pz amp	–0.0981	0.61
D – type & P300 Fz amp	–0.1409	0.49

ERP – event-related potential; MS – multiple sclerosis; SD – standard deviation; Fz – frontal region; Cz – central region; Pz – parietal region; lat – latency; amp – amplitude.

N200/P300 and PSS

A statistically significant directly proportional relationship was found between the amplitudes of the N200 component at each recording site and the 10-point PSS and 10-sten PSS (Table 6). No statistically significant differences

Table 6. Correlations between the latency and amplitude of N200 and PSS10 points and sten scores assessed using the standard Pearson coefficient

N200 amplitude vs PSS 10	R	p-value
Fz	0.37	0.04
Cz	0.43	0.02
Pz	0.45	0.01
N200 amplitude vs PSS stens		
Fz	0.38	0.04
Cz	0.42	0.02
Pz	0.48	0.01
N200 latency vs PSS 10		
Cz lat	–0.21	0.26
Pz lat	–0.18	0.35
Fz lat	–0.08	0.69
N200 latency vs PSS stens		
Cz	–0.23	0.21
Pz	–0.21	0.27
Fz	–0.07	0.7

PSS 10 – the perceived stress scale; Fz – frontal region; Cz – central region; Pz – parietal region.

were found between the latency of N200, the amplitude and the latency of P300 and the PSS10 (expressed in points or stens). An inversely proportional trend was observed between the P300 amplitudes recorded at Cz, 10-sten PSS (R = –0.25; p = 0.18) and the latency of the P300 potential recorded at Cz and 10-sten PSS (R = –0.24; p = 0.2).

Based on the PSS test results, the patients were divided into 3 groups depending on the intensity of perceived stress (Group I: 1–4 stens, Group II: 5–6 stens and Group III: 7–10 stens). The ERP parameters were assessed in all groups. Patients with high levels of perceived stress had significantly larger N200 amplitudes at the Pz recording site than those with low levels of perceived stress (8.2 ±4.4 vs 3.9 ±3.3; p = 0.03). A trend was also found toward higher N200 amplitudes at the Cz recording site (p = 0.06). The remaining ERP results did not show any statistically significant differences with regard to PSS results (Table 7).

Discussion

The present study investigated the level of perceived stress and personality type, as well as their correlation with electrophysiological parameters, in MS patients.

More than 60% of the MS patients experienced moderate or severe stress. Our data is comparable with the findings of Senders et al. (16.6 points vs 16.55 points), but is significantly lower than the results of Artemiadis et al. (16.6 points vs 24.9 points) and Pritchard et al. (16.6 points vs 21.22 points).[15–17] Those differences can be attributed to the larger sample size in our study and to the characteristics of our study group (a relatively low level of disability and short duration of illness, or the use of appropriate immunomodulatory treatment). Type D personality occurred much less commonly in the study group (23%) than in the general Polish population (34.8%). It was comparable to healthy populations in other European countries (16.6–38.5%).[12,18–21] Our results were similar to those obtained in patients with diabetes (20–29%), but lower than those obtained in patients with cardiovascular disease (31–72.1%) or on dialysis (41%).[18,22] In the study by Dubayova et al., Type D personality occurred much more commonly in MS patients (44.5%) than in our study.[23] However, that study was carried out on patients with a higher disability level (mean EDSS: 3.0)

Table 7. The mean values of the latency [ms] and amplitude [uV] of N200 and P300 potentials in patients with MS divided into 3 groups according to the score obtained in PSS

ERP	Group 1 (low) n = 11		Group 2 (medium) n = 6		Group 3 (high) n = 13		p-value
	mean	SD	mean	SD	mean	SD	
N200 Fz lat	214.1	26.0	215.2	8.8	208.0	22.4	0.68
N200 Fz amp	5.9	4.0	5.9	3.2	8.4	2.7	0.19
N200 Cz lat	212.5	20.6	210.7	24.6	204.8	19.4	0.39
N200 Cz amp	5.0	3.1	6.2	4.7	8.4	4.0	0.06
N200 Pz lat	216.1	21.1	213.7	25.1	212.9	31.7	0.64
N200 Pz amp	3.9	3.3	4.4	2.7	8.2	4.4	0.03
P300 Fz lat	337.5	21.5	347.0	18.7	335.3	27.4	0.36
P300 Fz amp	9.7	7.6	11.0	6.7	7.2	5.0	0.45
P300 Cz lat	334.5	29.3	347.7	18.1	332.8	21.3	0.25
P300 Cz amp	10.1	6.6	10.5	6.2	6.7	4.3	0.38
P300 Pz lat	338.8	23.3	348.5	19.5	333.9	20.5	0.27
P300 Pz amp	8.3	8.8	12.6	8.3	6.4	3.9	0.25

ERP – event-related potential; MS – multiple sclerosis; SD – standard deviation; Fz – frontal region; Cz – central region; Pz – parietal region; lat – latency; amp – amplitude.

and suffering from various types of the disease (70% relapsing–remitting, 30% secondary or primary progressive).

ERPs are formed in extensive neuronal CNS networks. The P300 component, which is the most frequently analyzed parameter in clinical practice, arises in the frontal lobe, medial temporal lobe, cingulate gyrus, thalamus, and structures of the limbic system.[24,25] The P300 wave reflects the complex neuronal processes involved in the reception and processing of sensory information and selective attention, indicating decision making and memory updating processes. The parameters of the P300 potential are characterized by large variability among individuals and can be influenced by numerous endogenous and exogenous factors (age, personality, intelligence, hemispheric dominance, fatigue, physical activity, drugs, smoking, and alcohol consumption).[26]

The latency of the P300 wave corresponds to the time needed for an impulse to be recognized and classified, and is a marker of the rate of information processing. The P300 amplitude (maximal near the centro-parietal site) corresponds to short-term memory, attention and involvement of the subject in the task.[26]

The N200 ERP component is analyzed much less frequently. It is generated in the sensory and frontal areas and is thought to be associated with the initial (subconscious) identification of a stimulus and the activation required to complete the given task.

In our study, we found MS patients to have longer P300 latencies than healthy controls. A trend towards a longer N200 latency was obtained at both the Fz and Pz sites.

In the available literature on MS, a prolongation of the P300 latency was most frequently described. Such prolongation correlated with the severity of white matter damage in the course of demyelination, the severity of cognitive impairment and the rate of depression.[27,28] Some authors also found a prolongation of the N200 latency.[29–31] Relationships between ERP parameters and the duration of the disease or the degree of disability were more disputable.[27,28,32] Sundgren et al. pointed to the prognostic importance of the P300 parameters.[33] They noted that the progression of cognitive disorders was accompanied by an increased latency and decreased amplitude of the P300 wave. This progression was slower in patients with an abnormality of only 1 parameter.

All the patients in our study had a normal SDMT result; thus, according to the screening test, they did not have significant cognitive impairment. It is interesting that there was no correlation between the SDMT result and the ERP parameters. This may suggest that ERP may be used to disclose subtle cognitive deficits.

We did not analyze the relationships between ERP parameters and other disease-related variables (disease duration or EDSS). However, all our patients presented with only mild disability (mean EDSS: 1.8). Auditory modality of ERP was also chosen to further eliminate the impact of MS-related neurological deficit upon electrophysiological parameters (with the auditory pathway much less commonly affected in the course of MS than the visual one).

We found that the patients with MS in our study had higher N200 amplitudes than the control group. Similar findings were not found in the literature. The higher N200 amplitudes in our patients may suggest increased cortical and subcortical activity. This may be explained by compensatory mobilization of larger neuronal networks (due to a decline in neuronal function) in order to ensure better stimulus analysis, or perhaps a more intensive neuronal stimulation caused by higher stress levels. A long-term exposure to stress has been shown to lead to a dysfunction of the bioelectric brain activity. This may particularly occur in the course of demyelinating inflammatory diseases, hormonal activation, activation of proinflammatory cytokines, oxidative stress, or excitotoxicity.[34–36]

Our findings seem to support the association between N200 amplitude and stress. We found higher N200 amplitudes in MS patients with a higher level of perceived stress and a significant correlation between the amplitude of the N200 wave and negative affectivity in the DS14 scale. No such correlation was found in the case of social inhibition. The influence of stress on the initial stages of stimulus processing (corresponding with N200 parameters) may be explained by the subjects' perception that an associated mental task is difficult. Senkowski and Herrmann conducted ERP in healthy subjects using a visual discrimination task, with either an easy or difficult version.[37] The authors showed that the N200 amplitude was higher when subjects carried out the more difficult version of the task. They attributed this phenomenon to early hyperactivity in the cerebral cortex in preparation for a difficult task.[38]

Electrophysiological parameters such as contingent negative variation (CNV) and ERP parameters (mainly amplitude) may be modulated by stress, anxiety and personality in patients and healthy subjects. CNVs were larger in subjects with high perceived stress and high levels of arousal. Similar correlations were found in subjects with prolonged stress, which was measured using the PSS. An interesting finding was made in subjects with high anxiety levels: they were able to perform tasks at a similar level to subjects with much lower anxiety levels. The former subjects had higher CNV amplitudes, which was explained by the need for more processing resources in order to maintain adequate performance. Anxiety and the perception of a stimulus considered threatening may cause more involvement of neuronal networks. On the other hand, an individual's engaging of greater cognitive reserves in preliminarily analyzing a stimulus may lead to depletion of those reserves, causing fatigue and emotional tension (another vicious circle?).[39–41] Our findings of increased N200 amplitudes in MS patients with high perceived stress and in patients with negative affectivity support the above described phenomenon.

This study focused on the topic of the relationships between perceived stress, personality traits and

neuroelectrophysiological parameters, which have remained poorly understood. The results suggest that evaluating these aspects in patients with MS of short disease duration and a low degree of disability may help to identify those who require more psychological support. Event-related potentials seem to deserve attention as an electrophysiological indicator of susceptibility to stress that may be used alongside psychological tests.

The limitations of our study include the small size of the study group and using only 1 time-point in a study of patients with MS, which is known to have a fluctuating course. However, ours was a pilot study whose findings might encourage further research. Our future studies will focus on monitoring stress levels and ERP parameters in the course of the disease and on analyzing the relationship between stress, personality type and the course of the disease (natural or modified using immunomodulatory treatment).

Conclusions

The majority of MS patients experience moderate or severe stress, which needs to be addressed with appropriate psychological support. Abnormalities of ERP were found in the MS patients without any overt cognitive decline and showed correlations with measures of stress and negative affectivity (one of the dimensions of the D-type personality scale). Event-related potentials may be considered in the assessment of the influence of stress and emotions on the course of MS.

References

1. Selmaj K. Stwardnienie rozsiane – kryteria diagnostyczne i naturalny przebieg choroby. *Pol Przeg Neurol*. 2005;1:99–105.
2. Wolińska A. Psychological stress and multiple sclerosis. *Neuropsychiat neuropsychol*. 2012;7:184–189.
3. Strober L, Arnett P. Unemployment among women with multiple sclerosis: The role of coping and perceived stress and support in the workplace. *Psychol Health Med*. 2015;12:1–9.
4. Mohr DC, Goodkin DE, Bacchetti P, et al. Psychological stress and the subsequent appearance of new brain MRI lesions in MS. *Neurology*. 2000;55:55–61.
5. Polich J. P300 clinical utility and control of variability. *J Clin Neurophysiol*. 1998;15:14–33.
6. Polman CH, Reingold SC, Banwell B, et al. Diagnostic criteria for multiple sclerosis: 2010 revisions to the McDonald criteria. *Ann Neurol*. 2011;69:292–302.
7. Kurtzke JF. Historical and clinical perspectives of the Expanded Disability Status Scale. *Neuroepidemiology*. 2008;31:1–9.
8. Rao S. *A Manual for the Brief, Repeatable Battery of Neuropsychological tests in multiple sclerosis*. New York, NY: National Multiple Sclerosis Society; 1991.
9. Smith A. The symbol-digit modalities test: A neuropsychologic test of learning and other cerebral disorders. In: Helmuth J, ed. *Learning disorder*. Seattle, WA: Special Child Publications; 1968:83–91.
10. Cohen S, Kamarck T, Mermelstein E. A global measure of perceived stress. *J Health Soc Behav*. 1983;24:385–396.
11. Juczyński Z, Ogińska-Bulik N. *Narzędzia pomiaru stresu i radzenia sobie ze stresem* [in Polish]. Warszawa: Pracownia Testów Psychologicznych; 2009.
12. Denollet J. DS14: Standard assessment of negative affectivity, social inhibition, and type D personality. *Psychosom Med*. 2005;67:89–97.
13. Parmenter BA, Weinstock-Guttman B, Garg N, Munschauer F, Benedict RH. Screening for cognitive impairment in multiple sclerosis using the Symbol Digit Modalities Test. *Mult Scler J*. 2007;13:52–57.
14. Duncan C, Barry R, Connolly J, et al. Event-related potentials in clinical research: Guidelines for eliciting, recording, and quantifying mismatch negativity, P300, and N400. *Clin Neurophysiol*. 2009;120:1883–1908.
15. Senders A, Bourdette D, Hanes D, Yadav V, Shinto L. Perceived stress in multiple sclerosis: The potential role of mindfulness in health and wellbeing. *J Evid Based Complementary Altern Med*. 2014;19:104–111.
16. Artemiadis A, Vervainioti A, Alexopoulos E, Rombos A, Anagnostouli M, Darviri C. Stress management and multiple sclerosis: A randomized controlled trial. *Arch Clin Neuropsychol*. 2012;27:406–416.
17. Pritchard M, Elison-Bowers P, Birdsall B. Impact of integrative restoration (iRest) meditation on perceived stress levels in multiple sclerosis and cancer outpatients. *Stress Health*. 2010;26:233–237.
18. Ogińska-Bulik N. Type D personality in Poland: Validity and application of the Polish DS14. *Pol Psychol Bul*. 2009;40:130–136.
19. Williams L, O'Connor R, Howard S, et al. Type-D personality mechanisms of effect: The role of health-related behavior and social support. *J Psychosom Res*. 2008;64;63–69.
20. Kunst M, Bogaerts S, Winkel F. Peer and inmate aggression, Type D personality and post-traumatic stress among Dutch prison workers. *Stress Health*. 2009;25:387–395.
21. Schiffer A, Smith O, Pedersen S, Widdershoven J, Denollet J. Type D personality and cardiac mortality in patients with chronic heart failure. *Int J Cardiol*. 2010;142:230–235.
22. Nefs G, Speight J, Pouwer F, Pop V, Bot M, Denollet J. Type D personality, suboptimal health behaviors and emotional distress in adults with diabetes: Results from Diabetes MILES–The Netherlands. *Diabetes Res Clin Pract*. 2015;108:94–105.
23. Dubayova T, Krokavcova M, Nagyova I, et al. Type D, anxiety and depression in association with quality of life in patients with Parkinson's disease and patients with multiple sclerosis. *Qual Life Res*. 2013;22:1353–1360.
24. Ludowig E, Bien C, Elger C. Two P300 generators in the hippocampal formation. *Hippocampus*. 2010;20:186–195.
25. Halgren E, Marinkovic K, Chauvel P. Generators of the late cognitive potentials in auditory and visual oddball tasks. *Electroencephalogr Clin Neurophysiol*. 1998;106:156–164.
26. Polich J. Meta-analysis of P300 normative aging studies. *Psychophysiology*. 1996;33:334–353.
27. Aminoff J, Goodin D. Long-latency cerebral event-related potentials in multiple sclerosis. *J Clin Neurophysiol*. 2001;18:372–377.
28. Elger T, Bethke F, Frese A, et al. Event-related potenctials in different subtypes of multiple sclerosis – A cross-sectional study. *J Neurol Sci*. 2002;205:35–40.
29. Pokryszko-Dragan A, Zagrajek M, Słotwiński K, Gruszka E, Bilińska M, Podemski R. Neuropsychological testing and event-related potentials in the assessment of cognitive performance in the patients with multiple sclerosis – A pilot study. *Clin Neurol Neurosurg*. 2009;111: 503–506.
30. Kocer B, Unal T, Nazliel B, et al. Evaluating sub-clinical cognitive dysfunction and event-related potentials (P300) in clinically isolated syndrome. *Neurol Sci*. 2008;29:435–444.
31. Gil R, Zai L, Neau JP, et al. Event-related auditory evoked potentials and multiple sclerosis. *Electroencephalogr Clin Neurophysiol*. 1993;88: 182–187.
32. Pokryszko-Dragan A, Zagrajek M, Slotwinski K, et al. Event-related potentials and cognitive performance in multiple sclerosis patients with fatigue. *Neurol Sci*. 2016;37(9):1545–1556.
33. Sundgren M, Nikulin VV, Maurex L, Wahlin L, Piehl F, Brismar T. P300 amplitude and response speed relate to preserved cognitive function in relapsing–remitting multiple sclerosis. *Clin Neurophysiol*. 2015;126:689–697.
34. Rogan M, Staubli U, LeDoux J. Fear conditioning induces associative long-term potentiation in the amygdala. *Nature*. 1997;390:604–607.
35. Maes M, Mihaylova I, Bosmans E. Not in the mind of neurasthenic lazybones but in the cell nucleus: Patients with chronic fatigue syndrome have increased production of nuclear factor kappa beta. *Neuro Endocrinol Lett*. 2007;28:456–462.

36. Maes M, Twisk FN, Kubera M, Ringel K. Evidence for inflammation and activation of cell-mediated immunity in myalgic encephalomyelitis/chronic fatigue syndrome (ME/CFS): Increased interleukin-1, tumor necrosis factor-α, PMN-elastase, lysozyme and neopterin. *J Affect Disord*. 2012;136:933–939.
37. Senkowski D, Herrmann C. Effects of task difficulty on evoked gamma activity and ERPs in a visual discrimination task. *Clin Neurophysiol*. 2002;113:1742–1753.
38. Duan H, Yuan Y, Yang C, Zhang L, Zhang K, Wu J. Anticipatory processes under academic stress: An ERP study. *Brain Cogn*. 2015;94: 60–67.
39. Brown D, Fenwick P, Howard R. The contingent negative variation in a Go/No Go avoidance task: Relationships with personality and subjective state. *Int J Psychophysiol*. 1989;7:35–45.
40. Nagai Y, Critchley H, Featherstone E, Fenwick P, Trimble M, Dolan R. Brain activity relating to the contingent negative variation: An fMRI investigation. *NeuroImage*. 2004;21:1232–1241.
41. Ansari T, Derakshan N. The neural correlates of cognitive effort in anxiety: Effects on processing efficiency. *Biol Psychol*. 2011;86: 337–348.

Hounsfield units from unenhanced 18F-FDG-PET/CT are useful in evaluating supradiaphragmatic lymph nodes in children and adolescents with classical Hodgkin's lymphoma

Radosław Chaber[1,A–D,F], Mateusz Łasecki[2,A–D], Justyna Kwaśnicka[3,B], Kornelia Łach[1,C], Zbigniew Podgajny[4,5,B,E], Cyprian Olchowy[2,B], Urszula Zaleska-Dorobisz[2,E,F]

[1] Department of Pediatric Oncology and Hematology, Faculty of Medicine, University of Rzeszów, Poland
[2] Department of General and Pediatric Radiology, Wroclaw Medical University, Poland
[3] Department of Pediatric Bone Marrow Transplantation, Oncology and Hematology, Wroclaw Medical University, Poland
[4] Affidea Center of Positron Emission Tomography and Computed Tomography, Wrocław, Poland
[5] Department of Endocrinology and Isotopes Therapy, Military Institute of Medicine, Warszawa, Poland

A – research concept and design; B – collection and/or assembly of data; C – data analysis and interpretation; D – writing the article; E – critical revision of the article; F – final approval of the article

Advances in Clinical and Experimental Medicine, ISSN 1899-5276 (print), ISSN 2451-2680 (online) *Adv Clin Exp Med*. 2018;27(6):795–805

Address for correspondence
Radosław Chaber
E-mail: radoslaw.chaber@gmail.com

Funding sources
None declared

Conflict of interest
None declared

Received on October 28, 2016
Reviewed on December 14, 2016
Accepted on February 14, 2017

Abstract

Background. The precise identification of the primarily-affected nodal regions in Hodgkin's lymphoma (HL) is essential in determining the stage of the disease and the intensity of chemotherapy and radiotherapy.

Objectives. The aim of this study was to use the degree of X-ray attenuation (XRA) in Hounsfield units (HU) and the lymph node-to-muscle attenuation ratio (LN/M) in computed tomography (CT) unenhanced imaging, routinely performed with 18F-fluorodeoxyglucose positron emission tomography (18F-FDG-PET), to distinguish HL-affected supradiaphragmatic lymph nodes.

Material and methods. The study included 52 patients with classical HL treated according to the EuroNet-PHL-C1 protocol. Patients received 2 chemotherapy cycles after 18F-FDG-PET/CT testing, followed by re-examination. The lymph nodes were evaluated according to the Society for Pediatric Oncology and Hematology's GPOH-HD-2002 study and Lugano criteria as not-involved (NI-LN) and involved (I-LN).

Results. A significant difference ($p < 0.001$) was found in the XRA and LN/M values between NI-LN and I-LN before treatment and after the 2 chemotherapy cycles. The optimal cut-off point for XRA (44.7 HU) and LN/M (0.79) values distinguishing I-LN from NI-LN nodes was determined by receiver operating characteristic (ROC) analysis. After 2 cycles of chemotherapy, higher XRA ($p = 0.002$) and LN/M ($p = 0.001$) values in the group with inadequate early CTx response were found.

Conclusions. The use of XRA in HU and LN/M, together with the existing standard, can improve the qualification of supradiaphragmatic lymph nodes in HL.

Key words: children, lymph nodes, Hodgkin's lymphoma, positron-emission tomography

DOI
10.17219/acem/68990

Introduction

Hodgkin's lymphoma (HL) is one of the most common neoplasms in adolescents of 15–20 years of age (approx. 12–29 cases per million per year in European countries and the USA; approx. 6% of all pediatric tumor cases).[1,2]

In recent decades, significant progress in the treatment of children with HL has been made. About 90–95% of patients survive many years relapse-free.[3] Currently, risk-adapted therapy (chemotherapy – CTx, potentially with radiotherapy – RTx), where the intensity of treatment depends on the presence of specific prognostic factors, is a standard procedure.

A health analysis of convalescents treated in childhood for HL revealed that, despite many years of remission, a large number of them suffered from numerous late effects of the administered therapy (e.g., secondary thyroid or breast cancer, leukemia, infertility, cardiomyopathy, failure of endocrine organs, or pulmonary fibrosis). These complications significantly diminish the quality of life and may even shorten it.[4–8] Contemporary regimens seek to reduce the toxicity of CTx and to completely eliminate RTx in those patients who respond well to CTx.[9] If RTx is necessary, it is limited to the lowest number of fields and doses.[10] The precise identification of affected lymph nodes (LN) in different regions is of fundamental importance in determining the intensity of CTx and specifying fields for possible irradiation. The selection of patients for additional RTx was based on the evaluation of morphological and functional response after the first 2 cycles of CTx.

The aim of this study was to use the degree of X-ray attenuation (XRA), expressed in Hounsfield units (HU), and the lymph node-to-muscle attenuation ratio (LN/M) in computed tomography (CT) unenhanced imaging, routinely performed with 18F-fluorodeoxyglucose positron emission tomography (18F-FDG-PET), to distinguish HL-affected nodes. Moreover, LN XRA values were measured after the first 2 cycles of CTx to assess morphological and functional response.

Material and methods

Patients

The study included 52 of a total of 61 consecutive patients diagnosed with classical HL between 2009 and 2015. In 7 patients it was impossible to locate the primarily affected LN or unaffected nodes. In another 2 cases, unsatisfactory technical quality made it impossible to measure XRA in control 18F-FDG-PET/CT tests. Each diagnosis was confirmed by centrally verified histopathology. The clinical characteristics of the patients are shown in Table 1. The initial staging and response to CTx assessments were performed according to the EuroNet PHL C1 protocol.[11,12] After 18F-FDG-PET/CT testing, all patients received 2 CTx cycles – vincristine (Oncovin), etoposide, prednisone, and doxorubicin (Adriamycin – OEPA) – followed by 18F-FDG-PET/CT re-examination. In the case of an unsatisfactory functional and/or morphological response to the administered CTx, the patient was subjected to RTx after all cycles of CTx.

Table 1. Characteristic of patients (n = 52)

Feature	
Male/female	24/28
Age	
range [years]	4–17.5
median	14
HL subtypes	
nodular sclerosis (NS)	47
mixed cellularity (MC)	2
lymphocyte depleted (LD)	2
not done	1
Initial staging (Ann Arbor)	
I	1
II	24
III	13
IV	14
B symptoms	28
"E" feature	14
Therapeutic groups	
TG 1	9
TG 2	15
TG 3	28
Early chemotherapy response adequate/inadequate	27/25

HL – Hodgkin's lymphoma; TG – therapeutic group.

Analysis of CT images

Unenhanced 18F-FDG-PET/CT studies were performed using a 16-row detector GE Discovery STE16 scanner (GE Healthcare, Milwaukee, United States) with variable voltage (100–140 keV) and intensity (10–150 mAs), single collimation width (SCW) 0.625–1.25, total collimation width (TCW) 10.0–20.0, and spiral pitch factor (SPF) 1.125–0.75. We analyzed 61 CT components performed at the time of initial diagnosis (Fig. 1 A, B) and 61 tests evaluating the early response to CTx – about 2–3 weeks after the second OEPA cycle (Fig. 1 C, D). All tests were performed as part of routine clinical diagnostics. Axial sections were used for the assessment and preference was given to those having the thinnest layers, which ranged from 1.25 to 3.75 mm, depending on the study/patient.

Principles for the evaluation of lymph nodes

Lymph nodes were evaluated according to the Society for Pediatric Oncology and Hematology's GPOH-HD 2002 study and Lugano criteria independently by 2 radiologists and a nuclear medicine specialist.[7,13] The Surveillance,

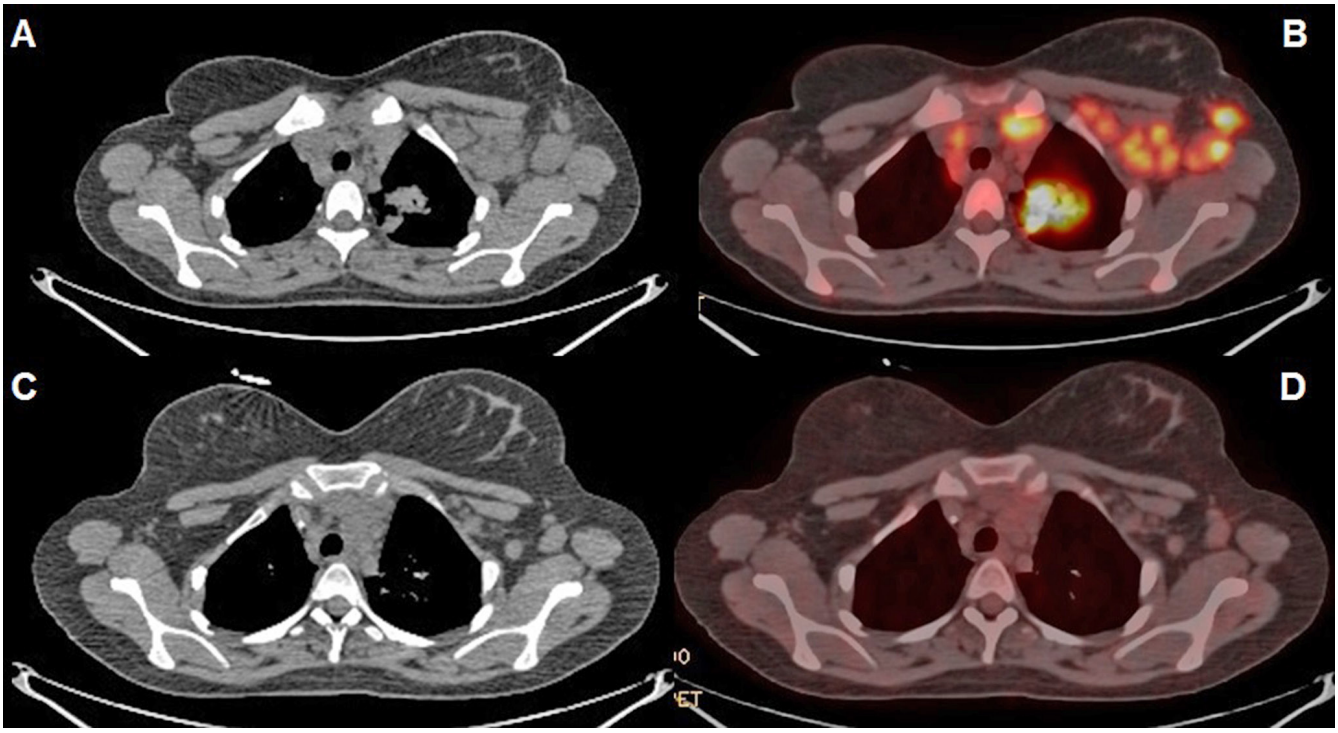

Fig. 1. A 17-year-old female with classical NS type HL; axial CT and PET-CT (fusion) images performed before (A, B) and after OEPA treatment (C, D)

A – malignant lymphadenopathy of the left axillary and subclavian lymph nodes; right axillary lymph nodes were normal; NS – nodular sclerosis; HL – Hodgkin's lymphoma, CT – computed tomography; PET – positron emission tomography; OEPA – vincristine (Oncovin), etoposide, prednisone, and doxorubicin (Adriamycin)

Epidemiology, and End Results program (SEER) database guidelines with minor modifications were adopted for the anatomic division of LN.[14]

The preferred normal LN locations were: axilliary (level 1 according to Berg), cervical (level 5 according to Som et al.), or the mandibular angle.[15,16] Nodes of normal morphology and size were excluded if an affected node existed within a distance of less than 2 cm. XRA measurement was made on an axial section of the node with the thickest cortical layer. The fatty hilum was disregarded for measurement as it would have lowered the average XRA value.

Involved nodes were selected based on the 18F-FDG-PET component, according to highest maximum standardized uptake value (SUV_{max}) and the largest area of peak SUV_{max} value occurrence. The most commonly elected LNs were: cervical (level 4 and 5 according to Som et al.), mediastinal (levels 2–7 according to International Symposium on Light Alloys and Composite Materials – ISLAC) and subclavian (axillary nodes level 2 and 3 according to Berg).[15–17] In each case, the XRA values were assessed in the section in which the fusion image showed the highest SUV_{max} value and in the 2 adjacent sections (due to the possibility of a small image shift in PET compared to the CT images, Fig. 2).[18,19] The arithmetic mean was calculated using these 3 measurements. One of the factors hindering the assessment was variable upper limb positioning by the patient in individual studies.

The group of normal nodes unaffected by HL (not-involved – NI-LN) included nodes whose largest dimension was <1 cm and whose SUV values did not exceed Deauville scale level 2. Nodes >2 cm rated Deauville scale level 4 or 5 were considered affected by HL (involved – I-LN). In each study, 2–5 supradiaphragmatic LNs categorized as NI-LN or I-LN were selected for analysis, and then the average XRA was calculated. In order to eliminate non-specific inter-individual variability related to different water and body fat content, the LN/M ratio was introduced. This value is obtained by dividing the average LN HU value by the HU value of the right erector spinae muscles. The results obtained are therefore also independent of the keV and mAs parameters used in the study.

The region of interest (ROI) calculation of LN is presented in Fig. 2.

Right erector spinae muscle selection

Measurements were made in axial sections of the CT between the places where the celiac and superior mesenteric arteries arise. This area was chosen due to the low variability of anatomical relations between the muscles and the surrounding structures in successive studies, ensuring the repeatability of measurements. The XRA measurements were performed maintaining a margin of 2–3 mm from fatty tissue clusters adjacent to the muscles. The region of interest included a field surface of 0.8–1 cm^2 every time.

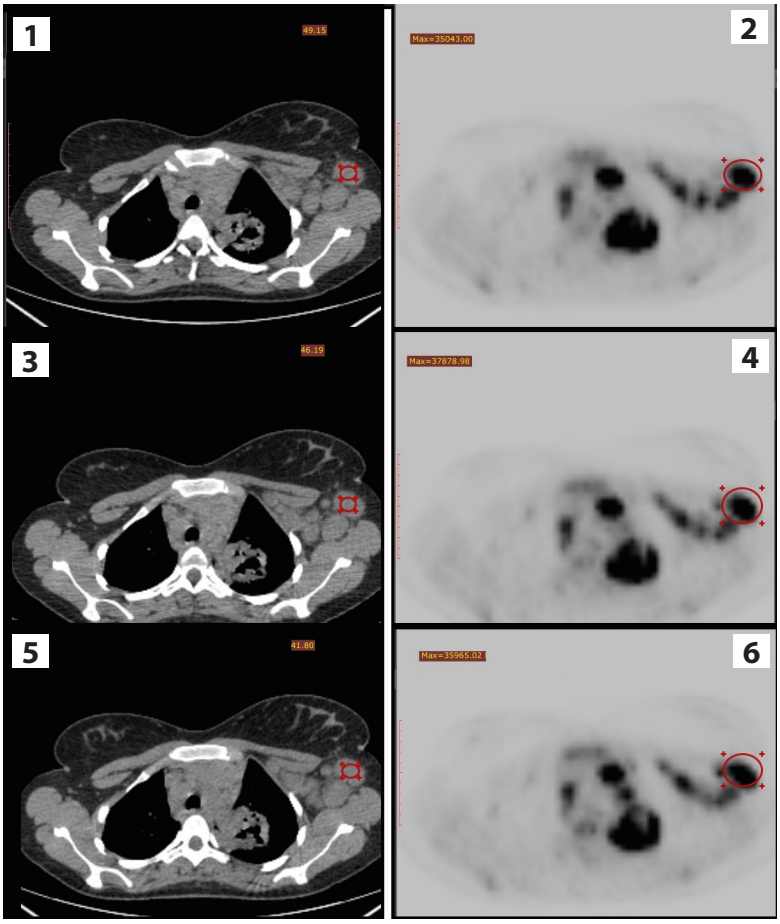

Fig. 2. This image presents the method of assessing mean density (in HU) of a malignant left axillary lymph node before CTx treatment. The ROI measurement was put on the central part of the lymph node (image 3). It should cover at least half of the area of the lymph node on the axial scan with the highest SUV_{max} value (image 4). Due to the risk of slight CT-PET image misalignment, density measurements were performed on 2 adjacent CT axial scans as well (images 1–2 and 5–6). The final HU value was an arithmetic mean of the 3 previous measurements

HU – Hounsfield units; ROI – the region of interest; CTx – chemotherapy; SUV_{max} – maximum standardized uptake value; CT – computed tomography; PET – positron emission tomography.

Three measurements were performed from the chosen cross-section and the arithmetic mean was calculated. The presence of hardened beam artifacts or of any focal lesions (e.g., intramuscular calcification) resulted in the exclusion of measurements.

Statistical analysis

The average XRA values and the LN/M ratios, as well as the differences depending on certain clinical parameters, were compared using Student's t-test. The Wilcoxon test for sequence pairs was used to analyze the differences of XRA and LN/M after 2 cycles OEPA relative to the primary results. The optimal cut-off point for distinguishing normal nodes from HL-affected nodes was determined using receiver operating characteristic analysis (ROC) implementing the Youden index. It was assumed that the cost of obtaining a false negative is twice as high as the cost of obtaining a false positive. The resulting area under the curve (AUC) was compared to an AUC equal to 0.5 using Hanley's algorithm.[20] The level of significance was $p < 0.05$. The calculations were performed using STATISTICA v. 12, Medical kit v. 3.0 (StatSoft, Tulsa, USA).

Table 2. Results of NI-LN vs I-LN group (n = 52)

Variable	Non-involved lymph nodes [NI-LN]	Involved lymph nodes [I-LN]	p-value
initial staging			
XRA range [HU]	18.5–73.7	34.0–108.7	<0.001
XRA average [HU] (SD)	40.1 (12.01)	56.63 (13.30)	
LN/M range	0.37–1.33	0.45–2.03	<0.001
LN/M average (SD)	0.70 (0.22)	1.01 (0.29)	
after 2 OEPA cycles			
XRA range [HU]	5.0–56.05	3.3–67.5	<0.001
XRA average [HU] (SD)	28.62 (10.68)	38.16 (11.58)	
LN/M range	0.09–1.04	0.06–1.22	<0.001
LN/M average (SD)	0.52 (0.21)	0.69 (0.20)	
Δ = XRA(LN/M) after 2 OEPA cycles/XRA (LN/M) initial staging			
range [HU]	0.14–1.91	0.05–1.60	0.66
average [HU] (SD)	0.75 (0.30)	0.71 (0.28)	
range LN/M	0.17–1.90	0.07–1.89	0.59
average LN/M (SD)	0.76 (0.34)	0.73 (0.31)	

XRA – X-ray attenuation; HU – Hounsfield units; LN/M – lymph node/muscle attenuation ratio; NI-L – not-involved lymph nodes; I-LN – involved lymph nodes; SD – standard deviation; OEPA – vincristine (Oncovin), etoposide, prednisone, and doxorubicin (Adriamycin)

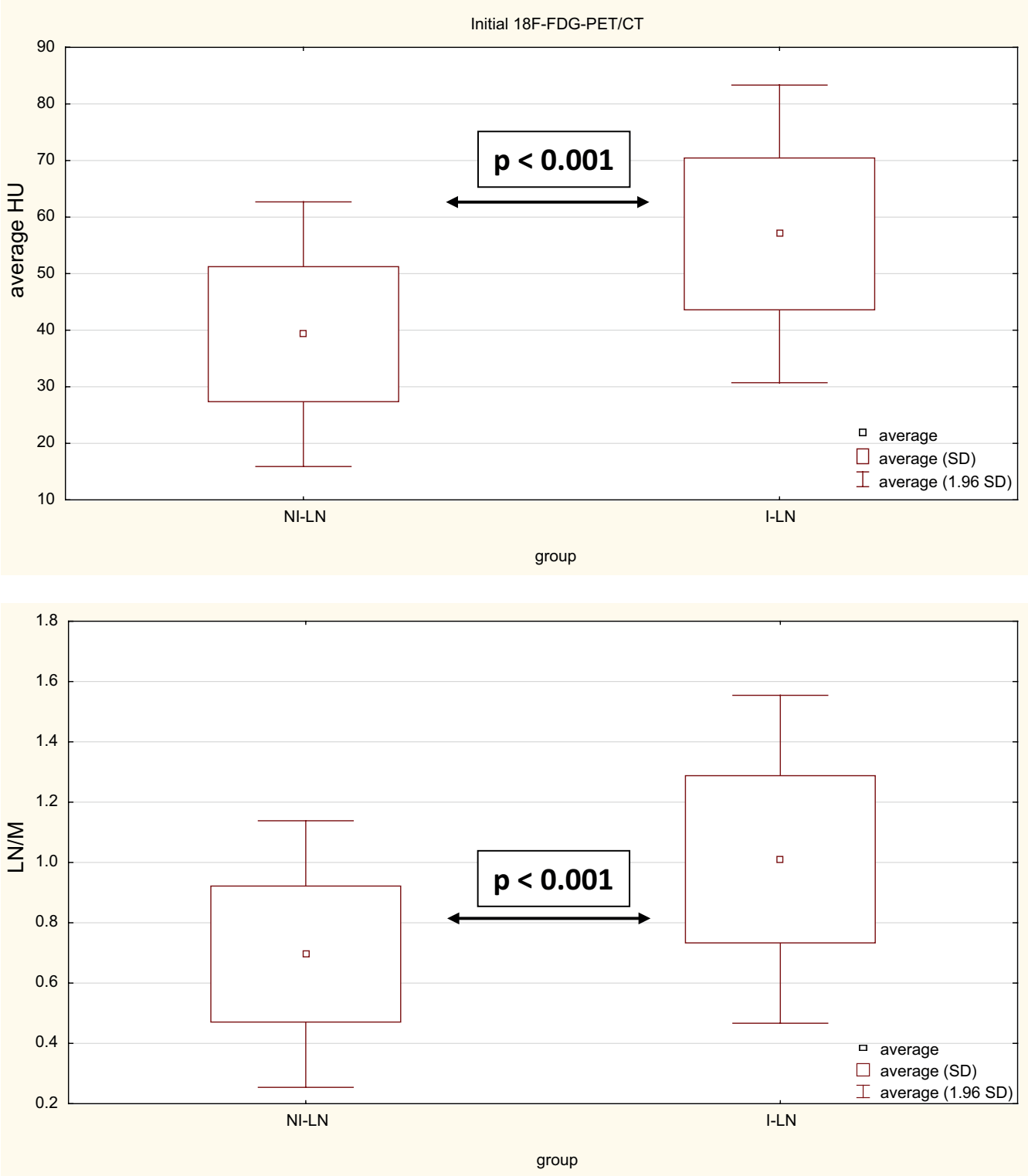

Fig. 3. Initial 18FDG-PET-CT not-involved vs involved lymph nodes [average HU; LN/M] (n = 52)

18FDG-PET-CT – 18F-fluorodeoxyglucose positron emission tomography; HU – Hounsfield units; LN/M – lymph node/muscle attenuation ratio; NI-L – not-involved lymph nodes; I-LN – involved lymph nodes; SD – standard deviation.

Results

The obtained results are compared in Table 2. The average values of XRA and LN/M from I-LN and NI-LN in primary 18F-FDG-PET/CT and the changes in these parameters after 2 cycles OEPA are presented. A significant difference was found in the XRA and the average LN/M values between the LNs assessed as HL-affected due to size and metabolic activity in 18F-FDG-PET/CT vs normal LNs. This difference was significant both in studies

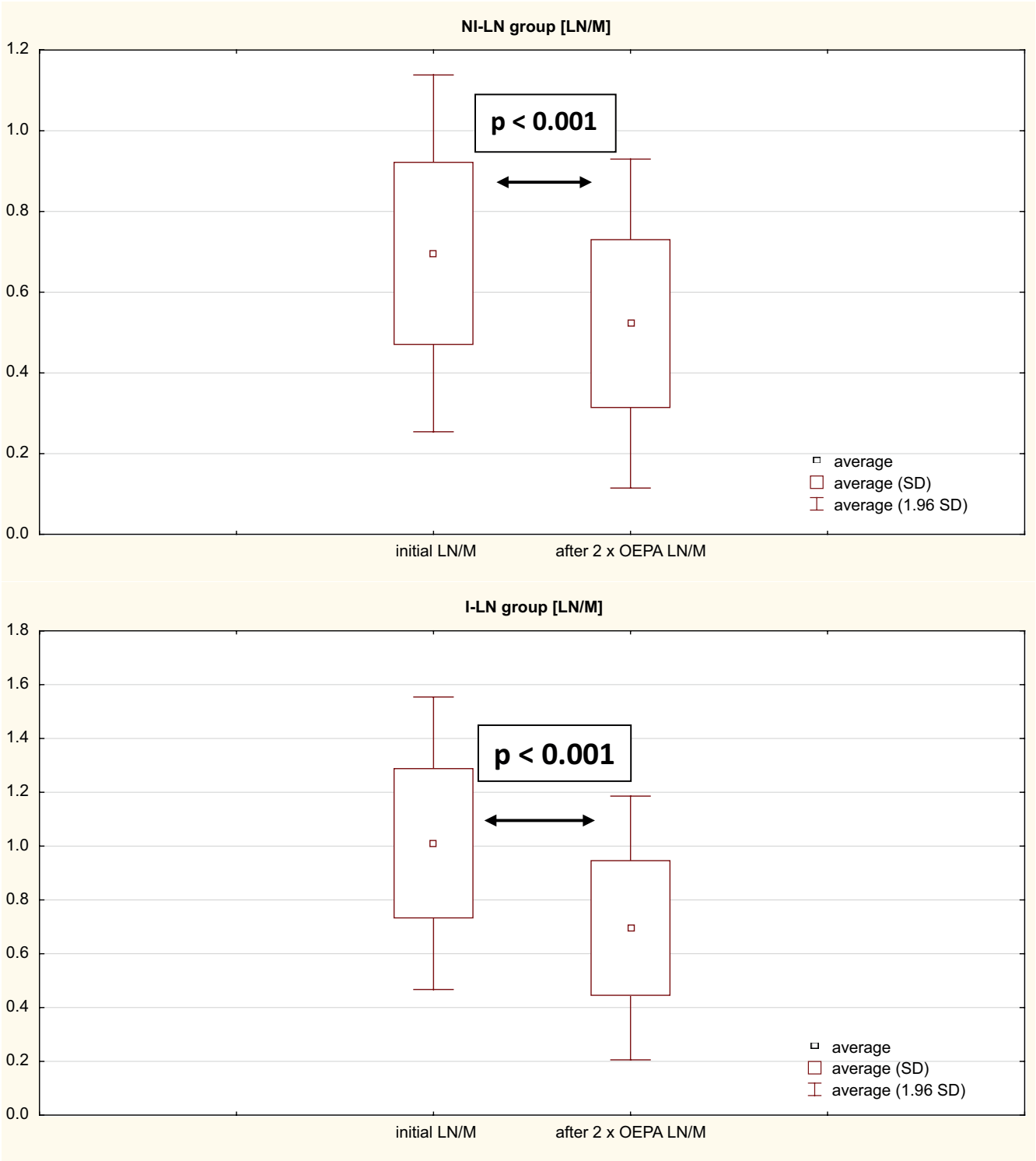

Fig. 4. 18F-FDG-PET/CT initial vs after 2 OEPA cycles [LN/M] (n = 52)

18FDG-PET-CT – 18F-fluorodeoxyglucose positron emission tomography; OEPA – vincristine (Oncovin), etoposide, prednisone, and doxorubicin (Adriamycin) LN/M – lymph node/muscle attenuation ratio; SD – standard deviation.

performed before treatment ($p < 0.001$; Fig. 3) and those performed during the assessment of treatment response after 2 OEPA cycles ($p < 0.001$). Significantly higher values of HU were observed in I-LN compared to NI-LN nodes. Comparing LN/M also revealed higher values in I-LN relative to NI-LN nodes.

In the 18F-FDG-PET/CT study performed after 2 OEPA cycles, both XRA and LN/M values were significantly lower compared to baseline, in both the I-LN and the NI-LN ($p < 0.001$, Table 2, Fig. 4). XRA and LN/M values after 2 cycles of OEPA compared with preliminary XRA and LN/M values for particular nodes (Δ) did not differ significantly

Table 3. Initial 18F-FDG-PET/CT, I-LN group (n = 52)

Variable		X-RA [HU] average ±SD	p-value	LN/M average ±SD	p-value
Age [years] (number of patients)	≤14 (28)	60.92 ±14.84	**0.010**	1.12 ±0.32	**0.002**
	>14 (24)	51.62 ±9.22		0.88 ±0.17	
Sex (number of patients)	male (24)	59.73 ±14.36	0.120	1.04 ±0.29	0.486
	female (28)	53.97 ±11.93		0.99 ±0.29	
HL (number of patients)	NS (47)	56.18 ±12.82	0.641*	1.01 ±0.28	0.756*
	non-NS (5)	65.48 ±18.04		1.07 ±0.38	
Stage$^{\$}$ (number of patients)	II (24)	56.70 ±16.72	0.896$^{\#}$	1.05 ±0.37	0.914$^{\#}$
	III (13)	56.96 ±11.51		0.97 ±0.23	
	IV (14)	56.46 ±8.69		0.98 ±0.18	
Early chemotherapy response (number of patients)	inadequate (25)	56.76 ±14.76	0.949	0.99 ±0.28	0.623
	adequate (27)	56.52 ±12.07		1.03 ±0.30	

* the Mann–Whitney U test; $^{\#}$ the Kruskal–Wallis test; $^{\$}$ without any patient with stage I; XRA – X-ray attenuation; HU – Hounsfield units; LN/M – lymph node/muscle attenuation ratio; I-LN – involved lymph nodes; SD – standard deviation; HL – Hodgkin's lymphoma; NS – nodular sclerosis; significant results in bold.

Table 4. 18F-FDG-PET-CT after 2 OEPA cycles, I-LN group (n = 52)

Variable		XRA [HU] average ±SD	p-value	LN/M average ±SD	p-value
Age [years] (number of patients)	≤14 (28)	37.16 ±12.70	0.508	0.68 ±0.27	0.738
	>14 (24)	39.33 ±10.41		0.70 ±0.19	
Sex (number of patients)	male (24)	36.44 ±9.22	0.327	0.67 ±0.19	0.606
	female (28)	39.64 ±13.37		0.70 ±0.27	
HL (number of patients)	NS (47)	38.86 ±12.73	0.663*	0.69 ±0.24	0.686*
	non-NS)	39.32 ±9.80		0.65 ±0.17	
Stage$^{\$}$ (number of patients)	II (24)	38.49 ±10.28	0.335$^{\#}$	0.69 ±0.23	0.734$^{\#}$
	III (13)	38.78 ±9.39		0.71 ±0.19	
	IV (14)	36.10 ±15.65		0.65 ±0.30	
Early chemotherapy response (number of patients)	inadequate (25)	43.26 ±10.35	**0.002**	0.80 ±0.21	**0.001**
	adequate (27)	33.45 ±10.90		0.58 ±0.20	

* the Mann–Whitney U test; $^{\#}$ the Kruskal–Wallis test; $^{\$}$ without any patient with stage I; XRA – X-ray attenuation; HU – Hounsfield units; LN/M – lymph node/muscle attenuation ratio; I-LN – involved lymph nodes; SD – standard deviation; HL – Hodgkin's lymphoma; NS – nodular sclerosis, OEPA – vincristine (Oncovin), etoposide, prednisone, and doxorubicin (Adriamycin); significant results in bold.

in either group (I-LN vs NI-LN p = 0.66 for XRA, and p = 0.59 for the LN/M, Table 2).

In the initial 18F-FDG-PET/CT study, a significant statistical difference was found between XRA (p = 0.001) and LN/M (p = 0.002) in the I-LN nodes in children aged up to 14 years in relation to children older than 14 years (Table 3). The difference is not as apparent after shifting the age limit to 16 years, or in the XRA for NI-LN, and in 18FDG-PET-CT after 2 OEPA cycles. There were no significant differences in HU values for HL-affected nodes depending on gender, histological type, stage and responses after 2 cycles of OEPA (Table 3).

In the measurements taken after 2 cycles of OEPA, no significant difference was found in XRA depending on the analyzed clinical parameters in the I-LN group other than significantly higher XRA (p = 0.002) and LN/M (p = 0.001) values in the group with inadequate CTx response (Table 4, Fig. 5).

The optimal cut-off point for XRA and LN/M values distinguishing I-LN from NI-LN nodes was determined by ROC analysis. The greatest test accuracy was obtained by selecting baseline node XRA values of 44.7 HU (Fig. 6, AUC = 0.836, 95% confidence interval – CI: 0.759–0.913; p < 0.001) and a LN/M ratio of –0.79 (AUC = 0.804, 95% CI: 0.721–0.887; p < 0.001). A comparison of the obtained ROC curve compared to a random node qualification curve demonstrated a significant statistical difference for XRA and LN/M (p < 0.001).

ROC analysis was also used to assess the response of initially affected nodes to early CTx (and thus to qualify for RTx) in 18F-FDG-PET/CT after 2 OEPA cycles. The highest test accuracy was obtained when selecting a cut-off

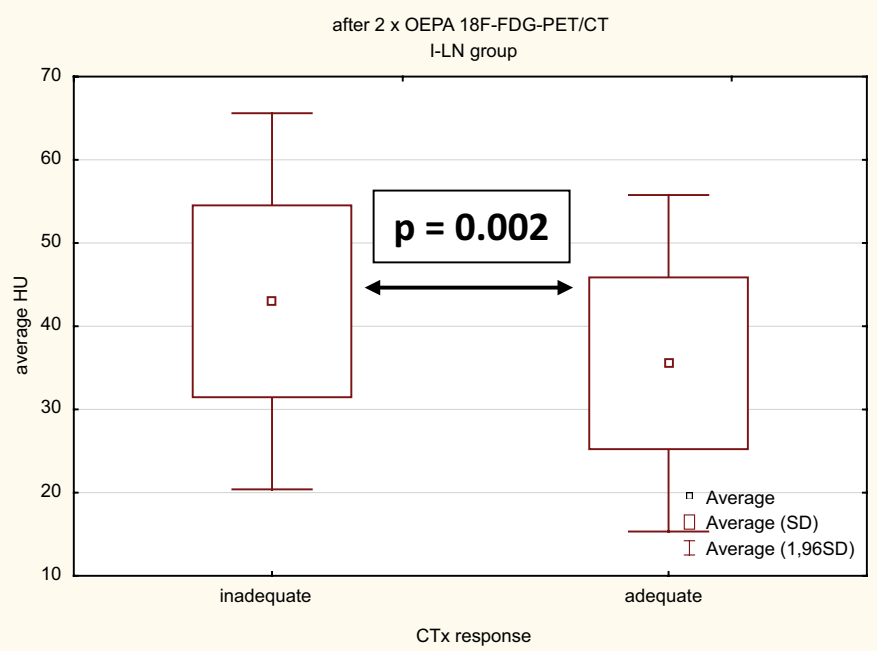

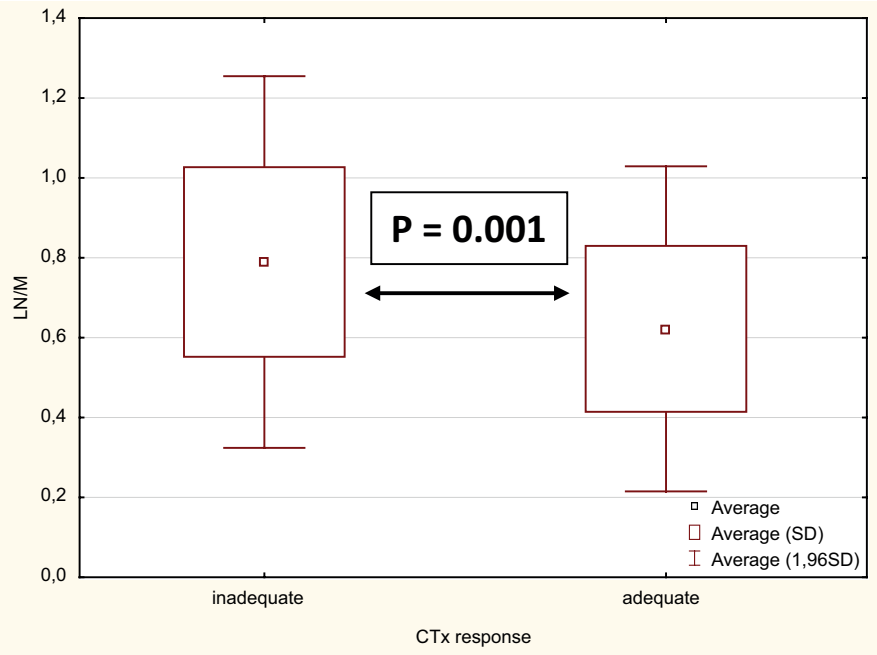

Fig. 5. 18F-FDG-PET/CT after 2 OEPA cycles, I-LN group (n = 52)

18FDG-PET-CT – 18F-fluorodeoxyglucose positron emission tomography; OEPA – vincristine (Oncovin), etoposide, prednisone, and doxorubicin (Adriamycin); I-LN – involved lymph nodes; SD – standard deviation.

point of 34.8 HU (AUC = 0.744, 0.95% CI: 0.608–0.879; p = 0.0004) and a LN/M ratio of –0.62 (AUC = 0.766, 0.95% CI: 0.632–0.900; p = 0.0001). Comparing the obtained ROC curve to a random node qualification curve showed no statistically significant difference for XRA (p = 0.12) or for the LN/M ratio (p = 0.11).

Discussion

Precise identification of all originally affected nodal regions and organs, and CTx response assessment using imaging and functional studies, are crucial in planning optimal treatment. The sensitivity and specificity of 18F-FDG-PET/CT tests in the evaluation of both initially affected LNs and the response to CTx in HL are high (90–100% sensitivity, 80–90% specificity) and exceed the diagnostic value of contrast CT.[21–23] 18F-FDG-PET/CT interpretation can be difficult in children due to frequent respiratory infections and the associated increased metabolic activity of the lymphatic system.

We have found no publications in which an attempt has been made to use XRA in CT directly for the differentiation of affected and unaffected LNs in children and adolescents with HL. One study, investigating a population of 25 adults with lymphoma, illustrates that LN XRA values were in most cases at the same level as soft tissue – only 2 patients attained lower values.[24] Similar analysis

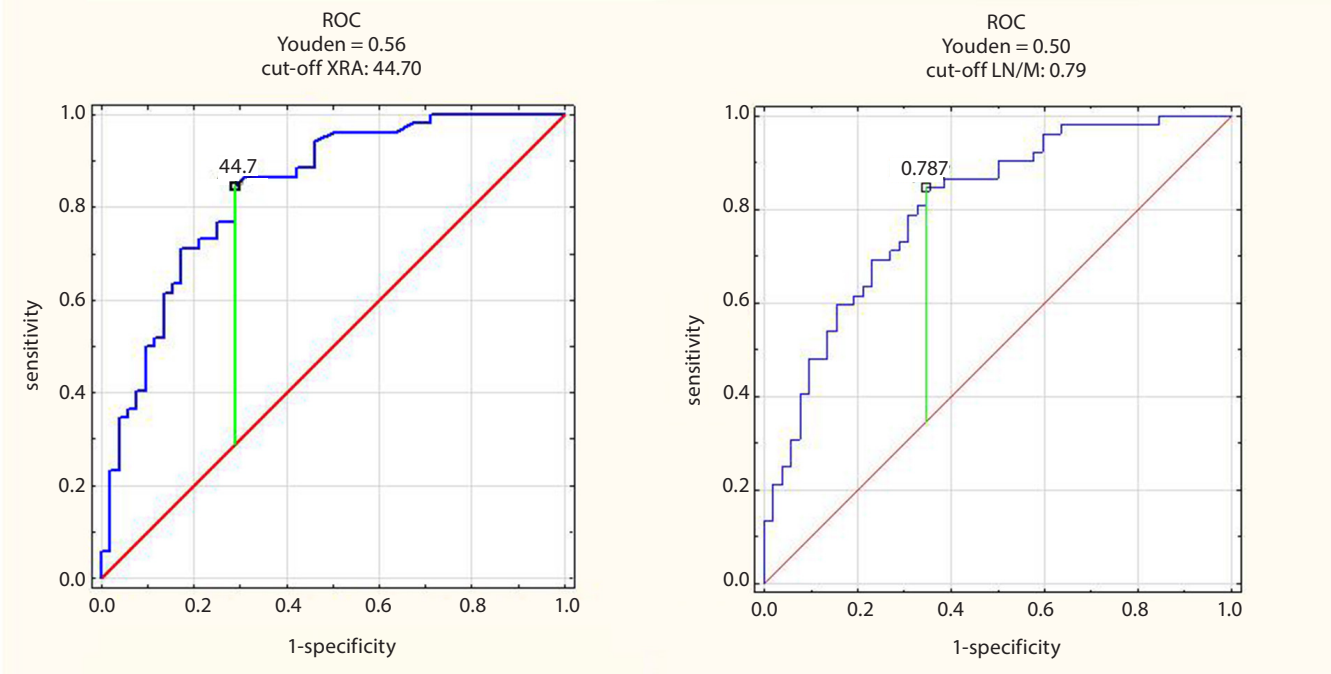

Fig. 6. Receiver operating characteristic (ROC). Initial 18F-FDG-PET/CT, NI-LN vs I-LN group (n = 52)

18FDG-PET-CT – 18F-fluorodeoxyglucose positron emission tomography; NI-LN – not involved lymph nodes; I-LN – involved lymph nodes.

in other neoplastic diseases also suggested this parameter's potential. In the study by Flechsig et al., which uses XRA to differentiate LNs in an orthotopic model of lung cancer in rats, it was proved that the XRA of metastatic LNs in the mediastinum was significantly higher than in those without metastatic foci.[25] Yoon et al. analyzed mediastinal LNs in 674 patients with non-small-cell lung cancer.[26] Nodes with XRA values >70 HU, despite 18FDG uptake, had a higher probability of not having metastatic foci. Measuring XRA is also used to distinguish normal from metastatic nodes in the axilliary region in patients with breast cancer. In a study by Urata et al., significantly higher XRA values in metastatic LNs as compared to unaffected nodes was shown.[27] Esophageal squamous cell carcinoma is another cancer in which the evaluation of XRA can be used to differentiate between metastatic and normal LNs. In the study by Kim et al., it was shown that the XRA for metastatic nodes was significantly lower than for unaffected nodes.[28]

In our study, we evaluated the unenhanced component of 18F-FDG-PET/CT. One undoubted advantage is the low dosage of X-rays used, which is important due to the young age of patients and the need for periodic examinations in the monitoring of the disease. For radiological protection, it is preferable to perform magnetic resonance imaging (MRI) and 18F-FDG-PET/MRI; however, CT remains the gold standard for imaging the chest and lungs. Another advantage of using the CT component is that administering iodine contrast agents is unnecessary, unlike with classic CT.[29] The administration of a contrast agent can cause many adverse effects and increases the radiation dosage in the child.[30–32] The use of unenhanced CT examination eliminates the risk of tissue size and density measurement errors due to beam hardening artifacts resulting from large residual amounts of concentrated contrast in the blood vessels.[33,34] An additional difficulty concerning this method is that even a slight disturbance in the contrast administration protocol or in the anatomy of the patient may significantly change the image of the scanned structures, which can cause an unwarranted increase in the planned radiation dose when administering radiation therapy.[35,36]

In this study we have shown that the XRA values are significantly higher in I-LN compared with NI-LN according to standard criteria. This difference is observed both in the baseline study and after 2 cycles of CTx. This may result from the different structure in nodes with active neoplastic disease compared to unaffected nodes. In neoplastic LNs, damaged internal structure with chaotic blood vessels can be seen. The presence of increased perinodular fatty tissue can also be observed.[37] Nodular sclerosis Hodgkin's lymphoma classical form dominates in the pediatric population. It is characterized by a high content of fibrous connective tissue (desmoplasia), among other things. Normal LNs are characterized by a more ordered structure with a well-separated vascular hilum and regular blood flow through the node. It can be supposed that the content of lymphomatous tissue with different XRA values compared to normal tissue in the evaluated LN will determine the final XRA value. This is consistent with the observation that the XRA/(LN/M) value decreased significantly after CTx administration, both in affected and

normal LNs, as a result of internal structural changes like desmoplasia. In patients who did not achieve an adequate morphological and functional response and were qualified for RTx, the XRA and LN/M values were higher. A weaker CTx effect on HL nodes may be visible as a "slower" decline in both the SUV and the dimensions of the I-LN, as well as the XRA (LN/M) values. The differences, however, are too small to be used as a standalone parameter for a reliable evaluation of the nodes' response to CTx.

According to our analysis, there is a visible difference in the XRA values of HL-affected nodes between children younger than 14 years and the group of older children and young adults (15–18 years old). Moving the age limit to 16 years reduces the relevance of the above difference, but it persists when the limit is shifted to 12 or 10 years. This relationship does not occur in unaffected nodes (NI-LN) or in imaging performed after 2 CTx cycles. This may be due to the slightly different biology and LN structure in younger children with HL.

It seems that measuring XRA/(LN/M) in 18F-FDG-PET/CT without contrast, including the assessment of size and SUV, may increase the accuracy of the qualification of LNs as HL-affected or unaffected. This parameter could potentially be of use, especially in case of doubt concerning the interpretation of radiological images. Large, obvious nodal lesions of over 2 cm in diameter typically do not cause diagnostic dilemmas. The assessment of nodes with so-called intermediate ("unclear") dimensions (1–2 cm) and SUV values (2–3 points on the Deauville scale) can be more problematic. Unfortunately, a limitation of our study is the unavailability of histopathological verification for each evaluated LN. Hodgkin's lymphoma most often affects many LNs in various parts of the body. Surgical biopsy of all lesions is not clinically justified and is not routinely done. Because of the impossibility of routine histopathological confirmation, the group of intermediate LNs had to be excluded from analysis.

Another limitation is assessing the HU values in 3-mm CT slices. Values of HU on image borders may be inaccurate for small structures such as LNs due to the partial volume effect, which specifically concerns images from PET-CT scanners.[38,39] In addition, HU values depend on the CT machine, the imaging conditions, and the specifications of the image processing software, which differ in every institution. For this reason, a direct comparison of exams carried out in different centers would not be reliable.[40] Introducing the LN/M and its analysis allows for the reduction of variability resulting from different technical parameters of CT scanners and exam protocols and from the impact of nonspecific external factors such as inter-individual variation.

Conclusions

Using XRA and the LN/M ratio in addition to the current standard criteria of assessing LNs in HL could be helpful and may improve the quality of their qualification as affected or unaffected. It can translate into more accurate staging and CTx response assessment in some groups of patients, and further, into reducing the incidence of the complications of RTx and CTx (the reliable determination of RTx fields and CTx intensity) and reducing the frequency of HL relapses in regions which were originally incorrectly labeled unaffected or wrongly classified as having an adequate response to CTx.

The XRA and LN/M values could be also an addition to standard criteria factors in the assessment of CTx early response in doubtful cases. Full recognition of the diagnostic value of these parameters requires further studies in larger groups of patients.

References

1. Ries LAG, Harkins D, Krapcho M, et al. (eds). SEER Cancer Statistics Review, 1975-2003, National Cancer Institute. Bethesda, MD, http://seer.cancer.gov/csr/1975_2003/, based on November 2005 SEER data submission, posted to the SEER web site, 2006.
2. de Alarcon PA, Metzger M, Al-Rahawan MM. Pediatric Hodgkin lymphoma. Medscape News & Perspective. http://emedicine.medscape.com/article/987101-overview#a5. Accessed April 30, 2015.
3. National Cancer Institute. PDQ® Childhood Hodgkin Lymphoma Treatment. National Cancer Institute, Bethesda. http://www.cancer.gov/types/lymphoma/hp/child-hodgkin-treatment-pdq. Accessed February 3, 2016.
4. van Nimwegen FA, Schaapveld M, Janus CP, et al. Cardiovascular disease after Hodgkin lymphoma treatment: 40-year disease risk. *JAMA Intern Med*. 2015;175(6):1007–1017.
5. Chemaitilly W, Mertens AC, Mitby P, et al. Acute ovarian failure in the childhood cancer survivor study. *J Clin Endocrinol Metab*. 2006;91(5):1723–1728.
6. Constine LS, Scott Gamis A, Gross TG, et al. PDQ® Childhood Hodgkin Lymphoma Treatment. National Cancer Institute, Bethesda. http://www.cancer.gov/types/lymphoma/hp/child-hodgkin-treatment-pdq. Accessed March 31, 2016.
7. Mauz-Körholz C, Hasenclever D, Dörffel W, et al. Procarbazine-free OEPA-COPDAC chemotherapy in boys and standard OPPA-COPP in girls have comparable effectiveness in pediatric Hodgkin's lymphoma: The GPOH-HD-2002 study. *J Clin Oncol*. 2010;28(23):3680–3686.
8. Maraldo MV, Brodin NP, Aznar MC, et al. Estimated risk of cardiovascular disease and secondary cancers with modern highly conformal radiotherapy for early-stage mediastinal Hodgkin lymphoma. *Ann Oncol*. 2013;24(8):2113–2118.
9. Raemaekers JM, Andre MP, Federico M, et al. Omitting radiotherapy in early positron emission tomography-negative stage I/II Hodgkin lymphoma is associated with an increased risk of early relapse: Clinical results of the preplanned interim analysis of the randomized EORTC/LYSA/FIL H10 trial. *J Clin Oncol*. 2014;32(12):1188–1194.
10. Specht L, Yahalom J, Illidge T, et al. Modern radiation therapy for Hodgkin lymphoma: Field and dose guidelines from the International Lymphoma Radiation Oncology Group (ILROG). *Int J Radiat Oncol Biol Phys*. 2014;89(4):854–862.
11. EuroNet-Paediatric Hodgkin's Lymphoma Group. First international Inter-Group Study for classical Hodgkin's Lymphoma in Children and Adolescents EuroNet-PHL-C1. http://www.lymphome.de/Gruppen/GPOH-HD/Protokolle/EuroNet-PHL-C1_und_R1/Synopsis.pdf. Accessed September 10, 2007.
12. EuroNet-Paediatric Hodgkin's Lymphoma Group. Recommendations for the diagnostics and treatment of children and adolescents with a classical Hodgkin`s Lymphoma during the interimphase between

the end of the EuroNet-PHL-C1 Study and the start of the EuroNet-PHL-C2 Study. https://www.skion.nl/workspace/uploads/EuroNet-PHL-Interim-Treatment-Guidelines-2012-12-3v0-2.pdf. Accessed January 30, 2013.
13. Barrington SF, Mikhaeel NG, Kostakoglu L, et al. Role of imaging in the staging and response assessment of lymphoma: Consensus of the International Conference on Malignant Lymphomas Imaging Working Group. *J Clin Oncol*. 2014;32(27):3048–3058.
14. Ries LAG, Melbert D, Krapcho M, et al. (eds). SEER Cancer Statistics Review, 1975-2005, National Cancer Institute. Bethesda, MD, https://seer.cancer.gov/csr/1975_2005/, based on November 2007 SEER data submission, posted to the SEER web site, 2008.
15. Berg JW. The significance of axillary node levels in the study of breast carcinoma. *Cancer*. 1995;8:776–778.
16. Som PM, Curtin HD, Mancuso AA. Imaging-based nodal classification for evaluation of neck metastatic adenopathy. *Am J Roentgenol*. 2000;174(3):837–844.
17. El-Sherief AH, Lau CT, Wu CC, Drake RL, Abbott GF, Rice TW. International Association for the Study of Lung Cancer (IASLC) lymph node map: Radiologic review with CT illustration. *Radiographics*. 2014;34(6):1680–1691.
18. Papathanassiou D, Becker S, Amir R, Menéroux B, Liehnet JC. Respiratory motion artefact in the liver dome on FDG PET/CT: Comparison of attenuation correction with CT and a caesium external source. *Eur J Nucl Med Mol Imaging*. 2005;32(12):1422–1428.
19. Pettinato C, Nanni C, Farsad M, et al. Artefacts of PET/CT images. *Biomed Imaging Interv J*. 2006;2(4):e60.
20. Hanley JA, Hajian-Tilaki HO. Sampling variability of nonparametric estimates of the areas under the receiver operating characteristic curves: An update. *Acad Radiol*. 1997;4:49–58.
21. Schaefer NG, Taverna C, Strobel K, Wastl C, Kurrer M, Hany TF. Hodgkin disease: Diagnostic value of FDG PET/CT after first-line therapy – is biopsy of FDG-avid lesions still needed? *Radiology*. 2007;244(1):257–262.
22. Jerusalem G, Beguin Y, Fassotte MF, et al. Whole-body positron emission tomography using 18F-fluorodeoxyglucose compared to standard procedures for staging patients with Hodgkin's disease. *Haematologica*. 2001;86(3):266–273.
23. Schaefer NG, Hany TF, Taverna C, et al. Non-Hodgkin lymphoma and Hodgkin disease: Coregistered FDG PET and CT at staging and restaging – do we need contrast-enhanced CT? *Radiology*. 2004;232(3):823–829.
24. Pombo F, Rodriguez E, Caruncho MV, Villalva C, Crespo C. CT attenuation values and enhancing characteristics of thoracoabdominal lymphomatous adenopathies. *J Comput Assist Tomogr*. 1994;18(1):59–62.
25. Flechsig P, Choyke P, Kratochwil C, et al. Increased X-ray attenuation in malignant vs. benign mediastinal nodes in an orthotopic model of lung cancer. *Diagn Interv Radiol*. 2015;22(1):35–39.
26. Yoon Kyung K, Kyung Soo L, Byung-Tae K, et al. Mediastinal nodal staging of nonsmall cell lung cancer using integrated 18F-FDG PET/CT in a tuberculosis-endemic country: Diagnostic efficacy in 674 patients. *Cancer*. 2007;109(6):1068–1077.
27. Urata M, Kijima Y, Hirata M, et al. Computed tomography Hounsfield units can predict breast cancer metastasis to axillary lymph nodes. *BMC Cancer*. 2014;14:730.
28. Kim SA, Lee KN, Kang EJ, Kim DW, Hong SH. Hounsfield units upon PET/CT are useful in evaluating metastatic regional lymph nodes in patients with oesophageal squamous cell carcinoma. *Br J Radiol*. 2012;85(1013):606–612.
29. Follows GA, Ardeshna KM, Barrington SF, et al. Guidelines for the first line management of classical Hodgkin lymphoma. *Br J Haematol*. 2014;166(1):34–49.
30. Dillman JR, Strouse PJ, Ellis JH, Cohan RH, Jan SC. Incidence and severity of acute allergic-like reactions to i.v. nonionic iodinated contrast material in children. *AJR Am J Roentgenol*. 2007;188(6):1643–1647.
31. Zo'o M, Hoermann M, Balassy C, et al. Renal safety in pediatric imaging: Randomized, double-blind phase IV clinical trial of Iobitridol 300 versus Iodixanol 270 in multidetector CT. *Pediatr Radiol*. 2011;41(11):1393–1400.
32. Amato E, Salamone I, Naso S, Bottari A, Gaetand M, Blandino A. Can contrast media increase organ doses in CT examinations? A clinical study. *AJR Am J Roentgenol*. 2013;200(6):1288–1293.
33. Birnbaum BA, Hindman N, Lee J, Babb JS. Renal cyst pseudoenhancement: Influence of multidetector CT reconstruction algorithm and scanner type in Phantom Model 1. *Radiology*. 2007;244(3):767–775.
34. Boas FE, Fleischmann D. CT artifacts: Causes and reduction techniques. *Imaging Med*. 2012;4(2):229–240.
35. Morrill SM, Langer ML, Lane RG, Rosen II. Tissue heterogeneity effects in treatment plan optimization. *Int J Radiat Oncol Biol Phys*. 1994;30(3):699–706.
36. Burridge NA, Rowbottom CG, Bur PA. Effect of contrast-enhanced CT scans on heterogeneity corrected dose computations in the lung. *J Appl Clin Med Phys*. 2006;7(4):1–12.
37. Elmore SA. Histopathology of the lymph nodes. *Toxicol Pathol*. 2006;34(5):425–454.
38. Tan BB, Flaherty KR, Kazerooni EA, Iannettoni MD. The solitary pulmonary nodule. *Chest*. 2003;123:89S–96S.
39. Gould MK, Maclean CC, Kuschner WG, Rydzak CE, Owens DK. Accuracy of positron emission tomography for diagnosis of pulmonary nodules and mass lesions: A meta-analysis. *JAMA*. 2001;285:914–924.
40. Bui AT, Taira RK. Medical data visualization: Toward integrated clinical workstations. In: Bui AT, Taira RK, eds. *Medical Imaging Informatics*. New York, NY: Springer Science & Business Media; 2010:139–193.

Lotus tetragonolobus, *Ulex europaeus*, *Maackia amurensis*, and *Arachis hypogaea* (peanut) lectins influence the binding of *Helicobacter pylori* to gastric carbohydrates

Iwona Radziejewska[1,A,B,D–F], Małgorzata Borzym-Kluczyk[2,C,D], Katarzyna Leszczyńska[3,B,D]

[1] Department of Medical Chemistry, Medical University of Bialystok, Poland
[2] Department of Pharmaceutical Biochemistry, Medical University of Bialystok, Poland
[3] Department of Microbiology, Medical University of Bialystok, Poland

A – research concept and design; B – collection and/or assembly of data; C – data analysis and interpretation; D – writing the article; E – critical revision of the article; F – final approval of the article

Advances in Clinical and Experimental Medicine, ISSN 1899-5276 (print), ISSN 2451-2680 (online) *Adv Clin Exp Med*. 2018;27(6):807–811

Address for correspondence
Iwona Radziejewska
E-mail: iwona@umb.edu.pl

Funding sources
This work was supported by Medical University of Białystok grant No. 143-03753F. This study was conducted with the use of equipment purchased by the Medical University of Bialystok as part of the OP DEP 2007–2013, Priority Axis I.3, contract No. POPW.01.03.00-20-008/09.

Conflict of interest
None declared

Acknowledgements
We would like to express our great appreciation to prof. Z. Namiot from the Department of Physiology, Medical University of Bialystok, for the provision of clinical material for our research.

Received March 22, 2016
Reviewed June 15, 2016
Accepted February 14, 2017

Abstract

Background. The carbohydrates of gastric mucins and other sugar structures are involved in interactions with *Helicobacter pylori* (*H. pylori*) adhesins. The binding of bacteria to mucins can protect the epithelium from direct contact with the pathogen and from developing infection because of a specific barrier created by the mucus. The pathogen also interacts with other carbohydrate structures of the epithelium. Direct contact between the bacteria and the epithelial cells facilitates infection development.

Objectives. The aim of this study was to assess the influence of *Maackia amurensis* (MAA), *Lotus tetragonolobus* (LTA), *Ulex europaeus* (UEA), and *Arachis hypogaea* (PNA) lectins on the binding of gastric carbohydrates with *H. pylori* adhesins.

Material and methods. Three patients' gastric juices and 12 *H. pylori* strains were included in the study. An ELISA test was used to assess the presence of MUC1 and MUC5AC mucins and the sugar structures recognized by all examined lectins. The binding of the bacterium to the sugar structures was analyzed by the ELISA method with and without the gastric juices pretreated with lectins.

Results. In the majority of the samples examined, MAA, LTA, UEA, and PNA lectins enhanced the binding of *H. pylori* to specific carbohydrate structures of gastric mucins.

Conclusions. Substances which influence the binding of the pathogen with specific carbohydrate receptors on gastric epithelial cells can favor inflammation development. However, if *H. pylori* binds with mucins, the bacterium can have difficulty reaching the epithelium and progressing with infection.

Key words: *Helicobacter pylori*, mucins, lectins

DOI
10.17219/acem/68987

Introduction

Helicobacter pylori, a Gram-negative bacterium, colonizes the human stomach of more than 50% of the world's population. It is said to be the most globally common bacterial infectious agent. *H. pylori* can cause chronic active gastritis, peptic ulceration, and gastric cancers. It is interesting that more than 80% of infected individuals remain asymptomatic.[1,2]

The mucosal surface, with its mucus layer constantly secreted by the epithelial cells, plays an important role in the protection of the human stomach against invading pathogens. The mucus layer is mainly comprised of 2 secreted mucins: MUC5AC and MUC6, the first produced by the surface epithelium and the second one by the glands.[3,4] There is also MUC1, the most highly expressed membrane-tethered mucin that is normally found on the apical surface of polarized epithelia, and is a major component of glycocalyx. It can initiate a signaling pathway in response to bacterial invasion and is thought to play an important role in cell–cell and cell–extracellular matrix interactions.[5–7] Mucins are heavily glycosylated glycoproteins with a large number of O-linked oligosaccharides with many sugar antigens which can be recognized by *H. pylori* adhesins.[8,9] It has been suggested that the bacterium can bind to both MUC1 and MUC5AC mucins via fucosylated and sialylated glycans.[10–12] Some authors suggest that a release of MUC1 following the binding to *H. pylori* can limit the adhesion of the bacterium to the cell surface. Besides, MUC1 forms a physical barrier and may protect the gastric epithelium from adhesion to non-mucin binding agents.[13]

The involvement of MUC1 and MUC5AC mucins in *H. pylori* infection development seems to be unquestionable. To prove the participation of mucin sugar antigens in binding with *H. pylori* adhesins, some substances which can inhibit or enhance interactions between bacteria and mucins can be used.[14] Anti-Lewis-x antibodies have been suggested as agents promoting *H. pylori* adhesion to gastric epithelial cells.[15] Our latest studies with anti-Lewis-b, anti-H type 1, and sialyl Lewis-x revealed the slight inhibitory effect of these antibodies on *H. pylori* binding to MUC1 mucin.[16] In the presented study, we used specific plant lectins in order to check their influence on *H. pylori* adhesion to gastric carbohydrates.

It seems clear that the explanation of the strategy used by *H. pylori* for colonizing the gastric epithelium could help reveal how pathogens overcome specific barriers to infection, such as the mucus layer.[17]

Material and methods

Patients and specimens

The gastric juices (as the source of mucins) of 3 *H. pylori*-infected patients with duodenal ulcers were included in the study. The patients were hospitalized in the Department of Medicine and Gastroenterology of the Regional Hospital of Bialystok, Poland. They were treated for 2 weeks by oral administration of omeprazole (2 × 20 mg per day), amoxicillin (2 × 100 mg), and tynidazole (2 × 500 mg). Gastric juices were taken on days 11–13 of the successful treatment. The presence of *H. pylori* was examined histopathologically and by the urease test with gastric cells scraped under endoscopic examination.

To obtain high-molecular-mass mucins, the juices were pretreated as described before.[18] The prepared samples of the juices were diluted to the same protein concentration (0.005 mg/mL) prior to further tests. The protein content was measured using the bicinchoninic acid method.[19]

Bacterial strains and culture conditions

Helicobacter pylori strains were isolated from the gastric epithelial cells of 12 patients suffering from gastritis. The scrapings were collected before the beginning of the treatment, under endoscopic examination, from the prepyloric area and the body of the stomach. The scrapings were immediately carried into the transport medium *Portagerm pylori* (bioMerieux, Marcy-l'Étoile, France). Then, after homogenization, the bacteria were cultured on Pylori Agar and Columbia Agar supplemented with 5% sheep blood (bioMerieux, France) for 7 days at 37°C under microaerophilic conditions using a Genbag microaer (bioMerieux, Marcy-l'Étoile, France). Microorgansms were identified upon the colony morphology by the Gram method. Additionally, the activity of the bacterial urease, catalase and oxidase were also determined. To prove *H. pylori* species, the ELISA test (HpAg48; EQUIPAR, Guadalajara, Mexico) was used. Then, the bacteria were subcultured in the same conditions and suspended at 1.2×10^9 bacteria/mL in PBS.

Determination of MUC1, MUC5AC and sugar antigens recognized by *Lotus tetragonolobus*, *Ulex europaeus*, *Maackia amurensis*, and *Arachis hypogaea* lectins in gastric juices

Aliquots (50 µL) of the samples of gastric juices (containing 0.005 mg of protein/mL) were coated onto microtiter plates (NUNC F96; Maxisorp, Roskilde, Denmark) at room temperature (RT) overnight. The plates were washed 3 times (100 µL) in the washing buffer PBS-T (PBS, 0.05% Tween, Sigma, St. Luis, USA) between all ensuing steps. Unbound sites were blocked with 100 µL of 1% blocking reagent for ELISA (Roche Diagnostics, Mannheim, Germany) for 1 h. Then the plates were incubated (2 h at RT) with 100 µL of anti-MUC1 and anti-MUC5AC monoclonal antibodies (for specifications and dilutions of antibodies, see Table 1) diluted in 1% bovine serum albumin (BSA) in PBS-T or with biotinylated *Lotus tetragonolobus* (LTA), *Ulex europaeus* (UEA), *Maackia amurensis* (MAA), or

Table 1. Specifications of antibodies used in the study

Antibody	Clone	Source	Dilution
Anti-MUC1	BC2	Thermo Scientific	1:400
Anti-MUC5AC	45M1	Sigma	1:400
Anti-*H. pylori* (polyclonal, biotin-conjugated)		Abcam	1:1,500
Horseradish peroxidase conjugated anti-mouse IgG		Sigma	1:1,500

Table 2. The major binding specifications of lectins used in the study

Origin and abbreviations of lectins	Binding preferences
Lotus tetragonolobus (LTA)	Fucα1-3GlcNAc
Ulex europaeus (UEA)	Fucα1-2Gal; Fucα1-3GlcNAc
Maackia amurensis (MAA)	NeuAcα2-3Gal
Arachis hypogaea (peanut) (PNA)	Galβ1-3GalNAc

Arachis hypogaea (PNA) lectins (diluted to 5 µg of lectin/mL in PBS-T-BSA (1%)) (Vector, Burlingame, USA) (for carbohydrate specifications of lectins, see Table 2). The lectin solutions were supplemented with metal cations: LTA, UEA, and PNA with 0.1 mmol/L $CaCl_2$; MAA with 0.1 mmol/L $CaCl_2$ and 0.01 mmol/L $MnCl_2$. Then the plates were incubated (2 h at RT) with 100 µL of secondary, rabbit anti-mouse IgG horseradish peroxidase (conjugated for MUC1 and MUC5AC detection) or with 100 µL of horseradish peroxidase avidin D (Vector, Burlingame, USA) (for lectin detection) diluted (1:2,000) in PBS-T-BSA (1%). Next, after washing 4 times in PBS, the colored reaction was developed by incubation with 100 µL of 2,2'-azino-bis(3-ethylbenzthiazoline-6-sulfonic acid) (ABTS) – the liquid substrate for horseradish peroxidase (Sigma, St. Louis, USA). Absorbance at 405 nm was measured after about 30–40 min. For controls, wells with no gastric juices were used. The test was performed twice with 3 replicates of each sample.

Binding of *H. pylori* to mucins

Aliquots of the samples of gastric juices were coated onto microtiter plates and incubated as described above. Then the plates were washed and blocked as before. The plates were incubated for 2 h at RT with aliquots (100 µL) of non-biotinylated LTA, UEA, MAA, and PNA lectins. Two concentrations of lectin were used (in PBS supplemented with metal cations – see above): 40 and 0.4 µg of lectin/mL of PBS-T-BSA (1%). Wells without added lectins served as controls. The bacteria were diluted with PBS to get 2.4×10^7 cells/mL and 100 µL of each strain solution were added to the wells and incubated at 37°C overnight. Then the wells were treated with anti-*H. pylori* polyclonal, biotin-conjugated antibody diluted with PBS-T-BSA (1%) at RT for 1 h. After being incubated with horseradish peroxidase-conjugated avidin D, the colored reaction was developed as described above.

Statistics

The binding of *H. pylori* to mucins of gastric juices (pretreated with lectins or not) was subjected to statistical analysis (using STATISTICA v. 10.1 (StatSoft, Tulsa, USA). The results are presented as mean ±SD. Post hoc analysis calculated by an NIR test was used. Statistical significance was assumed at $p < 0.05$.

The study was approved by the Institutional Ethical Committee with the principles of the Declaration of Helsinki and informed consent was obtained from all patients.

Results

Three examined gastric juices revealed the presence of MUC1 and MUC5AC mucins. Mucin expressions were determined as OD values (405 nm) in the ELISA test (Fig. 1).

Figure 2 shows the expression of specific carbohydrate structures on gastric glycoproteins, recognized by the examined lectins. Fuc linked by α1-2 bond to Gal or by α1-3 bond to GlcNAc, recognized by the UEA lectin is observed at the highest level. A high level of sialic acid linked by α2-3 bond to Gal, recognized by the MAA lectin, is also seen. Fuc linked by α1-3 to GlcNAc, recognized by the LTA lectin and the Galα1-3GalNAc structure, recognized by the PNA lectin, are observed at a much lower level.

The abovementioned lectins were used to check their influence on the binding of *H. pylori* to gastric mucins. Two concentrations of lectins were used: 40 and 0.4 µg/mL. In Fig. 3 we can observe that in all samples, the addition of UEA, MAA and PNA lectins (at a higher concentration) caused an increase in the binding of the bacterium

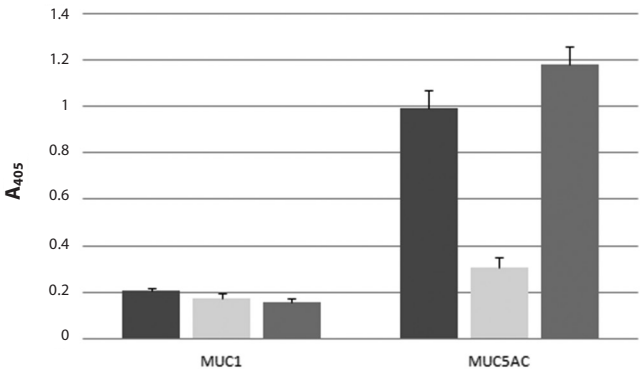

Fig. 1. The level of MUC1 and MUC5AC mucins in the gastric juices of 3 patients (each bar represents an individual patient); data is presented as the mean of 6 replicates ±SD

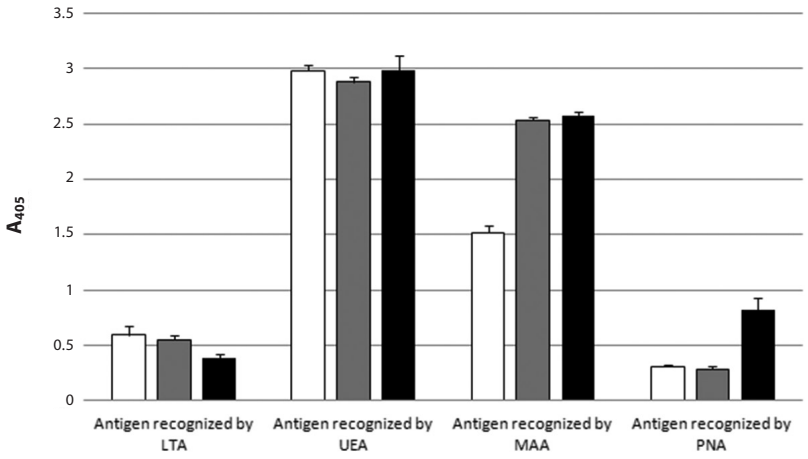

Fig. 2. The level of specific carbohydrate antigens (in the 3 examined gastric juices) recognized by LTA, UEA, MAA, and PNA lectins (bars represent individual patients); data is presented as the mean of 6 replicates ±SD

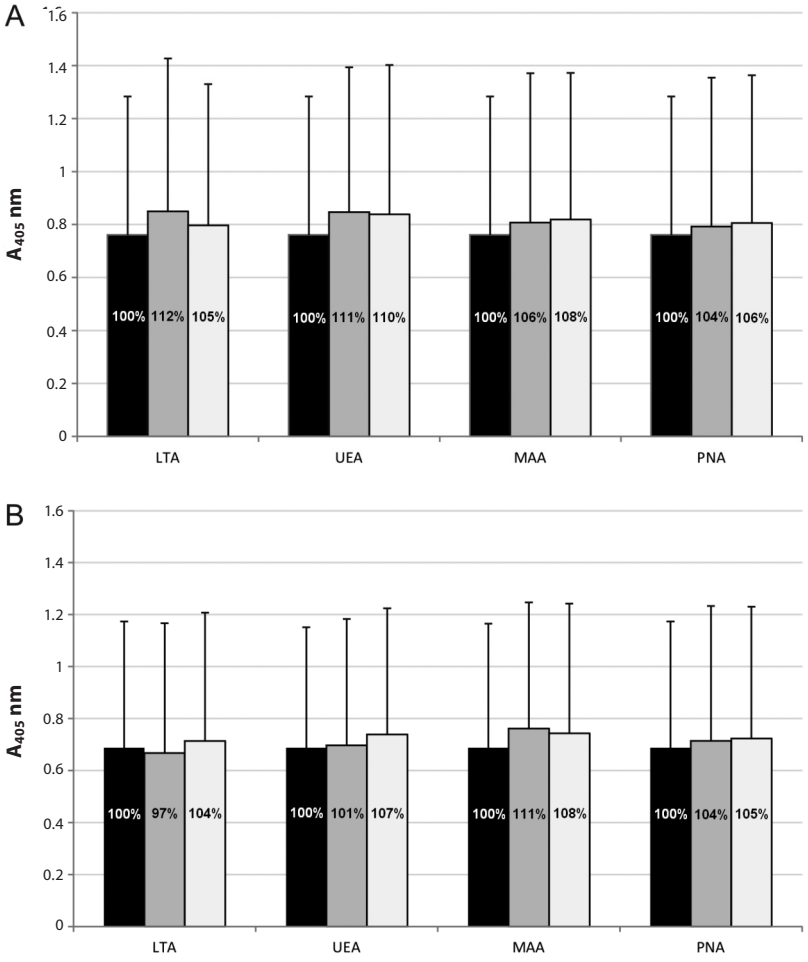

Fig. 3. LTA, UEA, MAA, and PNA lectins' additive effect on *Helicobacter pylori's* binding to gastric mucins

H. pylori (n = 12) was allowed to react with gastric mucins and the bound bacterium was assessed with polyclonal anti-*H. pylori* antibodies; black bars – samples without lectins; grey bars – samples treated with 40 µg/mL of specified lectins; white bars – samples treated with 0.4 µg/mL of specified lectins; A, B, C – results for individual patients; binding of *H. pylori* without pretreatment with lectins (black bars) is stated as 100%; bars represent ±SD.

to mucins. In the case of the LTA lectin, only in one sample (Fig. 3b) was a slight decrease in *H. pylori* binding observed for a lectin concentration of 40 µg/mL. Generally, it can be seen that a smaller dose of lectins (0.4 µg/mL) induced less of an increase in bacterium binding.

Discussion

Secretory MUC5AC and epithelial MUC1 mucins, with their specific carbohydrate structures, are said to be involved in interactions with *H. pylori* adhesins.[12,13] Some authors imply that Lewis antigens on the lipopolysaccharide (LPS) of *H. pylori* are also involved in bacterial adhesion.[15] However, the exact mechanism of interaction of *H. pylori* with the gastric epithelium still needs to be more precisely elucidated.

Some tested particles have been shown to inhibit or enhance the binding of the bacterium to epithelial carbohydrate antigens. It was revealed that anti-Le x MAb could promote the adhesion ability of an *H. pylori* strain with

high Le x expression.[15] According to the authors, MAb can serve as a kind of bridge to connect the Le x antigen of bacteria and the Le x antigen of the epithelium. These results are not in accordance with our latest studies with anti-Lewis b, anti-H type 1, and sialyl Lewis x antibodies. We revealed that the antibodies in question slightly inhibited the binding of bacteria to the MUC1 mucin.[16] In other studies, it was observed that neoglycoproteins of the Le b or sLe x oligosaccharides conjugated to human serum albumin (HSA) inhibited the adhesion of *H. pylori* to the gastric mucosa in vitro.[9,20] Glycoconjugates of porcine milk also showed the inhibition of *H. pylori* adhesion.[21] These findings give more insight into the participation of peculiar sugar structures in interactions with bacterial adhesins. The exact elucidation of the mechanisms that *H. pylori* uses to colonize mucosal surfaces could lead to a complete understanding of how pathogens overcome barriers to infection, such as the presence of a mucus layer.

The lectins isolated from certain plants which were used in our study are able to recognize specific sugar structures in a manner similar to antigen–antibody interactions. Some lectins require that the particular sugar be in a terminal non-reducing position in the oligosaccharide; others can bind to sugars within the oligosaccharide chain. The affinity between a lectin and its receptor may vary a great deal due to small changes in the carbohydrate structure of the receptor.[22]

In our study, we decided to use lectins that can recognize sugar structures which are said to act as carbohydrate receptors for *H. pylori* adhesins (LTA, UEA, or MAA) or are part of mucin structures (PNA) (Table 2). All the lectins used revealed the enhancement of *H. pylori* binding to gastric mucins. Despite the different levels of sugar structures in gastric juices recognized by lectins, the increased binding effect was similar in all of the samples. It can suggest that some non-specific interaction between lectins and carbohydrate structures in gastric juices are possible. The eventual participation of bacterial LPS carbohydrates in such interactions cannot be excluded. The lectins used, with their high affinity to specific sugar antigens, can act as agents which could crosslink bacterial and mucin carbohydrates, as well as other sugar structures of the gastric epithelium. The binding of the bacterium with mucins can protect the host from developing an infection because the pathogen would be trapped in mucus and washed away from the stomach. On the other hand, interactions of *H. pylori* with surface carbohydrates could favor infection development by direct interactions of the bacterium with the epithelium.

We want to emphasize that our study should be treated as a preliminary one. More detailed experiments are planned for the future in order to explore the subject more deeply.

References

1. Atherton JC. The pathogenesis of Helicobacter pylori induced gastro-duodenal diseases. *Annu Rev Pathol*. 2006;1:63–96.
2. Lillehoj EP, Guang W, Ding H, Czinn SJ, Blanchard TG. Helicobacter pylori and gastric inflammation: Role of MUC1 mucin. *J Pediatr Biochem*. 2012;2:125–132.
3. Lacunza E, Bara J, Segal-Eiras A, Croce MV. Expression of conserved mucin domains by epithelial tissues in various mammalian species. *Res Vet Sci*. 2009;86:68–77.
4. Navabi N, Johansson MEV, Raghavan S, Linden SK. Helicobacter pylori infection impairs the mucin production rate and turnover in the murine gastric mucosa. *Infect Immun*. 2013;81:829–837.
5. Guang W, Czinn SJ, Blanchard TG, Kim KC, Lillehoj EP. Genetic regulation of MUC1 expression by Helicobacter pylori in gastric cancer cells. *Biochem Biophys Res Commun*. 2014;445:145–150.
6. Guang W, Ding H, Czinn SJ, Kim KC, Blanchard TG, Lillehoj EP. Muc1 cell surface mucin attenuates epithelial inflammation in response to a common mucosal pathogen. *J Biol Chem*. 2010;285:20547–20557.
7. Jonckheere N, Van Seuningen J. The membrane-bound mucins: From cell signaling to transcriptional regulation and expression in epithelial cancers. *Biochimie*. 2010;92:1–11.
8. Ilver D, Arnqvist A, Ogren J, et al. Helicobacter pylori adhesion binding fucosylated histo-blood group antigens revealed by retagging. *Science*. 1998;279:373–377.
9. Mahdavi J, Sonden B, Hurtig M, et al. Helicobacter pylori SabA adhesion in persistent infection and chronic inflammation. *Science*. 2002; 297:573–578.
10. Linden S, Mahdavi J, Hedenbro J, Boren T, Carlstedt I. Effects of pH on Helicobacter pylori binding to human gastric mucins: Identification of binding to non-MUC5AC mucins. *Biochem J*. 2004;384:263–270.
11. Linden S, Nordman H, Hedenbro J, Hurtig M, Boren T, Carlstedt I. Strain- and blood group-dependent binding of Helicobacter pylori to human gastric MUC5AC glycoforms. *Gastroenterology*. 2002;123: 1923–1930.
12. Linden SK, Wickstrom C, Lindell G, Gilshenan K, Carlstedt I. Four models of adhesion are used during Helicobacter pylori binding to human mucins in the oral and gastric niches. *Helicobacter*. 2008;13:81–93.
13. Linden SK, Sheng YH, Every AL, et al. MUC1 limits Helicobacter pylori infection both by steric hindrance and by acting as a releasable decoy. *PLoS Pathog*. 2009;5:e1000617.
14. Radziejewska I, Borzym-Kluczyk M, Leszczyńska K. Are Lewis b and H type 1 on Helicobacter pylori involved in binding of bacteria to MUC1 mucin? *Adv Clin Exp Med*. 2013;22:347–353.
15. Sheu S, Sheu B, Yang H, Lei H, Wu J. Anti-Lewis x antibody promotes Helicobacter pylori adhesion to gastric epithelial cells. *Infect Immun*. 2007;75:2661–2667.
16. Radziejewska I, Leszczyńska K, Borzym-Kluczyk M. Influence of monoclonal anti-Lewis b, anti-H type 1, and anti-sialyl Lewis x antibodies on binding of Helicobacter pylori to MUC1 mucin. *Mol Cell Biochem*. 2014;385:249–255.
17. Dolan B, Naughton J, Tegtmeyer N, May FEB, Clyne M. The interaction of Helicobacter pylori with the adherent mucus gel layer secreted by polarized HT29-MTX-E12 cells. *PLoS One*. 2012;7:e47300.
18. Radziejewska I, Leszczyńska K, Borzym-Kluczyk M, Namiot Z. Assessment of interactions between mucins of gastric juice and Helicobacter pylori – preliminary study. *Hepatogastroenterology* 2010;57: 367–371.
19. Smith PK, Krohn RJ, Hermanson GT, et al. Measurement of protein using bicinchoninic acid. *Anal Biochem*. 1985;150:76–85. [Erratum: *Anal Biochem*. 1987;163:279]
20. Younson J, O'Mahony R, Liu H, et al. A human domain antibody and Lewis b glycoconjugate that inhibit binding of Helicobacter pylori to Lewis b receptor and adhesion to human gastric epithelium. *J Inf Dis*. 2009;200:1574–1582. [Erratum: *J Infect Dis*. 2010;201:481]
21. Gustafsson A, Hultberg A, Sjostrom R, et al. Carbohydrate-dependent inhibition of Helicobacter pylori colonization using porcine milk. *Glycobiology*. 2006;16:1–10.
22. Liener IE, Sharon N, Goldstein IL. *The Lectins. Properties, Functions and Applications in Biology and Medicine*. Orlando: Academic Press;1986.

Stool patterns and symptoms of disordered anorectal function in patients with inflammatory bowel diseases

Paweł W. Petryszyn[1,A–E], Leszek Paradowski[2,A,E,F]

[1] Department of Clinical Pharmacology, Faculty of Pharmacy with Division of Laboratory Diagnostics, Wroclaw Medical University, Poland
[2] Department of Gastroenterology and Hepatology, Faculty of Postgraduate Medical Training, Wroclaw Medical University, Poland

A – research concept and design; B – collection and/or assembly of data; C – data analysis and interpretation;
D – writing the article; E – critical revision of the article; F – final approval of the article

Advances in Clinical and Experimental Medicine, ISSN 1899-5276 (print), ISSN 2451-2680 (online) *Adv Clin Exp Med*. 2018;27(6):813–818

Address for correspondence
Paweł Petryszyn
E-mail: ppetryszyn@wp.pl

Funding sources
None declared

Conflict of interest
None declared

Received on April 24, 2016
Reviewed on June 29, 2016
Accepted on February 14, 2017

Abstract

Background. Crohn's disease (CD) and ulcerative colitis (UC) typically clinically manifest with symptoms like chronic diarrhea, cramps, abdominal pain, and rectal bleeding. However, symptoms of abnormal anorectal function seem to be of equal importance, regardless of the presence or absence of perianal disease.

Objectives. The aim of this study was to assess stool patterns and the prevalence of symptoms of disordered anorectal function, particularly urgency and fecal incontinence, and their severity in patients with inflammatory bowel diseases (IBDs).

Material and methods. Thirty-three patients with CD and 38 patients with UC completed a questionnaire. A push/strain maneuver was performed on all patients and 20 controls.

Results. Thirty-three patients had more than 3 bowel movements a day; 44 had loose/watery stools. Two patients had fewer than 3 bowel movements a week, 8 had hard/lumpy stools, and 3 used laxatives. Excessive straining and incomplete evacuation were reported by 17 and 38 patients, respectively. Fifty-two patients complained of urgency and 32 of tenesmus. Significantly, more UC patients than CD patients had urgency at least once a day ($p < 0.04$). The following symptoms were reported by patients in the following numbers: fecal incontinence (31), passive (20) and urge incontinence (16), incontinence to gas (24), as well as liquid (33) and solid stool (7). Stool/gas discrimination was defective in 28 patients. Eleven patients had to wear pads. Everyday functioning was worsened because of urgency/tenesmus in 39 patients and because of fecal incontinence in 28 patients. The push/strain maneuver was abnormal in 12 patients with CD, 15 patients with UC and 1 control subject. The differences between the 2 study groups and the controls were significant ($p < 0.03$ and $p < 0.01$).

Conclusions. A majority of patients with IBD complain of urgency. Fecal incontinence is reported by over 50% of patients. Both worsen patients' everyday functioning. A relevant proportion of patients have symptoms consistent with constipation, which is in connection with an abnormal push/strain maneuver in more than 1/3 of them.

Key words: high-resolution manometry, fecal incontinence, inflammatory bowel disease

DOI
10.17219/acem/68986

Introduction

Crohn's disease (CD) and ulcerative colitis (UC) belong to the group of inflammatory bowel diseases (IBDs). They typically clinically manifest with symptoms such as chronic diarrhea, cramps, abdominal pain, rectal bleeding, and low-grade fever. Some patients may even experience constipation, which is often overlooked when the frequent passage of blood and mucous is confused with diarrhea. The Rome III criteria for IBD are often met. In some patients with CD and UC, perianal diseases comprising ulcerations, fissures, abscesses, and fistulas are diagnosed. The symptoms of abnormal anorectal function, such as urgency, tenesmus and fecal incontinence, seem to be quite prevalent in patients with IBD, regardless of the presence or absence of perianal disease. These symptoms are extremely embarrassing, thus patients are unwilling to report them and very often doctors themselves do not ask about them. However, such symptoms may have a relevant impact on patients' quality of life that cannot be ignored.

Objectives

The aim of this study was to assess stool patterns and the prevalence of the symptoms of disordered anorectal function, urgency and fecal incontinence in particular, and their severity in patients with IBD.

Material and methods

Patients

Seventy-one patients with an established diagnosis of CD and UC, who were hospitalized in the Department of Gastroenterology and Hepatology of Wroclaw Medical University, Poland, between 2007 and 2008, were included in this study. Patients who had had a diverting ileostomy or colostomy, colectomy or subtotal colectomy, colectomy with ileorectal anastomosis, or restorative proctocolectomy with ileal pouch-anal anastomosis (IPAA), were excluded. The control group consisted of 20 volunteers without any symptoms of the lower gastrointestinal tract diseases and without any relevant concomitant chronic diseases, like diabetes mellitus or neurological disorders. The study group was divided into 2 subgroups: group I – patients with CD (n = 33), and group II – patients with UC (n = 38). Twelve operations for IBD were performed in 10 patients with CD. In addition, 3 patients had a hemorrhoidectomy and 1 was operated on because of anal fissure. In the CD patients, the disease was localized in the ileum (Montreal L1) in 3 patients, in the colon (Montreal L2) in 16 patients, and in both the ileum and colon (Montreal L3) in 12 patients. Thirteen patients had only luminal inflammatory changes (Montreal B1), 14 developed strictures (Montreal B2) and in 4 patients the disease had penetrating behavior (Montreal B3). Perianal disease (fistulas) was present in 3 patients. Among the UC group, in 4 patients IBD was restricted to the rectum (Montreal E1), 19 had left-sided UC (Montreal E2), and 13 patients presented extensive colitis (Montreal E3). A total of 15% of patients with CD and 42% of patients with UC were in clinical remission (Crohn's Disease Activity Index [CDAI] <150 and Rachmilewitz Index [IR] ≤4, respectively). Patient characteristics and clinical details are shown in Table 1.

Table 1. Patient characteristics and clinical details

Characteristic	CD	UC	Controls
Studied	33	38	20
Men/women	20/13	18/20	8/12
Age [years]*	40.8 (18–81)	45.5 (18–74)	41.4 (20–65)
Time since diagnosis			
<1 year	17	12	–
1–8 years	10	15	–
>8 years	6	11	–
Medication			
Sulfasalazine	10	20	–
Mesalazine	20	23	–
Prednisone	12	14	–
Budesonide	1	2	–
Azathioprine	18	16	–

CD – Crohn's disease; UC –ulcerative colitis; * data expressed as mean (range).

Questionnaire

All patients completed a questionnaire consisting of 70 questions divided into 6 categories: general questions (demographic, social and professional, as well as concerning smoking, nutrition); questions concerning the underlying disease (time since diagnosis, onset of symptoms, management, presence of symptoms within the last 6 months, most troublesome symptom, abdominal pain and its relief after defecation); questions concerning bowel movements (frequency, consistency, straining during bowel movement, feeling of incomplete evacuation, use of antidiarrheals and laxatives, Bristol stool form scale by Heaton and Lewis, questions concerning urgency and tenesmus (prevalence, frequency, deferral time); questions about fecal incontinence (type of incontinence – passive or urge, fecal seepage, frequency of incontinence to gas, liquid and solid stool, incontinence at night, discrimination between stool and gas, wearing pads) as well as about the impact of the symptoms on the patient's everyday functioning; and questions about factors which may influence anorectal function (concomitant chronic diseases, medication, anorectal disorders, past abdominal and pelvic operations or perianal disease operations, radiotherapy).[1] The women

answered 9 extra questions related to gynecological and obstetrical factors. After receiving detailed instructions, patients were asked to fill in the questionnaire on their own. The mean response time was approx. 15 min. Whenever a patient was unsure or had doubts, we discussed the answers with the patient the following day. This way, we tried to minimize the bias associated with inaccuracy or misunderstanding.

Anorectal manometry

In all patients and the 20 controls, a push/strain maneuver was performed by means of anorectal manometry with the use of a 4-lumen water-perfused catheter (Zinectics Manometric Catheter; Medtronic, Minneapolis, USA). The patient was asked to bear down as if to defecate. The test was considered abnormal if there was a paradoxical increase or decrease of less than 20% of the baseline anal resting pressure.

Statistical analysis

Statistical analysis was performed with the use of STATISTICA v. 7.0 PL (StatSoft, Tulsa, USA). Proportions were compared using a χ^2 test; $p < 0.05$ was considered statistically significant.

Ethical considerations

Written informed consent from all study participants was obtained. The study was approved by the Bioethical Committee of Wroclaw Medical University, Poland.

Results

Bowel movements

A total of 91% of patients with CD and 84% of patients with UC reported gastrointestinal symptoms within the last 6 months. The most common symptoms were abdominal pain, diarrhea and vomiting in CD, and diarrhea, rectal bleeding and bloating in UC. Over 40% of patients in both groups eliminated more than 3 stools a day in the week preceding hospitalization, and more than 60% of patients had loose or watery stools. Six of the CD patients and 10 UC patients used antidiarrheals. One patient with CD and 1 patient with UC had fewer than 3 stools a week; in 3 patients from group I and in 5 patients from group II, the stools were hard or lumpy. Approximately 25% of the patients reported excessive straining while passing stools and in 50% of the patients a feeling of incomplete evacuation was noted. The differences between groups I and II in the above-mentioned parameters characterizing bowel movements were not statistically significant (Table 2).

Table 2. Bowel movements (BMs) in patients with IBD

Characteristic		CD (n = 33)	UC (n = 38)	p-value
BMs	>3/day	15	18	ns
	≥6/day	3	8	ns
	<3/week	1	1	ns
	loose/watery	20	24	ns
	hard/lumpy	3	5	ns
Excessive straining		7	10	ns
Feeling of incomplete evacuation		16	22	ns
Use of antidiarrheals		6	10	ns
Use of laxatives		0	3	ns

CD – Crohn's disease; UC – ulcerative colitis; IBD – inflammatory bowel disease.

Defecatory maneuver

The defecatory maneuver was abnormal in 12 patients with CD, in 15 patients with UC and in 1 control (CD vs control, $p < 0.03$; UC vs control, $p < 0.01$).

Urgency and/or tenesmus

A total of 67% of patients with CD and 84% of the patients with UC reported urgency. It was present at least once a day in 25% of the patients with CD and in 50% of the patients with UC. The difference was statistically significant. Tenesmus was reported by more than 2/5 of patients in both groups. The period of time in which it is possible to defer defecation after the desire to evacuate, known as deferral time, was not longer than 5 min in 45% of CD patients and in 54% of UC patients. Urgency or tenesmus worsened everyday functioning in 55% of patients with CD and in 70% of patients with UC (Table 3).

Table 3. Urgency and tenesmus in patients with IBD

Characteristic	CD (n = 31)*	UC (n = 37)*	p-value
Urgency	21	31	ns
Urgency at least once a day	8	19	<0.04
Tenesmus	14	18	ns
Deferral time ≤5 min	14	20	ns
Worsened daily functioning because of urgency/tenesmus	17	22	ns

CD – Crohn's disease; UC – ulcerative colitis; IBD – inflammatory bowel disease; * data was not available in 2 patients with CD and 1 patient with UC.

Fecal incontinence

Fecal incontinence was present in 52% of patients diagnosed with CD and in 60% of patients diagnosed with UC. Ten patients in each group reported passive incontinence. Discharge of fecal matter in spite of efforts to retain

bowel contents – urge incontinence – affected almost 25% of the patients in the 2 study groups. In 6 patients from group I and 5 patients from group II symptoms of passive and urge incontinence were present. Five patients from group I and 8 patients from group II admitted experiencing leakage of a small amount of stool without their awareness or staining of undergarments following an otherwise normal evacuation, i.e., fecal seepage. In both groups, the discrimination between stool and gas was defective in more than 2/5 of patients, while 16% of them reported wearing pads because of incontinence (Table 4).

Table 4. Fecal incontinence in patients with IBD

Characteristic	CD (n = 33)*	UC (n = 38)*	p-value
Fecal incontinence	14	17	ns
Passive incontinence	10	10	ns
Urge incontinence	7	9	ns
Incontinence to gas	12	12	ns
Incontinence to liquid stool	13	19	ns
Incontinence to solid stool	3	4	ns
Defective discrimination between stool and gas	13	15	ns
Wearing pads	5	6	ns
Worsened daily functioning because of fecal incontinence	13	15	ns

CD – Crohn's disease; UC – ulcerative colitis; IBD – inflammatory bowel disease; * data was not available in 2 patients with CD and 1 patient with UC.

Table 4 differentiates patients with CD and UC depending on the type of fecal matter when incontinent. Grades I, II, and III, according to the Miller's Incontinence Score have the following significance: I – less often than once a month, II – from once a week to once a month, III – more than once a week.[2] Incontinence to gas was present in 39% of patients with CD and in 32% of patients with UC; incontinence to liquid stool was present in 45 and 51% of patients, respectively; and incontinence to solid stool was present in 10% and 11% of the patients, respectively (Table 5).

Fecal incontinence worsened everyday functioning of 42% of CD patients and 51% of UC patients (Table 4).

Discussion

Diarrhea is the most characteristic symptom of IBDs. In UC it is caused by rectal mucosal inflammation, but in CD its character strictly depends on the location of the disease. In Crohn's colitis, like in UC, especially when the rectum is inflamed, stools are frequent and scarce. As the inflammatory process and fibrosis of the rectal wall progresses, it becomes rigid and poorly extensible; diarrhea is the consequence of this decreased rectal compliance. In small bowel disease, stools are large in volume. Steatorrhea or chologenic

Table 5. Frequency of fecal incontinence based on the type of fecal matter in patients with IBD (according to Miller's score for fecal incontinence)[2]

Characteristic		CD (n = 33)	UC (n = 38)	p-value
Gas incontinence	I	4	3	ns
	II	3	6	
	III	5	3	
	pooled	12	12	
Liquid stool incontinence	I	5	6	ns
	II	2	7	
	III	7	6	
	pooled	14	19	
Solid stool incontinence	I	1	2	ns
	II	0	1	
	III	2	1	
	pooled	3	4	
n/a*		2	1	–

CD – Crohn's disease; UC – ulcerative colitis; IBD – inflammatory bowel disease; * data not available.

diarrhea are commonly observed. In our study, 40% of patients with CD and UC had more than 3 stools a day in the week preceding hospitalization. In more than 60% of patients, they were loose or watery.

However, 25% of patients with IBD reported excessive straining in order to defecate and more than 50% reported a feeling of incomplete evacuation. Constipation, defined as passing hard or lumpy stools, was present in 3 patients with CD and in 5 patients with UC. Three patients with UC used laxatives. Ulcerative colitis is commonly associated with symptoms such as diarrhea, rectal bleeding and abdominal pain. Rao et al. assessed the prevalence of bowel and anorectal symptoms in 96 patients with active, quiescent, as well as distal and total UC. Urgency was present in 85% of cases, a feeling of incomplete evacuation in 78% and tenesmus in 63% of patients with active UC. These symptoms were all significantly less common in patients with quiescent colitis. Their prevalence was similar among patients with distal and total colitis, which may indicate that they are related to an inflamed distal colon and rectum. A total of 27% of patients with active UC voided hard stools, which was a significantly higher proportion compared to patients with quiescent colitis.[3] When asked about the frequency of bowel movements, patients often attribute frequent passage of blood and mucous to diarrhea; this fact may lead to constipation being overlooked in many cases which otherwise would have been diagnosed if stool consistency would had been taken into consideration as a criterion.

Rao and Read also analyzed the colonic transit of a test meal and stool weight and frequency in 62 patients with UC as well as in 20 healthy volunteers. Whole gut transit time was unchanged in UC patients in comparison with the control group. The authors suggest that diarrhea in UC is associated with rectosigmoid inflammation rather

than rapid transit, and they recommend caution when prescribing such patients antidiarrheals, which could further impede proximal colonic transit.[4]

Constipation may be a dominant symptom of ulcerative proctitis, especially in elderly patients. Crispino et al. investigated the functional and morphologic features of the anorectal region in 11 patients with inactive UC and constipation, and in 10 patients with functional constipation. Patients with ulcerative proctitis had lower rectal compliance, prolonged left colon transit and lower lateral rectal diameter than patients with functional constipation. This, according to the authors, suggests that constipation in ulcerative proctitis may be correlated with rectal fibrosis.[5]

Symptoms such as abdominal pain, diarrhea, constipation, pain relief with bowel action, urgency, straining in order to defecate, a feeling of incomplete evacuation, and flatulence are characteristic of irritable bowel syndrome (IBS). Isgar et al., using the Manning criteria, demonstrated that 33% of patients with UC fulfilled the diagnostic criteria of IBS.[6] Patients with UC, both active and in remission, had increased low-amplitude colonic propulsive activity with respect to controls, while there was no difference in the frequency of propagated contractions between active colitis patients and patients with IBS and diarrhea.[7,8] This observation may at least partially explain the presence of IBS symptoms in UC patients. In the study of Simren et al., IBS symptoms were present in 33% of patients with UC and in 57% of patients with CD. Their presence was associated with increased levels of anxiety and depression and they worsened the patients' general well-being.[9]

The defecatory maneuver was abnormal in 1/3 of patients with CD and UC, which constituted a significantly higher percentage compared to the control group. Previously, only Loening-Baucke et al. assessed this parameter in IBD patients. The results of a balloon defecation test were similar in patients with active and inactive UC and in healthy subjects.[10] The lack of anal relaxation during straining in a large number of UC patients may explain the excessive straining in order to defecate and the feeling of incomplete evacuation. It should be noted that this examination is very subjective and dependent on many factors, e.g., the degree of privacy and the fact that impaired anal relaxation may be seen in more than 20% of healthy subjects.[11]

The frequency of urgency in patients with UC in our study was similar to the frequency of this symptom in the above-cited study by Rao et al., whereas tenesmus was present slightly more often (49% vs 63%).[3] Urgency at least once a day occurred twice as often in patients with UC than in patients with CD. The deferral time in a study by Mueller et al. was not longer than 5 min in 50% of CD patients without active disease in the rectum as determined by endoscopy.[12]

Urgency and tenesmus are particularly unpleasant symptoms which may persist in patients with IBD despite optimal medical treatment and may be an indication for surgery. Buchmann et al., who compared 20 patients with CD who were suffering from urgency with 19 patients who did not report its presence, did not find any difference in anal resting and squeeze pressures or anal response to passive rectal filling. The authors suggested the role of small and large intestine dysmotilityin the pathogenesis of urgency in CD.[13]

Fecal incontinence was present in more than 50% of patients with CD and in approx. 60% of patients with UC. In the above-cited study by Rao et al., fecal incontinence was present in 18% of patients with distal active UC and in 31% of patients with total active UC.[3] Fecal incontinence is an especially embarrassing medical condition and patients are reluctant to report it to a physician unless asked directly. In both studies, a questionnaire was used. Kangas et al., who studied anorectal function in 63 patients with CD, found 17% of patients to be partially incontinent and 5% of patients to be totally incontinent.[14] Urge incontinence affected almost 25% of patients with CD and UC, which generally reflects the proportions observed in the literature.[3,14]

Our data points out the scale of the problem of fecal incontinence in patients with IBD. In the study by Mueller et al., incontinence to gas, liquid stool and solid stool was diagnosed in 24%, 46% and 9% of patients with CD without endoscopic rectal changes, respectively.[12] In our study, proctitis was confirmed in 9 patients (27%) with CD.

Incontinence to gas mainly affected patients with CD, while incontinence to gas and liquid stool occurred more often in patients with UC. Discrimination between stool and gas was impaired in more than 40% of patients with both CD and UC, and 16% of them had to wear pads because of incontinence. In the study by Mueller et al., the ability to discriminate between stool and gas was defective in 24% of patients with CD. A total of 12% of these patients wore pads because of incontinence.[12]

Fecal incontinence worsened everyday functioning in 42% of patients with CD and in 51% of patients with UC. Fecal incontinence and its related concerns could represent the elements of the symptomatology of IBD which are most constricting in everyday life. In a study aiming to provide optimal nursing care, 5 young adults, who were asked what mattered most as they lived with IBD, pointed out embarrassment and concerns related to fecal incontinence, among other aspects.[15] In UC patients, fear of fecal incontinence can be obsessive and can lead to compulsive evacuation-checking. This can be called bowel obsession syndrome (BOS) and is a type of obsessive-compulsive disorder. Porcelli and Leandro described a male patient with UC and marked symptoms of BOS who was successfully treated with antidepressants.[16] Fear of fecal incontinence was the reason for sexual inactivity in 14% of women with CD in a study by Moody et al.[17]

Our data has clearly shown that fecal incontinence affects a large percentage of patients with both CD and UC, and constitutes an important element of the clinical picture which has a great impact However, the main limitation of this study is its relatively small overall sample size.

References

1. Lewis SJ, Heaton KW. Stool form scale as a useful guide to intestinal transit time. *Scand J Gastroenterol*. 1997;32(9):920–924.
2. Miller R, Bartolo DC, Locke-Edmunds JC, et al. Prospective study of conservative and operative treatment for fecal incontinence. *Br J Surg*. 1988;75(2):101–105.
3. Rao SS, Holdsworth CD, Read NW. Symptoms and stool patterns in patients with ulcerative colitis. *Gut*. 1988;29(3):342–345.
4. Rao SS, Read NW. Gastrointestinal motility in patients with ulcerative colitis. *Scand J Gastroenterol Suppl*. 1990;175:22–28.
5. Crispino P, Habib FI, Badiali D, et al. Colorectal motor and sensitivity features in patients affected by ulcerative proctitis with constipation: A radiological and manometric controlled study. *Inflamm Bowel Dis*. 2006;12:712–718.
6. Isgar B, Harman M, Kaye MD, et al. Symptoms of irritable bowel syndrome in ulcerative colitis in remission. *Gut*. 198;24:190–192.
7. Bassotti G, de Roberto G, Chistolini F, et al. Twenty-four-hour manometric study of colonic propulsive activity in patients with diarrhea due to inflammatory (ulcerative colitis) and non-inflammatory (irritable bowel syndrome) conditions. *Int J Colorectal Dis*. 2004;19:493–497.
8. Bassotti G, Villanacci V, Mazzocchi A, et al. Colonic propulsive and postprandial motor activity in patients with ulcerative colitis in remission. *Eur J Gastroenterol Hepatol*. 2006;18:507–510.
9. Simren M, Axelsson J, Gillberg R, et al. Quality of life in inflammatory bowel disease in remission: The impact of IBS-like symptoms and associated psychological factors. *Am J Gastroenterol*. 2002;97(2):389–396.
10. Loening-Baucke V, Metcalf AM, Shirazi S. Anorectal manometry in active and quiescent ulcerative colitis. *Am J Gastroenterol*. 1989;84(8):892–897.
11. Rao SS, Hatfield R, Soffer E, et al. Manometric tests of anorectal function in healthy adults. *Am J Gastroenterol*. 1999;94(3):773–783.
12. Mueller MH, Kreis ME, Gross ML, et al. Anorectal functional disorders in the absence of anorectal inflammation in patients with Crohn's disease. *Br J Surg*. 2002;89:1027–1031.
13. Buchmann P, Kolb E, Alexander-Williams J. Pathogenesis of urgency in defecation in Crohn's disease. *Digestion*. 1981;22(6):310–316.
14. Kangas E, Hiltunen KM, Matikainen M. Anorectal function in Crohn's disease. *Ann Chir Gynaecol*. 1992;81(1):43–47.
15. Daniel JM. Young adults' perceptions of living with chronic inflammatory bowel disease. *Gastroenterol Nurs*. 2002;25(3):83–94.
16. Porcelli P, Leandro G. Bowel obsession syndrome in a patient with ulcerative colitis. *Psychosomatics*. 2007;48(5):448–450.
17. Moody G, Probert CS, Srivastava EM, et al. Sexual dysfunction amongst women with Crohn's disease: A hidden problem. *Digestion*. 1992;52(3–4):179–183.

Insufficient modification of atherosclerosis risk factors in PAD patients

Katarzyna Skórkowska-Telichowska[1–3,B–D], Katarzyna Kropielnicka[1,4,B,C], Katarzyna Bulińska[1,4,B,C], Urszula Pilch[1,4,B,C], Marek Woźniewski[4,A,F], Andrzej Szuba[1–3,A,D–F], Ryszard Jasiński[4,B,F]

[1] WroVasc-Integrated Medical Cardiovascular Center, Regional Specialist Hospital, Research and Development Center, Wrocław, Poland
[2] Department of Internal Medicine, 4th Military Hospital, Wrocław, Poland
[3] Division of Angiology, Faculty of Health Sciences, Wroclaw Medical University, Poland
[4] Department of Rehabilitation, University School of Physical Education, Wrocław, Poland

A – research concept and design; B – collection and/or assembly of data; C – data analysis and interpretation; D – writing the article; E – critical revision of the article; F – final approval of the article

Advances in Clinical and Experimental Medicine, ISSN 1899-5276 (print), ISSN 2451-2680 (online) *Adv Clin Exp Med*. 2018;27(6):819–826

Address for correspondence
Katarzyna Skórkowska-Telichowska
E-mail: cathcor@poczta.onet.pl

Funding sources
This publication is a part of the "WroVasc – Integrated Cardiovascular Centre" project, co-financed by the European Regional Development Fund, within the Innovative Economy Operational Program, 2007–2013, conducted in the Regional Specialist Hospital, Research and Development Center in Wrocław, Poland.

Conflict of interest
None declared

Received on February 9, 2016
Reviewed on August 11, 2016
Accepted on February 14, 2017

Abstract

Background. An aggressive reduction of cardiovascular risk factors in patients with intermittent claudication (IC) is extremely important.

Objectives. The aim of this study was to investigate patients' adherence to current guidelines for the recognition and reduction of atherosclerosis risk factors in peripheral arterial disease (PAD) in Poland.

Material and methods. The study included 126 patients with PAD stage II, according to the Fontaine Classification, who over a period of 2 years attended an angiological outpatient clinic and were referred for physical rehabilitation.

Results. In the 77% of PAD patients diagnosed with dyslipidemia, 72% had hypertension and 31% had diabetes. Suboptimal treatment was being given to 85.5% of patients with dyslipidemia, to 26% of patients with hypertension and to 95% of diabetics. In this study, a diagnosis of dyslipidemia, hypertension and diabetes was made for the 1st time in 22%, 7% and 4% of patients, respectively. As many as 17.5% of PAD patients with claudication were not receiving any antiplatelet therapy.

Conclusions. The diagnosis of dyslipidemia was insufficient (about 1/3 of the patients were undiagnosed), and diagnoses of hypertension and diabetes prevailed. It was established that the effective control of risk factors using relevant treatment is insufficient in dyslipidemia, hypertension and diabetes. Antiplatelet therapy was not prescribed in approx. 20% of cases.

Key words: diabetes, smoking, arterial hypertension, antiplatelet therapy, dyslipidemia

DOI
10.17219/acem/68983

Introduction

The guidelines on the Diagnosis and Treatment of Peripheral Artery Disease, established by the European Society of Cardiology (ESC) and applicable in Poland, determine and facilitate the treatment of atherosclerosis that occurs in different vascular beds.[1] The guidelines should help angiologists make proper decisions in their daily practice. However, due to a lack of cohort studies, the very general nature of the recommendations and the conservative character of the guidelines, the final decisions concerning individual patients must be made by the responsible physician. In peripheral artery disease (PAD) patients, a multidisciplinary approach is recommended in order to establish a management strategy (class of recommendation: I, level of evidence: C). The most effective strategy for PAD treatment, according to the ESC guidelines, is the aggressive reduction of atherosclerosis risk factors, which include atherogenic dyslipidemia, hypertension, diabetes, obesity, and smoking.

Apart from lifestyle modifications, such as regular exercise, a Mediterranean diet and cessation of smoking, patient care should include pharmacological treatment to control blood pressure (treatment with angiotensin-converting enzyme [ACE] inhibitors and beta-blockers have shown beneficial effects), an appropriate lipid-lowering statin therapy, and glycaemia treatment in diabetic patients.[1] All PAD patients should receive antiplatelet therapy.[1]

The aim of this study was to determine the adherence to the current recommendations regarding the reduction of atherosclerosis risk factors in patients with PAD in Poland.

Material and methods

From a group of 219 subjects with atherosclerosis of the lower extremities who were examined in the angiology outpatient unit over a 2-year period (2011–2013), 126 subjects fulfilled the criteria for participation in physical exercise training and were enrolled in the study.

Recruitment into the rehabilitation program was limited to patients with stable claudication without any limitations or contraindications for physical exercise. The inclusion and exclusion criteria for participation in physical training are listed in Table 1.

Risk factor profile

The profile of risk factors and treatment were determined during admission to the angiology outpatient unit based on a self-reported medical history. Measurement of blood pressure and laboratory tests were also performed during the visit.

In the study, references to current treatment guidelines for dyslipidemia, hypertension and diabetes reflected the ESC Guidelines on the Diagnosis and Treatment of Peripheral Arterial Disease, 2011.[1]

Table 1. Inclusion and exclusion criteria for participation in the study[2]

Inclusion criteria
• Age over 40 years • Documented IC which is stable for at least 3 months, considered for physical rehabilitation program • IC distance: 30–320 m (stage II according to the Fontaine Classification), ABI ≤0.9
Exclusion criteria
• PAD Fontaine stage I (pain-free distance on a treadmill >500 m, unlimited walking ability) and stage III/IV (rest pain, ulcerations) • Physical limitation due to advanced cardiovascular disease, orthopedic disorders, balance disorders, or dementia • Vascular surgery or other invasive treatment during the last 3 months • Logistical obstacles: distance to the place of physical rehabilitation • Simultaneous participation in another research programs • Anticipated problems with patients' compliance with the program

ABI – ankle brachial index; IC – intermittent claudication; PAD – peripheral artery disease.

Dyslipidemia was defined in accordance with the Third Report of the Adult Treatment Panel (ATP III) of the National Cholesterol Education Program guidelines as a high concentration of total cholesterol, low-density lipoprotein (LDL) cholesterol ≥100 mg/dL, triglycerides ≥150 mg/dL, and/or a low high-density lipoprotein (HDL) cholesterol level of <40 mg/dL for men and <50 mg/dL for women.[3]

Optimal treatment of previously recognized dyslipidemia was defined as an LDL cholesterol level of ≤100 mg/dL (in asymptomatic PAD patients), or ideally, a level of ≤70 mg/dL (in symptomatic patients – that is, with intermittent claudication [IC]), and all cholesterol and triglyceride counts within normal ranges.

Arterial hypertension was outlined by the 8th Joint National Committee guidelines and defined as an systolic blood pressure/diastolic blood pressure (SBP/DBP) of ≥140/90 mm Hg in patients aged <60 years and ≥150/90 mm Hg in patients aged ≥60 years, with or without antihypertensive treatment.[4]

Optimal treatment in patients with previously diagnosed arterial hypertension was defined as an SBP/DBP of ≤140/90 mm Hg in patients aged ≤60 years and of ≤150/90 mm Hg in patients aged ≥60 years.

A glycated hemoglobin (HbA_{1c}) level of ≥7% indicated suboptimal glycemic control in diabetics. Newly diagnosed diabetes was defined as a fasting glucose concentration of ≥126 mg/dL accompanied by symptoms of uncontrolled diabetes. Impaired fasting glucose (defined as prediabetes) was established as a fasting glucose level between 110 mg/dL and 125 mg/dL.[5]

Routine laboratory tests were performed on peripheral blood collected in the morning after an 8-h fast. Laboratory tests included a complete blood count with a differential and biochemical profile, including blood urea, creatinine, C reactive protein (CRP), fibrinogen, a lipid panel with total cholesterol, HDL cholesterol, LDL cholesterol, and triglycerides, as well as sodium, potassium and glucose levels.

Table 2. Entire population data (patients' characteristics and disease history). Descriptive data is presented as mean ± standard deviation or number (%)

General information	
Number of subjects	126
Age [years]	67.4 ±8.3
Gender	
Female, n (%)	34 (27)
Male, n (%)	92 (73)
BMI [kg/m^2]	27.5 ±4
City dwellers, n (%)	120 (95.3)
Village dwellers, n (%)	6 (4.7)
Angiological profile	
Type of ischemia, n (%)	
Aorto-iliac	9 (7)
Femoro-popliteal	74 (59)
Infra-popliteal	24 (19)
Multilevel lesions	19 (15)
Fontaine class, n (%)	
Class II a (>200 m)	8 (6.4)
Class II b (<200 m)	118 (93.6)
ABI	0.61 ±0.22
Initial claudication distance [m]	95.9 ±58
Absolute claudication distance [m]	175.6 ±98.8
Medical history, n (%)	
Diagnosed diabetes type 2	39 (31)
Diagnosed arterial hypertension	91 (72)
Diagnosed dyslipidemia	97 (77)
Diagnosed CHD	54 (42.8), after ACS 20 (15.8); stabile angina pectoris 34 (27)
History of CHF	41 (32.5)
History of stroke	13 (10.3)
History of cancer	15 (11.9)
History of thyroid diseases	10 (7.94)
History of kidney failure	15 (11.9)
Chronic venous insufficiency	11 (8.7)
Osteoarthritis	37 (29.3)
COPD	2 (1.6)
Osteoporosis	2 (1.6)

ABI – ankle brachial index; ACS – acute coronary syndrome; BMI – body mass index; CHD – coronary heart disease; CHF – chronic heart failure; COPD – chronic obstructive pulmonary disease.

This was performed using standard laboratory techniques carried out in the angiology unit (Table 2).

The patients' profile of atherosclerosis risk factors allowed for the division of the subjects into 3 groups:

1. Patients with previously diagnosed risk factors, treated optimally according to applicable standards;
2. Patients with previously diagnosed risk factors whose treatment was not optimal (the therapeutic objectives were not achieved);
3. Patients in whom atherosclerosis risk factors had not previously been diagnosed.

Statistical analysis

Normality was tested using the D'Agostino-Pearson test. Comparison between quantitative variables was performed using the Mann-Whitney U test (for 2 variables) and the Kruskall-Wallis test (for more than 2 variables). Analysis of the relationships between qualitative variables was performed using the χ^2 test. Statistical analysis was performed using R for Windows (v. 3.1.2). All results with $p < 0.05$ were considered significant. The demographic and clinical characteristics of the study group were reported as median and interquartile ranges or as counts and percentages, as appropriate.

Ethical approval

Ethical approval was obtained from the local bioethics committee (Bioethics Committee, Wroclaw Medical University, Poland, No. 130/2008 KB). All the patients were provided with written information on the purpose and design of the study.

Results

The main clinical and biochemical data of the examined group are summarized in Table 3.

Dyslipidemia

A history of dyslipidemia was reported in 97 subjects (77%), with a mean level of total cholesterol amounting to 167 ±36 mg/dL, mean LDL cholesterol of 92 ±30 mg/dL, mean HDL cholesterol of 46.5 ±11 mg/dL, and a mean level of triglycerides of 141 ±80 mg/dL.

Optimal therapy was observed in 14 subjects (14.4% of the 97 patients) with a mean level of total cholesterol amounting to 122 ±17 mg/dL, mean LDL cholesterol of 53 ±9 mg/dL, mean HDL cholesterol level of 49 ±11 mg/dL, and triglycerides of 97 ±34 mg/dL.

Suboptimal therapy was observed in 83 subjects (85.5% of the 97 patients) with a mean level of total cholesterol amounting to 174 ±33 mg/dL, mean LDL cholesterol of 98 ±27 mg/dL, mean HDL cholesterol of 46 ±11 mg/dL, and triglycerides of 148 ±83 mg/dL. Undiagnosed cases of dyslipidemia were found in 28 subjects (22% of the total sample of 126 patients). These were new cases of dyslipidemia with mean levels of total cholesterol amounting to 202 ±42 mg/dL, mean LDL cholesterol of 123 ±32 mg/dL, mean HDL cholesterol of 45 ±8 mg/dL, and triglycerides of 154 ±84 mg/dL. Patients that had not been diagnosed before participating in the study had significantly higher total cholesterol levels than the group undergoing treatment ($p = 0.0003$) and significantly higher LDL cholesterol levels ($p = 0.0001$). HDL cholesterol levels and triglycerides were higher in the untreated group, but not significantly.

Table 3. Risk factor profile of PAD patients (n = 126). Descriptive data is presented as mean ± standard deviation or number (%)

Variable	Entire population (n = 126)	A: patients with diagnosed diabetes (n = 39; 30.952%)	B: patients without diabetes (n = 87; 69.047%)	p-value (A vs B)
Fasting glucose level [mg/dL]	117 ±35	147 ±35	103 ±24	0.0001
HbA_{1c} [%]	10 ±0.5	10 ±0.5	–	–
Total cholesterol [mg/dL]	174 ±41	169 ±39	177 ±41	0.26
LDL cholesterol [mg/dL]	98 ±33	93 ±30	101 ±34	0.12
HDL cholesterol [mg/dL]	46 ±10	44 ±10	47 ±10	0.16
Triglycerides [mg/dL]	144 ±81	149.5 ±73	141 ±85	0.19
CRP [mg/L]	6 ±13	6.5 ±20	6 ±9	0.022
Homocysteine [umol/L]	14 ±5	13 ±5	15 ±5	0.16
Fibrynogen [g/L]	4 ±1	4 ±1	4 ±1	0.46
SBP [mm Hg] DBP [mm Hg]	133 ±15 78 ±7	133 ±15 77 ±8	133 ±15 78 ±7	0.62
Pulse rate [bpm]	75 ±12	74 ±12	76 ±13	0.85
ABI	0.6 ±0.2	0.64 ±0.3	0.60 ±0.1	0.92
BMI [kg/m^2]	27.5 ±4	28.7 ±3	27.0 ±4	0.018
Current smokers, n (%)	32 (25%)	10 (8%)	22 (17.5%)	0.43
Ever-smokers, n (%)	17 (13.5%)	3 (2.3%)	14 (11%)	0.43
Initial claudication distance [m]	95.9 ±58	106 ±72	91 ±50	0.94
Absolute claudication distance [m]	175 ±99	179 ±107	174 ±95	0.76

p-value of <0.05 was considered statistically significant; BMI – body mass index; CRP – C reactive protein; LDL – low-density lipoprotein; HDL – high-density lipoprotein; SBP – systolic blood pressure; DBP – diastolic blood pressure; ABI – ankle brachial index.

An absence of dyslipidemia was observed in only 1 case, with a total cholesterol amounting to 116 mg/dL, LDL cholesterol level of 70 mg/dL, HDL cholesterol of 33 mg/dL, and triglyceride level of 65 mg/dL.

In subjects with previously diagnosed dyslipidemia, the most commonly prescribed medications were statins (88 subjects – 91%), while 5 subjects (5%) were taking 2 cholesterol-lowering agents (statin + fibrate) and 4 subjects (4%) were on fibrate therapy. Two main types of statins were being administered: 76% of patients (n = 67) received atorvastatin and 20% (n = 17) were given simvastatin. The patients considered to be receiving optimal treatment had significantly lower total cholesterol levels (p = 0.0001), LDL cholesterol levels (p = 0.0001) and triglycerides (p = 0.022). HDL cholesterol levels did not vary significantly, but were higher in the group treated optimally.

Hypertension

Arterial hypertension was diagnosed in 91 subjects prior to the study, representing 72% of the study sample; in this group of patients, the mean SBP was 134 ±16 mm Hg and DBP was 77 ±8 mm Hg.

Management of hypertension was suboptimal in 24 subjects (26% of subjects with hypertension). In this group, the mean SBP was 156 ±9 mm Hg and DBP was 80 ±7 mm Hg.

The optimal treatment was prescribed in 67 patients (74% of subjects with hypertension) with a mean SBP amounting to 127 ±10 mm Hg and DBP of 76 ±8 mm Hg.

Hypertension was unrecognized in 7% (n = 9) of the sample with a mean SBP of 150 ±8 mm Hg and DBP of 88 ±5 mm Hg. All 3 groups of patients (those treated optimally, treated suboptimally and undiagnosed) differed significantly in terms of both SBP (p = 0.0005) and DBP (p = 0.0001). An absence of hypertension was observed in 26 patients (20.63%).

In patients with previously diagnosed hypertension, 20% (n = 18) were receiving monotherapy, while 21% (n = 19) were receiving dual hypertensive therapy. Triple therapy had been prescribed in 30% of subjects (n = 27), representing the most common regimen. A combination of 4 medicines was prescribed to 21% of patients (n = 19). Five medicines had been prescribed less frequently (6%; n = 6), though 2 patients (2%) were taking 6 medicines. There were no significant differences in SBP or DBP relative to the number of antihypertensive medications used; nevertheless, the lowest pressure was observed in patients treated with 3 medications.

The most frequently used medications were ACE inhibitors (57% of subjects with diagnosed hypertension, n = 52) and diuretics (54% of subjects with diagnosed hypertension, n = 49), followed by calcium channel blockers and other kinds of antihypertensive medications. Of the ACE inhibitors, the most frequently prescribed medications were ramipril (54%, n = 28), followed by perindopril (23%, n = 12), quinapril (15%, n = 8) and other medications. The most frequently prescribed diuretics were Indapen® SR (45% of patients who received diuretics,

n = 22), hydrochlorothiazide (26.5% of patients who received diuretics, n = 13), and loop diuretics, such as furosemide and torasemide (28.6% of patients who received diuretics, n = 14).

Fifty-five patients (43.6% of the entire study population) were using beta-blockers, bisoprolol being the most frequently prescribed medication (54.5%, n =30), followed by carvedilol (18%, n = 10), metoprolol (12.7%, n = 7) and nebivolol (9%, n = 5).

The most frequently administered drug combination, which was given to 14 patients (15%), consisted of perindopril and Indapen® SR.

Diabetes

A history of diabetes was reported in 39 patients (31%). The mean fasting blood glucose level was 147 ±36 mg/dL, and the mean HbA_{1c} level was 10 ±0.5%.

Suboptimal glycemic control was found in 37 cases (95%), in which the mean fasting blood glucose level was 152 ±4 mg/dL. In 2 patients (5%) who exhibited optimal glucose control, the mean fasting blood glucose was 85.5 ±0.7 mg/dL.

During the study, prediabetes (impaired fasting glucose) was diagnosed for the 1st time in 14 subjects (11%); the mean fasting glucose level in this group was 116 ±5 mg/dL. Newly diagnosed cases of diabetes affected 5 patients (4%). The mean fasting glucose level in this group was 181 ±40 mg/dL.

Normal glucose control was found in 68 patients (54%) with fasting blood glucose levels of 91 ±7 mg/dL. All 3 groups of patients (those with diagnosed diabetes, those with existing but previously undiagnosed diabetes, and healthy individuals without diabetes) differed significantly in terms of fasting glucose levels (p = 0.0001).

Out of the 39 subjects who had diabetes, 29 were taking oral hypoglycemic medications, 3 subjects were being treated with insulin therapy and 7 subjects received both insulin and oral hypoglycemic therapy. In the group of patients who were administered oral medicines, 16 received monotherapy (a mean fasting glucose level of 125 ±37 mg/dL), 11 patients received double therapy (a mean fasting glucose level of 152 ±21 mg/dL) and 2 patients were administered triple therapy (with a mean fasting glucose level of 152.5 ±37 mg/dL). The most frequently prescribed oral hypoglycemic medicine was metformin. Patients who were treated with insulin had a mean fasting glucose level of 144.6 ±5 mg/dL.

Diabetes, hypertension and dyslipidemia were observed in 28 subjects concomitantly (22.2% of the entire study population). Diabetes plus hypertension was observed in 6 subjects (5% of the entire study population). Diabetes plus dyslipidemia (without hypertension) was observed in 2 cases (1.6%). Only 3 subjects who were diagnosed with diabetes did not have either hypertension or dyslipidemia.

Anticoagulation/antiplatelet therapy

Antiplatelet therapy was being used by 104 subjects (82.5% of the 126 patients), the most common being monotherapy. Aspirin monotherapy was being taken by 74 subjects (59%), followed by clopidogrel (1.6%, n = 2) and ticlopidine (1.6%, n = 2). Dual therapy was administered to 19 patients (15%). The most common therapies were the concomitant treatment of aspirin with clopidogrel (17 patients, 13.5%) and aspirin with ticlopidine (2 patients, 1.6%). The prescription of dual therapy was not the result of previous invasive interventional cardiology, but was due to atherosclerosis of the lower limbs. One subject (0.8%) was administered triple therapy: aspirin, clopidogrel and acenokumarol. Anticoagulation therapy was being given to 3 patients only (4%). Twenty-two individuals (17.5%) were not currently receiving anticoagulant or antiplatelet therapy.

Other medicines taken for peripheral artery disease

Thirty-five subjects from the entire study population (28%) were taking pentoxifylline, the average dose being 1200 mg per day (600–1800 mg). Sulodexide was taken by 13 patients (10.3%) with an average dose of 500 mg per day. Bencyclane was taken by 15 patients (12%); the average dose was 400 mg per day.

Smokers

In the entire study group, 49 patients (39%) were current or ex-smokers, and 32 patients (25%) were current smokers. None of them had previously received any pharmacological tobacco cessation therapy, according to their self-declared medical history. The patients smoked 20 cigarettes a day on average. Ex-smokers accounted for 14% (n = 17) of the study population.

Physical activity

None of the patients in the study group were participating in any regular, long-lasting physical activity.

Discussion

The main finding of this study is that in the group of PAD claudicants admitted to an angiology outpatient unit, the atherosclerosis risk factors had been underestimated and when diagnosed, they were treated incorrectly. The current study revealed that 77% of PAD patients were diagnosed with dyslipidemia, 72% had hypertension and 31% had diabetes. Suboptimal treatment was received by 85.5% of patients with dyslipidemia, 26% of patients with hypertension and 95% of diabetics. In this study, dyslipidemia,

hypertension and diabetes were diagnosed for the 1st time in 22%, 7% and 4% of the subjects, respectively. A total of 17.5% of PAD patients with claudication were not receiving any antiplatelet therapy.

Lipid-lowering therapy

The ESC guidelines require an active search for atherogenic dyslipidemia in symptomatic PAD patients and, following diagnosis, aggressive lipid-lowering therapy. All patients with PAD should have their serum LDL cholesterol reduced to <100 mg/dL, or to <70 mg/dL, ideally; when the target level cannot be reached, the physician should consider lowering the LDL cholesterol by 50% or more of the level before treatment, according to the guidelines (class of recommendation: I, level of evidence: C). The most important medications which reduce the risk of mortality, cardiovascular events and stroke, and those which increase the absolute walking distance in patients with PAD with and without coronary heart disease (CHD), are statins, especially simvastatin.[1,3,6–8]

The data revealed that 77% of PAD patients were dyslipidemic before the study began, and that a further 22% of subjects were not diagnosed with dyslipidemia beforehand. Nonetheless, when dyslipidemia was diagnosed, only 14.4% of the affected subjects achieved the goals of ESC treatment for LDL levels. These results could be the consequence of not following the guidelines or they may suggest a lack of awareness on the part of physicians and patients, who did not test for dyslipidemia. The 2 main types of statins administered were atorvastatin in 76% of patients (n = 67) and simvastatin in 20% of patients (n = 17).

Antihypertensive drugs

All patients with PAD, according to the ESC guidelines, should have their blood pressure reduced to ≤140/90 mm Hg (class of recommendation: I, level of evidence: A).[1,4] Treatment with angiotensin-converting enzyme inhibitors has shown a beneficial effect by lowering blood pressure in high-risk groups.[9,10] Importantly, beta-blockers are not contraindicated in patients with PAD (class of recommendation: IIa, level of evidence: B). Beta-blockers should be considered in the treatment of concomitant coronary artery disease and/or heart failure (class of recommendation: IIa, level of evidence: B).[11]

According to the results of this study, hypertension was detected in 72% of the study group, which was higher than the findings of the Framingham Offspring Study (69%) and lower than the findings in the PARTNERS study (88%).[12,13] The detection of hypertension is imperative, but of even more importance to the current study is that 26% of patients with recognized hypertension were receiving suboptimal treatment. Seven percent of the entire study group had unrecognized hypertension.[1,6] The detection of atherosclerosis risk factors and the achievement of treatment goals are better in the case of hypertension than in dyslipidemia in Poland. Nevertheless, almost 1/3 of antihypertensive PAD subjects were receiving suboptimal treatment.

Diabetes

In patients with PAD and diabetes, the recommended HbA_{1c} level is ≤6.5% according to ESC criteria (class of recommendation: I, level of evidence: C)[1] and ≤7% according to American Diabetes Association (ADA) criteria (level of evidence: B).[14] Diabetic PAD patients have poorer leg function, higher body mass index (BMI), increased neuropathy, and more cardiovascular comorbidities than PAD patients without diabetes.[15–17] Additionally, inadequate treatment of diabetes increases the risk of mortality in PAD patients.[12] For these reasons detection and treatment of diabetes in PAD patients should be imperative.

In the current study, 31% of patients had previously diagnosed diabetes. Prediabetes was found in 11% of cases and unrecognized diabetes was found in 4%, using only the venous fasting glycaemia test. The majority of diabetics (95%) were being undertreated, with an HbA_{1c} level higher than the recommended range. The study revealed that although the recognition of diabetes seems to be sufficient in PAD patients in Poland, the level of inadequate treatment is considerable and requires improvement.

Antiplatelet and antithrombotic therapy

According to ESC guidelines, the incidence of vascular death, non-fatal myocardial infarction and non-fatal stroke was significantly reduced at follow-up by the use of antiplatelet drugs (class of recommendation: I, level of evidence: C).[1,18] A low dose of aspirin (75–100 mg daily) was at least as effective as higher daily doses.[1] The CAPRIE trial demonstrated that clopidogrel is as efficacious as aspirin in preventing major cardiovascular events in patients with PAD.[19] The insignificant benefits of dual antiplatelet therapy do not overcome the increased risk of bleeding in patients with PAD, so its recommendation is not justified.[20,21] Antiplatelet therapy is recommended in all patients with symptomatic PAD.[1]

In the current study, 82.5% of the entire population were using antiplatelet therapy. Aspirin (an average daily dose of 150 mg), as a recommended therapy, was the most common antiplatelet therapy (59%), followed by clopidogrel and ticlopidine in the same proportions (1.6%). Anticoagulation therapy was being used in 4% of cases. Approximately 17.5% of the patients in the study sample (n = 22) were not currently receiving antiplatelet or anticoagulant therapy, but no contraindications to this therapy were identified in this group of patients. Moreover, 15% of the subjects were administered dual antiplatelet therapy, without any cardiological or angiosurgical indications for such treatment.

Other medicines taken for peripheral artery disease

Phosphodiesterase inhibitor was one of the 1st drugs used in patients with arteriosclerosis obliterans. It improves the rheological properties of blood and is also believed to increase the claudication distance by about 100 m.[22] Our study revealed that 35 subjects from the entire population (only 28%) were taking pentoxifylline, with an average dose of 1200 mg per day (600–1800 mg). Sulodexide was taken by 13 patients (10.3%), with an average dose of 500 mg per day. Bencyclane was taken by 15 patients (12%) at an average dose of 400 mg per day.

Lifestyle modifications

Smoking is an important risk factor for PAD. In the general population, smoking increases the risk of PAD between 2-fold and 6-fold. Current smokers with PAD have an increased risk of limb amputation and are at an increased risk of postoperative complications and mortality.[23–25] Smokers should be advised to quit smoking and be offered smoking cessation programs (class of recommendation: I, level of evidence: B).[1]

A limitation of the study was the use of self-reported smoking history without validating it by means of biological markers. Out of the 126 patients who were admitted to the outpatient angiology unit with a low walking distance, 25% were active smokers. This number seems very low in comparison to the PARTNERS study and the Rotterdam Study, in which 70% of the PAD patients were active smokers.[25]

Non-pharmacological methods of improving the length and quality of life in the form of a balanced diet, weight control and regular exercise were not being used by any of the patients.

Conclusions

There is a strong need to carefully diagnose dyslipidemia in PAD patients. The prescription of antiplatelet therapy to PAD patients should be more widespread. The rate of hypertension and diabetes in PAD patients appears to be high, but physicians should place greater emphasis on achieving optimal treatment goals.

References

1. European Stroke Organisation, Tendera M, Aboyans V, Bartelink ML, et al.; ESC Committee for Practice Guidelines. ESC Guidelines on the diagnosis and treatment of peripheral artery diseases. *Eur Heart J*. 2011;32(22):2851–2906.
2. Gardner A, Montgomery P, Flinn W, Katzel LI. The effect of exercise intensity on the response to exercise rehabilitation in patients with intermittent claudication. *J Vasc Surg*. 2005;42(4):702–709.
3. Goff DC, Bertoni AG, Kramer H, et al. Dyslipidemia prevalence, treatment, and control in the multi-ethnic study of atherosclerosis (MESA): Gender, ethnicity, and coronary artery calcium. *Circulation*. 2006;113(5):647–656.
4. James PA, Oparil S, Carter BL, et al. Evidence-based guideline for the management of high blood pressure in adults: Report from the panel members appointed to the Eighth Joint National Committee (JNC 8). *JAMA*. 2014;311(5):507–520.
5. World Health Organization. Definition and diagnosis of diabetes mellitus and intermediate hyperglycaemia: Report of a WHO/IDF consultation. Geneva, Switzerland: World Health Organization; 2006.
6. Graham I, Atar D, Borch-Johnsen K, et al.; European Society of Cardiology (ESC); European Association for Cardiovascular Prevention and Rehabilitation (EACPR); Council on Cardiovascular Nursing; European Association for Study of Diabetes (EASD); International Diabetes Federation Europe (IDF-Europe); European Stroke Initiative (EUSI); International Society of Behavioral Medicine (ISBM); European Society of Hypertension (ESH); European Society of General Practice/Family Medicine (ESGP/FM/WONCA); European Heart Network (EHN). European guidelines on cardiovascular disease prevention in clinical practice: Executive summary. Fourth Joint Task Force of the European Society of Cardiology and other societies on cardiovascular disease prevention in clinical practice (constituted by representatives of nine societies and by invited experts). *Eur Heart J*. 2007;28:2375–2414.
7. European Association for Cardiovascular Prevention & Rehabilitation, Reiner Z, Catapano AL, De Backer G, et al.; ESC Committee for Practice Guidelines (CPG) 2008–2010 and 2010–2012 Committees. ESC/EAS guidelines for the management of dyslipidaemias: The Task Force for the management of dyslipidaemias of the European Society of Cardiology (ESC) and the European Atherosclerosis Society (EAS). *Eur Heart J*. 2011;32(14):1769–1818.
8. Collins R, Armitage J, Parish S, Sleigh P, Peto R; Heart Protection Study Collaborative Group. MRC/BHF Heart Protection Study in cholesterol-lowering with simvastatin in 5963 people with diabetes: A randomized placebo-controlled trial. *Lancet*. 2003;361(9374):2005–2016.
9. The Heart Outcomes Prevention Evaluation Study Investigators, Yusuf S, Sleight P, Pogue J, Bosch J, Davies R, Dagenais G. Effects of an angiotensin-converting-enzyme inhibitor, ramipril, on cardiovascular events in high risk patients. *N Engl J Med*. 2000;342(3):145–153.
10. ONTARGET Investigators, Yusuf S, Teo KK, Pogue J, et al. Telmisartan, ramipril or both in patients at high risk for vascular events. *N Engl J Med*. 2008;358(15):1547–1559.
11. Radack K, Deck C. Beta-adrenergic blocker therapy does not worsen intermittent claudication in subjects in peripheral arterial disease. A meta-analysis of randomized, controlled trials. *Arch Intern Med*. 1991;151(9):1769–1776.
12. Murabito JM, Evans JC, Nieto K, Larson MG, Levy D, Wilson PW. Prevalence and clinical correlates of peripheral arterial disease in the Framingham Offspring Study. *Am Heart J*. 2002;143(6):961–965.
13. Hirsh AT, Criqui MH, Treat-Jacobson D, et al. Peripheral arterial disease detection, awareness, and treatment in primary care. *JAMA*. 2001;286(11):1317–1324.
14. American Diabetes Association. Standards of Medical Care in Diabetes – 2014. *Diabetes Care*. 2014;37(Suppl 1):S14–80.
15. Resnic H, Shorr R, Kuller L. Prevalence and clinical implications of American Diabetes Association-defined diabetes and other categories of glucose dysregulation in older adults: The health, aging and body composition study. *J Clin Epidemiol*. 2001;54(9):869.
16. Hiatt WR. Preventing atherotrombotic events in peripheral arterial disease: The use of antiplatelet therapy. *J Intern Med*. 2002;251(1):93–206.
17. Dawson DL, Hiatt WR, Creager MA, Hirsch AT. Peripheral arterial disease: Medical care and prevention of complications. *Prev Cardiol*. 2002;5:119–130.
18. Antithrombotic Trialists' (ATT) Collaboration, Baigent C, Blackwell L, Collins R, et al. Aspirin in the primary and secondary prevention of vascular disease: Collaborative meta-analysis of individual participant data from randomized trials. *Lancet*. 2009;373(9678):1849–1860.
19. CAPRIE Steering Committee. A randomized, blinded, trial of clopidogrel versus aspirin in patients at risk of ischemic events (CAPRIE). *Lancet*. 1996;348(9038):1329–1339.
20. Bhatt DL, Fox KA, Hacke W, et al. CHARISMA Investigators. Clopidogrel and aspirin versus aspirin alone for the prevention of atherotrombotic events. *N Engl J Med*. 2006;354(16):1706–1717.
21. Cacoub PP, Bhatt DL, Steg PG, Topol EJ, Creager MA; CHARISMA Investigators. Patients with peripheral arterial disease in the CHARISMA trial. *Eur Heart J*. 2009;30(2):192–201.

22. Momsen AH, Jensen MB, Norager CB, Madsen MR, Vestergaard-Andersen T, Lindholt JS. Drug therapy for improving walking distance in intermittent claudication: A systematic review and meta-analysis of robust randomized controlled studies. *Eur J Vasc Endovasc Surg*. 2009;38(4):463–474.
23. Fowkes FG, Housley E, Riemersma RA, et al. Smoking, lipids, glucose intolerance, and blood pressure as risk factors of peripheral atherosclerosis compared with ischaemic heart disease in the Edinburgh Artery Study. *Am J Epidemiol*. 1992;135(4):331–340.
24. Criqui MH. Peripheral artery disease – epidemiological aspects. *Vasc Med*. 2001;6:3–7.
25. Powell JT, Edwards RJ, Worrell PC, Franks PJ, Greenhalgh RM, Poulter NR. Risk factors associated with the development of peripheral arterial disease in smokers: A case-control study. *Atherosclerosis*. 1997;129(1):41–1248.

High prevalence of antinuclear antibodies in patients following venous thromboembolism

Joanna Natorska[1,B–D], Magdalena Celińska-Löwenhoff[2,D,E], Anetta I. Undas[1,A,E,F]

[1] Institute of Cardiology, Jagiellonian University Medical College, Kraków, Poland
[2] Department of Internal Medicine, Jagiellonian University Medical College, Kraków, Poland

A – research concept and design; B – collection and/or assembly of data; C – data analysis and interpretation;
D – writing the article; E – critical revision of the article; F – final approval of the article

Advances in Clinical and Experimental Medicine, ISSN 1899-5276 (print), ISSN 2451-2680 (online) *Adv Clin Exp Med*. 2018;27(6):827–832

Address for correspondence
Joanna Natorska
E-mail: j.natorska@szpitaljp2.krakow.pl

Funding sources
The study was supported by the grant from the National Centre of Science to UMO-2013/09/B/NZ5/00254 to AU.

Conflict of interest
None declared

Received on July 21, 2016
Reviewed on September 20, 2016
Accepted on October 6, 2017

Abstract

Background. Growing evidence suggests that activation of blood coagulation exerts protective functions during inflammation. However, it has been hypothesized that dysregulated immunothrombosis may lead to venous thromboembolism (VTE). Antinuclear antibodies (ANAs) are considered to promote the thrombotic tendency but there have been no reports on the association between ANAs and VTE.

Objectives. The objective of this study was to investigate if the presence of ANAs is associated with VTE.

Material and methods. We enrolled 283 consecutive patients, aged 18–66 years old, following a VTE episode, and 165 age-matched healthy controls. Patients with documented autoimmune diseases (n = 56, 19.79%), including antiphospholipid syndrome (n = 48, 16.9%), were excluded. Antinuclear antibodies were determined based on immunofluorescence. The specific immunofluorescence patterns observed at serum dilution equal to or greater than 1:100 were considered as positive ANAs.

Results. The final analysis included 227 patients (aged 41.07 ±11.4, 98 males, 129 females) following provoked (n = 111) or unprovoked (n = 116) VTE. Ninety-four (42.2%) patients had positive ANAs, including 32 (33.3%) with ANAs titer ≥1:320, whereas as few as 14 (8.4%) controls had positive ANAs ($p < 0.007$). ANA-positive patients were more commonly diagnosed with unprovoked (n = 55; 57.4%) than provoked VTE (n = 39; 40.6%) ($p = 0.03$). A similar observation was made for ANAs titer ≥1: 320 (26 patients with unprovoked vs 20 patients with provoked VTE, $p = 0.04$). The presence of ANAs in the patient group did not correlate with age, sex, time since the VTE event, type of anticoagulation and its quality, inflammatory markers and D-dimer.

Conclusions. The prevalence of positive ANAs was 5 times higher among VTE patients than in controls. Antinuclear antibodies occur commonly in VTE and might be involved in the pathogenesis of unprovoked VTE.

Key words: venous thromboembolism, deep vein thrombosis, antinuclear antibodies

DOI
10.17219/acem/78361

Introduction

Venous thromboembolism (VTE), encompassing deep vein thrombosis (DVT) and pulmonary embolism (PE), is a multifactorial disease.[1] Venous thromboembolism is considered to be "provoked" in the presence of a temporary or reversible risk factor (such as surgery, trauma, immobilization, pregnancy, oral contraceptive use or hormone replacement therapy) within the last 6 weeks to 3 months before diagnosis, and "unprovoked" in the absence thereof. The identification of potential risk factors plays a crucial role in the decision-making process about the duration of therapy. Patients with antiphospholipid syndrome, those with a deficiency of antithrombin, protein C or protein S, and patients homozygous for factor V Leiden or prothrombin G20210A (PTG20210A), may be candidates for indefinite anticoagulant treatment after a 1st unprovoked VTE.[2] Modern thrombophilia testing fails to identify any underlying prothrombotic tendency in a significant number of patients presenting with objectively confirmed VTE.[3] Overall, 25–50% of patients with the first-time VTE have an idiopathic condition, without a readily identifiable risk factor.[4]

Correlative studies have hinted at a relationship between DVT and immune responses mainly associated with DNA and neutrophils leading to a concept of immunothrombosis.[5] Growing evidence suggests that activation of blood coagulation exerts critical protective functions during inflammation. However, it has been hypothesized that dysregulated immunothrombosis may lead to VTE.

Antinuclear antibodies are considered to promote the thrombotic tendency directly by causing intimal damage due to their binding to the intimal cell wall and indirectly by causing a disorder of the intimal function due to their binding to intracellular structures of intimal cells such as the nucleus and cytoplasm.[6,7] Unlike antiphospholipid antibodies, which bind to the cell wall in a restricted manner, ANAs bind to various cell components and may contribute to the thrombotic tendency by diverse mechanisms. Moreover, ANAs are involved in vascular disorders such as Raynaud's phenomenon.[7]

To the best of our knowledge, there have been no reports on the association between ANAs and VTE. Thus, the aim of our study was to investigate the prevalence of ANAs in patients following VTE.

Material and methods

Patients

We recruited 283 consecutive patients following documented provoked or unprovoked VTE (aged 18–66 years) who were referred to the Center for Coagulation Disorders in the John Paul II Hospital (Kraków, Poland) for further laboratory work-up between June 2013 and September 2015. Minimum time from the acute VTE episode prior to recruitment was 3 months. All the patients were treated with low molecular weight heparins followed by oral anticoagulants. The exclusion criteria were: acute coronary syndrome or stroke within the preceding 6 months, known malignancy, signs of acute infection or acute VTE, long-term antithrombotic treatment for other indications, e.g., atrial fibrillation or prosthetic cardiac valve implantation, pregnancy or postpartum period, end-stage kidney disease, documented autoimmune diseases (n = 56, 19.79%), including antiphospholipid syndrome (APS) diagnosed in 48 patients (16.9%). Patients receiving anticoagulant therapy were eligible. The final analysis included 227 VTE patients. The Bioethics Committee of the Jagiellonian University approved the study. All the participants signed written informed consent.

The data on demographic characteristics, risk factors for VTE, comorbidities and medications was collected. The diagnosis of DVT of the lower or upper limb required a positive finding of color duplex sonography; an iliac/caval DVT was defined as abnormal duplex flow patterns typical of thrombosis or an intraluminal filling defect on contrast computed tomography or magnetic resonance venography. The diagnosis of PE was based on the presence of typical symptoms and positive results of high-resolution spiral computed tomography. Individuals with thrombosis at unusual sites were also diagnosed. Cerebral sinus venous thrombosis and hepatic/portal/splanchnic vein thrombosis was objectively documented using computed tomography angiography, magnetic resonance or magnetic resonance angiography.

Provoked VTE, i.e., associated with a known transient risk factor, was diagnosed in patients with VTE who experienced immobilization, surgery with the use of general anesthetic, major trauma, leg fracture or lower extremity plaster cast or hospitalization in the past month, intake of estrogen-containing oral contraceptives or hormone replacement therapy (HRT), as well as pregnancy or delivery within 3 months preceding the index event. Unprovoked (idiopathic) VTE episode was defined in patients who had no history of cancer, surgery, major trauma, plaster cast or hospitalization in the past month, pregnancy or delivery in the past 3 months.

A control population consisted of concurrent age-matched healthy 165 participants.

Laboratory tests

After an overnight fast, venous blood was drawn from the antecubital vein into citrated tubes (9:1 of 0.106 M sodium citrate) and was centrifuged at 2500 g at 20°C for 10 min and stored in aliquots at –80°C until analysis. Blood drawn into serum tubes was centrifuged at 2500 g at –20°C for 10 min and stored at –80°C. To determine blood cell count, lipid profile, glucose, creatinine and thyroid-stimulating hormone (TSH), routine laboratory assays were used. High-sensitivity C-reactive protein (CRP) was determined using immunoturbidimetry (Roche Diagnostics, Mannheim, Germany). Fibrinogen was measured

by the von Clauss method (Instrumentation Laboratory, Bedford, USA). Plasma D-dimer was measured with the Innovance D-dimer assay (Siemens, Marburg, Germany).

Antibodies directed at various cellular compartments including nuclear constituents, components of the nuclear envelope, mitotic spindle apparatus, cytosol, cytoplasmic organelles and cell membranes (ANAs) were tested by immunofluorescence (IIF) in IgG isotype (HEp2 cells and the conjugate; Euroimmun, Lübeck, Germany). Patients' sera were diluted with the cut-off 1:100 in PBS with Tween 20 (Sigma-Aldrich, St. Louis, USA), according to the international recommendations for the assessment of autoantibodies to cellular antigens.[8] Visual determination of the staining pattern was assessed using the Nikon Eclipse E400 fluorescence microscope (Nikon Instruments Europe B.V., Amsterdam, Netherlands). The specific immunofluorescence patterns observed at serum dilution equal to or greater than 1:100 were considered as positive ANAs. An additional analysis for subjects with ANAs titer ≥1:320 was performed to confirm and strengthen the observations made for the whole ANA-positive patients' group.

The anti-DFS70 pattern was characterized by dense fine speckles distributed in the nucleus, confirmed in a reference laboratory of Euroimmun in Lübeck and subjected to semiquantitative enzyme-linked immunosorbent assay (ELISA) analysis (Euroimmun, Lübeck, Germany), according the manufacturer's instructions.

All patients were screened for thrombophilia, including the factor V Leiden mutation, prothrombin G20210A, as well as deficiency of antithrombin, protein C or protein S. Inherited thrombophilia was defined as the presence of either of the 2 mutations or a deficiency of 1 of the 3 coagulation inhibitors. Genotypes of FV Leiden (*rs6025*) and prothrombin G20210A (*rs1799963*) polymorphisms were ascertained by the allelic discrimination test using the TaqMan Genotyping assay on the ABI PRISM 7900HT Fast Real-Time PCR System (Life Technologies Co., Carlsbad, USA). Antithrombin anti-FX activity was measured using a chromogenic method in the presence of heparin (HemosIL™ TH, Instrumentation Laboratory SpA, Milan, Italy). Plasma PC was quantified using the HemosIL™ Protein C chromogenic assay (Instrumentation Laboratory SpA, Milan, Italy). Free PS was quantified using the HemosIL™ Free Protein S latex ligand immunoassay (Instrumentation Laboratory SpA, Milan, Italy).

To exclude APS based on the modified APS classification criteria by Miyakis et al., lupus anticoagulant (LA) was estimated using a clot-based assay, according to the recommendations published in 2009.[9,10] Anticardiolipin and anti-β_2GP-I antibodies were determined by immunoenzymatic assays (INOVA Diagnostics, San Diego, USA). Reference ranges for IgG were up to 15 IgG phospholipid unit (GPL) and 8 standard IgG β-2 glycoprotein unit (SGU), respectively, and for IgM up to 17 IgM phospholipid unit (MPL) and 10 standard IgM β-2 glycoprotein unit (SMU), respectively. All positive cases were reevaluated after 12–16 weeks.[11]

Serum protein profile was evaluated using serum protein electrophoresis (SPE) with the fully automated instrument Interlab G26 (Interlab, Rome, Italy) on agarose gel plates at pH 8.9. The final protein concentration ranged from 60 g/L to 80 g/L. Densitometry of the pattern was determined for the relative quantification of protein zones.

Statistical analysis

Continuous variables were presented as median and interquartile range. Categorical variables were presented as the number and percentages. The Shapiro-Wilk test was used to test the normality of continuous variables. To examine the differences between the independent groups, the Kruskal-Wallis test was used. The χ^2 or Pearson's exact tests were used for categorical variables. Statistical analysis was performed with STATISTICA v. 12.0 (StatSoft, Tulsa, USA).

Results

The demographic and laboratory data of the control and VTE patients are summarized in Table 1. Of the 165 control subjects, as few as 14 (8.4%) individuals had positive ANAs, of whom 8 (4.8%) had ANAs titer = 1:100 and 6 (3.6%) had ANAs titer = 1:320.

Of the 227 VTE patients studied, 94 (42.2%) individuals had positive ANAs, including 62 patients (64.6%) with ANAs titer <1:320 and 32 patients (33.3%) with ANAs titer ≥1:320.

The prevalence of positive ANAs was 5 times higher among VTE patients compared with the controls (42.2% vs 8.4%, p = 0.007). Of importance, patients with unprovoked VTE had positive ANAs more commonly (n = 55; 57.4%) than those with provoked VTE (n = 39; 40.6%) (p = 0.03). A similar observation was made regarding the ANAs titer ≥1:320 (26 (27.1%) patients with unprovoked vs 20 (20.8%) patients with provoked VTE, p = 0.04).

The presence of ANAs was correlated with albumin (r = 0.4, p = 0.014) and gamma globulin levels (r = 0.5, p = 0.019). The positive ANAs did not correlate with any other examined demographic or clinical variables like age, gender, body mass index (BMI), smoking, C-reactive protein (CRP), glucose, fibrinogen, D-dimer, time since last VTE event, as well as type of anticoagulation and its quality.

Anti-DFS70 antibodies were screened in 149 (90.3%) control patients and 222 (97.8%) VTE patients. There was no difference in the prevalence of anti-DFS70 antibodies in the control and VTE patients (n = 6 (4.03%) vs n = 9 (4.05%), respectively, p = 0.8). The DFS70 positive patients from the 2 groups did not differ in any of the examined demographic or clinical variables (data not shown).

The ANA-negative patients did not differ from ANA-positive patients in any of examined parameters such as lipid profile, glucose, CRP, fibrinogen, D-dimer, TSH or time since the VTE event.

Table 1. Characteristics of control and venous thromboembolism (VTE) patients

Variables	Controls n = 165	VTE total n = 227	VTE ANA (–) (n = 133) (58.6%)	VTE ANA <1:320 (n = 62) (27.3%)	VTE ANA ≥1:320 (n = 32) (14.1%)
	(A)	(B)	(C)	(D)	(E)
Age [years]	38 (20–60)	40.5 (18–66)	39.5 (18–64)	43 (20–64)	43 (19–66)
Male [n] (%)	77 (46)	101 (44.5)	62 (41.89)	26 (41.94)	13 (40.63)
Body mass index [kg/m^2]	23.68 (17.1–34.78)	27.21 (17.01–49.72)*	27.65 (17.58–47.09)	28.23 (17.01–49.72)	25.59 (18.59–41.96)
Laboratory parameters at enrollment					
White blood cells [10^3/μL]	5.86 (3.15–9.27)	6.18 (2.83–18.89)*	6.14 (2.83–18.89)	6.04 (3.86–14.97)	6.55 (3.24–11.93)
Hemoglobin [g/dL]	14.2 (9.5–16.7)	14.1 (9.2–17.2)	14.05 (9.2–17.2)	14 (10–17.5)	14.1 (9.8–16)
Platelets [10^3/μL]	240 (106–396)	239.5 (77–539)	242.5 (77–501)	238.5 (150–539)	233 (169–352)
Creatinine [μmol/L]	74 (51–116)	70 (31–139)	71 (47–139)	70 (47–110)	69 (31–101)
Glucose [mmol/L]	4.9 (3.3–6.2)	5.1 (2.8–8.2)	5.2 (2.8–8.2)	5.3 (4.3–8.2)	5.15 (4.5–7.2)
Cholesterol [mmol/L]	4.96 (3.37–7.18)	5.14 (2.96–8.83)	5.19 (2.96–8.35)	5.17 (3.37–8.66)	4.84 (3.78–8.83)
Triglycerides [mmol/L]	1.13 (0.44–5.06)	1.17 (0.35–7.02)	1.23 (0.35–7.02)	1.26 (0.56–4.33)	1.24 (0.45–4.85)
LDL-cholesterol [mmol/L]	3.08 (1.11–5.4)	3.29 (1.36–7.14)*	3.37 (1.36–6.33)	3.19 (1.62–7.14)	2.92 (1.76–6.51)
HDL-cholesterol [mmol/L]	1.67 (0.8–2.34)	1.5 (0.56–3.03)*	1.55 (0.63–3.03)	1.45 (0.9–2.97)	1.49 (0.97–2.87)
Thyroid-stimulating hormone [mU/L]	1.74 (0.31–4.02)	1.57 (0.01–25.19)*	1.57 (0.24–5.05)	1.56 (0.01–25.19)	1.57 (0.42–3.51)
C-reactive protein [mg/L]	1.23 (0.15–5.93)	1.45 (0.15–20.6)	1.39 (0.15–20.6)	2 (0.35–15.1)	1.12 (0.15–17.51)
Fibrinogen [g/L]	2.46 (1.69–4.96)	3.11 (1.84–6.43)*	3.07 (1.84–6.43)	3.16 (2.1–5.04)	3.15 (1.96–5.25)**
D-dimer [ng/mL]	199 (171–870)	211 (117–7778)	199 (170–7778)	222.5 (117–1897)	288.5 (170–1327)
DVT alone, n (%)	-	79 (34.8)	47 (40.6)	22 (35.48)	10 (31.25)
PE [n] (%)	-	62 (27.3)	35 (26.3)	21 (33.87)	6 (18.75)
DVT+PE, n (%)	-	70 (30.8)	39 (29.3)	17 (27.43)	14 (43.75)
Other thrombosis***, n (%)	-	16 (7.1)	12 (9)	2 (3.23)	2 (6.25)
Inherited thrombophilia (FVL, G20210A, antithrombin, protein C or protein S deficiency), n (%)	-	104 (45.8)	39 (29.3)	47 (75.8)	18 (56.25)**
Vitamin K antagonists, n (%)	-	81 (35.7)	54 (40.6)	22 (35.5)	5 (15.63)**
Non-vitamin K antagonist oral anticoagulants, n (%)	-	97 (42.7)	50 (36.7)	29 (46.78)	18 (56.25)
Acetylsalicylic acid, n (%)	-	16 (7.1)	10 (7.52)	2 (3.23)	4 (5.71)
Statins, n (%)	-	28 (12.3)	10 (7.35)	8 (12.9)	10 (31.25)**
Positive family history, n (%)	-	78 (34.36)	44 (32.35)	21 (33.87)	13 (40.63)
Arterial hypertension, n (%)	-	67 (29.5)	36 (26.47)	22 (35.48)	9 (28.13)
Diabetes mellitus, n (%)	-	12 (5.29)	5 (3.38)	4 (6.45)	3 (9.38)
Hypercholesterolaemia, n (%)	-	149 (65.64)	91 (66.9)	39 (62.9)	19 (59.38)

Continuous variables are presented as median and interquartile range (min–max). Categorical variables are presented as the number and percentages. ANA - antinuclear antibodies; HDL – high-density lipoprotein; LDL – low-density lipoprotein; VTE – venous thromboembolism; DVT – deep vein thrombosis; PE – pulmonary embolism; * $p < 0.05$ comparison for groups A and B; ** $p < 0.05$ comparison for groups C, D and E; *** cerebral venous sinus thrombosis, upper limb thrombosis, portal or hepatic vein thrombosis.

Discussion

To our knowledge, this study is the first to show that the presence of ANA among patients with VTE is higher than in control subjects. Based on this finding we hypothesize that ANA may play a potential role in the pathogenesis of VTE and might have a predictive value when it persists. Our rationale is that the individuals with autoimmune diseases are at a higher risk of VTE. However, this risk was mainly attributed to APS and/or exacerbation of autoimmune diseases, with the maximum rates within the first years since diagnosis, in particular in systemic lupus erythematosus (SLE) and anti-neutrophil cytoplasmic antibodies.[12,13] Surprisingly, little is known about ANA in VTE patients without diagnosed autoimmune disease.

The link of APS to VTE is well established.[14] Antiphospholipid syndrome is a complex autoimmune thrombotic disorder with defined clinical phenotypes, and experimental evidence suggests that antiphospholipid antibodies (aPLAs) play a causative role in vascular thrombosis and obstetric complications; however, the mechanisms are not well understood.[15]

Numerous mechanisms of thrombosis in the APS have been proposed.[16] At least some of the variety of mechanisms may be explained by the spectrum of autoantibody. Mechanisms of autoantibody-mediated thrombosis may be divided into 2 general types: (1) autoantibodies interfere with hemostatic components occurring on membrane surfaces, for example the ability of certain autoantibodies to prolong in-vitro coagulation assays, and (2) autoantibody engagement of antigens on cell surfaces leads to transduction of a signal and altered cell activity.[17,18]

Moreover, several studies have reported that autoantibodies are associated with increased procoagulant activity on circulating blood monocytes. Tissue factor (TF), a major initiator of normal and pathological blood coagulation, can be expressed in larger amounts on monocytes and endothelial cells by a variety of stimuli, including circulating antibodies.[19] Moreover, monocyte-derived TF has been shown to be a key player in the initiation and propagation of VTE.[5] It might be speculated that the presence of ANA may enhance TF expression and contribute to a low grade prothrombotic state, which increases the risk of thrombosis and/or its recurrence especially when additional thrombotic risk factors occur, e.g. immobilization, obesity or HRT.

A separate issue that needs to be addressed is the potential involvement of autoantibodies in immunothrombosis. It has been demonstrated that autoantibodies against beta2-glycoprotein I (β_2GPI) promote thrombin generation in vitro.[19] This potentially sets up a vicious prothrombotic cycle and predisposes to VTE. It is, therefore, likely that other autoantibodies in a similar manner might lead to the activation of thrombotic mechanisms by endothelial cell damage and dysfunction. Since it is known that as few as 2–5% patients with elevated aPLAs levels do not develop thromboembolic events, it is possible that positive ANAs could also have some predictive value.[20]

ANA detected in our group of patients were unspecific; we did not find any disease-specific antibodies. The subset of autoantibodies most commonly found in "apparently healthy" individuals and several inflammatory non-rheumatic diseases are anti-DFS70 antibodies, directed against epithelium-derived growth factor *p75*, which are usually absent in defined autoimmune diseases.[21] Recently, positive anti-DFS70 antibodies have been shown to be associated with idiopathic VTE, arterial thrombosis and/or obstetric complications.[22] In our study, however, we did not observe any association of anti-DFS70 antibodies and VTE, which might be explained by the analysis of patients below 65 years of age free of known autoimmune disorders. A potential role of anti-DFS70 antibodies in VTE requires further investigation.

Furthermore, it remains to be elucidated whether ANAs in VTE are primary or rather result from the disease itself, which is important for elucidating their role in thrombosis. Therefore, it might be useful to monitor the persistence of ANAs over a longer period of time.

It also is important to note that it is likely that by defining the potential relationship between ANAs and VTE, we might develop new diagnostic tools to identify patients at risk of VTE, especially unprovoked episodes.

In conclusion, our study indicates that positive ANAs, though at low titers, are common in young and middle-aged patients following VTE, regardless of the time since the event, its type and anticoagulant therapy. More commonly, ANAs can be detected among patients after unprovoked VTE, which might suggest that autoimmune reactions could be involved in the pathogenesis of VTE. It would be also of interest to assess the role of ANAs as a potential risk factor of the VTE recurrence during a long-term follow-up in a large cohort study. Moreover, the predictive role of VTE in the development of symptomatic autoimmune disease in the future requires a further follow-up study.

References

1. Rosendaal FR. Venous thrombosis: A multicausal disease. *Lancet*. 1999;353:1167–1173.
2. Konstantinides SV, Torbicki A, Agnelli G, et al.; Task Force for the Diagnosis and Management of Acute Pulmonary Embolism of the European Society of Cardiology (ESC). 2014 ESC guidelines on the diagnosis and management of acute pulmonary embolism. *Eur Heart J*. 2014;43:3033–3069.
3. Jenkins PV, Rawley O, Smith OP, O'Donnell JS. Elevated factor VIII levels and risk of venous thrombosis. *Br J Haematol*. 2012;157:653–663.
4. de Groot PG, Derksen B, Lisman T, Meijers JC, Rosendaal FR. Lupus anticoagulants and the risk of a first episode of deep venous thrombosis. *J Thromb Haemost*. 2005;3:1993–1997.
5. von Brühl ML, Stark K, Steinhart A, et al. Monocytes, neutrophils and platelets cooperate to initiate and propagate venous thrombosis in mice in vivo. *J Exp Med*. 2012;209:819–835.
6. Yamazaki M. Antiphospholipid antibody syndrome. In: Ichinose A, ed. *Sciences of Thrombi, Hemostasis, and Angiology*. Tokyo, Japan: Chugai-Igakusha; 2005:410–421.

7. Kobayashi Y, Numano F. Angiitis. In: Morishita R, ed. *Vascular Medicine*. Tokyo, Japan: Medical Review; 2001:565–576.
8. Agmon-Levin N, Damoiseaux J, Kallenberg C, et al. International recommendations for the assessment of autoantibodies to cellular antigens referred to as anti-nuclear antibodies. *Ann Rheum Dis*. 2014;73:17–23.
9. Miyakis S, Lockshin MD, Atsumi T, et al. International consensus statement on an update of the classification criteria for definite antiphospholipid syndrome (APS). *J Thromb Haemost*. 2006;4:295–306.
10. Pengo V, Tripodi A, Reber G, et al.; Subcommittee on Lupus Anticoagulant/Antiphospholipid Antibody of the Scientific and Standardisation Committee of the International Society on Thrombosis and Haemostasis. Update of the guidelines for lupus anticoagulant detection. *J Thromb Haemost*. 2009;7:1737–1740.
11. Tripodi A, de Groot PE, Pengo V. Antiphospholipid syndrome: Laboratory detection, mechanisms of action and treatment. *J Intern Med*. 2011;270:110–122.
12. Aviña-Zubieta JA, Vostretsova K, De Vera MA, Sayre EC, Choi HK. The risk of pulmonary embolism and deep venous thrombosis in systemic lupuserythematosus: A general population-based study. *Semin Arthritis Rheum*. 2015;45:195–201.
13. Merkel PA, Lo GH, Holbrook JT, et al.; Wegener's Granulomatosis Etanercept Trial Research Group. High incidence of venous thrombotic events among patients with Wegener granulomatosis: The Wegener's Clinical Occurrence of Thrombosis (WeCLOT) study. *Ann Intern Med*. 2005;142:620–626.
14. Mustonen P, Lehtonen KV, Javela K, Puurunen M. Persistent antiphospholipid antibody (aPL) in asymptomatic carriers as a risk factor for future thrombotic events: A nationwide prospective study. *Lupus*. 2014;23:1468–1476.
15. Pierangeli SS, Chen PP, Raschi E, et al. Antiphospholipid antibodies and the antiphospholipid syndrome: Pathogenic mechanisms. *Semin Thromb Hemost*. 2008;34:236–250.
16. Roubey RA. Immunology of the antiphospholipid antibody syndrome. *Arthritis Rheum*. 1996;391:1444–1454.
17. Vlachoyiannopoulos PG, Routsias JG. A novel mechanism of thrombosis in antiphospholipid antibody syndrome. *J Autoimmun*. 2010;35:248–255.
18. Roubey RA, Hoffman M. From antiphospholipid syndrome to antibody-mediated thrombosis. *Lancet*. 1997;350:1491–1493.
19. Yalavarthi S, Gould TJ, Rao AN, et al. Release of neutrophil extracellular traps by neutrophils stimulated with antiphospholipid antibodies: A newly identified mechanism of thrombosis in the antiphospholipid syndrome. *Arthritis Rheumatol*. 2015;67:2990–3003.
20. Ortel TL. Thrombosis and the antiphospholipid syndrome. *Hematology Am Soc Hematol Educ Program*. 2005;1:462–468.
21. Basu A, Sanchez TW, Casiano CA. DFS70/LEDGFp75: An enigmatic autoantigen at the interface between autoimmunity, AIDS and cancer. *Front Immunol*. 2015;6:116. doi: 10.3389/fimmu.2015.00116
22. Marlet J, Ankri A, Charuel JL, et al. Thrombophilia associated with anti-DFS70 autoantibodies. *PLoS One*. 2015;10(9):e0138671. doi: 10.1371/journal.pone.0138671

Expression profiles of selected genes in tumors and matched surgical margins in oral cavity cancer: Do we have to pay attention to the molecular analysis of the surgical margins?

Joanna K. Strzelczyk[1,A–F], Łukasz Krakowczyk[2,B,E,F], Karolina Gołąbek[1,C–D,F], Aleksander J. Owczarek[3,C,F]

[1] Department of Medical and Molecular Biology, School of Medicine with the Division of Dentistry in Zabrze, Medical University of Silesia in Katowice, Poland
[2] Clinic of Oncological and Reconstructive Surgery, Maria Skłodowska-Curie Memorial Cancer Center and Institute of Oncology, Gliwice, Poland
[3] Department of Statistics, School of Pharmacy with the Division of Laboratory Medicine in Sosnowiec, Medical University of Silesia in Katowice, Poland

A – research concept and design; B – collection and/or assembly of data; C – data analysis and interpretation;
D – writing the article; E – critical revision of the article; F – final approval of the article

Advances in Clinical and Experimental Medicine, ISSN 1899-5276 (print), ISSN 2451-2680 (online) *Adv Clin Exp Med*. 2018;27(6):833–840

Address for correspondence
Joanna Strzelczyk
E-mail: jstrzelczyk@sum.edu.pl

Funding sources
None declared

Conflict of interest
None declared

Acknowledgements
We would like to thank professor Andrzej Wiczkowski for advice on the design of this study and Ms. Anna Plachetka for technical assistance.

Received on April 4, 2017
Reviewed on July 23, 2017
Accepted on November 7, 2017

Abstract

Background. Head and neck squamous cell carcinomas (HNSCCs) are associated with an interplay between genetics and the environment; they account for 3% of all diagnosed malignant tumors in men and 2% of those in women.

Objectives. The aim of the study was to analyze the significance of *TIMP3*, *SFRP1*, *SFRP2*, *CDH1*, *RASSF1*, *RORA*, and *DAPK1* gene expression in head and neck squamous cell carcinoma tumors, and in matching surgical margin samples. We also analyzed the association between clinical parameters and the expression of the selected genes.

Material and methods. Following surgical resection, 56 primary HNSCC tumors and matching surgical margin samples were collected from patients at the Clinic of Oncological and Reconstructive Surgery of Maria Skłodowska-Curie Memorial Cancer Center and the Institute of Oncology in Gliwice, Poland. The gene expression levels were analyzed by quantitative reverse transcription (qRT)-PCR.

Results. *SFRP1* gene expression was statistically significantly lower in the tumor samples than in the surgical margins (0.30 ±0.36 vs 0.62 ±0.36; $p < 0.01$). No correlation was found between gene expression and clinical parameters, except *DAPK1*, where low expression correlated with alcohol abuse (0.85 ±1.19 vs 1.97 ±3.22; $p = 0.074$). Moreover, patients with G3 grade tumors, i.e., poorly differentiated tumors, had significantly higher values of *DAPK1* gene expression than the G1 (well-differentiated tumors) and G2 (moderately differentiated) groups.

Conclusions. There are many different reasons and concepts for altered gene expression in tumors and surgical margin tissue. Tumor heterogeneity and its microenvironment are undoubtedly linked to the biology of HNSCC. In order to understand specific tumor behavior and the microenvironment, further studies are needed. To find markers connected with cancer development and to provide insight into the earliest stages of cancer development, attention should also be focused on molecular analysis of the surgical margins.

Key words: gene expression, surgical margin, oral cavity, head and neck cancer

DOI
10.17219/acem/79846

Introduction

Head and neck squamous cell carcinomas (HNSCCs) account for 3% of all diagnosed malignant tumors in men and 2% of those diagnosed in women.[1] Head and neck cancer is associated with an interplay between genetics and environment. It is associated with abnormalities in proliferation, apoptosis, differentiation, cell cycle regulation, DNA repair, signal transduction, and angiogenesis.[2] The instability of the genome, chromosomal rearrangement and loss of DNA fragments are associated with carcinogenesis of HNSCC.[3] Califano et al. proposed a model for the dynamics of chromosomal damage in the course of cancers of the head and neck.[4] Through progression, an increased amount of chromosomal loss takes places. The conversion from normal mucosa to invasive cancer is linked with an accumulation of genetic changes in tumor suppressor genes and proto-oncogenes. Furthermore, adjacent areas share similar genetic alterations. For HNSCC, the list of environmental risk factors includes alcohol consumption, tobacco use, poor oral hygiene, chronic exposure to certain industrial agents, and infection with specific subtypes of human papillomavirus (HPV).[1] Slaughter et al. first proposed the idea of "field cancerization" as the "preconditioning of an area of the epithelium to cancer growth by a carcinogenic agent", which means that an area with genetically altered cells could play a crucial role in the carcinogenic process based on many molecular findings.[5,6] The initiation of field cancerization is associated with various types of molecular damage, e.g., altered gene expression. The residual field in the region adjacent to the tumor can cause local recurrences and 2nd primary tumors after surgical intervention for the primary carcinoma. Actually, there are many theories interpreting oral field cancerization.[7] The "cancer field effect" has been explained by the presence of cells with genetic alterations; however, involvement of epigenetic alterations in field cancerization has also been shown. Epigenetic changes are defined as alterations in gene expression that are not coded in the DNA sequence. Among epigenetic mechanisms, such as DNA methylation at CpG sites or histone modifications, aberrant DNA methylation has been frequently analyzed in various types of cancer. Hypomethylation leads to the activation of cancer-associated genes, whereas hypermethylation of promoter CpG islands is associated with the silencing of various tumor-suppressor genes. Several environmental factors could induce epigenetic modifications.[8] In this study, we have analyzed the gene expression of *TIMP3, SFRP1, SFRP2, CDH1, RASSF1, RORA,* and *DAPK1* in primary HNSCC tumors and matching surgical margin samples. We selected genes involved in degradation of the extracellular matrix, cellular proliferation, migration, and apoptosis. Disruption of these processes can lead to carcinogenesis. The characteristics of these genes are shown in Table 1.[9–15]

The main aim of the study was to provide more information concerning the molecular mechanism of oral malignancy based on gene expression, which could provide valuable information for a better understanding of the oral carcinogenesis process.

Material and methods

Patients and tissue samples

We collected 56 primary HNSCC tumors and 56 matching surgical margin samples following surgical resection from patients at the Clinic of Oncological and Reconstructive Surgery of Maria Skłodowska-Curie Memorial Cancer Center and the Institute

Table 1. The characteristics of selected genes

Symbol	Name	Location	Function	Reference
TIMP3	tissue inhibitor of metalloproteinases 3	22q12.3	The proteins encoded by this gene family are inhibitors of the matrix metalloproteinases, a group of peptidases involved in the degradation of the extracellular matrix (ECM).	9
SFRP1	secreted frizzled-related protein 1	8p11.21	This gene encodes secreted frizzled-related protein 1, a negative modulator of the Wnt signaling pathway.	10, 11
SFRP2	secreted frizzled-related protein 2	4q31	This gene encodes secreted frizzled-related protein 2 (SFRP2), a negative modulator of the Wnt signaling pathway.	10, 11
CDH1	cadherin 1 also known as E-cadherin	16q22.1	This gene encodes a calcium-dependent protein. E-cadherin plays an important role in the maintenance of cell differentiation and the normal architecture of epithelial tissues.	12
RASSF1	Ras association (RalGDS/AF-6) domain family member 1	3p21.3	This gene encodes RASSF1A. It inhibits cell cycle progression at the G1/S transition by preventing the accumulation of cyclin D1.	13
RORA	RAR-related orphan receptor A	15q22.2	This gene encodes RORA. The protein encoded by this gene is a member of the NR1 subfamily of nuclear hormone receptors. These receptors are critical in the regulation of a number of physiological processes. RORA has also been suggested to be involved in lipid metabolism and to possess immunomodulatory activity.	14
DAPK1	death-associated protein kinase 1	9q21.33	This gene encodes calmodulin-dependent serine-threonine kinase. *DAPK1* is involved in programmed cell death.	15

of Oncology in Gliwice, Poland. After resection, these specimens were submerged in the tissue storage and ribonucleic acid (RNA) stabilization solution, RNA*later*® (Sigma-Aldrich, Saint Louis, USA), then frozen at –80°C until RNA extraction. All the tumors collected during surgery were oral cavity cancers (comprising the maxilla, mandible, floor of the mouth, tongue, and cheek, with the highest number being mandible and tongue cases). Representative tumor samples were histologically confirmed by pathologists from Maria Skłodowska-Curie Memorial Cancer Center and the Institute of Oncology in Gliwice, and were classified as primary HNSCC tumors. Oral mucosal biopsy specimens were taken from the surgical margin at least 10 mm from the tumor border and were histologically confirmed as being free of cancer. Intraoperative histopathological examinations were performed whenever positive margins were suspected.

The Institutional Review Board on Medical Ethics of Maria Skłodowska-Curie Memorial Cancer Center and the Institute of Oncology in Gliwice approved the study protocol (nos. KB/493-15/08 and KB/430-47/13). An informed consent form was obtained from all patients. None of the patients included in this study had preoperative radio- or chemotherapy. The average age of the patients was 56.05 years (range: 29–77 years, median: 58.5 years). There were 37 men (66%) and 19 women (34%); 80% of the patients (45/56) were smokers; 73% of them (41/56) reported alcohol consumption; 64% (36/56) were both smokers and alcohol consumers. Tumor staging was based on the pathology findings and then revised according to the 2007 version of the American Joint Committee on Cancer (AJCC) staging system for analysis.[16,17] The clinical parameters of the patients are shown in Table 2.

Table 2. Clinical features of patients

Clinical parameters	Patients, n (%)
Histological grading	
G1 (well-differentiated)	5 (8.9)
G2 (moderately differentiated)	44 (78.6)
G3 (poorly differentiated)	7 (12.5)
T classification	
T1	3 (5.4)
T2	6 (10.7)
T3	13 (23.2)
T4	34 (60.7)
Nodal status	
N0	21 (37.5)
N1	22 (39.3)
N2	13 (23.2)

Homogenization and ribonucleic acid extraction

The tissue samples were fixed in RNA*later*® Stabilisator Reagent (Sigma-Aldrich, Saint Louis, USA) and frozen to –80°C, then thawed slowly at room temperature and homogenized with FastPrep®-24 homogenizer (MP Biomedicals, Santa Ana, USA) using tubes with ceramic beads for tissue homogenization, Lysing Matrix D (MP Biomedicals, Santa Ana, USA). The RNA was isolated using an RNeasy® Mini Kit (Qiagen, Hilden, Germany). In addition to the standard procedure, DNase I digestion was performed on the extracted RNA (RNase Free DNase Set, Qiagen, Hilden, Germany) to remove the residual genomic DNA.

The RNA was quantified by measuring the UV absorbance at 260/280 nm (NanoDrop™ ND, 1000 Spectrophotometer, Thermo Fisher Scientific, Waltham, USA) and the integrity was assessed by electrophoresis on 1.2% agarose gel stained with ethidium bromide (Serva, Heidelberg, Germany). Additionally, the RNA integrity number (RIN) was derived with an Agilent Bioanalyzer 2100 (Agilent Technologies, Santa Clara, USA) using an Agilent RNA 6000 Nano Kit (Agilent Technologies, Santa Clara, USA); this helped to ensure RNA quality.

Complementary DNA (cDNA) synthesis

The total RNA from each tumor and surgical margin sample was reverse-transcribed into cDNA using a High Capacity cDNA Reverse Transcription Kit with RNase Inhibitor (Applied Biosystems, Foster City, USA). The Total RNA (30 ng) was reverse-transcribed into cDNA. The reaction was performed with a volume of 20 µL according to the manufacturer's instructions and using Mastercycler® Personal (Eppendorf, Hamburg, Germany). To avoid multiple thawing, cDNA samples were divided into a number of portions, which were sufficient for all subsequent quantitative polymerase chain reactions (Q-PCR); these portions were frozen at –80°C.

Quantitative polymerase chain reaction

The gene expression analysis was performed by quantitative reverse transcription (qRT)-PCR using specific TaqMan® Gene Expression Assays (Applied Biosystems, Foster City, USA). Q-PCR was performed for 7 genes: *TIMP3* (Hs00165949_m1), *SFRP1* (Hs00610060_m1), *SFRP2* (Hs00293258_m1), *CDH1* (Hs01023894_m1), *RASSF1* (Hs00200394_m1), *RORA* (Hs00536545_m1), and *DAPK1* (Hs00234489_m1).

The Q-PCR for all genes was performed in a volume of 20 µL using 1 µL of cDNA, 10 µL of TaqMan® Gene Expression Master Mix (Applied Biosystems, Foster City, USA), 1 µL of primer and probe mix (TaqMan® Gene Expression Assays), and 8 µL of H_2O (Qiagen, Hilden, Germany). All assays were carried out in 96-well plates (Applied Biosystems, Foster City, USA) on a 7300 Real-Time PCR System and were analyzed by SDS v. 1.4 software (Applied Biosystems, Foster City, USA). The glyceraldehyde-3-phosphate dehydrogenase gene (*GAPDH*, Hs99999905_m1) was used as an internal control. The expression levels of all these genes were normalized to those of *GAPDH*. In all amplification reactions, a negative control was also included: water free

of DNase, RNase, and protease (5Prime, Hilden, Germany) was used in place of cDNA. Thermal cycling for all analyzed genes and *GAPDH* was 95°C for 10 min, followed by 40 cycles at 95°C for 15 s and at 60°C for 1 min. The comparative threshold cycle (Ct) method $2^{-\Delta\Delta Ct}$ was used to determine the relative gene expression levels (relative quantification – RQ) for each of the 7 target genes. Five surgical margin samples were used as a calibrator. Relative mRNA expression was determined from the tumor and surgical margin samples using mRNA expression from the calibrator.

Statistical analysis

Statistical analysis was performed using STATISTICA v. 10.0 PL (QUEST, Tulsa, USA). Statistical significance was set at a p-value of less than 0.05. All tests were two-tailed. Imputations were not performed for missing data. Nominal and ordinal data were expressed as percentages, while interval data were expressed as means ±standard deviation. The distribution of variables was evaluated by the Shapiro-Wilk test and the homogeneity of variances was assessed by the Levene test. For comparison of data between 2 groups, the Student's t-test was used for independent data. For comparison between different histological grades, one-way analysis of variance (ANOVA) was used with an LSD post-hoc test.

Results

When gene expression levels were compared between the tumor samples and the margin samples, a statistically significantly lower gene expression of *SFRP1* was found in the tumor samples. The RQ values of the selected genes are reported in Table 3.

Table 3. Relative quantification (RQ) values in tumor vs surgical margin in patients with HNSCC

Gene	Tumor mean RQ ±SD	Margin mean RQ ±SD	p-value
TIMP3	0.62 ±0.80	0.97 ±0.80	0.113
SFRP1	0.30 ±0.36	0.62 ±0.36	<0.01
SFRP2	0.60 ±0.66	0.54 ±0.66	0.609
CDH1	0.70 ±0.45	0.68 ±0.45	0.846
RASSF1	0.71 ±0.49	0.64 ±0.49	0.465
RORA	0.46 ±0.66	0.54 ±0.66	0.423
DAPK1	1.07 ±1.44	1.24 ±1.45	0.654

SD – standard deviation.

We also analyzed the correlation of the clinical parameters with the expression levels of selected genes. No association was found between the gene expression levels and clinical parameters, except *DAPK1*, in which a low gene expression level statistically correlated with alcohol abuse (Table 4). Moreover, the one-way ANOVA showed a significant influence of the histological stage. The LSD post-hoc test showed that the patients with high-grade G3 tumors – i.e., poorly differentiated – had a significantly higher gene expression level of *DAPK1* than the patients with low-grade G1 (well-differentiated) tumors ($p < 0.05$) or G2 (moderately differentiated) tumors ($p < 0.01$). These results are shown in Fig. 1.

Table 4. Relative quantification (RQ) values of *DAPK1* in the group of patients with HNSCC with/without alcohol abuse

Alcohol	*DAPK1* (mean RQ ±SD)	p-value
Alcohol +	0.85 ±1.19	0.074
Alcohol –	1.97 ±3.22	

SD – standard deviation.

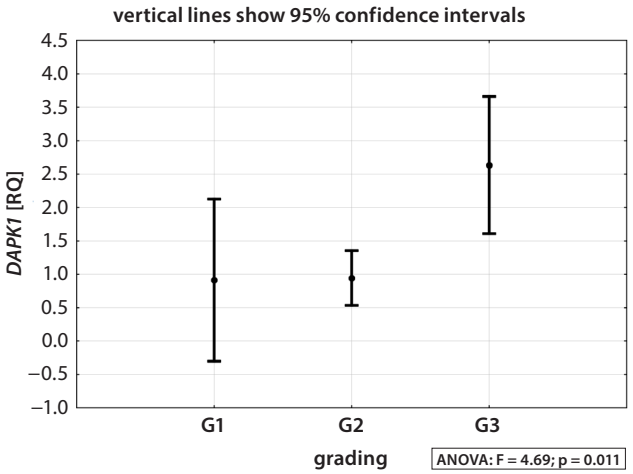

Fig. 1. Relative quantification (RQ) values of *DAPK1* in the group of patients with HNSCC according to G1, G2 and G3 grading stage

Discussion

In the literature, the expression profiles of many genes have been reported in different types of human cancer,[18–21] including HNSCC.[12,22–27] The majority of the research has compared tumor tissue from patients with normal tissue from healthy individuals or normal human cells obtained commercially.[12,18,20–22,28,29] Simultaneous analysis of gene expression levels in the tumor and surgical margins has rarely been performed.[23,26,30] Cancer development is the result of the accumulation of genetic and epigenetic alterations. Because changes in certain genes occur in the very early stages of tumorigenesis, the detection of preneoplastic alterations in the surgical margin could facilitate the detection of cancer. A molecular approach to the matching margin can contribute to cancer prevention and control; therefore, we studied the tumors and matched surgical margins from the patients. Moreover, in our study, the expression levels of the *TIMP3, SFRP1, SFRP2, CDH1, RASSF1*, and *RORA* genes did not

correlate with any of the clinical-pathological parameters, whereas *DAPK1* correlated with both the histological grade of the tumor and alcohol consumption. In addition, in some findings there was a significant correlation between clinical and pathological parameters and gene expression, but in others there was no significant association.[22,25–28,31–33]

TIMP3

The expression of *TIMPs* in oral squamous cell carcinoma (OSCC) shows a trend that is higher in tumors than in normal tissue, and which correlates with an increased risk of metastasis and regional lymph node involvement, although some deviations from this have been noted.[34] There are suggestions that *TIMP3* protects against tumor development by suppressing angiogenesis, tumor growth and metastasis through inferred apoptosis.[9]

Coskunpinar et al. analyzed the expression levels of 88 genes in laryngeal carcinoma using a PCR array and showed an altered expression of 16 genes when compared to paired cancer-free tissue.[30] One of the altered genes in which expression was significantly higher in the tumor tissue was the *TIMP1* gene. *TIMP1* protein expression was significantly higher in laryngeal squamous cell carcinoma than in adjacent non-cancerous tissues.[19] Similarly, an increased expression of *TIMP2* has been observed in tumor tissues compared with normal tissues.[26] Burduk et al. described oropharyngeal cancer without lymph node metastasis showing lower *TIMP1* and *TIMP2* protein expression in cancer cells and stroma compared to patients with lymph node metastasis.[35] On the other hand, it has been reported that a downregulated expression of the *TIMP3* protein in esophageal adenocarcinoma is associated with enhanced tumor invasiveness and reduced patient survival[9] and that the downregulation of *TIMP3* stimulates growth and invasion in endometrial cancer cell lines.[36] The present study of *TIMP3* gene expression in tumors and surgical margin tissues and the correlation between gene expression and clinical-pathological parameters in oral cavity cancers indicated no significant differences (Table 3).

SFRP1 and *SFRP2*

Research has shown that the expression of *SFRP* genes is often downregulated in many cancers, indicating that *SFRP* functions as a tumor suppressor gene.[37–39] In our study, we examined *SFRP1* and *SFRP2* gene expression levels and found a statistically significantly lower expression of *SFRP1* in tumor samples compared to margin samples, although the difference was not significant for the *SFRP2* gene (Table 3). Sogabe et al. proved that in OSCC cell lines, the silencing of *SFRP* genes and their loss of function lead to cell proliferation during oral carcinogenesis.[38] Similarly, Xiao et al. showed that *SFRP2* mRNA expression was downregulated in tumor samples of OSCC compared to tumor-adjacent normal tissue, and that the loss of expression was connected with hypermethylation of the gene promoter.[39] Reduced *SFRP1* expression was also detected by immunohistochemical staining in a group of patients diagnosed with mucoepidermoid carcinoma of the salivary glands.[40] The *SFRP1* protein can act as a Wnt signaling inhibitor by attaching extracellular Wnt ligands or directly binding to the transmembranous receptor FZD. Its role as a potential progression marker was clarified in a study by Rogler et al. which used cell cultures and tumor samples of bladder cancer.[37] They demonstrated that the function of *SFRP1* in the process of oncogenesis is more complicated, considering the non-canonical Wnt- and mitogen-activated protein kinase (MAPK) signaling pathways.

CDH1

A dysfunction of cadherin 1 is involved in carcinogenesis, and a loss of function has been demonstrated to promote tumor invasion and metastasis in different cancer models.[41] It has been reported that the loss of protein expression of *CDH1* is also associated with an increased invasive potential in head and neck cancer.[42] In a study conducted on clinical samples collected from patients with tongue squamous cell carcinoma, a significantly lower *CDH1* mRNA expression level than in the corresponding non-cancerous tissues was shown.[31] In our study, no significant differences were found between the *CDH1* gene expression levels of the tumors and the surgical margin samples. Similar results were obtained by Kordi-Tamandani et al., who found no significant differences between the mRNA expression of the *CDH1* gene of patients with oral cavity cancer and that of a healthy control group.[12]

RASSF1

Another gene that plays an important role in human cancer cell growth and progression is *RASSF1*, and an abnormal expression of *RASSF1* could be an important step in oncogenesis.[21] In the case of the *RASSF1* gene, we found no significant differences in our study. A downregulated expression of *RASSF1A* transcripts and protein in tumor tissues in esophageal and nasopharyngeal carcinomas were observed by Lo et al.; moreover, a reduced expression correlated with the histological grade of the tumor.[33] The mRNA expression of *RASSF1A* was also downregulated in primary tumors in a group of patients with cutaneous melanoma and lacrimal gland carcinoma compared to healthy groups, and was also downregulated in lung and breast cancer cell lines.[18,21,43] Furthermore, aberrant methylation of *RASSF1A* has been observed in several cancer types[43] and a few reports have been focused on the methylation of this gene in HNSCC.[44,45] It is well known that hypermethylation is one of the important epigenetic mechanisms responsible for inactivation of the gene, in addition to genetic alterations of gains and losses.[12,43]

RORA

RORA is a steroid hormone receptor involved in cellular processes, including metabolism, angiogenesis, inflammation, and the circadian rhythm. There are several diseases where *RORs* are integral to the onset and progression, such as autoimmune diseases, inflammation, osteoporosis, and cancer, and it has been proven that in tumor cell lines and cancerous tissues, *ROR* mRNA levels are often downregulated.[46] *RORA* expression was analyzed in colorectal adenocarcinomas, where *RORA* mRNA expression was downregulated in comparison to normal colonic tissue.[47]

In this study, we found no significant differences in *RORA* gene expression, and to our knowledge there have been insufficient studies on the expression of this gene in patients with head and neck cancer. Sørensen et al. analyzed gene expression in human squamous cell carcinoma cell lines and observed a higher level of *RORA* gene expression in the hypoxia group compared to the control group; this was one of the genes induced at low oxygen independent of pH.[29] Genes upregulated by low oxygen have been considered endogenous markers for tumor hypoxia.

DAPK1

DAPK1 is a regulator of apoptosis; suppression of this gene is thought to be critical in the development of tumors. Lower mRNA and protein expression of *DAPK1* was observed in a group of patients with primary gastric cancer compared with adjacent non-tumor tissues.[48] Mariano et al. detected that even with losses of copy numbers for the *DAPK1* gene, the immunohistochemical reaction showed protein expression of this gene in a group of patients with salivary gland neoplasms.[49] Our study showed no significant differences in *DAPK1* gene expression between the tumors and the surgical margin tissues, but there was a significant association between *DAPK1* gene expression and tumor grade. Patients with G3 tumors had significantly higher RQ values of *DAPK1* than patients with G1 and G2 tumors. Figure 1 shows the histological findings of the tumors as related to the gene expression of *DAPK1.* It is often difficult to compare findings between studies because of the different populations and methods used, but our results regarding *DAPK1* are not compatible with other studies. Another study revealed that the methylation of the *DAPK1* gene was associated with the progression of HNSCC.[44,45] Aberrant promoter DNA methylation of this gene has been examined in other types of cancer, including breast cancer; furthermore, tumors with an advanced T-category revealed a higher frequency of *DAPK1* methylation.[50] Surprisingly, the data of Brait et al. on *DAPK1* promoter methylation showed the frequencies of methylation for *DAPK1* in normal thyroid samples to be higher than the frequencies in cancer samples.[51] According to the research, these results limit the usefulness of this gene as a diagnostic marker; additionally, the hypermethylation in the tumors in neoplastic relevance is questionable. Our understanding of the physiological role of the gene is still at an early stage. Furthermore, our studies of the selected tumor histological grade were done on a small population; we must carry out further studies on a larger population in order to verify this result.

Interestingly, we also found a lower *DAPK1* gene expression in the group of patients with alcohol abuse (0.85 vs 1.97; Table 4). This finding could be explained by an epigenetic mechanism after exposure to a risk factor like alcohol consumption, as different lifestyle factors induce expression changes in different genes. Also, low transcription could be associated with methylation induction, as genes specific to a factor could be methylated.[8] In the development of upper aerodigestive tract cancer, alcohol and tobacco are 2 well-established associated risk factors.[52]

There are many different reasons and hypotheses for altered gene expression in tumors and surgical margin tissue. A tumor's heterogeneity and microenvironment are undoubtedly linked to the biology of HNSCC. The clinical application of genetic alterations and their role in HNSCC progression are still being discussed.[41] Different mutations of the *TP53* gene are most prevalent among the numerous observed mutations in HNSCC. An association between the specific mutations of this gene and the biological and clinical course of cancer has been found.[53] Moreover, epigenetic events, such as aberrant promoter gene hypermethylation, are often observed not only in tumor tissue, but also in surgical margins.[39,54,55] Abnormal DNA methylation patterns in promoter regions can inactivate genes and facilitate tumor formation and progression.[56] Environmental factors like exposure to alcohol and cigarettes can influence aberrant methylation patterns, too.[57] Apart from tobacco and alcohol consumption, HPV has been named as a causative agent in a subset of this cancer.[58] HPV infection leads to deregulation of the cell cycle and it is well-known that additional genetic changes are needed for HPV-mediated oncogenesis.[59] It was found that an overexpression of *p16* was connected with molecular events occurring after HPV infection and *p16* has been used as a surrogate marker for evaluation of HPV status.[60,61] Interestingly, HPV was also found to deregulate the methylation levels in individuals with HPV infection.[62] Recently, *Helicobacter pylori* was detected in samples collected from malignancies in the oropharyngeal area and its influence on carcinogenesis was also suggested.[63] It is essential to further study the methylation status in this group of patients, and papers on this subject are currently in progress. One limitation of this study was the fact that we did not investigate the patients' HPV status; we are also considering further investigation of this issue.

In our study population, 80% of the patients were current smokers (most of them smoked more than 1 pack per day); 73% of them reported alcohol consumption, and 64%

both smoked and consumed alcohol. Given the important role that environmental factors such as alcohol abuse and tobacco exposure play in the onset of cancer, it is clear that some genetic or epigenetic alteration occurs in non-cancerous tissues adjacent to the tumor tissue.[1] As many of the patients studied were exposed to these factors, they showed altered expression levels, and the lack of statistically significant differences between the tumor and the margin can also be interpreted in terms of "field cancerization." It is known that patients with head and neck cancer subsequently have increased morbidity and mortality and that subsequent primary tumors are the main reason for mortality in this group of patients.[64] It is well-known that the carcinogenic process involves a progressive accumulation of genetic abnormalities and that HNSCC is a diverse disease with complex molecular abnormalities. A special model of genetic alterations and the progression of squamous dysplasia to invasive carcinoma has been described, including the clonal growth of transformed cells with the formation of an abnormal genetic field.[65] Moreover, oral field cancerization suggests that oral cancer does not arise as an isolated cellular phenomenon but rather as an anaplastic tendency involving many cells at once and it results in the multifocal development of cancer at varied rates within the total field as a reaction to a carcinogen, particularly tobacco. This concept could explain the appearance of multiple primary cancers and recurrences despite the total excision of oral cancer.[7] Tabor et al. found genetically altered fields in the non-neoplastic mucosa surrounding the tumors of 10 out of 28 patients (36%) with HNSCC – the size of the fields was variable. Moreover, in 7 out of 10 patients the field extended beyond the surgical margin.[66]

In order to understand specific tumor behavior and the microenvironment, further studies are needed. As a lot of clinical procedures are limited predictors of tumor progression, many authors suggest that the detection of abnormalities in the field defect can be a useful diagnostic marker to help in assessing the risk of cancer.[67,68] It would be favorable to change the assessment of a safe margin extension or to expand the irradiation field.[69] The discovery of a marker of cancerization is important, but the oncogenesis process is very complicated and molecular techniques have limitations as well. Finding a marker for the development of cancer which provides insight into its earliest stages requires attention to also be focused on a molecular analysis of the surgical margin.

Conclusions

To find markers connected with cancer development and to provide insight into the earliest stages of cancer development, attention should be focused on a molecular analysis of the surgical margins. More investigation is required to completely understand all of the components.

References

1. Ignacio DN, Griffin JJ, Daniel MG, et al. An evaluation of treatment strategies for head and neck cancer in an African American population. *West Indian Med J.* 2013;62:504–509.
2. Demokan S, Chuang A, Suoğlu Y, et al. Promoter methylation and loss of p16(INK4a) gene expression in head and neck cancer. *Head Neck.* 2012;34:1470–1475.
3. Sang-Hyuk Lee SH, Lee NH, Jin SM, et al. Loss of heterozygosity of tumor suppressor genes (p16, Rb, E-cadherin, p53) in hypopharynx squamous cell carcinoma. *Otolaryngol Head Neck Surg.* 2011;145:64–70.
4. Califano J, van der Riet P, Westra W, et al. Genetic progression model for head and neck cancer: Implications for field cancerization. *Cancer Res.* 1996;56:2488–2492.
5. Slaughter DP, Southwick HW, Smejkal W. Field cancerization in oral stratified squamous epithelium: Clinical implications of multicentric origin. *Cancer.* 1953;6:963–968.
6. Braakhuis BJ, Tabor MP, Kummer JA, Leemans CR, Brakenhoff RH. A genetic explanation of Slaughter's concept of field cancerization: Evidence and clinical implications. *Cancer Res.* 2003;63:1727–1730.
7. Angadi PV, Savitha JK, Rao SS, et al. Oral field cancerization: Current evidence and future perspectives. *Oral Maxillofac Surg.* 2012;16:171–180.
8. Ushijima T. Epigenetic field for cancerization. *J Biochem Mol Biol.* 2007;40:142–150.
9. Darnton SJ, Hardie LJ, Muc RS, et al. Tissue inhibitor of metalloproteinase-3 (TIMP-3) gene is methylated in the development of esophageal adenocarcinoma: Loss of expression correlates with poor prognosis. *Int J Cancer.* 2005;115:351–358.
10. Frank B, Hoffmeister M, Klopp N, et al. Single nucleotide polymorphisms in Wnt signaling and cell death pathway genes and susceptibility to colorectal cancer. *Carcinogenesis.* 2010;8:1381–1386.
11. Tremblay K, Daley D, Chamberland A, et al. Genetic variation in immune signaling genes differentially expressed in asthmatic lung tissues. *J Allergy Clin Immunol.* 2008;122:529–536.
12. Kordi-Tamandani DM, Moazeni-Roodi AK, Rigi-Ladiz MA, et al. Promoter hypermethylation and expression profile of MGMT and CDH1 genes in oral cavity cancer. *Arch Oral Biol.* 2010;55:809–814.
13. Oh HJ, Lee KK, Song SJ, et al. Role of the tumor suppressor RASSF1A in Mst1-mediated apoptosis. *Cancer Res.* 2006;66:2562–2569.
14. Zhu Y, McAvoy S, Kuhn R, et al. RORA, a large common fragile site gene, is involved in cellular stress response. *Oncogene.* 2006;25:2901–2908.
15. Lin Y, Hupp TR, Stevens C. Death-associated protein kinase (DAPK) and signal transduction: Additional roles beyond cell death. *FEBS J.* 2010;277:48–57.
16. Brunner M, Ng BC, Veness MJ, et al. Comparison of the AJCC N staging system in mucosal and cutaneous squamous head and neck cancer. *Laryngoscope.* 2014;124:1598–1602.
17. Rodrigues PC, Miguel MC, Bagordakis E, et al. Clinicopathological prognostic factors of oral tongue squamous cell carcinoma: A retrospective study of 202 cases. *Int J Oral Maxillofac Surg.* 2014;43:795–801.
18. Marini A, Mirmohammadsadegh A, Nambiar S, et al. Epigenetic inactivation of tumor suppressor genes in serum of patients with cutaneous melanoma. *J Invest Dermatol.* 2006;126:422–431.
19. Cao XL, Xu RJ, Zheng YY, et al. Expression of type IV collagen, metalloproteinase-2, metalloproteinase-9 and tissue inhibitor of metalloproteinase-1 in laryngeal squamous cell carcinomas. *Asian Pac J Cancer Prev.* 2011;12:3245–3249.
20. McCormack A, Kaplan W, Gill AJ, et al. MGMT expression and pituitary tumors: Relationship to tumor biology. *Pituitary.* 2013;16:208–219.
21. Zeng CH, Guo B, Chen J, et al. Expression profile of tumor suppressor gene RASSF1 in lacrimal gland carcinoma. *Genet Mol Res.* 2015;14:6993–6998.
22. Belbin TJ, Singh B, Barber I, et al. Molecular classification of head and neck squamous cell carcinoma using cDNA microarrays. *Cancer Res.* 2002;62:1184–1190.
23. El-Naggar AK, Kim HW, Clayman GL, et al. Differential expression profiling of head and neck squamous carcinoma: Significance in their phenotypic and biological classification. *Oncogene.* 2002;21:8206–8219.
24. Maiti GP, Mondal P, Mukherjee N, et al. Overexpression of EGFR in head and neck squamous cell carcinoma is associated with inactivation of SH3GL2 and CDC25A genes. *PLoS One.* 2013;8:e63440.

25. Schena M, Guarrera S, Buffoni L, et al. DNA repair gene expression level in peripheral blood and tumor tissue from non-small cell lung cancer and head and neck squamous cell cancer patients. *DNA Repair (Amst).* 2012;11:374–380.
26. Stokes A, Joutsa J, Ala-Aho R, et al. Expression profiles and clinical correlations of degradome components in the tumor microenvironment of head and neck squamous cell carcinoma. *Clin Cancer Res.* 2010;16:2022–2035.
27. Tsuchiya R, Yamamoto G, Nagoshi Y, et al. Expression of adenomatous polyposis coli (APC) in tumorigenesis of human oral squamous cell carcinoma. *Oral Oncol.* 2004;40:932–940.
28. Dünne AA, Mandic R, Falkenberg S, et al. RT-PCR expression profiling of matrix metalloproteinases and their specific inhibitors in cell lines and fresh biopsies of squamous cell carcinomas of the head and neck. *In Vivo.* 2005;19:943–948.
29. Sørensen BS, Toustrup K, Horsman MR, et al. Identifying pH independent hypoxia induced genes in human squamous cell carcinomas in vitro. *Acta Oncol.* 2010;49:895–905.
30. Coskunpinar E, Oltulu YM, Orhan KS, et al. Identification of a differential expression signature associated with tumorigenesis and metastasis of laryngeal carcinoma. *Gene.* 2014;534:183–188.
31. Fujii R, Imanishi Y, Shibata K, et al. Restoration of E-cadherin expression by selective Cox-2 inhibition and the clinical relevance of the epithelial-to-mesenchymal transition in head and neck squamous cell carcinoma. *J Exp Clin Cancer Res.* 2014;33:40.
32. Ito S, Ohga T, Saeki H, et al. Promoter hypermethylation and quantitative expression analysis of CDKN2A (p14ARF and p16INK4a) gene in esophageal squamous cell carcinoma. *Anticancer Res.* 2007;27:3345–3353.
33. Lo PH, Xie D, Chan KC, et al. Reduced expression of RASSF1A in esophageal and nasopharyngeal carcinomas significantly correlates with tumor stage. *Cancer Lett.* 2007;257:199–205.
34. Pérez-Sayáns García M, Suárez-Peñaranda JM, Gayoso-Diz P, et al. Tissue inhibitor of metalloproteinases in oral squamous cell carcinomas – a therapeutic target? *Cancer Lett.* 2012;323:11–19.
35. Burduk PK, Bodnar M, Sawicki P, et al. Expression of metalloproteinases 2 and 9 and tissue inhibitors 1 and 2 as predictors of lymph node metastases in oropharyngeal squamous cell carcinoma. *Head Neck.* 2015;37:418–422.
36. Yu D, Zhou H, Xun Q, et al. microRNA-103 regulates the growth and invasion of endometrial cancer cells through the downregulation of tissue inhibitor of metalloproteinase 3. *Oncol Lett.* 2012;3:1221–1226.
37. Rogler A, Kendziorra E, Giedl J, et al. Functional analyses and prognostic significance of SFRP1 expression in bladder cancer. *J Cancer Res Clin Oncol.* 2015;141:1779–1790.
38. Sogabe Y, Suzuki H, Toyota M, et al. Epigenetic inactivation of SFRP genes in oral squamous cell carcinoma. *Int J Oncol.* 2008;32:1253–1261.
39. Xiao C, Wang L, Zhu L, et al. Secreted frizzled-related protein 2 is epigenetically silenced and functions as a tumor suppressor in oral squamous cell carcinoma. *Mol Med Rep.* 2014;10:2293–2298.
40. Lee CH, Hung YJ, Lin CY, et al. Loss of SFRP1 expression is associated with aberrant beta-catenin distribution and tumor progression in mucoepidermoid carcinoma of salivary glands. *Ann Surg Oncol.* 2010;17:2237–2246.
41. Hardisson D. Molecular pathogenesis of head and neck squamous cell carcinoma. *Eur Arch Otorhinolaryngol.* 2003;260:502–508.
42. Fan CC, Wang TY, Cheng YA, et al. Expression of E-cadherin, Twist, and p53 and their prognostic value in patients with oral squamous cell carcinoma. *J Cancer Res Clin Oncol.* 2013;139:1735–1744.
43. Burbee DG, Forgacs E, Zöchbauer-Müller S, et al. Epigenetic inactivation of RASSF1A in lung and breast cancers and malignant phenotype suppression. *J Natl Cancer Inst.* 2001;93:691–699.
44. Righini CA, de Fraipont F, Timsit JF, et al. Tumor-specific methylation in saliva: A promising biomarker for early detection of head and neck cancer recurrence. *Clin Cancer Res.* 2007;13:1179–1185.
45. Choudhury JH, Ghosh SK. Promoter hypermethylation profiling identifies subtypes of head and neck cancer with distinct viral, environmental, genetic and survival characteristics. *PLoS One.* 2015;10:e0129808.
46. Ranhotra HS. The interplay between retinoic acid receptor-related orphan receptors and human diseases. *J Recept Signal Transduct Res.* 2012;32:181–189.
47. Kottorou AE, Antonacopoulou AG, Dimitrakopoulos FI, et al. Altered expression of NFY-C and RORA in colorectal adenocarcinomas. *Acta Histochem.* 2012;114:553–561.
48. Ye M, Li D, Zhou F, et al. Epigenetic regulation of death-associated protein kinase expression in primary gastric cancers from Chinese patients. *Eur J Cancer Prev.* 2012;21:241–246.
49. Mariano FV, Rincon D, Gondak RO, et al. Carcinoma ex-pleomorphic adenoma of upper lip showing copy number loss of tumor suppressor genes. *Oral Surg Oral Med Oral Pathol Oral Radiol.* 2013;116:69–74.
50. Tserga A, Michalopoulos NV, Levidou G, et al. Association of aberrant DNA methylation with clinicopathological features in breast cancer. *Oncol Rep.* 2012;27:1630–1638.
51. Brait M, Loyo M, Rosenbaum E, et al. Correlation between BRAF mutation and promoter methylation of TIMP3, RARβ2 and RASSF1A in thyroid cancer. *Epigenetics.* 2012;7:710–719.
52. Hashibe M, Boffetta P, Zaridze D, et al. Evidence for an important role of alcohol- and aldehyde-metabolizing genes in cancers of the upper aerodigestive tract. *Cancer Epidemiol Biomarkers Prev.* 2006;15:696–703.
53. Erber R, Conradt C, Homann N, et al. TP53 DNA contact mutations are selectively associated with allelic loss and have a strong clinical impact in head and neck cancer. *Oncogene.* 1998;16:1671–1679.
54. Hayashi M, Wu G, Roh JL, et al. Correlation of gene methylation in surgical margin imprints with locoregional recurrence in head and neck squamous cell carcinoma. *Cancer.* 2015;121:1957–1965.
55. Wei DM, Liu DY, Lei DP, et al. Aberrant methylation and expression of DAPk1 in human hypopharyngeal squamous cell carcinoma. *Acta Otolaryngol.* 2015;135:70–78.
56. Baylin SB, Ohm JE. Epigenetic gene silencing in cancer – a mechanism for early oncogenic pathway addiction? *Nat Rev Cancer.* 2006;6:107–116.
57. Wong TS, Man MW, Lam AK, et al. The study of p16 and p15 gene methylation in head and neck squamous cell carcinoma and their quantitative evaluation in plasma by real-time PCR. *Eur J Cancer.* 2003;39:1881–1887.
58. Leemans CR, Braakhuis BJ, Brakenhoff RH. The molecular biology of head and neck cancer. *Nat Rev Cancer.* 2011;11:9–22.
59. Doorbar J. Molecular biology of human papillomavirus infection and cervical cancer. *Clin Sci (Lond).* 2006;110:525–541.
60. Sritippho T, Pongsiriwet S, Lertprasertsuke N, et al. p16 – a possible surrogate marker for high-risk human papillomaviruses in oral cancer? *Asian Pac J Cancer Prev.* 2016;17:4049–4057.
61. Garnaes E, Frederiksen K, Kiss K, et al. Double positivity for HPV DNA/p16 in tonsillar and base of tongue cancer improves prognostication: Insights from a large population-based study. *Int J Cancer.* 2016;139:2598–2605.
62. Lim Y, Wan Y, Vagenas D, et al. Salivary DNA methylation panel to diagnose HPV-positive and HPV-negative head and neck cancers. *BMC Cancer.* 2016;16:749.
63. Pavlik E, Nartova E, Astl J, et al. Detection of Helicobacter pylori and human papillomavirus in peroperative tissue biopsies collected from malignancies in oropharyngeal area. *Am J Clin Exp Med.* 2015;3:364–367.
64. Braakhuis BJ, Tabor MP, Leemans CR, et al. Second primary tumors and field cancerization in oral and oropharyngeal cancer: Molecular techniques provide new insights and definitions. *Head Neck.* 2002;24:198–206.
65. Perez-Ordoñez B, Beauchemin M, Jordan RC. Molecular biology of squamous cell carcinoma of the head and neck. *J Clin Pathol.* 2006;59:445–453.
66. Tabor MP, Brakenhoff RH, van Houten VM, et al. Persistence of genetically altered fields in head and neck cancer patients: Biological and clinical implications. *Clin Cancer Res.* 2001;7:1523–1532.
67. Braakhuis BJ, Tabor MP, Kummer JA, et al. A genetic explanation of Slaughter's concept of field cancerization: Evidence and clinical implications. *Cancer Res.* 2003;63:1727–1730.
68. Tabor MP, Brakenhoff RH, Ruijter-Schippers HJ, et al. Genetically altered fields as origin of locally recurrent head and neck cancer: A retrospective study. *Clin Cancer Res.* 2004;10:3607–3613.
69. Szukała K, Brieger J, Bruch K, el al. Loss of heterozygosity on chromosome arm 13q in larynx cancer patients: Analysis of tumor, margin and clinically unchanged mucosa. *Med Sci Monit.* 2004;10:CR233–240.

Early hypophosphatemia in very low birth weight preterm infants

Agata Pająk[B–D], Barbara Królak-Olejnik[A,D–F], Agnieszka Szafrańska[A,C,D]

Department and Clinic of Neonatology, University Hospital, Wroclaw Medical University, Poland

A – research concept and design; B – collection and/or assembly of data; C – data analysis and interpretation;
D – writing the article; E – critical revision of the article; F – final approval of the article

Advances in Clinical and Experimental Medicine, ISSN 1899-5276 (print), ISSN 2451-2680 (online) *Adv Clin Exp Med*. 2018;27(6):841–847

Address for correspondence
Agata Pająk
E-mail: agata_pa@wp.pl

Funding sources
None declared

Conflict of interest
None declared

Acknowledgements
The authors would like to acknowledge Beata Kołaczyńska for her involvement in the laboratory diagnosis.

Received on August 30, 2016
Reviewed on February 15, 2017
Accepted on March 31, 2017

Abstract

Refeeding Syndrome (RFS) is a well-known group of symptoms which occur after the introduction of enteral or parenteral nutrition in undernourished patients. Intrauterine growth restriction (IUGR) is the equivalent of postnatal RFS following the beginning of feeding. The aggressive parenteral nutrition of neonates with very low birth weight (VLBW) resulting from the termination of intrauterine transplacental nutrition is a source of biochemical disorders. The aim of this study was to analyze metabolic disorders in preterm infants during the 1st week of life and to determine the hypophosphatemia risk factors in low birth weight neonates receiving parenteral nutrition. The retrospective analysis covered 49 neonates, aged between 24 0/7 and 32 6/7 weeks of gestation. The examined patients were divided into 2 groups according to the level of phosphates during the 1st week of life: HP (n = 18) with aggravated hypophosphatemia (≤3.1 mg/dL) and NP (n = 31) with normal phosphatemia (>3.1 mg/dL). Hypophosphatemia was observed in the first days of life in 61% of children, in 45% of whom a subsequent test revealed a further fall in the phosphate level. In the rest of the preterm neonates (39%), hypophosphatemia was revealed between the 4th and 7th day of life. The risk of early hypophosphatemia was higher in neonates with IUGR ($p = 0.0001$; RR 5.2, 95% CI 2.2–12.4) and extremely low birth weight (ELBW) preterm infants ($p < 0.05$). Early hypophosphatemia should be closely monitored early in life, especially in newborns with ELBW and IUGR. Further research is needed to develop an optimal nutritional regimen from the first days of life.

Key words: nutrition, neonatology, hypophosphatemia, metabolic, preterm infant

DOI
10.17219/acem/70081

Introduction

Nutrition is an essential element in the intensive care of preterm newborns. Not only does it affect the results of treatment, but it also influences susceptibility to diseases in adulthood and it has lifelong cognitive impact. The aim of administering aggressive parenteral nutrition is to promote continued growth (increased weight and length) equivalent to that of a fetus's normal intrauterine life.[1–4] Refeeding Syndrome (RFS) is a well-known group of symptoms which occur after the introduction of enteral or parenteral nutrition in undernourished patients. RFS can be prevented by the correction of electrolyte disorders and by vitamin B intake at the beginning of nutrition.[5,6] The symptoms result from the quick conversion of catabolic metabolism to anabolic – from the transformation of free fatty acids and ketones released during the transformation of bicarbonates as a primary source of energy.[7,8] Intrauterine growth restriction is the equivalent of postnatal RFS after nutrition has begun. Aggressive parenteral feeding of neonates with very low birth weight (VLBW) resulting from the interruption of intrauterine transplacental nutrition is a source of biochemical disorders.

The term Placental Incompletely Restored Feeding syndrome (PI-ReFeeding syndrome) was proposed for preterm newborns because of the lack of adequate intake of other nutrients in relation to amino acids and energy. Amino acids are responsible for an increase in the production of endogenous insulin. Insulin induces intracellular redistribution of phosphates and potassium, which leads to the lowering of their concentration in blood serum. Moreover, the acceleration of anabolism results in the increased reprocessing of phosphates and potassium.[9] The clinical implication of hypophosphatemia are multi-system disorders occurring mainly in energy-active organs; thus, heart or respiratory failure, muscle hypotension, neurological symptoms, hematological disorders, insulin-resistant hyperglycemia, or metabolic acidosis may occur. However, indications for the modification of the phosphate intake of nutritional treatment, which, according to current recommendations, are introduced on the 3rd day of a neonate's life, have not yet been established.

The aims of this study were:

- to analyze metabolic disorders in preterm infants during the 1st week of life, especially hypophosphatemia; and
- to determine the hypophosphatemia risk factors in low birth weight neonates receiving parenteral nutrition.

Material and methods

The research was carried out from August 2013 to July 2014 in the Neonatal Intensive Care Unit of the Department of Neonatology at the University Hospital in Wrocław. During this period, 2,316 neonates were hospitalized in the department, 84 of whom were born before 33 0/7 weeks of gestation, which constituted 3.6% of all labors. The retrospective analysis covered 49 neonates aged between 24 0/7 and 32 6/7 weeks of gestation. The study included children whose phosphate concentration was measured at least twice during the 1st week of their lives: between the 1st and 3rd day of life (M1), and between the 4th and 7th day of life (M2). Patients with congenital malformations were excluded from the analysis. Two groups of neonates were identified by means of Fenton centile growth charts for preterm neonates: appropriate for gestational age (AGA) and small for gestational age (SGA).[10]

Starting parenteral nutrition sets were prepared by the hospital pharmacy and contained amino acids (1.5 g/kg), glucose and calcium (0.5 mmol/kg), but no phosphates. According to the Guidelines for Paediatric Parenteral Nutrition published by the European Society for Paediatric Gastroenterology, Hepatology and Nutrition (ESPGHAN) in 2005, a minimum amino acid intake of 1.5 g/kg/day is necessary to prevent a negative nitrogen balance.[11] Patients in the study received amino acids (3.0 g/kg/day) and lipids (3 g/kg/day) from the 2nd day of life.

The patients received Glycophos (Fresenius Kabi, Uppsala, Sweden) in parenteral nutrition from the 2nd or 3rd day of life (range: 2nd–5th day of life), according to current recommendations.[11]

Phosphate supplementation was continued in the form of human milk fortifier and/or a sodium-phosphate mixture in all enterally-fed patients with hypophosphatemia.

A phosphate level <4.4 mg/dL (1.4 mmol/L) in preterm neonates in the 1st week of life was diagnosed as hypophosphatemia. Severe hypophosphatemia was set at a phosphate level of <3.1 mg/dL (1 mmol/L), and hypocalcemia and hypomagnesemia were diagnosed at calcium and magnesium levels <8.0 mg/dL and 1.5 mg/dL, respectively. The biochemical tests on blood serum were performed using the Beckman Coulter analyzer (Beckman Coulter Polska Sp. z o. o., Warszawa, Poland) in the Department of Analytical Laboratory of the University Hospital in Wrocław.

The Bioethical Commission of Wroclaw Medical University granted permission to carry out the retrospective analysis of the patients' medical records.

The characteristics of the examined patients, divided into 2 groups according to the level of phosphates (HP – aggravated hypophosphatemia, ≤3.1 mg/dL; and NP – normal phosphatemia, >3.1 mg/dL]) are presented in Table 1.

Statistical analyses were performed using either version N-1 of the χ^2 test for categorical variables, or the Mann–Whitney test or Student's t-test for continuous variables. The data was expressed as mean ±SD for normally distributed continuous variables, or as median and range for variables not normally distributed. Categorical variables were described using absolute (n) and relative (%) frequencies. For categorical variables, the relative risk (RR) was calculated with 95% confidence intervals (CI). Simple and multiple regression were also used. A p-value <0.05 was considered significant.

The analysis was performed using Stargraphics Centurion XVII (Stargraphics Technologie Inc., Virginia, USA) and MedCalc v. 16.2 (MedCalc, Ostend, Belgium) for Windows.

Results

A phosphate concentration in blood serum within the proper laboratory range (4.4–6.7 mg/dL) was observed in only 25% of infants. A value below the lower range limit was observed in 75% of neonates, and in 2 children (4%) phosphate concentration barely exceeded the upper range limit (Fig. 1).

Hypophosphatemia was observed in the first days of life in 61% of children, in 45% of whom a subsequent test revealed a further fall in the phosphate level. In 39% of the examined preterm neonates, hypophosphatemia was recognized between the 4th and 7th day of life (Fig. 2).

On the basis of phosphate concentration, the neonates were divided into 2 groups: those with aggravated hypophosphatemia (≤3.1 mg/dL) and those with normal phosphatemia (>3.1 mg/dL).

The median concentration of phosphates in 1–3-day-old newborns' blood serum was 3.1 mg/dL in the HP group and 5 mg/dL in the NP group; however, in the tests

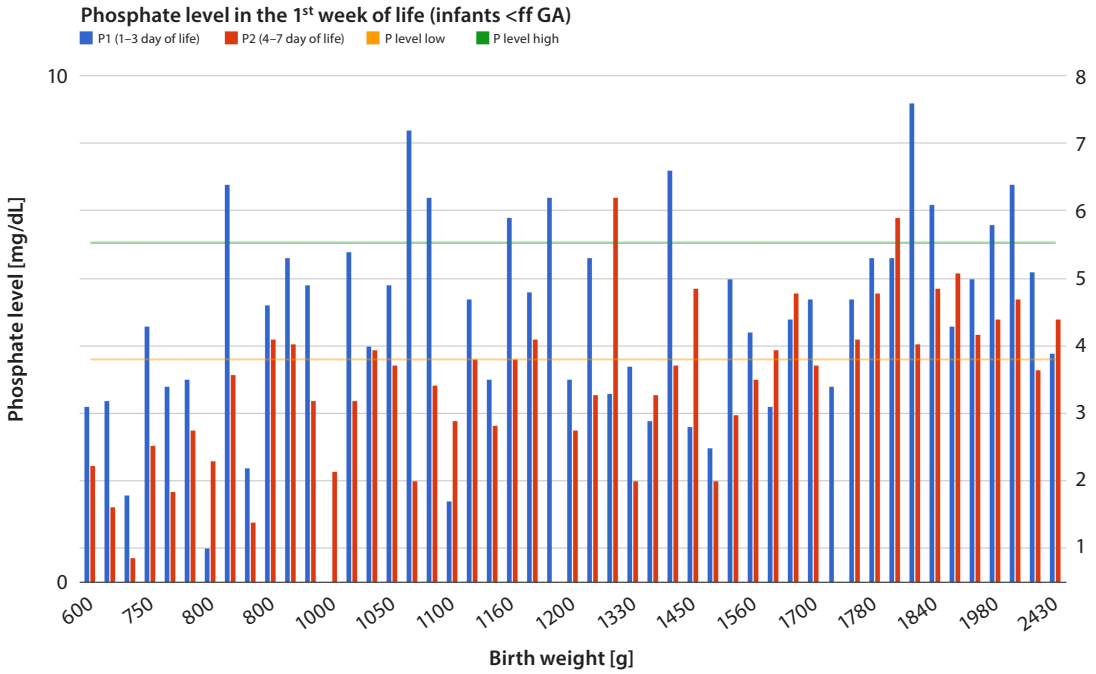

Fig. 1. Phosphate concentration in blood serum of preterm infants

green line – upper range limit; orange line – lower range limit, blue column – level of phosphates in the 1st–3rd day of life; red column – level of phosphates in 4th–7th day of life.

Table 1. Characteristics of the preterm infants: A comparison of HP and NP

Characteristics	HP (n = 18)	NP (n = 31)	RR 95% CI	p-value
Gestational age weeks, mean ±SD	29.2 ±2.2	29.8 ±2.4	–	0.3576^{t}
GA <28 HBd , n (%)	3 (17)	7 (23)	RR 0.74 CI 0.22–2.50	0.6215^{X}
Birth weight [g], mean ±SD	1029 ±315	1477 ±447	–	0.0005^{t}
Small for gestational age, n (%)	11 (61)	3 (10)	RR 6.32 CI 2.03–19.68	0.0002^{X}
TPN initial glucose intake [g/kg/day], mean ±SD[1] initial amino acids intake [g/kg/day], mean ±SD[1] initial P intake [mmol/kg/day], median (range)[2] initial K intake [mmol/kg/day], median (range)[2]	 8.97 ±1.24 2.72 ±0.31 3 (1–5) 3 (2–5)	 8.89 ±1.21 2.69 ±0.45 4 (2–5) 4 (2–7)	 – – – –	 0. 8192^{t} 0.7891^{t} 0.7273^{M-W} 0.0528^{M-W}
Days of TPN (for survivors), median (range)	13 (5–30)	10.5 (3–35)	–	0.3919^{M-W}
Days of hospital stay (for survivors)	53 (31–89)	35 (15–104)	–	0.0324^{M-W}

HP – study group; NP – control group; n – number of patients; RR – relative risk; CI – confidence interval; SD – standard deviation; GA – gestational age; HBd – hebdomas; TPN – total parenteral nutrition; ^{X} χ^2 test; t Student's t-test; $^{M-W}$ Mann-Whitney test.

carried out between the 4th and 7th day of life, the concentrations were 2.35 mg/dL (HP) and 5.5 mg/dL (NP). The lowest level of phosphates was observed up to the 10th day of life (median: the 6th day of life). The neonates received phosphates in parenteral nutrition from the 3rd day of life (range: 2nd–5th day of life). Phosphorus supplementation was continued in the form of human milk fortifier and/or a phosphate-sodium mixture in all patients with hypophosphatemia.

There was a statistically significant relationship between the minimum level of phosphorus (P_{min}) [mg/dL] and birth weight [g] with a 95% CI; p-value <0.05 (p = 0.0000).

$$P_{min}\ [mg/dL] = -14.6492 + 2.53301 \times \ln(\text{birth weight [g]})$$

The R^2 value indicates that the model as fitted explains 46.3533% of the variability in P_{min} [mg/dL] after transforming to a Y/(1-Y) scale to linearize the model. The correlation coefficient equals 0.680833, indicating a moderately strong relationship between the variables (Fig. 3).

Neonates with intrauterine growth restriction (IUGR) (RR 5.2 95% CI 2.2–124; p = 0.0001) and extremely low birth rate (ELBW) (p < 0.05) were at risk of early hypophosphatemia; however, the difference in gestational age between the NP and HP groups was statistically insignificant.

Even though insulin, catecholamine and invasive ventilation were more frequently administered, and complications such as intraventricular hemorrhages (IVH), early infections, bronchopulmonary dysplasia (BPD), death, or biochemical disorders (hypertriglyceridemia, hypocalcemia or hyperglycemia) occurred more often in the HP group than in the NP one, they were statistically insignificant.

Discussion

Considering the problem of hypophosphatemia in neonates, the question of how and when to diagnose it must be answered.

The assessment of hypophosphatemia is necessarily based on the level of phosphorus in serum; thus, it is vital to be fully familiar with the normal range. It is also essential to bear in mind pre-analytical errors – sample hemolysis falsely increases the phosphate concentration results, as do hypertriglyceridemia and hyperbilirubinemia in intensive care unit patients. The phosphate concentration in a fetus's blood may be adopted as the golden standard for determining a preterm neonate's biochemical condition.[12] Based on the assessment of phosphate concentration in 560 neonates' umbilical blood, Fenton set referential values for preterm newborns and term-born babies dependent on gestational age within 4 age ranges. The lower range limit for preterm neonates with 28–31 weeks of gestation was 1.4 mmol/L, the same as in our study. However, the upper range limit in our study was higher than that in Fenton (2.7 vs 2.1 mmol/L). In neonates, the norms depend on gestational age; phosphate concentration in umbilical blood decreases with GA, while the level of sodium increases.

Adults are also considered to develop serious symptoms at phosphorus levels lower than 1–1.5 mg/dL (<0.32–0.5 mmol/L).[8,13] In the developmental period, however, phosphatemia norms depend on age – the lower the age, the higher the norms. The highest values are observed in babies, so extrapolation seems inaccurate. Safe phosphatemia ranges in neonates, especially in VLBW ones, need to be determined in the near future. Both the frequency and intensity of the described disorders in a specific study

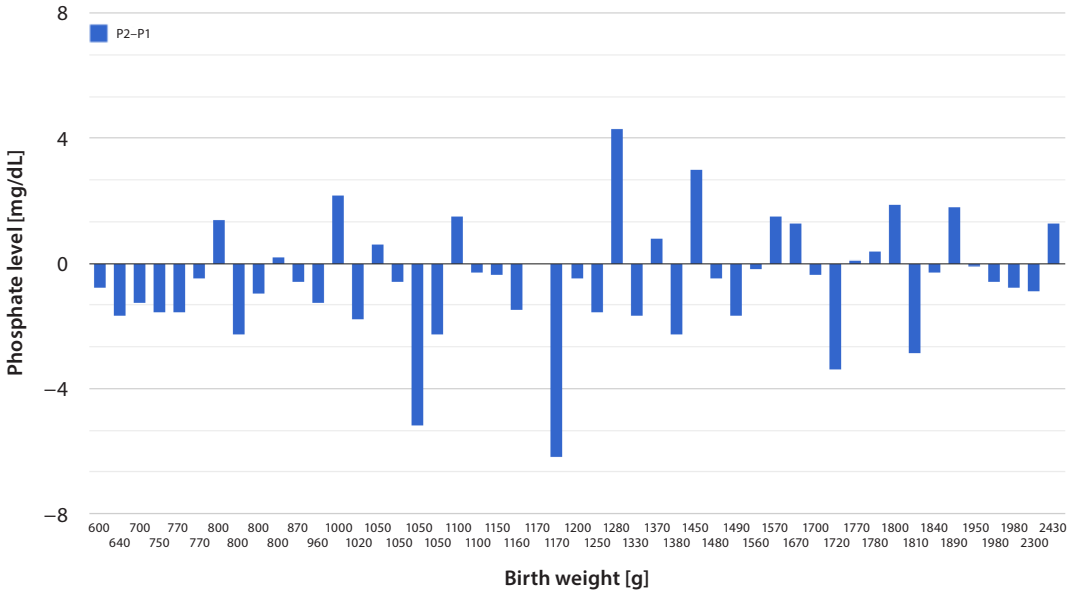

Fig. 2. Difference in phosphate level depending on the body weight of newborn infants

are influenced by the range of the adopted norm. In order to increase the possibility of revealing hypophosphatemia complications, we used aggravated hypophosphatemia (defined as a phosphorus level of <1 mmol/L) for the purpose of statistical analysis. In publications, hypophosphatemia is set at various phosphorus concentrations ranging from <0.8 mmol/L to ≤ 0.9 mmol/L or ≤ 1 mmol/L.[9,14–16]

Therefore, which level should require intensive phosphate supplementation? In other words, when should hypophosphatemia be diagnosed? It may be necessary to review the results of the studies conducted with metabolic methods, which can precisely pinpoint the ranges of clinically significant hypophosphatemia.[17,18]

Just 10 years ago, hypophosphatemia in neonates, as well as in babies, was associated with a metabolic bone disease diagnosed at the end of the 1st month of life; and in the early neonatal period, this age group was actually expected to develop hyperphosphatemia.

On the basis of both our own studies and published works, it may be concluded that after changing the nutrition protocol, hypophosphatemia is not a rare complication in VLBW infants and it often occurs in the 1st week of life.[9,14,19–21] The early hypophosphatemia observed in VLBW infants and those who are small for gestational age (SGA) suggest that it may have the same mechanism as RFS. VLBW neonates with sepsis require special attention, because they present even lower values of phosphorus concentration in blood.[14,20] Three out of 4 neonates from our study group diagnosed with sepsis within the first 2 weeks of life had pronounced early hypophosphatemia (<3.1 mg/dL); 2 of them died. Transient hypophosphatemia is also observed in both children and adults in the course of diagnosed infections; phosphorus concentration is inversely proportionate to C-reactive protein (CRP) level, so other anti-inflammatory factors are said to take part in the process (tumor necrosis factor alpha and interleukin 6).[22,23] When should phosphorus concentration be monitored, then? Unfortunately, there are no generally accepted protocols, but there is increasing evidence which indicates that it is important to measure phosphate concentration within the first days of life.[4,15,21] However, the number of additional tests in infants is limited not only by indications for their use, but also by the amount of circulating blood and the risk of iatrogenic anemia. There are suggestions that phosphate concentration should be monitored twice a day before stabilization.[24] Other authors argued for monitoring the clinical and biochemical parameters of RFS in the 3rd or 4th day of life in infants at risk, including VLBW or ELBW neonates requiring parenteral nutrition.[19]

Based on the data which we obtained, the 1st measurement of phosphorus should be taken by the 3rd day of life and it should be retaken every 2 or 3 days within the 1st week of life due to the risk of increased hypophosphatemia. While correcting acute hypophosphatemia, the concentration in blood serum should be measured 2 h after infusion.[8] The dose and timing of phosphorus intake in parenteral and enteral feeding with a high protein and energy intake is crucial in order to avoid RFS in infants.[25] In neonatology, tailored nutrition prescriptions

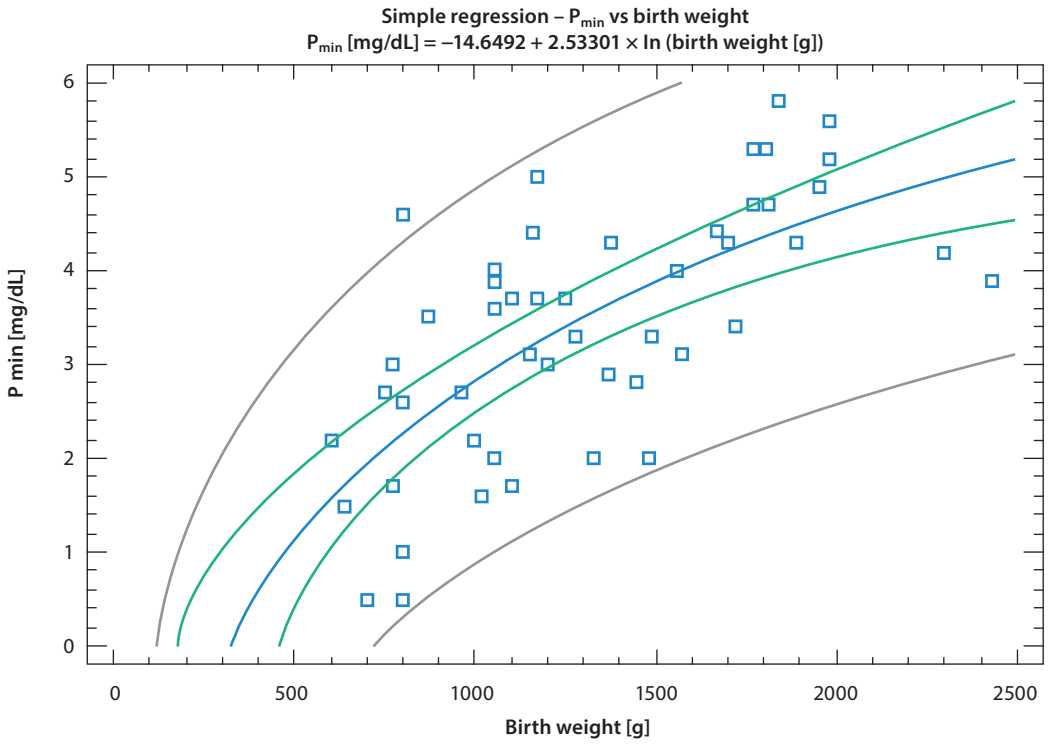

Fig. 3. Relationship between P_{min} [mg/dL] in blood serum during the 1st week of life and birth weight [g] of the preterm infants

are typically administered. More and more data advocate intake safety from the 1st day of standard nutrition which contains phosphates.[26–28] However, phosphorus supplementation is currently recommended from the 3rd day of life; before that, neonates receive only a small amount of phosphorus in a lipid solution. Fears of early phosphate intake result from the need to intake sodium and potassium simultaneously, which is not recommended in the first days of life until diuresis stabilizes. The complications from phosphorus intake, especially intravenous feeding, also include hypocalcemia and excess intake resulting in hyperphosphatemia.[11] It is important to point out that regardless of phosphate supplementation, a decrease in phosphate concentration was observed in 66% of preterm neonates with parenteral nutrition older than 3 days of life whom we examined, a fact that indicates insufficient intake. While performing parenteral intake of Ca or P in the amount of 3 and 1.92 mmol/kg/day, respectively, in the 3rd day of life, Christman et al. administered the maximum recommended phosphate doses to preterm infants <34 GA; however, as many as 34% of babies had a phosphorus level of <1.8 mmol/L in the 5th day of life.[21]

The study we carried out is a preliminary one. The small group of patients studied made it impossible for us to present conclusive results concerning RFS clinical symptoms in preterm neonates with aggravated hypophosphatemia. Prospective studies are currently being conducted in our center.

Conclusions

Early hypophosphatemia is a common metabolic complication in neonates with <33 GA who receive parenteral feeding. Thus, thorough monitoring is necessary from the very first days of life, especially in VLBW and SGA neonates. It is necessary to carry out further studies in order to determine optimal nutritional standards in the early stages of life. It is also essential to identify risk groups of infants who may have higher requirements for supplemented phosphates within the 1st week of life to prevent RFS.

What is new:

– adequate phosphate intake is important for prevention of metabolic bone disease in preterm infants;
– recommendations for neonatal mineral intake are based on in utero acceleration rates, but supplementation requirements of preterm neonates vary between studies.

What is known:

– early hypophosphatemia is a common metabolic complication in neonates before 32 GA receiving parenteral nutrition;
– thus, thorough monitoring is necessary from the very first days of life, especially in VLBW and SGA neonates.

References

1. Adamkin D, Radmacher P. Current trends and future challenges in neonatal parenteral nutrition. *J Neonatal Perinatal Med*. 2014;7:157–164.
2. Nehra D, Carlson S, Erica M, et al. The American Society for Parenteral and Enteral Nutrition (ASPEN) clinical guidelines: Nutrition support of neonatal patients at risk for metabolic bone disease. *J Parenter Enteral Nutr*. 2013;37:570–598.
3. Hay WW, Jr. Aggressive nutrition of the preterm infant. *Curr Pediatr Rep*. 2013;1(4):222–239. doi:10.1007/s40124–013-0026-4
4. Embleton ND, Morgan C, King C. Balancing the risks and benefits of parenteral nutrition for preterm infants: Can we define the optimal composition? *Arch Dis Child Fetal Neonatal Ed*. 2015;100:F72–F75.
5. Crook MA, Hally V, Panteli JV. The importance of the refeeding syndrome. *Nutrition*. 2001;17:632–637.
6. Khan LU, Ahmed J, Khan S, Macfie J. Refeeding syndrome: A literature review. *Gastroenterol Res Pract*.2011;410971. doi:10.1155/2011/410971
7. Skipper A. Refeeding syndrome or refeeding hypophosphatemia: A systematic review of cases. *Nutr Clin Pract*. 2012;27:34–40.
8. Byrnes MC, Stangenes J. Refeeding in the ICU: An adult and pediatric problem. *Curr Opin Clin Nutr Metab Care*. 2011;14:186–192.
9. Bonsante F, Iacobelli S, Latorre G, et al. Initial amino acid intake influences phosphorusus and calcium homeostasis in preterm infants: It is time to change the composition of the early parenteral nutrition. *PLoS ONE*. 2013;8:e72880. doi:10.1371/journal.pone.0072880
10. Fenton TR, Kim JH. A systematic review and meta-analysis to revise the Fenton growth chart for preterm infants. *BMC Pediatr*.2013;13:59. doi:10.1186/1471-2431-13-59
11. Koletzko B, Goulet O, Hunt J, Krohn K, Shamir R. Guidelines on Paediatric Parenteral Nutrition of the European Society of Paediatric Gastroenterology, Hepatology and Nutrition (ESPGHAN) and the European Society for Clinical Nutrition and Metabolism (ESPEN), supported by the European Society of Paediatric Research (ESPR). *J Pediatr Gastroenterol Nutr*. 2005;41:1–87.
12. Fenton TR, Lyon AW, Rose MS. Cord blood calcium, phosphate, magnesium, and alkaline phosphatase gestational age-specific reference intervals for preterm infants. *BMC Pediatr*. 2011;11:76. doi:10.1186/1471-2431-11-76
13. Sikora P. Phosphataemia disturbances in children. *Pediatr Dypl*. 2014;18:37–44.
14. Moltu SJ, Strømmen K, Blakstad EW, et al. Enhanced feeding in very-low-birth-weight infants may cause electrolyte disturbances and septicemia: A randomized, controlled trial. *Clin Nutr*. 2013;32:207–212.
15. Ross JR, Finch C, Ebeling M, Taylor SN. Refeeding syndrome in very-low-birth-weight intrauterine growth-restricted neonates. *J Perinatol*. 2013;33:717–720.
16. Boubred F, Herlenius E, Bartocci M, et al. Extremely preterm infants who are small for gestational age have a high risk of early hypophosphatemia and hypokalemia. *Acta Paediatr*. 2015;104:1077–1083.
17. Moco S, Collino S, Rezzi S, Martin FP. Metabolomics perspectives in pediatric research. *Pediatr Res*. 2013;73:570–576.
18. Alexandre-Gouabau MC, Courant F, Moyon T, et al. Maternal and cord blood LC-HRMS metabolomics reveal alterations in energy and polyamine metabolism, and oxidative stress in very-low-birth-weight Infants. *J Proteome Research*.2013;12:2764–2778.
19. Mizumoto H, Mikami M, Oda H, Hata D. Refeeding syndrome in a small-for-dates micro-preemie receiving early parenteral nutrition. *Pediatr Int*.2012;54:715–717.
20. Brener Dik PH, Galletti MF, Fernández Jonusas SA, et al. Early hypophosphatemia in preterm infants receiving aggressive parenteral nutrition. *J Perinatol*. 2015;35:712–715.
21. Christmann V, de Grauw AM, Visser R, Matthijsse RP, van Goudoever JB, van Heijst AF. Early postnatal calcium and phosphorusus metabolism in preterm infants. *J Pediatr Gastroenterol Nutr*. 2014;58:398–403.
22. Antachopoulos C, Margeli A, Giannaki M, et al. Transient hypophosphataemia associated with acute infectious disease in paediatric patients. *Scand J Infect Dis*. 2002;34:836–839.
23. Naffaa ME, Mustafa M, Azzam M, et al. Serum inorganic phosphorous level predict 30-day mortality in patients with community acquired pneumonia. *BMC Infect Dis*.2015;15:332. doi:10.1186/s12879-015-1094-6
24. Koletzko B, Poindexter B, Uauy R. Nutritional care of preterm infants: Scientific basis and practical guidelines. *Indian J Med Res*. 2016;143(4):531–532. doi:10.4103/0971-5916.184296

25. Lafeber HN, van de Lagemaat M, Rotteveel J, van Weissenbruch M. Timing of nutritional interventions in very-low-birth-weight infants: Optimal neurodevelopment compared with the onset of the metabolic syndrome. *Am J Clin Nutr*. 2013;98:556–560.
26. Jamin A, D'Inca R, Le FN, et al. Fatal effects of a neonatal high-protein diet in low-birth-weight piglets used as a model of intrauterine growth restriction. *Neonatology*. 2010;97:321–328.
27. Bolisetty S, Pharande P, Nirthanakumaran L, et al. Improved nutrient intake following implementation of the consensus standardized parenteral nutrition formulations in preterm neonates before-after intervention study. *BMC Pediatr*. 2014,14:309. doi:10.1186/s12887-014-0309
28. Imel EA, Econs MJ. Approach to the hypophosphatemic patient. *J Clin Endocrinol Metab*. 2012;97:696–706.

CXCL9, CXCL10, CXCL11, and their receptor (CXCR3) in neuroinflammation and neurodegeneration

Olga M. Koper[1,A–D,F], Joanna Kamińska[1,B,C,E,F], Karol Sawicki[2,C,E,F], Halina Kemona[1,E,F]

[1] Department of Clinical Laboratory Diagnostics, Medical University of Bialystok, Poland
[2] Department of Neurosurgery, Medical Clinical Hospital in Bialystok, Poland

A – research concept and design; B – collection and/or assembly of data; C – data analysis and interpretation; D – writing the article; E – critical revision of the article; F – final approval of the article

Advances in Clinical and Experimental Medicine, ISSN 1899-5276 (print), ISSN 2451-2680 (online) *Adv Clin Exp Med*. 2018;27(6):849–856

Address for correspondence
Olga M. Koper
E-mail: o.koper@wp.pl

Funding sources
None declared

Conflict of interest
None declared

Acknowledgements
The authors are grateful to Piotr Abramowicz for his technical help in preparing the figure.

Received on April 18, 2016
Reviewed on September 15, 2016
Accepted on February 7, 2017

Abstract

The aim of this review is to present data from the available literature concerning CXCL9, CXCL10 and CXCL11, as well as their receptor 3 (CXCR3) in selected diseases of the central nervous system (CNS), such as tick-borne encephalitis (TBE), neuroborreliosis (NB), Alzheimer's disease (AD), and multiple sclerosis (MS). CXCL9, CXCL10, and CXCL11 lack glutamic acid-leucine-arginine (ELR), and are unique, because they are more closely related to each other than to any other chemokine. The aforementioned chemokines are especially involved in Th1-type response and in various diseases, as their expression correlates with the tissue infiltration of T cells. Their production is strongly induced by interferon gamma (IFN-Y), the most typical Th1 cytokine. They act by binding to the CXC3 receptor. Knowledge about the action mechanism of CXCR3 and its ligands may be useful in the treatment of CNS diseases. However, data in the literature concerning the evaluation of CXCL9, CXCL10, CXCL11, and their receptor with the use of the enzyme-linked immunosorbent assay (ELISA) method is limited.

Key words: chemokines, neurodegeneration, neuroinflammation, CXCR3

DOI
10.17219/acem/68846

Introduction

Chemokines are crucial proteins that take part in the regulation of the migration of leukocytes in peripheral lymphatic organs. In pathological conditions, they take part in the migration of immunocompetent cells to the sites of inflammation and are also involved in neoplastic processes, or even may provide an entrance for pathogens into the body.[1]

The literature indicates that chemokines and their receptors might also play a role in the central nervous system (CNS). They are constitutively present in the brain on glial cells and neurons, take part in intracellular communication, and play a pivotal role during the pathogenesis of various CNS diseases.[2–4] Central nervous system cells, upon stimulation by pathogens, release chemokines and are able to respond to them using their receptors. Under normal conditions, the CNS is an immune-privileged site because of a highly selective blood-brain barrier (BBB), separating the brain from the circulating blood. A pathological process leads to the activation of microglia, and this leads to neuronal and glial cell injury, as well as to death through the production of chemokines. These events enable the migration of immune cells across the BBB.[4]

This review is focused on CXCL9/MIG (monokine-induced by IFN-ϒ), CXCL10/IP-10 (interferon-inducible 10 kDa protein) and CXCL11/I-TAC (inducible T cell-α chemoattractant), and their chemokine (C-X-C motif) receptor 3 (CXCR3/CD183).[3,5,6] Our aim is to present the data available in the literature, concerning the above-mentioned chemokines and their receptor in selected CNS diseases, such as tick-borne encephalitis (TBE), neuroborreliosis (NB), Alzheimer's disease (AD), and multiple sclerosis (MS). These CNS diseases have different etiologies: TBE is the most common viral tick-borne disease, NB is the most common bacterial disease transmitted by ticks and AD is the most common form of dementia in elderly people, while MS is the most common disabling inflammatory demyelinating CNS disease in young adults. The cells of the CNS are capable of releasing chemokines upon stimulation; moreover, CNS cells are also able to respond to them by their receptors. There is evidence which identifies chemokines and their receptors as potential therapeutic targets.[4] According to the best of our knowledge and the available literature, data regarding the role and evaluation of concentrations of CXCL9, CXCL10 and CXCL11, and their receptor in CNS diseases is limited and not well-studied.

Chemokines

Chemokines are small proteins (8–15 kDa), consisting of approx. 70–90 amino acids.[1,3,7] Based on the position of conservative cysteines (C) in their sequence, they are divided into 4 structural subfamilies: CXC (alpha), CC (beta), C (gamma), and CXC3 (delta).[8,9] The CXC chemokines are additionally subdivided into those containing a glutamic acid-leucine-arginine motif (ELR) near their N-terminus and those which do not contain this motif (non-ELR).[3]

Chemokines were originally discovered by their adhesion, chemotaxis and leukocyte activation abilities, both in vivo and in vitro.[2,7] They are also involved in immune surveillance and the location of lymphocytes B or T with an antigen.[3,10] Based on their primary function, chemokines have also been classified into inflammatory chemokines, homeostatic chemokines and dual function chemokines (involved in both of the aforementioned processes).[8]

Chemokines mediate their function by activating 7-transmembrane G protein-coupled receptors, and thus induce cells to migrate through a concentration gradient.[1,10] Chemokine receptors were identified as CXCR, CCR, CR, and CX_3CR.[11,12] These receptors are part of a larger superfamily, including receptors for inflammatory mediators, hormones and neurotransmitters, as well as paracrine substances.[8] The conformational change of the chemokine, which makes the N terminus larger and more flexible, allows for receptor activation. The activation of the chemokine receptor leads to an exchange of bound GDP to GTP in the α subunit of the G protein, which disassociates from the receptor, and thus activates the downstream of several effector molecules, resulting in a cascade of signaling events within the cytoplasm.[10]

The number of chemokine receptors is significantly lower (approx. 20) than their ligands (approx. 50), which means that various chemokines share a single, common receptor. On the other hand, individual chemokines can also bind multiple receptors. Monogamous chemokine receptor–ligand interactions have been observed only in the case of CXCL12/CXCR4 and CX_3CL1/CX_3CR1.[8]

CXCL9, CXCL10 and CXCL11

CXCL9, CXCL10 and CXCL11 are the 3 chemokines that lack ELR (Glu-Leu-Arg). They are more closely related to each other than to any other chemokine, with an amino acid sequence similarity of about 40%.[5] The *CXCL9*, *CXCL10* and *CXCL11* gene is located on chromosome 4q21.21.[12] The above-mentioned chemokines are especially involved in Th1 response. In various diseases, their expression correlates with the tissue infiltration of T cells.[7] Under physiological conditions, they are not detectable in most non-lymphoid tissues. However, in the case of infection, immunoinflammatory response or injury, their production by blood and tissue cells is strongly induced by IFN-ϒ – the most typical Th1 cytokine (Fig. 1).[3,5]

It is interesting that the actions of the individual CXCR3 ligands can be distinct: a carboxy-terminal domain is required by CXCL9 and CXCL10, while CXCL11 requires the 2nd domain, residing in the 3rd intracellular loop.[3] CXCL9, CXCL10 and CXCL11 may also act as natural antagonists for the receptor for eotaxin (CCR3) and a few other CC chemokines.[5]

Data in the literature indicates a significant role for CXCL9, CXCL10 and CXCL11, and their receptor in the CNS, in both physiological processes and pathological processes. CXCL11 was originally identified in interferon beta (IFN-β) treated mouse astrocytes. It was shown that IFN-Ɣ alone or with interleukin (IL)-1 had the ability to stimulate *CXCL11* gene expression by human astrocytes and fetal human microglia. Similarly, CXCL10 was identified in the context of *IFN-inducible* genes, expressed by murine-cultured astrocytes and microglia. CXCR3/CXCL10 signaling is crucial in microglia recruitment and essential for neuronal reorganization.[13] CXCL9 is constitutively expressed on human brain-derived microvascular endothelial cells and astrocytes.[3]

The CXC3 receptor

CXC3 receptor (*CXCR3*) gene is located on chromosome Xq13. *CXCR3* is a classic 7-transmembrane receptor coupled to the G protein. Historically, this was the 3rd chemokine receptor discovered. It encloses an extracellular domain, which contains 3 potential amino-glycosylation sites, 7 transmembrane-spanning domains and intracellular carboxyl-terminal regions with 3 intracellular loop regions, and it shares a 30% identity with CXCR1 (CD181) and CXCR2 (CD182).[14]

CXCR3 is linked to several pathways, including Src, PI3K and MAPK signaling pathways, and it is expressed in a few forms (CXCR3-A, CXCR3-B and CXCR3-alt). The classic form, CXCR3-A, is expressed on $CD4^+$ Th1 cells, naïve and memory $CD8^+$ T cells, natural killer (NK) cells, and activated B cells. It can also be induced on all T cell subsets within the first few days after activation.[3,15] The role of CXCR3-A consists in mediating the direct migration of T cells to inflamed lymph nodes and other sites of inflammation.[6,15] Studies showed that Th1 cells in vitro generate higher levels of CXC3 receptor expression and migrate better to CXCL11, CXCL10 and CXCL9 than Th2 cells.[5]

CXCR3-B is an alternatively spliced variant of the CXCR3 gene and it contains a longer NH2-terminal extracellular domain.[3,15] While CXCR3-A supports cell survival and chemotaxis, the role of CXCR3-B consists in DNA synthesis inhibition and the induction of apoptosis. CXCR3-B also has an angiostatic effect on tumor-associated blood vessels and acts as a functional receptor for platelet factor 4 (CXCL4/PF4).[6,16] CXCR3-alt is the 3rd variant that contains a truncated C-terminus, as it lacks an intact 3rd and 2nd extracellular loop. Cells showing an expression of this form in vitro are capable of migrating in response to stimulation with CXCL11.[15]

Tick-borne encephalitis

Tick-borne encephalitis (TBE) is one of the most significant human arboviral infections of the CNS.[2,17] It is endemic to regions where transmission vectors are distributed: *Ixodes ricinus*-dominated, *Ixodes persulcatus*-dominated

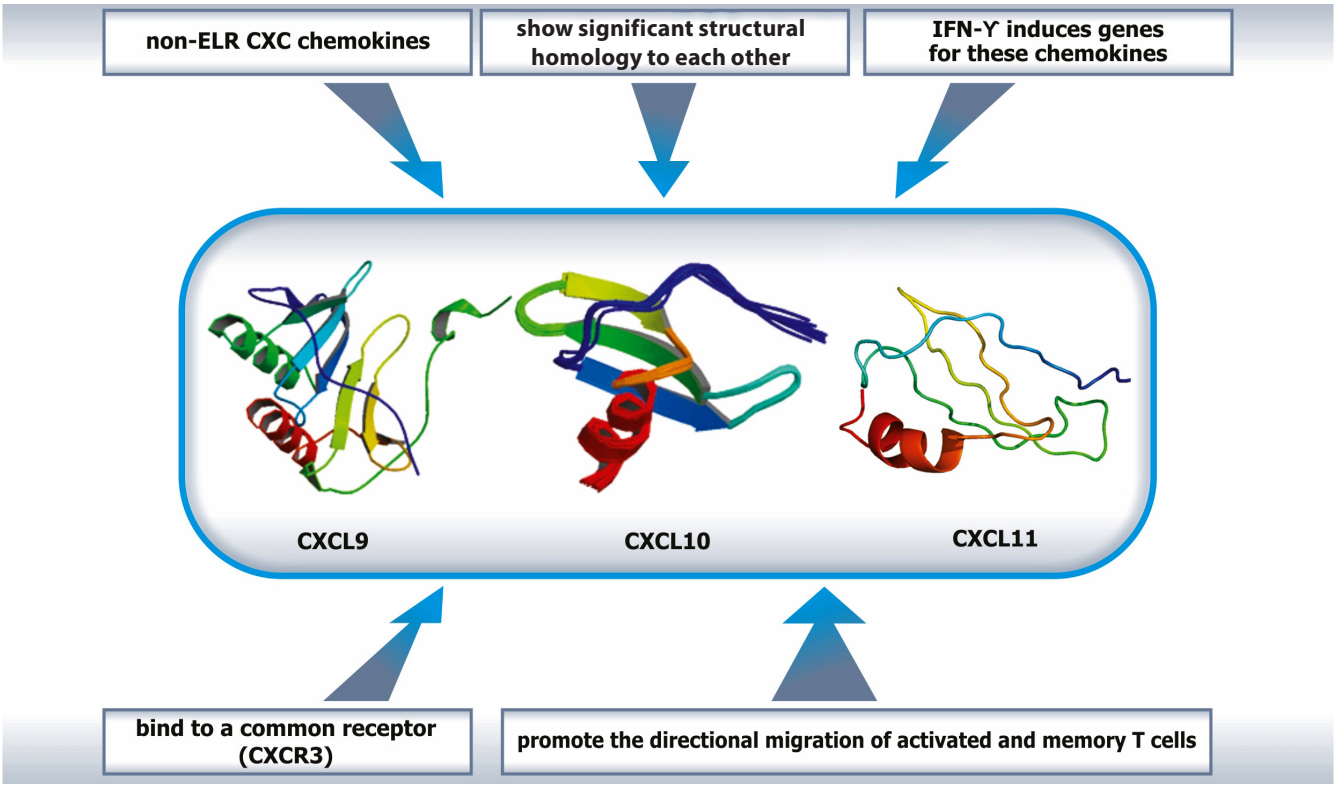

Fig. 1. The characteristics of CXCL9, CXCL10 and CXCL11 chemokines

and mixed regions.[17,18] So far, 3 genotypes of TBE viruses have been described: the European subtype transmitted by *I. ricinus* and the Siberian and Far-Eastern subtypes transmitted by *I. persulcatus*. Recently, the incidence of TBE has significantly increased, particularly in Germany, Switzerland, Lithuania, Latvia, and Poland.[17,18] Approximately 40% of infectious TBE cases might be asymptomatic; however, TBE is generally associated with a flu-like syndrome and causes moderate to severe injuries of the CNS.[17] The 2nd neurological phase may occur: with aseptic meningitis (in 50% of the cases), meningoencephalitis (40%) or meningoencephalomyelitis (10%).[17]

Chemokines are responsible for attracting leukocytes into the CNS and the cerebrospinal fluid (CSF) across the BBB in meningitis and meningoencephalitis. Holub et al. showed that the majority of cells in the early stage of TBE are T lymphocytes and only a small number consist of B lymphocytes and NK cells.[19]

There is not much data concerning the possible involvement of CXCL9, CXCL10 or CXCL11 chemokines, and their receptor in TBE. So far, the role and diagnostic usefulness of the aforementioned chemokines in TBE have been tested only by Zajkowska et al. and Koper et al.[20,21] Zajkowska et al. noted that serum CXCL10 concentrations were significantly increased in the acute phase of TBE as compared to the control group. CXCL10 and CXCL11 concentrations were also significantly higher in the CSF than in the serum, which might suggest that local production in the CSF is their source.[20] Moreover, the authors suggested that the concentration gradients of CXCL10 and CXCL11 between the CSF and the serum may recruit lymphocytes T to the CSF. Cerebrospinal fluid CXCL10 and CXCL11 concentrations were lower in TBE patients after treatment than before treatment; however, they still remained higher than in the control group (Table 1).[20] With the use of receiver operator characteristic (ROC) curves, Zajkowska et al. also assessed the diagnostic usefulness of these chemokines in the diagnosis and monitoring of inflammatory process in TBE.[20] The ROC curves analysis of CXCL10 and CXCL11 in TBE patients before and after treatment showed significant differences between these 2 groups. Additionally, CXCL10 and CXCL11 in the CSF were highly useful diagnostically ($p < 0.050$). According to Zajkowska et al., these chemokines might be useful parameters in monitoring the course of TBE.[20]

CXCL9 concentrations in TBE were analyzed by Koper et al., who revealed that the CSF and serum CXCL9 levels were significantly higher as compared to the controls. Cerebrospinal fluid CXCL9 demonstrated a tendency for higher concentrations, while serum CXCL9 tended to be lower in the acute phase of TBE in comparison to the TBE patients after a 2-week follow-up. However, neither difference was statistically significant (Table 1). To exclude the possible impairment of the blood-CSF barrier and/or BBB functions as potential sources influencing CXCL9 concentrations, the authors then related CSF CXCL9 concentrations to the serum levels in order to calculate the CXCL9 index (I_{CXCL9}). The levels of I_{CXCL9} in the acute phase of TBE and after a 2-week follow-up were significantly higher compared to the controls, and significantly decreased after the resolution of the symptoms. To sum up their findings, Koper et al. concluded that the CXCL9 index may be a better indicator of symptom resolutions in TBE than CSF or serum CXCL9 concentrations.[21]

The data presented in Table 1 indicates that higher concentrations of CXCL9 and CXCL10 are noted in the CSF as compared to serum samples. Among all 3 chemokines presented in this review, CXCL9 seems to be more specific for TBE than CXCL10 and CXC11, regardless of the type of material obtained from the patient for analysis.

Neuroborreliosis

Borreliosis (Lyme disease, Lyme borreliosis, LB) is a chronic disease, caused by etiologic factors which are spirochaetes *Borrelia burgdorferi* sensu lato. Annually, there are about 85,500 LB cases reported worldwide (approx. 65,500 cases in Europe, 16,500 in North America, 3,500 in Asia).[22]

It is estimated that neurological forms of Lyme disease develop in about 40% of the patients suffering from *B. burgdorferi*. Henningsson et al. reported that the number of neuroborreliosis (NB) cases in Sweden between 2000 and 2005 increased from 5/100,000 to 10/100,000 inhabitants/year.[23]

Table 1. CXCL9, CXCL10 and CXCL11 tested by the ELISA method in tick-borne encephalitis. Values are expressed in pg/mL

Zajkowska et al., 2011 TBE (n = 15), controls (n = 8)	CSF	Serum
CXCL10	• TBE1 (9360) vs C (338) – p* • TBE2 (1500) vs C (338) – p[a] • TBE1 (9360) vs TBE2 (1500) – p*	• TBE1 (127) vs C (69) – p* • TBE2 (192) vs C (69) – p[a] • TBE1 (127) vs TBE2 (192) – NS
CXCL11	• TBE1 (68) vs C (4.6) – p* • TBE2 (26) vs C (4.6) – p[a] • TBE1 (68) vs TBE2 (26) – p*	• TBE1 (80) vs C (91) – NS • TBE2 (132) vs C (91) – p[a] • TBE1 (80) vs TBE2 (132) – NS
Koper et al., 2018 TBE (n = 24), controls (n = 13)	**CSF**	**Serum**
CXCL9	• TBE1 (215) vs C (6) – p* • TBE2 (166) vs C (6) – p* • TBE1 (215) vs TBE2 (111) – NS	• TBE1 (111) vs C (58) – p* • TBE2 (138) vs C (58) – p* • TBE1 (111) vs TBE2 (138) – NS

C – controls; CSF – cerebrospinal fluid; ELISA – enzyme-linked immunosorbent assay; n – the number of subjects included in the study; NS – not statistically significant; [a] p-value not presented in the paper; * p-value significantly higher ($p < 0.05$); TBE – tick-borne encephalitis; TBE1 – material of TBE patients tested at the time of diagnosis; TBE2 – material of TBE patients tested after follow-up.

Approximately 15% of the patients suffering from NB are affected by lymphocytic cerebrospinal meningitis. The coexistence of meningitis symptoms, painful radicular syndrome and cranial nerve paralysis is called Bannwarth syndrome. Myeloencephalitis develops with a much lower frequency (in about 0.1% of patients).[23]

Lepej et al. evaluated the contribution of chemokine receptor CXCR3 and its ligands CXCL10 and CXCL11 to the recruitment of peripheral blood memory CD4+ T cells into the CSF of patients with acute NB.[24] In their studies, the percentage of memory CD45RO+CD4+ T cells expressing CXCR3 was significantly higher in the CSF compared to the peripheral blood. Additionally, concentrations of CXCL10 and CXCL11 in the CSF of NB patients were significantly higher compared to the corresponding serum samples. Regarding control samples, similar findings were observed only in the case of CXCL11. The authors suggested that in NB, CXCL10 and CXCL11 create a chemokine gradient between the CSF and serum, and recruit CXCR3-expressing memory CD4+ T cells into the CSF in patients with NB.[24]

Rupprecht et al. showed increased CXCL11 concentrations in the CSF of patients with NB as compared to the patients with noninflammatory CNS diseases.[25] Additionally, in their studies, CSF CXCL11 concentrations were significantly correlated with white blood cell count (Table 2). They also found that CSF CXCL11 concentrations of NB patients are statistically more chemotactic for mononuclear cells than those of control patients and that the chemotactic index was correlated with the CSF white blood cell count.[25]

Henningsson et al. showed that patients with confirmed NB and possible early NB had significantly higher CSF concentrations of CXCL10 as compared to the non-NB group and the control group.[26] Moreover, CSF CXCL10 correlated with CSF pleocytosis, but not with clinical parameters or the levels of anti-*Borrelia*-antibodies. In their opinion, time is probably an important factor for the chemokine profile, because Th1 cells dominate in the early stage of inflammation, which may be observed in patients with early NB. Thereafter, this response is counter-balanced by a Th2 response, which might be observed in patients with confirmed NB.[26] In the serum samples, CXCL10 concentrations were significantly higher in the confirmed NB group, as well as controls, as compared to subjects with possible early NB and the non-NB group. They also found that CSF CXCL10 concentrations did not correlate with the corresponding serum concentrations, which may indicate that the CSF is better material for the evaluation of the tested chemokine.

Moniuszko et al. revealed that pre-treatment serum CXCL10 and CXCL11 concentrations were significantly higher compared to the control group (Table 2).[27] After treatment, only serum CXCL10 concentrations revealed statistically significant outcomes as compared to the controls. In the CSF, only pre-treatment and post-treatment CXCL11 concentrations were notably higher when compared to the control group (Table 2). The analysis of diagnostic usefulness showed that CXCL10 differentiates NB and controls, while CXCL11 can only distinguish between the pre-treatment NB cases and healthy subjects.[27] According to Moniuszko et al., CXCL10 and CXCL11 are involved in the inflammatory process in NB; however, their results indicate that the chemokine patterns vary between the CSF and serum.[27]

The data in Table 2 indicates that both before and after antibiotic therapy, higher concentrations of CXCL10 in NB are noted in the CSF as compared to the serum samples. Data concerning the evaluation of the CXCL11 levels in NB is not coherent, thus this aspect requires further studies.

Alzheimer's disease

The most common form of dementia in elderly people is Alzheimer's disease (AD).[28,29] About 70% of late-life mental failure is caused by AD, which affects more than 25 million people worldwide.[30] Of crucial relevance in the development of AD is the deposition of β amyloid

Table 2. CXCL10 and CXCL11 tested by the ELISA method in neuroborreliosis. Values are expressed in pg/mL

Lepej et al., 2005 Acute NB before AT (n = 20); C (n = 11)	CSF	Serum
CXCL10	• NB (733) vs C (9) – p*	• NB (155) vs C (99) – p*
CXCL11	• NB (17) vs C (70) – p*	• NB (7) vs C (9) – NS
Rupprecht et al., 2005 Acute NB before AT (n = 17); C (n = 20) ELISA method		
CXCL11, CSF	• NB (100) vs C (55) – p* • CXCL11 significantly correlated with the CSF cell count ($p < 0.001$; $r = 0.57$)	
Moniuszko et al., 2014 Confirmed NB (n = 19); C (n = 8) ELISA method	CSF	Serum
CXCL10	• NB1 (465) vs C (274) – NS • NB2 (441) vs C (274) – NS • NB1 (465) vs NB2 (441) – NS	• NB1 (333) vs C (70) – p* • NB2 (145) vs C (70) – p* • NB1 (333) vs NB2 (145) – p*
CXCL11	• NB1 (111) vs C (4.2) –p* • NB2 (19) vs C (4.2) – p* • NB1 (111) vs NB2 (19) – p*	• NB1 (167) vs C (88) – p* • NB2 (105) vs C (88) – NS • NB1 (167) vs NB2 (105) – NS

AT – antibiotic therapy; C – controls; CSF – cerebrospinal fluid; ELISA – enzyme-linked immunosorbent assay; n – the number of subjects included in the study; NB1 – material tested before AT; NB2 – material tested after AT; NS – not statistically significant; * p-value significantly higher.

(1-42) in association with neurofibrillary tangle (NFT) formation in the brain, which leads to irreversible neuronal damage (severe reduction in the brain weight of more than 35% post-mortem AD cases was noted).[28,30]

The literature widely emphasizes the role of inflammation in neurodegenerative disorders such as AD. The expression of inflammatory mediators in the affected brain regions of AD cases has been demonstrated.[31] It was shown that in primary cortical neurons of mice, CXCL9 and CXCL10 were able to induce the activation of extracellular signal-regulated kinases (ERK1/2), which are members of the mitogen-activated-protein kinase. It is suggested that these chemokines might be involved in a neuronal–glial interaction.[11] The up-regulation of chemokines and their receptors was also found in human AD brains.[11,28]

Xia et al. showed that CXCR3 regional pattern staining did not differ in AD as compared to the control brain tissues, with the exception of diminished neuronal staining in regions of marked neuronal loss in AD.[11] Senile plaques of AD were not stained. Additionally, it was demonstrated that the CXCL10 expression defined a subpopulation of reactive astrocytes (the overall staining was higher in AD than in the controls).[18]

The CXCL10 over-expression in AD elicits apoptosis in fetal neurons. However, the mechanism of CXCL10-mediated neurotoxicity is not clearly understood. Sui et al. demonstrated that the treatment of fetal neuron cultures with exogenous CXCL10 leads to the elevated levels of intracellular Ca^{2+} via the binding of CXCL10 to its receptor (CXCR3).[32] Increased Ca^{2+}, which is available for uptake by the mitochondria, is associated with membrane permeabilization, and cytochrome c is released from this compartment. In the next step, cytochrome c initiates active caspase-9, which sequentially activates the effector caspase-3. This directly leads to apoptosis. The authors suggested that their results may provide putative targets for pharmaceutical intervention.[32]

Galimberti et al. showed that CSF CXCL10 concentrations in AD patients, as well as in mild cognitive impairment subjects, were significantly higher compared to the controls (Table 3), which suggests a role of this chemokine in the early stage of the disease, during which inflammation is likely to be more pronounced. In AD subjects, CXCL10 also positively correlated with the mini-mental state examination (MMSE).[28] However, further studies did not confirm their previous findings. They only indicated that the tested chemokine significantly correlated with age in the overall population.[29]

Corrêa et al. found a positive correlation between CXCL10 and β-amyloid in AD patients; however, CXCL10 concentrations did not differ in AD as compared to the controls (Table 3).[33]

The data included in Table 3 indicates that so far only CXCL10 concentrations have been analyzed in AD patients; however, the results obtained did not confirm the utility of the evaluation of this chemokine by the enzyme-linked immunosorbent assay (ELISA) method.

Multiple sclerosis

Multiple sclerosis (MS) attacks the myelinated axons in the CNS, and thus leads to the destruction of myelin and axons. The central mechanism of MS pathogenesis is the organ-specific traffic of T cells into the brain.[34]

The genetic contribution to susceptibility to MS has been established. So far, 57 genetic loci associated with MS have been identified; however, the meta-analysis undertaken by O'Gorman et al. has shown that MS results from multiple genetic susceptibility factors and environmental factors.[35] Kułakowska et al. analyzed 3,581 patients with MS (2,494 women and 1,030 men) and reported that a family history of MS was positive in only 6.4% of the cases.[36]

Research undertaken by Salmaggi et al. on microvascular endothelial cells and astrocytes from the human brain showed that CXCL9 behaved as a homing chemokine, while CXCL10 and CXCL11 were induced only after inflammatory stimuli.[37] Additionally, CXCL10 statistically correlated with the CXCR3 expression on CSF CD4+ T cells. From among CXCL9, CXCL10 and CXCL11, probably only CXCL10 is involved in the maintenance of intrathecal inflammation in MS.[38–40]

It is widely accepted that the recruitment of leukocytes to the sites of inflammation is very important in MS pathology. In MS, activated T cells and macrophages cross through the BBB. To better understand the involvement

Table 3. CSF CXCL10 tested by the ELISA method in Alzheimer's disease. Values are expressed in pg/mL

Galimberti et al., 2003 AD (n = 36); MCI (n = 38); C (n = 41)	• AD (103), MCI (128) vs C (69) – p*
Galimberti et al., 2006 AD (n = 48); MCI (n = 36); C (n = 29)	• AD (108) vs MCI (121) vs C (103) – NS
Corrêa et al., 2011 AD (n = 22); C (n = 27)	• AD vs C – NS

AD – Alzheimer's disease; C – controls; CSF – cerebrospinal fluid; ELISA – enzyme-linked immunosorbent assay; n – the number of subjects included in the study; NS – not statistically significant; MCI – mild cognitive impairment; * p-value significantly higher ($p < 0.05$).

Table 4. CSF CXCL10 tested by the ELISA method in multiple sclerosis. Values are expressed in pg/mL

Sørensen et al., 2001 CDMS (n = 36); MON (n = 12); C (n = 19)	• CDMS (2.6) vs C (1.8) – NS • CDMS (2.6) vs MON (2.1) – NS
Mahad et al., 2002 MS (n = 43); BH (n = 12); NIND (n = 44); IND (N = 24)	• MS, NIND and IND vs BH – p* • MS, IND vs NIND – p* • MS vs IND – NS

BH – patients with benign headaches; C – controls; CDMS – clinically definite multiple sclerosis; CSF – cerebrospinal fluid; ELISA – enzyme-linked immunosorbent assay; IND – inflammatory neurological diseases; n – the number of subjects included in the study; NIND – non-inflammatory neurological diseases; NS – not statistically significant; MON – monosymptomatic optic neuritis, * p-value significantly higher.

of chemokines in this mechanism, Simpson et al. examined post-mortem the CNS tissue from MS cases at different stages of lesion development.[39] Based on their findings, Simpson et al. suggested a sequence of events which might occur in MS formation. In the first step, activated T cells in the perivascular environment express IFN-ϒ. Next, IFN-ϒ induces the CXCL9 and CXCL10 expression in the surrounding glial cells, which finally selectively recruit further activated T-lymphocytes expressing CXCR3 to the site of inflammation.[39]

Mahad et al. showed significantly increased CXCL10 concentrations in the CSF of patients with MS, other inflammatory neurological diseases (IND) and non-inflammatory neurological diseases (NIND) as compared to subjects with benign headaches (control group).[38] However, CXCL10 concentrations between MS and IND were not significantly different (Table 4). CXCL10 concentrations were also notably higher in patients with relapsing-remitting MS than in the case of secondary progressive MS, which means that CXCL10 tends to decrease over time following a clinical relapse, and suggests a role of this chemokine in the inflammatory and demyelinating processes involved in MS relapses. CXCL10 also correlated with the CXCR3 expression on CD4+ T cells from the CSF. The authors suggested that this correlation may be related to the chemoattractant role of CXCL10 for activated lymphocytes.[38]

The studies of Sørensen et al. indicated increased levels of CXCL10 in MS patients in comparison with controls; however these differences were not statistically significant (Table 4).[41] CXCL10 concentration also did not change after 3 weeks of treatment (with methylprednisolone or placebo). In their research, CXCL10 concentrations in the patients' group were positively correlated with the parameters of intrathecal inflammation, such as neopterin, MMP-9, leukocyte count, and intrathecal IgG and IgM synthesis. The correlation between CSF CXCL10 and leukocyte count was not observed in the control group; however, it should be noted that only 2 of the 19 control subjects had normal CSF leukocyte counts. The authors emphasized that their findings suggest a strong role of CXCL10 accumulation in acute CNS inflammation. On the other hand, they showed that CCL2 concentrations were significantly lower in the group of patients than in the controls. The aforementioned parameters also negatively correlated with the measures of inflammation, which may directly suggest that CXCL10 is likely involved in the maintenance of intrathecal inflammation.[41]

The data presented in Table 4 indicates that only CXCL10 was tested with the use of the ELISA method in MS; however, the results obtained are not cohesive.

Conclusions

The literature indicates the significant role of CXCL9, CXCL10, CXCL11, and their receptor (CXCR3) in the physiology and the pathophysiology of the CNS. Knowledge about the mechanism of action of CXCR3 and its ligands may be useful in the treatment of CNS diseases. However, literature data concerning the evaluation of CXCL9, CXCL10, CXCL11, and their receptor with the use of the ELISA method is limited. Available papers indicate that CXCL9 seems to be more specific for TBE than CXCL10 and CXC11, regardless of the type of patient material obtained for analysis (the CSF or serum). Data concerning NB indicates the importance of CXCL10 in this disease. Information regarding the evaluation of CXCL11 concentrations in NB is not coherent, so this aspect requires further study. From among the above-mentioned chemokines, so far only the CXCL10 levels have been analyzed in AD; however, the studies have not proven the utility of the CXCL10 evaluation by means of the ELISA method. Similarly to AD, in MS, only CXCL10 has been analyzed so far, but the results obtained are not coherent.

References

1. Mazur G, Jaskuła E, Kryczek I, et al. Proinflammatory chemokine gene expression influences survival of patients with non-Hodgkin's lymphoma. *Folia Histochem Cytobiol*. 2011;49(2):240–247.
2. Banisadr G, Rostène W, Kitabgi P, Parsadaniantz SM. Chemokines and brain functions. *Curr Drug Targets Inflamm Allergy*. 2005;4(3):387–399.
3. Müller M, Carter S, Hofer MJ, Campbell IL. Review: The chemokine receptor CXCR3 and its ligands CXCL9, CXCL10, and CXCL11 in neuroimmunity – a tale of conflict and conundrum. *Neuropathol Appl Neurobiol*. 2010;36(5):368–387.
4. Ramesh G, MacLean AG, Philipp MT. Cytokines and chemokines at the crossroads of neuroinflammation, neurodegeneration, and neuropathic pain. *Mediators Inflamm*. 2013:480739. doi.org/10.1155/2013/480739
5. Clark-Lewis I, Mattioli I, Gong JH, Loetscher P. Structure-function relationship between the human chemokine receptor CXCR3 and its ligands. *J Biol Chem*. 2003;278(1):289–295.
6. Lazzeri E, Romagnani P. CXCR3-binding chemokines: Novel multifunctional therapeutic targets. *Curr Drug Targets Immune Endocr Metabol Disord*. 2005;5(1):109–118.
7. Bajetto A, Bonavia R, Barbero S, Florio T, Schettini G. Chemokines and their receptors in the central nervous system. *Front Neuroendocrinol*. 2001;22(3):147–184.
8. Bendall L. Chemokines and their receptors in disease. *Histol Histopathol*. 2005;20:907–926.
9. Sorce S, Myburgh R, Krause KH. The chemokine receptor CCR5 in the central nervous system. *Prog Neurobiol*. 2011;93(2):297–311.
10. Fernandez EJ, Lolis E. Structure, function, and inhibition of chemokines. *Annu Rev Pharmacol Toxicol*. 2002;42:469–499.
11. Xia MQ, Bacskai BJ, Knowles RB, Qin SX, Hyman BT. Expression of the chemokine receptor CXCR3 on neurons and the elevated expression of its ligand IP-10 in reactive astrocytes: In vitro ERK1/2 activation and role in Alzheimer's disease. *J Neuroimmunol*. 2000;108(1–2):227–235.
12. Zlotnik A, Yoshie O. Chemokines: A new classification system and their role in immunity. *Immunity*. 2000;12(2):121–127.
13. Li H, Gang Z, Yuling H, et al. Different neurotropic pathogens elicit neurotoxic CCR9- or neurosupportive CXCR3-expressing microglia. *J Immunol*. 2006;177(6):3644–3656.
14. Loetscher M, Loetscher P, Brass N, Meese E, Moser B. Lymphocyte-specific chemokine receptor CXCR3: Regulation, chemokine binding and gene localization. *Eur J Immunol*. 1998;28(11):3696–3705.
15. Fulton AM. The chemokine receptors CXCR4 and CXCR3 in cancer. *Curr Oncol Rep*. 2009;11(2):125–131.
16. Lasagni L, Francalanci M, Annunziato F, et al. An alternatively spliced variant of CXCR3 mediates the inhibition of endothelial cell growth induced by IP-10, Mig, and I-TAC, and acts as functional receptor for platelet factor 4. *J Exp Med*. 2003;197(11):1537–1549.
17. Herpe B, Schuffenecker I, Pillot J, et al. Tick-borne encephalitis, southwestern France. *Emerg Infect Dis*. 2007;13(7):1114–1117.

18. Bormane A, Lucenko I, Duks A, et al. Vectors of tick-borne diseases and epidemiological situation in Latvia in 1993–2002. *Int J Med Microbiol*. 2004;293(37):36–47.
19. Holub M, Klucková Z, Beran O, Aster V, Lobovská A. Lymphocyte subset numbers in cerebrospinal fluid: Comparison of tick-borne encephalitis and neuroborreliosis. *Acta Neurol Scand.* 2002;106(5):302–308.
20. Zajkowska J, Moniuszko-Malinowska A, Pancewicz SA, et al. Evaluation of CXCL10, CXCL11, CXCL12 and CXCL13 chemokines in serum and cerebrospinal fluid in patients with tick borne encephalitis (TBE). *Adv Med Sci*. 2011;56(2):311–317.
21. Koper OM, Kamińska J, Grygorczuk S, Zajkowska J, Kemona H. CXCL9 concentrations in cerebrospinal fluid and serum of patients with tick-borne encephalitis. *Arch Med Sci*. 2018;14(2):313–320.
22. Hubálek Z. Epidemiology of Lyme borreliosis. *Curr Probl Dermatol*. 2009;37:31–50.
23. Henningsson AJ, Malmvall BE, Ernerudh J, Matussek A, Forsberg P. Neuroborreliosis – an epidemiological, clinical and healthcare cost study from an endemic area in the south-east of Sweden. *Clin Microbiol Infect*. 2010;16(8):1245–1251.
24. Lepej SZ, Rode OD, Jeren T, Vince A, Remenar A, Barsić B. Increased expression of CXCR3 and CCR5 on memory CD4+ T-cells migrating into the cerebrospinal fluid of patients with neuroborreliosis: The role of CXCL10 and CXCL11. *J Neuroimmunol*. 2005;163(1–2): 128–134.
25. Rupprecht TA, Koedel U, Muhlberger B, Wilske B, Fontana A, Pfister HW. CXCL11 is involved in leucocyte recruitment to the central nervous system in neuroborreliosis. *J Neurol*. 2005;252(7):820–823.
26. Henningsson AJ, Tjernberg I, Malmvall BE, Forsberg P, Ernerudh J. Indications of Th1 and Th17 responses in cerebrospinal fluid from patients with Lyme neuroborreliosis: A large retrospective study. *J Neuroinflammation*. 2011;20:8–36.
27. Moniuszko A, Czupryna P, Pancewicz S, et al. Evaluation of CXCL8, CXCL10, CXCL11, CXCL12 and CXCL13 in serum and cerebrospinal fluid of patients with neuroborreliosis. *Immunol Lett*. 2014;157(1–2):45–50.
28. Galimberti D, Schoonenboom N, Scarpini E, Scheltens P; Dutch-Italian Alzheimer Research Group. Chemokines in serum and cerebrospinal fluid of Alzheimer's disease patients. *Ann Neurol*. 2003;53(4):547–548.
29. Galimberti D, Schoonenboom N, Scheltens P, et al. Intrathecal chemokine levels in Alzheimer disease and frontotemporal lobar degeneration. *Neurology*. 2006;66(1):146–147.
30. Farfara D, Lifshitz V, Frenkel D. Neuroprotective and neurotoxic properties of glial cells in the pathogenesis of Alzheimer's disease. *J Cell Mol Med*. 2008;12(3):762–780.
31. Schwab C, McGeer PL. Inflammatory aspects of Alzheimer disease and other neurodegenerative disorders. *J Alzheimers Dis*. 2008;13:359–369.
32. Sui Y, Stehno-Bittel L, Li S, et al. CXCL10-induced cell death in neurons: Role of calcium dysregulation. *Eur J Neurosci*. 2006;23(4):957–964.
33. Corrêa JD, Starling D, Teixeira AL, Caramelli P, Silva TA. Chemokines in CSF of Alzheimer's disease patients. *Arq Neuropsiquiatr*. 2011;69(3):455–459.
34. Goldenberg MM. Multiple sclerosis review. *P&T*. 2012;37(3):175–184.
35. O'Gorman C, Lin R, Stankovich J, Broadley SA. Modelling genetic susceptibility to multiple sclerosis with family data. *Neuroepidemiology*. 2013;40(1):1–12.
36. Kułakowska A, Bartosik-Psujek H, Hożejowski R, Mitosek-Szewczyk K, Drozdowski W, Stelmasiak Z. Wybrane aspekty epidemiologiczne stwardnienia rozsianego w Polsce – wieloośrodkowe badanie pilotażowe. *Neurol Neurochir Pol*. 2010;44(5):443–452.
37. Salmaggi A, Gelati M, Dufour A, et al. Expression and modulation of IFN-gamma-inducible chemokines (IP-10, Mig, and I-TAC) in human brain endothelium and astrocytes: Possible relevance for the immune invasion of the central nervous system and the pathogenesis of multiple sclerosis. *J Interferon Cytokine Res*. 2002;22(6):631–640.
38. Mahad DJ, Howell SJ, Woodroofe MN. Expression of chemokines in the CSF and correlation with clinical disease activity in patients with multiple sclerosis. *J Neurol Neurosurg Psychiatry*. 2002;72(4):498–502.
39. Simpson JE, Newcombe J, Cuzner ML, Woodroofe MN. Expression of the interferon-gamma-inducible chemokines IP-10 and Mig and their receptor, CXCR3, in multiple sclerosis lesions. *Neuropathol Appl Neurobiol*. 2000;26(2):133–142.
40. Balashov KE, Rottman JB, Weiner HL, Hancock WW. CCR5(+) and CXCR3(+) T cells are increased in multiple sclerosis and their ligands MIP-1alpha and IP-10 are expressed in demyelinating brain lesions. *Proc Natl Acad Sci USA*. 1999;96(12):6873–6878.
41. Sørensen TL, Sellebjerg F, Jensen CV, Strieter RM, Ransohoff RM. Chemokines CXCL10 and CCL2: Differential involvement in intrathecal inflammation in multiple sclerosis. *Eur J Neurol*. 2001;8(6):665–672.

Fibrin sealants in cardiac surgery: The last five years of their development and application

Robert Novotny[1–3,A–D], Jaroslav Hlubocký[1,2,E], Petr Mitáš[1,2,B,C], Jaroslav Lindner[1,2,E,F]

[1] 2nd Surgical Clinic of Cardiovascular Surgery, General Teaching Hospital, Prague, Czech Republic
[2] 1st Faculty of Medicine, Charles University, Prague, Czech Republic
[3] Transplant Surgery Department, Institute for Clinical and Experimental Medicine, Prague, Czech Republic

A – research concept and design; B – collection and/or assembly of data; C – data analysis and interpretation;
D – writing the article; E – critical revision of the article; F – final approval of the article

Advances in Clinical and Experimental Medicine, ISSN 1899-5276 (print), ISSN 2451-2680 (online) *Adv Clin Exp Med*. 2018;27(6):857–862

Address for correspondence
Robert Novotny
E-mail: novotny_robert@hotmail.com

Funding sources
None declared

Conflict of interest
None declared

Received on July 9, 2016
Reviewed on August 29, 2016
Accepted on February 14, 2017

Abstract

This review article describes the use of fibrin glue or fibrin sealants and their development over the past 5 years, with a focus on cardiac surgery. The roles of various types of sealants that are available in hemostasis control are reviewed briefly, together with the various potential risks and side effects of their use. The results of experimental work reported during the last 5 years, clinical data from the same period and the safety aspects of fibrin-based glues and sealants are summarized, showing many advantages of their clinical application over the use of synthetic glues or sealants that may be stronger in some cases, but less safe. It can be concluded that the widespread use of fibrin sealants is fully justified, as it benefits the patient as well as the surgeon through the improved control of hemostasis without increasing any adverse effects or complications during surgical procedures.

Key words: hemostasis, cardiac surgery, fibrin sealants

DOI
10.17219/acem/68981

Introduction

Sealants were developed in the previous century during World War II, when the need for a fast and reliable method of sealing injuries was obvious. The aim of sealing battle-related injuries was to completely stop bleeding, even with the use of sutures or – to replace the sutures – ligatures or cautery. Sealants are a modern-day auxiliary adjuncts in surgery.[1] The sealants, including fibrin-based sealants, are studied in approx. 200 scientific and clinical reports each year.[2] Consequently, it is obvious that the use of sealants in modern-day surgery is of interest for surgeons of various surgical specialties, with the main goal being an improvement in patient care.

The role of sealants in surgery

Presently, sealants are used in cardiac surgery for several reasons: (a) they help to control hemostasis through the control of bleeding in the area of surgical intervention (as auxiliary sutures, not as suture replacement); (b) they seal the openings made by standard sutures; and (c) they are useful in sealing off the hollow organs of the body. Ideally, they also should (d) improve wound healing and (e) may be useful in the delivery of medication to tissues exposed during surgery. Obviously, the use of sealants in surgery should be simple, safe and well-received by patients. The process of the sealant's disintegration should not cause inflammation or any type of unwanted or pathological process, immunological or other. Moreover, the cost of the use of sealants in surgery should not be prohibitive.

Types of sealant in surgery

Sealants in surgery may be classified according to various aspects of their production and structure; i.e., based on biological materials (fibrin) or synthetic substances (cyanoacrylates), the number of substances involved in inducing the sealing action, the tediousness of their use, and the safety and cost of various types of sealants.

The main types of sealants and glues used in medicine are as follows: (a) fibrin sealants; (b) cyanoacrylates; (c) gelatin and thrombin-based products; (d) polyethylene glycol polymers; and (e) albumin and glutaraldehyde-based products.

Fibrin sealants

These are blood-based. They are well-absorbed and easy to use. Their most prevalent use is to control hemostasis in cardiac surgery, liver surgery and after splenic trauma.[3,4]

Cyanoacrylates

These are synthetic sealants/glues. There are various cyanoacrylates on the market. However, the substances used for medical purposes are *n*-butyl or 2-octyl cyanoacrylate. The bond which is formed is strong enough to make the removal of sutures unnecessary.[5,6]

Gelatin and thrombin-based products

In principle, these products may be used in many types of surgery. These products (as all other natural/biological products) are relatively non-toxic.[7]

Polyethylene glycol polymers

These are oligomers or polymers of ethylene oxide and are biodegradable within 6 weeks of their use. They are used mainly in neurosurgery.[8,9]

Albumin and glutaraldehyde-based products

These mixed-origin products (natural albumin and synthetic glutaraldehyde) have excellent bonding ability in a mere 2–3 min.[10] These products are used in cardiac surgery.[11]

Fibrin blood clot formation

Fibrin plays an essential role in hemostasis. It is a fibrous protein that has an important part in blood clot formation. It is formed through the polymerization of fibrinogen (Factor I of blood coagulation) through an action of the protease enzyme thrombin, formed from prothrombin (Factor II). Additionally, thrombin activates other factors of the blood coagulation cascade, such as Factor V (proaccelerin), Factor VIII (antihemophilic factor) and Factor XIII (transglutaminase). Fibrin and platelets (with thrombin receptors) form a hemostatic clot that should close a natural, pathological or surgery-related tissue wound.[12]

Fibrin originates from fibrinogen, which is a peptide of relatively large molecules (molecular weight: 340 kDa). It consists of 2 tripeptide units connected at their *N*-terminal regions by disulfide bonds. The aggregation of fibrinogen particles is prevented by charge-charge repulsion. Thrombin cleaves the *N*-terminal structures and makes the resulting fibrin molecules capable of aggregation, resulting in the formation of a "soft" clot that is consequently stabilized by fibrin cross-linking.[12] Thus, the processes of sealing by fibrin sealants reproduces the final phase of physiological coagulation, the conversion of fibrinogen into fibrin. This whole process is an advantage of fibrin sealants, as it is a process natural to the body.

The 1st commercially available fibrin sealants to be approved for clinical use in the United States by the Food and Drug Administration (FDA) in 1998 was developed in Europe (TISSEEL; Baxter International Inc., Deerfield, USA).[13]

Fibrin as a biological structure is normally well-tolerated by patients. However, there are a few considerations.

1. The risk of an immunological reaction to animal (bovine) or human proteins present in sealants. It was reported that around 2% or even 5% of patients may develop anti-thrombin antibodies.[14,15]

2. The risk of excessive or uncontrolled clotting.

3. The potential (currently very small) for the transmission of some diseases, especially the transmission of some viral pathogens, i.e., human parvovirus B19.[16,17] Additional concerns for hepatitis B, hepatitis C and HIV transmission are justified. However, such cases have not been reported in the scientific literature. What is important is the fact that this aspect of fibrin sealant use not only threatens patients, but is also potentially risky for the sealant-handling health-care workers.

Recent uses of fibrin-based sealants in cardiac surgery: Experimental work

Significant scientific work has been done in the area of sealants' suitability and use in surgery. Current studies focus on several aspects of sealant application and on clarifying their possible benefits. The studies from the last 5 years were not only done in a clinical environment, but some were also done under experimental conditions.

Many such experiments compare different types of sealants to obtain information that is not yet available in order to optimize the use of these products. A very important demonstration of not only platelet-rich fibrin-based glue's excellent biocompatibility, but also of the upregulation of neovascularization was shown in experimental conditions using a rat model.[18] Additionally, aminomethylbenzoic acid prevents or slows down the degradation of fibrin glue.[18]

Recently, the possibility of using a sutureless approach through the application of a fibrin-based hemostat (TachoComb®; CSL Behring, Tokyo, Japan) was investigated in experiments on rabbit skin and porcine hearts.[19] It was found that the adhesive strength of the sealant is significantly increased through the application of polyglycolic acid sheets and fibrin glue together with the sealant. Thus, combining a hemostat with a polyglycolic acid sheet and fibrin glue seems to be a suitable method for difficult clinical situations, such as hemorrhage of the left ventricle. Fibrin glue itself seems to be very suitable for filling the needle holes created during cardiac or vascular surgery.[20] As much as this use of glue in surgery is obvious, not many studies of glue application for improved hemostasis are available. The report compared different methods of glue application: the drip method, the spray method, the rub and spray method, and the rub and rub method.[20] A comparison of hole-filling methods has shown that rubbing the fibrin glue onto a hole is the most effective approach. This was also confirmed by microscopic evaluation which documented that needle holes can be effectively clogged by rubbing the glue.[20] One important finding was documented on the superior effect of fibrin glue compared to a cyanoacrylate-based sealant in experiments using rabbit aortic wall.[20] The use of a cyanoacrylate-based sealant resulted in thinning of the rabbit aorta, while no such thinning was observed with a fibrin-based sealant.[20] Additionally, no apoptotic or necrotic cells were found by histological examination of the aortic tissue.

An interesting study devoted to the extraction of endoprostheses implanted in the aorta of experimental pigs was published.[21] The role of fibrin glue was evaluated in forming the interface between the endoprosthesis and tissue. Fibrin glue between the stent graft and the arterial wall increases the incorporation of the endoprosthesis.[21]

Recent reports on using of fibrin-based sealants in cardiac surgery: Clinical data

Significantly more reports available in the scientific literature deal with sealants or glues used in clinical situations. We have included only the reports where the use fibrin glue or sealant was described, and omitted reports whose authors used non-fibrin glue or sealant.

A review summarizing the available clinical data from controlled and uncontrolled clinical trials in cardiovascular surgery devoted to the use of various sealants appeared in 2013.[22] However, it deals with only some of the many products available on the market, mainly the product sold under the name TISSEEL. This review did not raise any concerns regarding the sealants' safety or tolerability, while emphasizing that they provide effective hemostasis control in cardiac and vascular surgery.[23]

The role of bleeding as an important predicting factor in morbidity was analyzed in the report on the use of a sealant in composite aortic root replacement in 56 patients.[24] The suture line in these operations was sealed with fibrin glue to prevent possible blood leakage. Only 1 patient required surgical re-exploration for bleeding and no case of operative or hospital death appeared. This was attributed to fibrin sealant application (spraying).[24] In another report, fibrin sealant was reported to have been successfully used in the case of left ventricular rupture, when it was combined with external sutures.[25]

A multicenter, parallel-group, randomized, controlled, open-label Phase II/III study was performed in Italy to address the question of fibrin sealant safety.[26] Two hundred patients were included in this retrospective

clinical trial study concentrating on thoracic surgery. Again, no increased risk of any type of adverse effects or surgical complications in relation to the use of fibrin sealant was observed.[26]

An evaluation of the efficacy and cost-effectiveness of a fibrinogen/thrombin-coated collagen patch (TachoSil®; CSL Behring, Tokyo, Japan) used for intraoperative hemostasis in patients younger than 16 years with congenital heart disease requiring reoperation during childhood was performed.[27] The surgeries of 117 patients took place between 2009 and 2011. The reasons for performing reoperations were reinforcement of suture lines, lung lesions, epicardial lesions, and chest wall lesions. A significant association was observed between the use of fibrinogen/thrombin-coated collagen patch and a decreased need for packed red blood cells. This, with the elimination of the use of other hemostatic or sealant agents, contributed to the decreased cost of the operations. This is important, especially because the patch served as an effective hemostatic agent.[28] Similar results for the same product were reported for patients who developed lymphatic leakage during an operation for congenital heart disease. The use of fibrinogen/thrombin-coated collagen patch was not only safe, but it also prevented the development of chylothorax during the postoperative period.[28]

A scientific study was published that described the success of using platelet and fibrin glue for a desirable non-invasive treatment of non-healing wounds in the sternal region after a coronary artery bypass operation.[29] Six patients were treated for serious, life-threatening chronic sternum wounds with multi-drug-resistant microbial pathogens. The topical application of platelet and fibrin glue every 2 days led to the complete healing of the wound in 5 patients and to significant improvement in 1 patient without any local or systemic complications or any abnormalities in tissue scarring or other type of tissue formation.[29] However, it was also reported that the use of platelet and fibrin glue sealant may lead to an increased rate of superficial sternal infections.[30]

Fibrin glue may also be successfully applied in cases of gunshot wounds.[31] It was shown that heart lacerations are successfully healed when mattress sutures with felt strips are covered with fibrin glue. In such cases, the use of fibrin glue contributes to an efficient medical care applied in emergencies.

Safety aspects in using glues or sealants in cardiac surgery

Fibrin glues or fibrin sealants as such are suitable for use in surgery because of their biological origin. The only unwanted effect that may take place is an immunological reaction. There is no report available to us from the last 5 years indicating some fibrin glue-related problems in cardiac surgery.[32] It is essential to note that the adhesive strength of fibrin glue or sealant is lower than that of glues based on cyanoacrylate or a gelatin-resorcin-formalin mixture. Lack of reported toxicity resulting from the use of fibrin sealant or glue use in cardiac surgery to repair a dissected aorta is obviously a great advantage over other sealant types, as there are some reports indicating issues with non-fibrin glues or sealants.[32] For example, there are several reports available on complications related the use of an albumin cross-linked glutaraldehyde glue (BioGlue®; CryoLife, Roberts Blvd., Kennesaw, USA). This product was implicated in a case report describing a patient treated for developed stenosis of the saphenous vein and internal thoracic artery bypass grafts.[33] The fibrotic narrowings which occurred were close to the BioGlue® site of application. The fibrotic reactions were likely associated with a reaction to the glue. Additionally, pulmonary embolism related to the use of BioGlue® was reported in the case of a type A aortic dissection repair.[34] Additionally, a delayed aorto-pulmonary artery wall disruption with false aneurysm formation after the repair of an acute type of aortic dissection with BioGlue® has also been reported.[35] There are other reports on BioGlue®--related complications, i.e., a case of ostial left main coronary artery stenosis possibly related to the use of BioGlue® and another report on several patients developing late wound healing problems after the use of BioGlue® for apical hemostasis during transapical aortic valve implantation.[36,37]

Closing remarks on the clinical use of some specific fibrin sealants

The accumulated data on fibrin-based and other sealants have created the basis for their broad application in practical cardiac surgery applications. In modern surgery, any sealant used in an operating room is of the highest quality and of an approved standard. These sealants are usually approved by the FDA and by other similar administrations in particular countries. The specific applications of some selected sealants are presented for further elucidation of the topic.

TachoSil®, according to the FDA, "is a fibrin sealant patch indicated for use with manual compression in adult and pediatric patients as an adjunct to hemostasis in cardiovascular and hepatic surgery, when control of bleeding by standard surgical techniques (such as suture, ligature or cautery) is ineffective or impractical".[38] In other words, TachoSil® is used in cardiac surgery in situations where the surgical treatment of bleeding is unavailable due to its anatomical location or because it would cause more damage to the anatomical structures. Other examples of TachoSil® applications include the repair of a ventricular rupture, a post-infarction repair of a ventricular septal defect and hemostatic support in reoperations. However, it is necessary to emphasize that TachoSil® (and also other sealants) should not be used in place of sutures or other forms of mechanical ligation in the treatment of major arterial or venous bleeding.[39–41]

BioGlue®, according to the FDA, is indicated as a supporting method for achieving hemostasis in adult patients in the open surgical repair of large vessels.[42] BioGlue® has a broad spectrum of use in cardiac surgery, such as repair of proximal aortic dissection, aortic root reconstruction procedures, aortic arch reconstruction procedures, ventricular rupture or injury, post-infarction ventricular septal defect repair, and valve repair and replacement procedures.[43–48] BioGlue® has also shown to be a very effective tool in patients with weakened tissue.[49]

CoSeal® (Baxter International Inc., Deerfield, USA), according to the FDA,is a hydrogel that works as a vascular sealant.[50] CoSeal® is indicated for use in reconstructive surgery to achieve adjunctive hemostasis by mechanically sealing leakage. Its main use is in the prevention of adhesions in surgery in high-risk or young patients, where reoperation is expected. Also, CoSeal® is used as either a supplement or an alternative to suture repair, obtaining hemostasis both in high-pressure ventricular repair and in the rupture of a friable coronary sinus adjacent to vital structures.[51,52]

Conclusions

Based on clinical experience and the results of experimental work, it can be concluded that the widespread use of fibrin sealants is fully justified, as it benefits the patient as well as the surgeon through the improved control of hemostasis while not increasing any adverse effects or complications during surgical procedures.

References

1. Spotnitz WD. Hemostats, sealants, and adhesives: A practical guide for the surgeon. *Am Surg*. 2012;78:1305–1321.
2. Spotnitz WD. Fibrin sealant: The only approved hemostat, sealant, and adhesive – a laboratory and clinical perspective. *ISRN Surg*. 2014;203943. doi: 10.1155/2014/203943
3. Schexneider KI. Fibrin sealants in surgical or traumatic hemorrhage. *Curr Opin Hematol*. 2004;11:323–326.
4. Kouba E, Tornehl C, Lavelle J, Wallen E, Pruthi RS. Partial nephrectomy with fibrin glue repair: Measurement of vascular and pelvicalyceal hydrodynamic bond integrity in a live and abbatoir porcine model. *J Urol*. 2004;172:326–330.
5. Dalvi AA, Faria MM, Pinto AA. Non-suture closure of wound using cyanoacrylate. *J Postgrad Med*. 1986;32:97–100. Accessed Junuary 13, 2018.
6. Duvvi SK, Lo S, Kumar R, Spraggs P. Superglue (cyanoacrylate) in the nose. *Otolaryngol Head Neck Surg*. 2005;133:803–804.
7. Ellegala DB, Maartens NF, Laws ER Jr. Use of FloSeal hemostatic sealant in transsphenoidal pituitary surgery: Technical note. *Neurosurgery*. 2002;51:513–515.
8. Krause TL, Bittner GD. Rapid morphological fusion of severed myelinated axons by polyethylene glycol. *Proc Natl Acad Sci USA*. 1990;87:1471–1475.
9. Stavisky RC, Britt JM, Zuzek A, Truong E, Bittner GD. Melatonin enhances the in vitro and in vivo repair of severed rat sciatic axons. *Neurosci Lett*. 2005;376:98–101.
10. Miscusi M, Polli FM, Forcato S, et al. The use of surgical sealants in the repair of dural tears during non-instrumented spinal surgery. *Eur Spine J*. 2014;23:1761–1766.
11. Bhamidipati CM, Coselli JS, LeMaire SA. BioGlue in 2011: What is its role in cardiac surgery? *J Extra Corpor Technol*. 2012;44:6–12.
12. Smith TE. Mechanism of blood coagulation. In: Devlin TM, ed. *Textbook of Biochemistry with Clinical Correlations*. 7th ed. Hoboken, NJ: John Wiley & Sons; 2010:1031–1048.
13. Immuno AG. Tisseel® Product Information, 1998. http://www.fda.gov/downloads/biologicsbloodvaccines/bloodbloodproducts/approvedproducts/licensedproductsblas/fractionatedplasmaproducts/ucm073008.pdf. Accessed December 20, 2015.
14. Gupta N, Chetter I, Hayes P, et al. Randomized trial of a dry-powder, fibrin sealant in vascular procedures. *J Vasc Surg*. 2015;62:1288–1295.
15. Verhoef C, Singla N, Moneta G, et al. Fibrocaps for surgical hemostasis: Two randomized, controlled phase II trials. *J Surg Res*. 2015;194:679–687.
16. Kawamura M, Sawafuji M, Watanabe M, Horinouchi H, Kobayashi K. Frequency of transmission of human parvovirus B19 infection by fibrin sealant used during thoracic surgery. *Ann Thorac Surg*. 2002;73:1098–1100.
17. Hino M, Ishiko O, Honda KI, et al. Transmission of symptomatic parvovirus B19 infection by fibrin sealant used during surgery. *Br J Haematol*. 2000;108:194–195.
18. Wu X, Ren J, Yao G, et al. Biocompatibility, biodegradation, and neovascularization of human single-unit platelet-rich fibrin glue: An in vivo analysis. *Chin Med J (Engl)*. 2014;127:408–411.
19. Kasahara H, Hayashi I. Polyglycolic acid sheet with fibrin glue potentiates the effect of a fibrin-based haemostat in cardiac surgery. *J Cardiothorac Surg*. 2014;9:121. doi: 10.1186/1749-8090-9-121
20. Kin H, Nakajima T, Okabayashi H. Experimental study on effective application of fibrin glue. *Gen Thorac Cardiovasc Surg*. 2012;60:140–144.
21. Almeida MJ, Yoshida WB, Hafner L, et al. Biomechanical and histologic analysis in aortic endoprosthesis using fibrin glue. *J Vasc Surg*. 2011;53:1368–1374.
22. Oda S, Morita S, Tanoue Y, Eto M, Matsuda T, Tominaga R. Experimental use of an elastomeric surgical sealant for arterial hemostasis and its long-term tissue response. *Interact Cardiovasc Thorac Surg*. 2010;10:258–261.
23. Rousou JA. Use of fibrin sealants in cardiovascular surgery: A systematic review. *J Card Surg*. 2013;28:238–247.
24. Della Corte A, Baldascino F, La Marca F, et al. Hemostatic modifications of the Bentall procedure: Imbricated proximal suture and fibrin sealant reduce postoperative morbidity and mortality rates. *Tex Heart Inst J*. 2012;39:206–210.
25. Garcia-Villarrea OA, Casillas-Covarrubias LE. Fibrin sealant for left ventricular rupture after mitral valve replacement. *Asian Cardiovasc Thorac Ann*. 2008;16:152–153.
26. Cardillo G, Carleo F, Carbone L, et al. Adverse effects of fibrin sealants in thoracic surgery. The safety of a new fibrin sealant: Multicenter, randomized, controlled, clinical trial. *Eur J Cardiothorac Surg*. 2012; 41:657–662.
27. Vida VL, De Franceschi M, Barzon E, Padalino MA, Scattolin F, Stellin G. The use fibrinogen/thrombin-coated equine collagen patch in children requiring reoperations for congenital heart disease: A single center clinical experience. *J Cardiovasc Surg (Torino)*. 2014;55:401–406.
28. Vida VL, Padalino MA, Barzon E, Stellin G. Efficacy of fibrinogen/thrombin-coated equine collagen patch in controlling lymphatic leaks. *J Card Surg*. 2012;27:441–442.
29. Tashnizi MA, Alamdari DH, Khayami ME, et al. Treatment of non-healing sternum wound after open-heart surgery with allogenic platelet-rich plasma and fibrin glue-preliminary outcomes. *Indian J Plast Surg*. 2013;46:538–542.
30. Sakic A, Chevtchik O, Kilo J, et al. Simple adaptations of surgical technique to critically reduce the risk of postoperative sternal complications in patients receiving bilateral internal thoracic arteries. *Interact Cardiovasc Thorac Surg*. 2013;17:378–382.
31. Suzuki T, Wada T, Funaki S, et al. Traumatic left ventricular free-wall laceration by a gunshot: Report of a case. *Surg Today*. 2014;44:1152–1155.
32. Suzuki S, Masuda M, Imoto K. The use of surgical glue in acute type A aortic dissection. *Gen Thorac Cardiovasc Surg*. 2014;62:207–213.
33. Khan H, Chaubey S, Desai J. Early failure of coronary artery bypass grafts: An albumin cross-linked glutaraldehyde (BioGlue) related complication. *J Card Surg*. 2011;26:264–266.

34. Rubio Alvarez J, Sierra Quiroga J, Martinez de Alegria A, Delgado Dominguez C. Pulmonary embolism due to biological glue after repair of type A aortic dissection. *Interact Cardiovasc Thorac Surg*. 2011;12:650–651.
35. Alameddine A, Alimov VK, Rousou JA, Freeman J. Aorto-pulmonary artery disruption following acute type-A aortic dissection repair with the use of BioGlue®. *J Card Surg*. 2012;27:371–373.
36. Modi A, Bull R, Tsang G, Kaarne M. Ostial left coronary stenosis following aortic root reconstruction with BioGlue. *Interact Cardiovasc Thorac Surg*. 2011;13:243–245.
37. Pasic M, Unbehaun A, Drews T, Hetzer R. Late wound healing problems after use of BioGlue for apical hemostasis during transapical aortic valve implantation. *Interact Cardiovasc Thorac Surg*. 2011;13:532–534.
38. TachoSil. U.S. Food and Drug Administration. https://www.fda.gov/BiologicsBloodVaccines/BloodBloodProducts/ApprovedProducts/LicensedProductsBLAs/FractionatedPlasmaProducts/ucm207482. Accessed March 31, 2010.
39. Feng W, Coady M. Epicardial tachosil patch repair of ventricular rupture in a 90-year-old after mitral valve replacement. *Ann Thorac Surg*. 2016;101(6):2361–2363.
40. Giordano R, Palma G, Palumbo S, Cioffi S, Russolillo V, Vosa C. Use of biological hemostatic support TachoSil® for reoperation in pediatric cardiac surgery. *Minerva Pediatr*. 2016;68(3):240–241.
41. Labrousse L, Barandon L, Choukroun E, Deville C. 'Double patch and glue' technique for early repair of posterior post-infarction ventricular septal defect. *Interact Cardiovasc Thorac Surg*. 2006;5(3):195–196.
42. BioGlue. U.S. Food and Drug Administration. https://www.accessdata.fda.gov/cdrh_docs/pdf/p010003b.pdf. Accessed December 14, 2001.
43. Zehr KJ. Use of bovine albumin-glutaraldehyde glue in cardiovascular surgery. *Ann Thorac Surg*. 2007;84:1048–1052.
44. Higashi R, Matsumura Y, Yamaki F. Posterior ventricular septal perforation: Sandwich technique via right ventriculotomy using BioGlue. *Gen Thorac Cardiovasc Surg*. 2013;61(8):460–462. doi:10.1007/s11748-012-0172-6
45. Masroor S, Schor J, Carrillo R, Williams DB. Endoventricular pocket repair of type I myocardial rupture after mitral valve replacement: A new technique using pericardial patch, Teflon felt, and BioGlue. *Ann Thorac Surg*. 2004;77:1439–1441.
46. Dunst KM, Antretter H, Bonatti J. Control of suture hole bleeding after aortic valve replacement by application of BioGlue during circulatory arrest. *Int Heart J*. 2005;46:175–179.
47. Leva C, Bruno PG, Gallorini C, et al. Complete myocardial revascularization and sutureless technique for left ventricular free wall rupture: Clinical and echocardiographic results. *Interact Cardiovasc Thorac Surg*. 2006;5:408–412.
48. Durukan AB, Serter FT, Gurbuz HA, Tavlasoglu M, Ucar HI, Yorgancioglu C. Biological glue application in repair of atrioventricular groove rupture: A case report. *J Tehran Heart Cent*. 2014;9(3):137–139.
49. Gil-Jaurena JM, Aroca Á, Pérez-Caballero R, Pita A. Free wall rupture after arterial switch operation. *Ann Thorac Surg*. 2014;98(6):2230–2231. doi:10.1016/j.athoracsur.2014.01.072
50. CoSeal. U.S. Food and Drug Administration. www.accessdata.fda.gov/cdrh_docs/pdf/p010022b.pdf. Accessed February 25, 2002.
51. Pace Napoleone C, Valori A, Crupi G, et al. An observational study of CoSeal for the prevention of adhesions in pediatric cardiac surgery. *Interact Cardiovasc Thorac Surg*. 2009;9(6):978–982. doi:10.1510/icvts.2009.212175
52. Garcia-Morales LJ, Ramchandani M, Loebe M, Reardon MJ, Bruckner BA, Ramlawi B. Intraoperative surgical sealant application during cardiac defect repair. *Tex Heart Inst J*. 2014;41(4):440–442. doi:10.14503/THIJ-13-3347

Advances
in Clinical and Experimental
Medicine